United States
Environmental Protection
Agency

Environmental Sciences
Research Laboratory
Research Triangle Park
NC 27711

EPA-600/9-78-020a
August 1978

Research and Development

EPA

Workshop Proceedings on Primary Sulfate Emissions from Combustion Sources

Volume 1
Measurement Technology

RESEARCH REPORTING SERIES

Research reports of the Office of Research and Development, U.S. Environmental Protection Agency, have been grouped into nine series. These nine broad categories were established to facilitate further development and application of environmental technology. Elimination of traditional grouping was consciously planned to foster technology transfer and a maximum interface in related fields. The nine series are:

1. Environmental Health Effects Research
2. Environmental Protection Technology
3. Ecological Research
4. Environmental Monitoring
5. Socioeconomic Environmental Studies
6. Scientific and Technical Assessment Reports (STAR)
7. Interagency Energy-Environment Research and Development
8. "Special" Reports
9. Miscellaneous Reports

This document is available to the public through the National Technical Information Service, Springfield, Virginia 22161.

EPA-600/9-78-020a
August 1978

Workshop Proceedings on Primary Sulfate Emissions from Combustion Sources

Volume 1
Measurement Technology

Sponsorship by
U.S. Environmental Protection Agency
April 24-26, 1978
Southern Pines, North Carolina 28287

Coordination and Editing by
Kappa Systems, Inc.
Arlington, Virginia 22209

Workshop Chairman
John S. Nader
Emission Measurements and Characterization Division
Environmental Sciences Research Laboratory
Research Triangle Park, North Carolina 27711

Environmental Sciences Research Laboratory
Office of Research and Development
U.S. Environmental Protection Agency
Research Triangle Park, North Carolina 27711

DISCLAIMER

This report has been reviewed by the Environmental Sciences Research Laboratory, U.S. Environmental Protection Agency, and approved for publication. Approval does not signify that the contents necessarily reflect the views and policies of the U.S. Environmental Protection Agency, nor does mention of trade names or commercial products constitute endorsement or recommendation for use.

In general, the technical content of the papers included in this report have been reproduced in the form submitted by the authors.

Any papers included in the Program and not included herein were not submitted for publication.

Preface

This volume contains the technical papers presented at the Workshop on Measurement Technology and Characterization of Primary Sulfur Oxides Emission from Combustion Sources held in Southern Pines, North Carolina, April 24-26, 1978. In addition, reports on deliberations and recommendations of four Working Groups (corresponding to the four sessions of technical presentations) are included.

A Working Group was formed for each of the four sessions of technical presentations and consisted of all the speakers of that session. Each Working Group met in a Working Group Session, reviewed and critiqued the session presentations, and made its initial report to all attendees in a summary session. The report summarized what is known and deemed acceptable and what further research activity needs to be pursued to provide desirable data and information. At the summary session, the initial report of each Working Group was discussed and further modified to reflect the comments and interaction between the Working Groups. The report of each Working Group resulting from this summary session is presented in this volume and follows the set of papers presented at the session it addresses.

The focus of sulfur pollutants impacting on ambient air quality has been the criteria pollutant, sulfur dioxide and its oxidation products, sulfuric acid and sulfate salts. Considerable attention has been directed to the sulfuric acid and sulfate salts resulting from the chemical transformation of SO_2 both temporally and spatially in the atmosphere. These are referred to as secondary sulfates. Sulfuric acid and sulfate salts emitted directly as emissions from combustion sources also impact on the ambient levels of sulfate.

These direct emissions of sulfuric acid and sulfate salts are referred to as primary sulfates.

Since sulfates at this time are not criteria pollutants and emission standards are not prescribed, no reference method is established for their measurement in combustion source emissions. With the current and ongoing concern about sulfur in fuels, there is increasing effort in measuring and characterizing sulfur-containing emissions from combustion sources. There is a need to identify valid measurement techniques for primary sulfates, specifically sulfuric acid, and to provide an accurate and consistent base of characterization data on primary sulfate emissions from the various combustion processes. There is also the need to determine what emission data on primary sulfates are available, their acceptability as valid measurements, and what further research effort needs to be conducted to provide a good data base for a good understanding of the contribution of primary sulfate emissions to ambient sulfate levels.

The purpose of this Workshop was to help meet these needs.

I am grateful for the active participation of the Workshop attendees who were invited to present and discuss their activities and studies in the area of primary sulfate emissions and for their contributions which made the Workshop an interesting and significant accomplishment. In particular, I want to thank the Session Chairmen (James Dorsey, Kenneth Knapp, James Homolya, and John Bachmann) and the Working Group Chairmen (Paul Urone, Dale Lundgren, James Howes, and David Natusch) for their assistance in implementing the Workshop agenda so effectively. I also want to include my appreciation for the efforts and cooperation of Ann Mitchell and Wendy Martin of Kappa Systems in coordinating the Workshop and in editing the Proceedings.

John S. Nader
Workshop Chairman

Contents

VOLUME 1

SECTION 1 -- Gas Sampling and Analysis

An Evaluation of a Modified Method 6 Flue Gas Sampling Procedure 3

Russell N. Dietz
Robert F. Wieser
Leonard Newman

Measurements of Sulfur Trioxide at Tennessee Valley Authority Coal-Fired Power Plants Using the Condenser Method 27

Elizabeth M. Bailey
H. A. Ruddock

Measurement of SO_3/H_2SO_4 Concentration in Kraft Recovery Furnace Stack Gas Using Controlled Condensation 41

Ashok K. Jain
R. O. Blosser
Howard S. Oglesby

Characterization of Combustion Source Sulfate Emissions with a Selective Condensation Sampling System 53

James L. Cheney
James B. Homolya

A Specific Method for the Determination of Sulfuric Acid Emissions from Combustion Sources 63

Paul Urone
Robert A. Lucas

Measurements of Sulfuric Acid Vapor by Infrared Spectroscopy 79

Roosevelt Rollins

Chemical Speciation and Concentration Monitoring of Sulfur Oxides by Laser-Raman Scattering 97

Richard K. Chang
Robert E. Benner

Report of the Working Group on Measurement of Gaseous Sulfur Oxides Emissions 137

Russell N. Dietz, Reporter

SECTION 2 -- Particulate Sampling and Analysis

Collection Methods for the Determination of Stationary Source Particulate Sulfur and Other Elements 145

Kenneth T. Knapp
Roy L. Bennett
Robert J. Griffin
Raymond C. Steward

A Stack Gas Sulfate Aerosol Measurement Problem 161

Dale A. Lundgren
Paul Urone
Thomas Gunderson

Sulfur Oxide Interaction with Filters Used for Method 5 Stack Sampling 179

Edward T. Peters
Jeffrey W. Adams

Particulate Sampling in Process Streams in the Presence of Sulfur Oxides 203

Kenneth M. Cushing

Primary Aerosol Sulfur Size Distribution Measurements Using a Low Pressure Impactor 227

Richard C. Flagan

Use of a High-Flow Stack Sampler for Determination of Particulate Sulfate Emissions 241

A. Jack O'Neal, Jr.
Harold Cowherd

Inorganic Compound Identification by Fourier Transform Infrared Spectroscopy 253

Robert J. Jakobsen
R. M. Gendreau
William M. Henry
Kenneth T. Knapp

Report of the Working Group on Measurement of Particulate Sulfur Oxides Emissions 275

Richard C. Flagan, Reporter

Appendix - Participants and Observers 277

VOLUME 2

SECTION 1 -- Gas Emissions

An Assessment of Sulfuric Acid and Sulfate Emissions from the Combustion of Fossil Fuels 3

James B. Homolya
James L. Cheney

Sulfur Oxides Emissions from Boilers, Turbines, and Industrial Combustion Equipment 13

Skillman C. Hunter
Paul K. Engel

Some Recent Data on SO_3 and SO_4 Levels in Utility Boilers 53

Brian W. Doyle
Richard C. Booth

Measurement of Sulfur Oxides from Coal-Fired Utility and Industrial Boilers 67

William R. McCurley
Daryl G. DeAngelis

Sulfur Oxide Measurements of Utility Power Plant Emissions 87

James E. Howes, Jr.

Effects of Combustion Modification on SO_3 Formation in Combustion 99

Arthur Levy
John F. Kircher
Earl L. Merryman

Impact of Sulfuric Acid Emissions on Plume Opacity 121

John S. Nader
William D. Conner

Query: Is There a Connection between the Expansion of Areas of Acid Rain and a Shift from Coal to Oil for Small-Scale Heat Needs? 137

Arthur M. Squires

Report of the Working Group on Characterization of Gaseous Sulfur Oxides Emissions 143

Arthur M. Squires, Reporter

SECTION 2 -- Particulate Emissions

Characterization of Fly Ash from Coal Combustion 149

David F. S. Natusch

Sulfur and Trace Metal Particulate Emissions from Combustion Sources 165

Roy L. Bennett
Kenneth T. Knapp

Inorganic Compounds Present in Fossil Fuel Fly Ash Emissions 185

William M. Henry
Ralph I. Mitchell
Kenneth T. Knapp

Investigation of Particulate Sulfur by ESCA 209

Arthur S. Werner

Sulfur Emissions Sampling and Analysis 219

Ray F. Maddalone

Operating Parameters Affecting Sulfate Emissions from an Oil-Fired Power Unit 239

Russell N. Dietz
Robert F. Wieser
Leonard Newman

Report of the Working Group on Characterization of Particulate Sulfur Oxides Emissions 271

Ray F. Maddalone, Reporter

Appendix - Participants and Observers 275

Section 1

Gas Sampling and Analysis

An Evaluation of a Modified Method 6 Flue Gas Sampling Procedure

Russell N. Dietz
Robert F. Wieser
Leonard Newman
Brookhaven National Laboratory

ABSTRACT

The character of primary sulfate emissions (i.e., H_2SO_4 and water-soluble sulfate salts) must be determined using flue gas sampling methods that differentiate between the acid form and the less nocuous sulfates. These methods must be used in considering potential health effects and in determining the mechanisms and parameters that affect the magnitude and distribution of such emissions.

As recommended, the Modified EPA Method 6 does not provide for specific determination of sulfate particulates and H_2SO_4. A Brookhaven modification, based on an isokinetically-sized nozzle and quartz fiber filter assembly, has been shown to collect quantitatively, in situ, all the particulate sulfate. Sulfuric acid was passed through the filter for subsequent quantitative collection, and no spurious formation of acid by oxidation of SO_2 was found on the filter. Problems associated with sub-isokinetic particulate sampling, leading to significant positive sulfate measurement errors, will be discussed.

In many cases, the isopropyl alcohol (IPA) used to collect the H_2SO_4 vapor contained sufficient oxidant to produce positive errors 10-fold or more when actual flue gas acid levels were less than 1 ppm. In addition, stripping experiments demonstrated the presence of dissolved SO_2 equivalent to 1 ppm to 3 ppm of flue gas acid even after 16- to 32-minute purging periods. The significance of these errors and simple corrective procedures will be presented.

INTRODUCTION

The character of primary sulfate emissions (i.e., H_2SO_4 and water-soluble metal sulfates) must be determined with flue gas sampling methods that differentiate between the acid form and the less nocuous metal sulfates, both for consideration of potential health effects and for determination of the mechanisms and parameters which affect the magnitude and distribution of those emissions.

As presently recommended, the modified version (1) of the EPA Method 6 (2) does not provide for specific determination of particulate metal sulfates and H_2SO_4. A Brookhaven modification, based on an isokinetically-sized nozzle and quartz fiber filter assembly (3), has been shown to quantitatively collect, in situ, all the particulate metal sulfates. Sulfuric acid was quantitatively passed through the filter for subsequent collection in the probe and the final collection stages--either an isopropyl alcohol (IPA) midget bubbler and filter (EPA Method 6) or a multi-turn condensation coil and filter (controlled condensation system). The latter is described in detail elsewhere (3) and, for the purposes of this paper, will be considered to be an absolute method to which other techniques will be compared.

Two problems have been encountered with the utilization of the Method 6 IPA midget bubbler for collection of H_2SO_4. In some preliminary field experiments (3) employing the IPA bubblers, we noted both the presence of an oxidant in the IPA solution which converted dissolved SO_2 to H_2SO_4 and the tendency of the solutions to retain dissolved SO_2 even after the recommended purging period with ambient air. The presence of oxidant in the IPA solutions has been noted by others (4)(5).

This paper describes an improved version of the IPA bubbler technique for collection of sulfuric acid--a version which can reduce the errors associated with neglecting the correction for the presence of an oxidant in the IPA and the inability to entirely strip the dissolved SO_2 prior to determination of H_2SO_4. Laboratory and field experimental results confirmed the existence of both phenomena as well as the apparent existence of a volatile oxidant in the flue gas which converted SO_2 to H_2SO_4 in the IPA. Because of the significant errors associated with even this improved version, especially at fossil-fueled combustion sources utilizing low sulfur and low vanadium fuels, it is recommended that the Modified EPA Method 6 using IPA bubblers be replaced by a miniaturized version of a controlled condensation system. Errors associated with non-isokinetic sampling of the particulate metal sulfates will be presented.

THE SAMPLING APPARATUS

Modifications to the EPA Method 6 were made in order to quantitatively separate the particulate metal sulfates from the sulfuric acid in the flue gas. This section describes the sampling apparatus employed to implement the separation in the Brookhaven Method 6 (BM6).

Nozzle and Filter Assembly (Metal Sulfates Collection)

The first significant modification, a miniaturized version of the Brookhaven controlled condensation system (CCS) in situ flue gas nozzle and filter assembly (NFA), was designed and fabricated as shown in Figure 1. The nozzle inside diameter was 1 mm for isokinetic sampling (100 ft/sec velocity) at 1 ℓ/min and 2 mm for 25 ft/sec. In order to compare isokinetic sampling for particulate metal sulfates with the non-isokinetic approach sampling normal to the direction of flue gas flow, a tube and filter assembly was also devised to approximate the dimension in the EPA version (1). The efficiency of the acid-treated quartz fiber filter used in both assemblies has been well documented for nearly 100% collection of the particulate metal sulfates while passing generally 95% or more of the flue gas H_2SO_4 (3). The trace amount of H_2SO_4 retained by the filter was recoverable by washing first with 100% IPA before washing with water for recovery of the water-soluble metal sulfates.

Probe and Bubbler Assembly (H_2SO_4 Collection)

After passing through the NFA and heated probe (~350° to 450°F), the particulate-free flue gas then passed through the second major Brookhaven modification--two midget bubblers separated by a quartz fiber filter--shown schematically in Figure 2. The first of the two midget bubblers, each containing 15 mℓ of 80% IPA for collection of H_2SO_4 aerosol, was followed by a heat and acid-treated quartz fiber filter mounted in an assembly shown in detail in Figure 3. As demonstrated in laboratory studies, the filter would not allow any acid aerosol to pass into the second bubbler.

Sulfur dioxide in the flue gas was collected by the two midget impingers each containing 15 mℓ of 3% H_2O_2 with a third impinger remaining empty to collect any entrained solution. The dried gas was then pumped through the dry test meter for an accurate measure of the sampled volume with a small portion (~0.4 ℓ) collected in the pre-evacuated gas bottle sampler at a constant rate for about 20 minutes (controlled by the critical orifice size). A photograph of the ice bath vessel (190 mm diameter by 100 mm high) containing

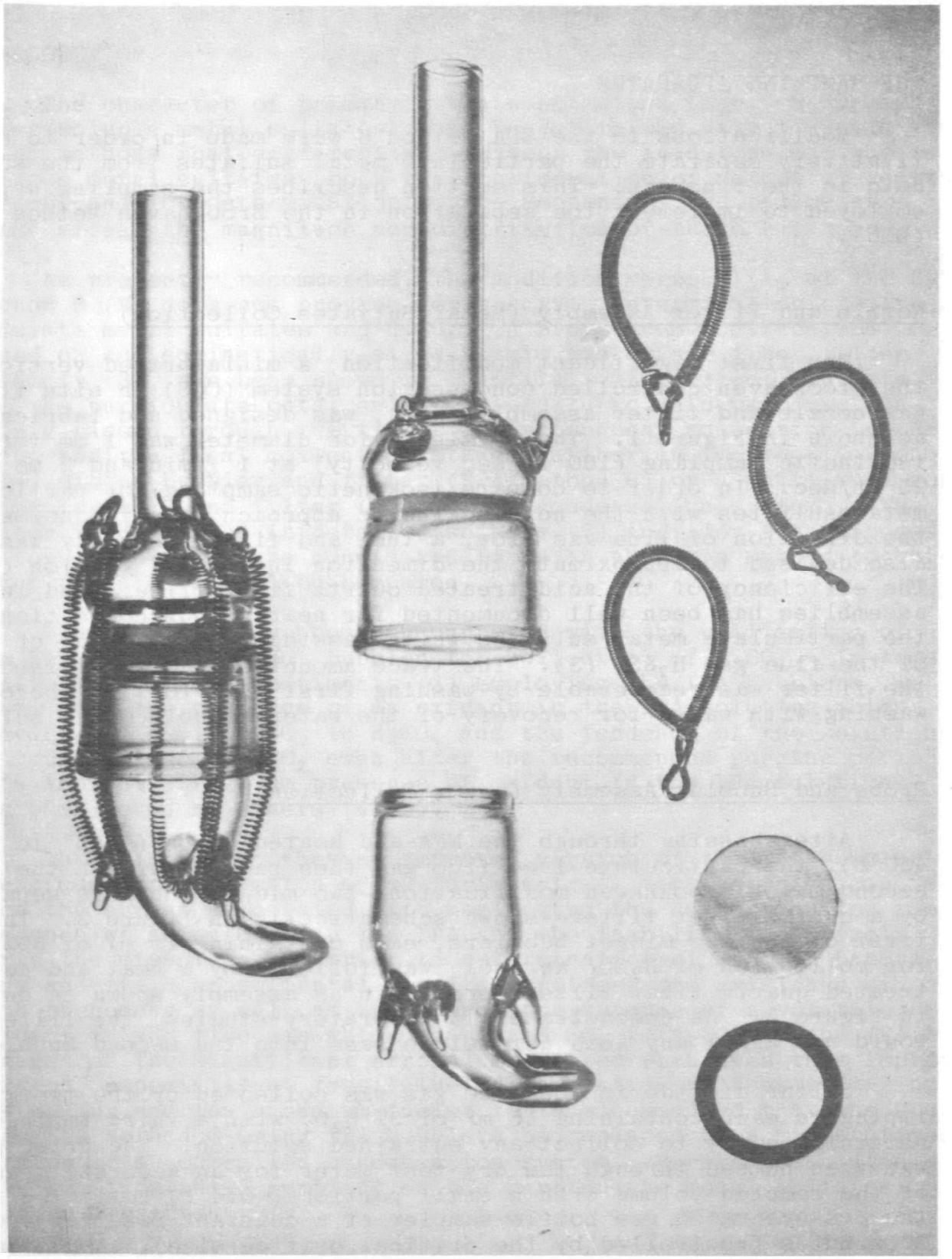

Figure 1. Flue gas isokinetic nozzle and filter assembly.

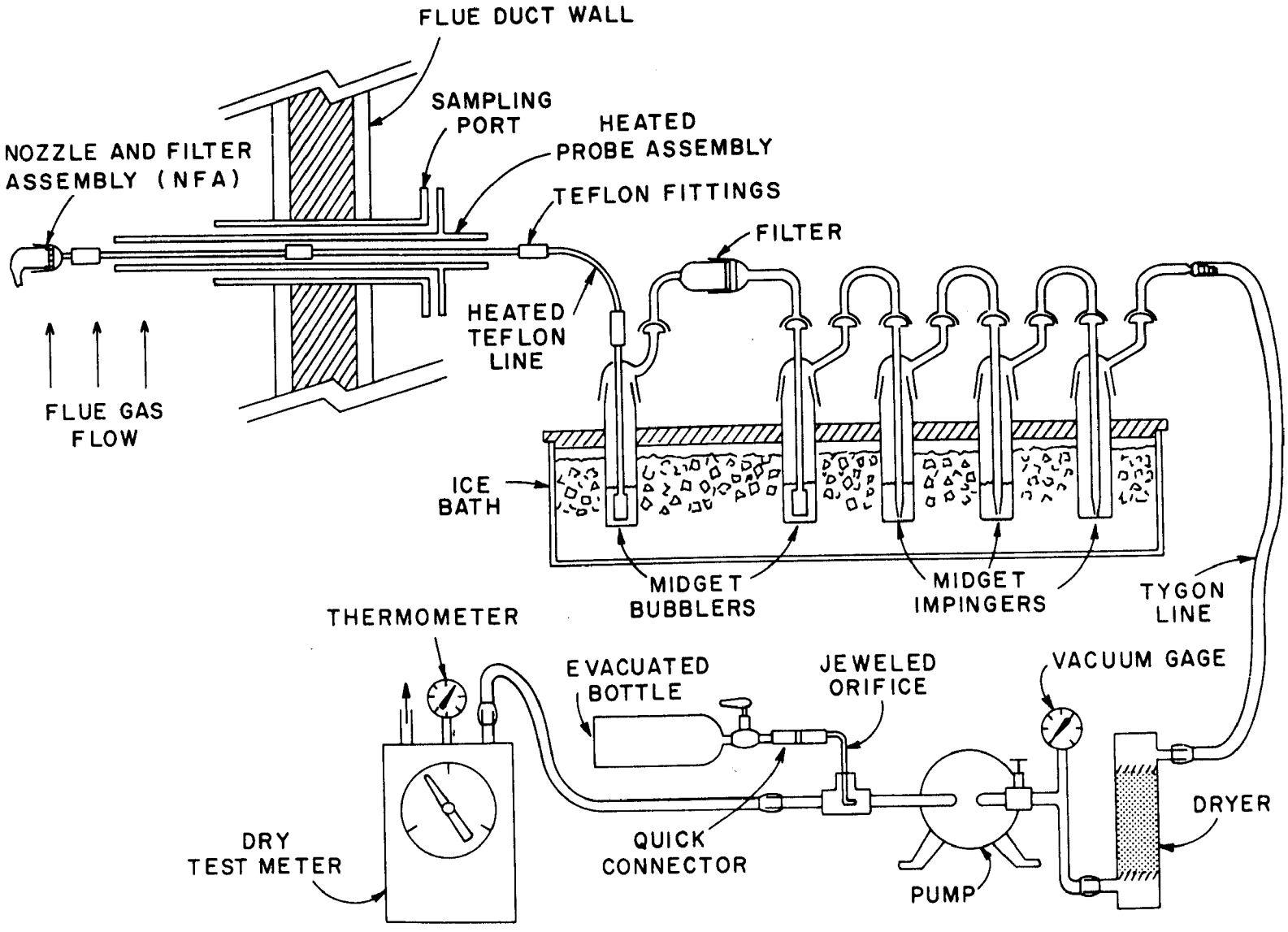

Figure 2. Schematic diagram of Brookhaven Method 6 apparatus.

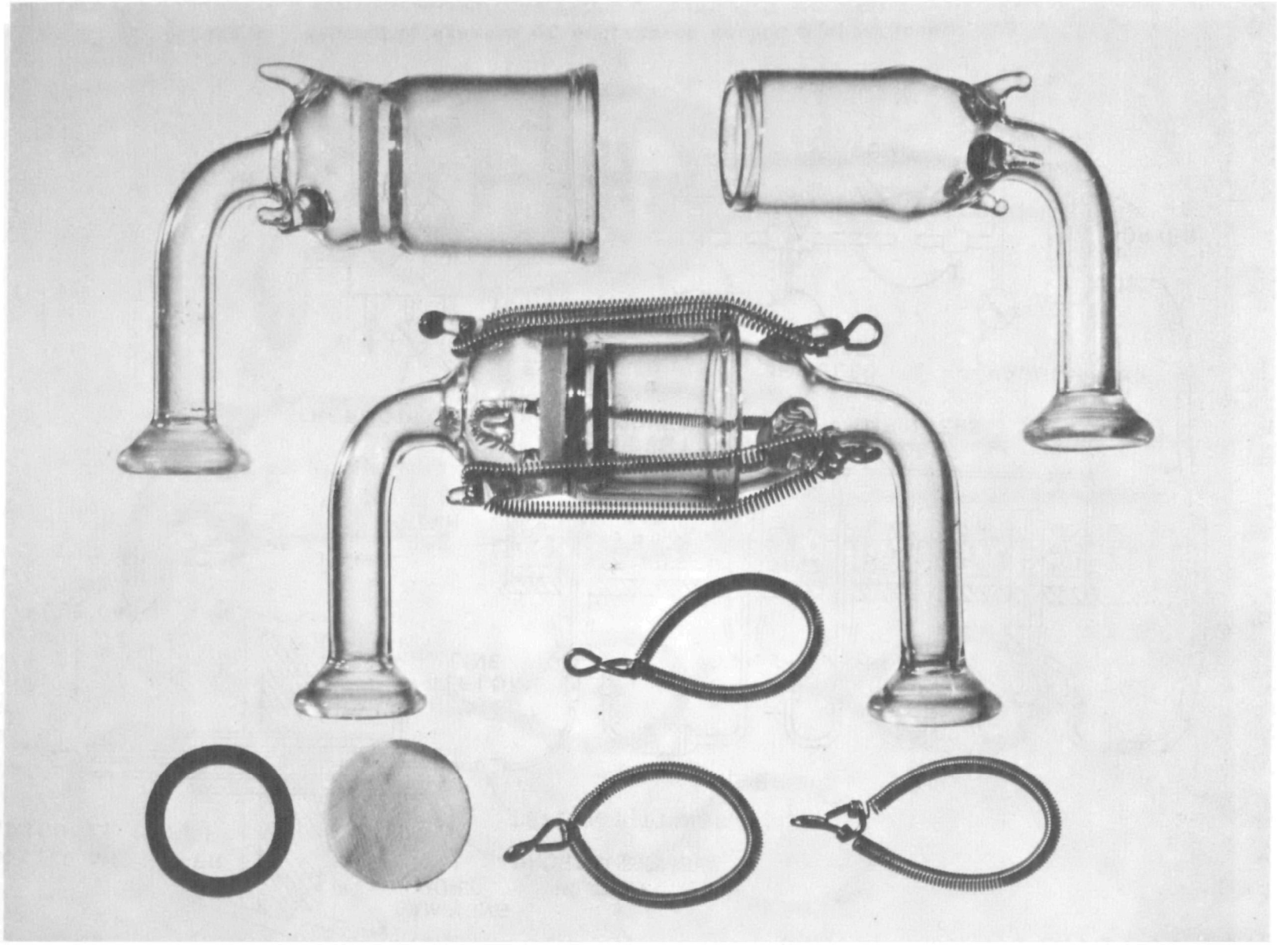

Figure 3. Midget bubbler filter assembly.

the five midget contactors is shown in Figure 4. The inlet to the first bubbler (on the left) is connected to the probe via a heated Teflon line and a Teflon fitting (Beckman union shown). Oxygen and carbon monoxide content of the flue gas was determined chromatographically from the contents of the gas bottle sampler (6).

LABORATORY EXPERIMENTS

Determination and Treatment of IPA Oxidant

Earlier tests at Brookhaven (3) and elsewhere (4) indicated that an oxidant, in varying amounts depending on the batch, was present in the IPA, as received. Spot tests with 2% KI solution, which released the yellow color of I_2 in the presence of a strong oxidant, confirmed these observations. A treatment procedure involving copper powder or wire was found to completely reduce the oxidant. By acidifying a batch of IPA with HCl to a pH of 4.0 to 4.5 (the treatment time at a pH of 5.8 was more than 20 hours) and exposing the solution to pre-cleaned copper powder or copper wire (cleaned in concentrated HCl and rinsed in IPA) with gentle stirring for about 16 hours, no residual oxidant could be detected as shown by the tests in Table 1.

Table 1. IPA Oxidant Tests

Test	IPA Solution	Flush Time, Min.	Flush Vol., ℓ	Total Dissolved SO_2, meq. Bubbler 1 Direct	Bubbler 1 Evap.	Bubbler 2 Direct	Bubbler 2 Evap.
1	U1	16	8.7	0.0124	0.0080	0.0204	0.0116
2	Cu P1	16	9.2	0.0064	0.0000	0.0116	0.0000
3	Cu W1	16	11.9	0.0072	0.0000	0.0100	0.0000
4	U2	16	11.9	0.0072	0.0022	0.0076	0.0028
5	U3	16	12.1	0.0048	0.0000	0.0032	0.0000
6	Cu W1	8	6.3	--	0.0000	--	0.0000
		(24 days later)			<0.0002		<0.0002

That series of tests was performed with 15 mℓ of 80% IPA solution in each bubbler sparged with 1400 ppm of SO_2 in simulated

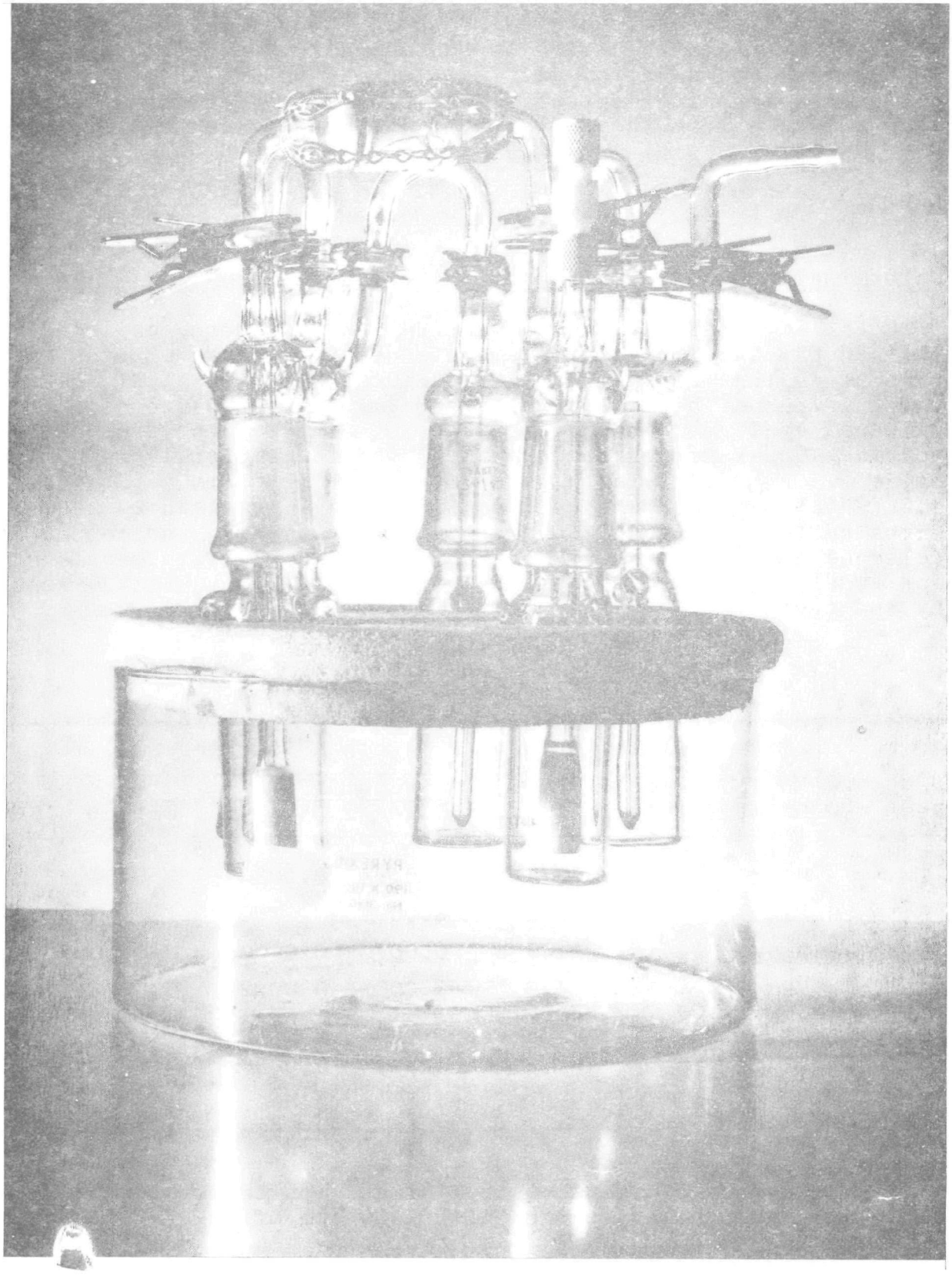

Figure 4. Midget contactors in portable ice bath.

flue gas for 20 to 30 minutes using the BM6 apparatus followed by a flushing period for the times and volumes indicated using SO_2-free air. Half the diluted solutions from each bubbler were titrated directly with 0.02 N NaOH and the other half after evaporation to "dryness" to expel the last traces of dissolved SO_2 ("dryness" in the presence of saturated $CaCl_2$ solution in a vacuum oven). It was apparent in every test that evaporation markedly reduced the level of detected SO_2, indicating that 9 ℓ to 12 ℓ of flushing air was not sufficient to expel all dissolved SO_2. In Test 1, the SO_2 remaining after evaporation can be attributed to that which was oxidized by the oxidant to H_2SO_4. SO_2 was always higher in the second bubbler compared to the first in the direct titration because the second bubbler was flushed with air containing some SO_2 that was stripped from the first. However, if a fixed amount of oxidant (e.g., H_2O_2) were present in the IPA, the expected residual SO_2 (i.e., H_2SO_4) in each bubbler after evaporation should have been identical. That it was not in Test 1 indicated that the oxidation must have continued to some degree during the evaporation when more SO_2 was present in the second bubbler. Thus the oxidant was at least not entirely attributable to H_2O_2.

Tests 2 and 3 showed that the copper treatment was successful in removing the last traces of oxidant, as evidenced by the lack of any acid in the evaporated samples. Tests 4 and 5 with two different batches of untreated IPA showed the variability of the oxidant level; for U3 the oxidant was apparently not present. The final test with copper wire treated IPA (preferred over the copper powder) included an evaluation of 24 days exposure time of the SO_2-containing solution prior to evaporation. There was essentially no H_2SO_4 found and hence no artifact formation from possible trace amounts of Cu ions. Several of the evaporated solutions which showed no trace of acid were re-analyzed by ion chromatography yielding negligible (<0.0006 meq) sulfate.

To determine if H_2SO_4 could be recovered equally well from treated as from untreated IPA solution, several tests were performed in which 0.0394 meq of H_2SO_4 were added to both versions of solution. The recovery of H_2SO_4 as acid was identical in both treated and untreated IPA, averaging 97 $\pm$ 1% from evaporated solutions. For several 0.01 meq H_2SO_4 aliquots, recovery from evaporated solutions ranged typically from 80% to 90%.

Although we have demonstrated a successful method for treating IPA to remove unwanted oxidants, it is preferable to use IPA that is initially free of oxidant. A procedure of testing for oxidant by using the 1400 ppm SO_2 simulated flue gas standard and checking for residual acid after evaporation was adopted as standard practice prior to and after field utilization of the BM6.

SO_2 Stripping Tests of IPA

The field procedure for sampling the flue gas consisted of collecting a sample for ~40 minutes at about 0.75 ℓ/min, followed by an ambient air purge for about 15 to 20 minutes in order to strip away any dissolved SO_2 prior to acid determination in the midget bubblers. If any dissolved SO_2 remained in the solution, a positive error in the acid determination could result.

Utilizing the BM6 apparatus, copper wire treated IPA (15 mℓ of 80% solution) was used in two bubblers which were sparged with 15 ℓ of 1400 ppm SO_2 (equivalent to 1.71 meq of SO_2) to fully saturate the solutions. In one series of experiments, the solutions in the bubbler were flushed with air at 0.78 ℓ/min for periods of from 2 to 32 minutes (1.5 to 25 ℓ). Half of each solution was immediately analyzed for residual SO_2. The balance, when brought to "dryness," showed no presence of acid, indicating that only dissolved SO_2 had been measured in the non-evaporated solutions. Assuming that 30 liters of flue gas would normally be sampled during field utilization of the method, the residual dissolved SO_2 was converted to an apparent H_2SO_4 concentration in the flue gas as shown in Figure 5. With a midget bubbler, even after stripping with 12 ℓ to 25 ℓ of air, residual dissolved SO_2 could cause errors from 1 ppm to 3 ppm equivalent sulfuric acid.

Saturated solutions of 80% IPA at 0°C in contact with 1400 ppm SO_2 flue gas were found to contain 0.103 meq of SO_2 per 15 mℓ of solution (equivalent to 40 ppm H_2SO_4 in 30 ℓ of flue gas). That was approximately two-thirds the reported solubility in water (Chemistry and Physics Handbook). Considering the bubbler to be a well-stirred vessel with the purge air containing SO_2 in equilibrium with the remaining dissolved SO_2 and that Henry's Law prevailed, the apparent H_2SO_4 concentration in the flue gas as a function of time was derived to be

$$[H_2SO_4] = 40\, e^{-\frac{FH}{24.5v}\, t} \qquad [1]$$

where $[H_2SO_4]$ = flue gas H_2SO_4 concentration, vol. ppm

F = flow of purge air, ℓ/min

H = Henry's Law constant, 0.41 atm ℓ/mole at 0°C

t = purging time, min

v = volume of IPA solution, liters

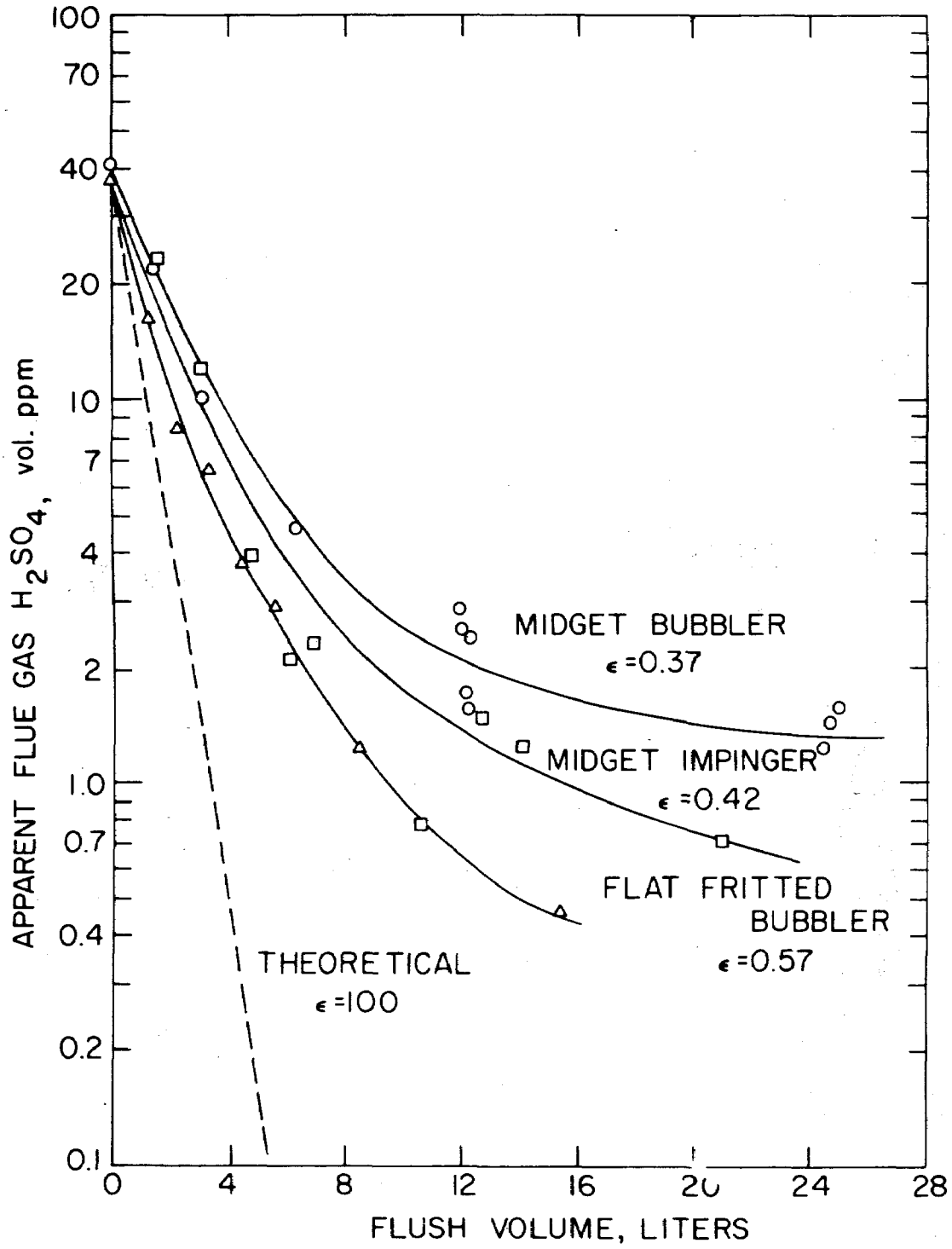

Figure 5. Residual dissolved SO_2 as apparent flue gas H_2SO_4 versus the volume of flushing air used.

For the conditions used in these tests, the theoretical residual SO_2 as H_2SO_4 was given by

$$[H_2SO_4] = 40\ e^{-1.12\ V} \qquad [2]$$

where V = volume of purge air, liters

which is plotted in Figure 5 as the dashed line.

Since the measured values for the midget bubbler curve deviated immediately and quite significantly from the theoretical dilution line, it was concluded that the midget bubbler was not an ideal well-stirred vessel. Inspection of the bubbler in action supported that conclusion. From a series of stripping tests using a midget impinger and then a flat-fritted bubbler, a different curve was generated for each device as shown in the plot. Using mathematically derived slopes from least mean square empirical correlations of the data, it was determined that the midget bubbler gave the poorest approach (ϵ = 0.37) to a well-stirred vessel (ϵ = 1.00) with the flat-fritted bubbler performing the best of the three (ϵ = 0.57). Statistically there was no difference in the residual dissolved SO_2 in the presence of added acid (0.01 meq)--i.e., equivalent to 4 ppm H_2SO_4 in 30 ℓ of flue gas.

FLUE GAS SAMPLING RESULTS

From July 1977 to March 1978, a number of flue gas sampling measurements using the Brookhaven Method 6 and the Brookhaven controlled condensation system (CCS) were performed at the Long Island Lighting Company (LILCO) power stations at Northport (Units 2 and 3) and Island Park, New York (Barrett Unit 1). The Northport units generally used No. 6 oil containing 2.4% S with significant amounts of vanadium (300 ppm to 400 ppm V). Barrett Unit 1 was a low sulfur oil-fired boiler (0.3% S) having much less vanadium (5 ppm to 30 ppm V).

Details of the results of sampling at these units have been reported elsewhere (7)(9). In this section, the measurement of particulate metal sulfates at isokinetic and non-isokinetic sampling velocities, as well as the determination of H_2SO_4 at high (>10 ppm) and low (<1 ppm) levels with the IPA approach compared with the more reliable CCS, will be presented.

BM6 Field Utilization--Particulate Metal Sulfates

When sampling into the direction of flue gas flow, sub-isokinetic runs at Barrett Unit 1 gave particulate metal sulfates 1.32 ± 0.08 times the isokinetic value when sampling at about 10% of isokinetic velocity. At Northport Unit 3 at the electrostatic precipitator (ESP) outlet, for the same approximate 10% of isokinetic velocity, the particulate metal sulfates were 4.4 ± 1.1 times the isokinetic value. The ratio of measured to isokinetic metal sulfates was plotted versus the ratio of nozzle velocity to flue gas velocity in Figure 6. Since sub-isokinetic sampling tends to bias the particulate collected with an excess of large particulate, it is apparent that most of the sulfate-bearing particulates at Barrett were quite small even though the unit had no particulate controls. Surprisingly, the substantial increase in sulfate with sub-isokinetic sampling at the ESP outlet of Northport Unit 3 indicated that a major fraction of the sulfate particles were larger in size (probably greater than 1 μm to 3 μm), even though at the ESP outlet.

Northport Unit 2, essentially the same as Unit 3 except that Unit 2 had no ESP, gave results not significantly different from those obtained at Barrett. The presence of a significant portion of larger particulates at Northport Unit 3 may have been due to the low furnace oxygen levels (0.0% to 0.2%) normally used at that unit compared to the others (typically 1.0% to 1.5% O_2).

The recommended Modified EPA Method 6 probe tip consisted of an 11 mm inside diameter glass probe end, with sampling occurring normal to the direction of flue gas flow (1). The straight nozzle and filter assembly devised at Brookhaven to duplicate the extremely low sub-isokinetic conditions gave the results shown at the left in Figure 6. Two of the runs gave particulate metal sulfate measurements approximately 50% greater than the isokinetic value when utilized at Northport Unit 2.

When sampling nearly isokinetically (within ± 20%) by either BM6 or CCS, into the direction of flue gas flow, the measured particulate metal sulfates were within about ± 20% of the isokinetic value. The EPA straight probe method on the average gave higher (about 30%) results than the isokinetic value, but a statistically significant number of runs was not made. Comparative measurements between the straight nozzle and the isokinetic approach at Northport Unit 3, because of the significant velocity dependence at that unit, would be of interest.

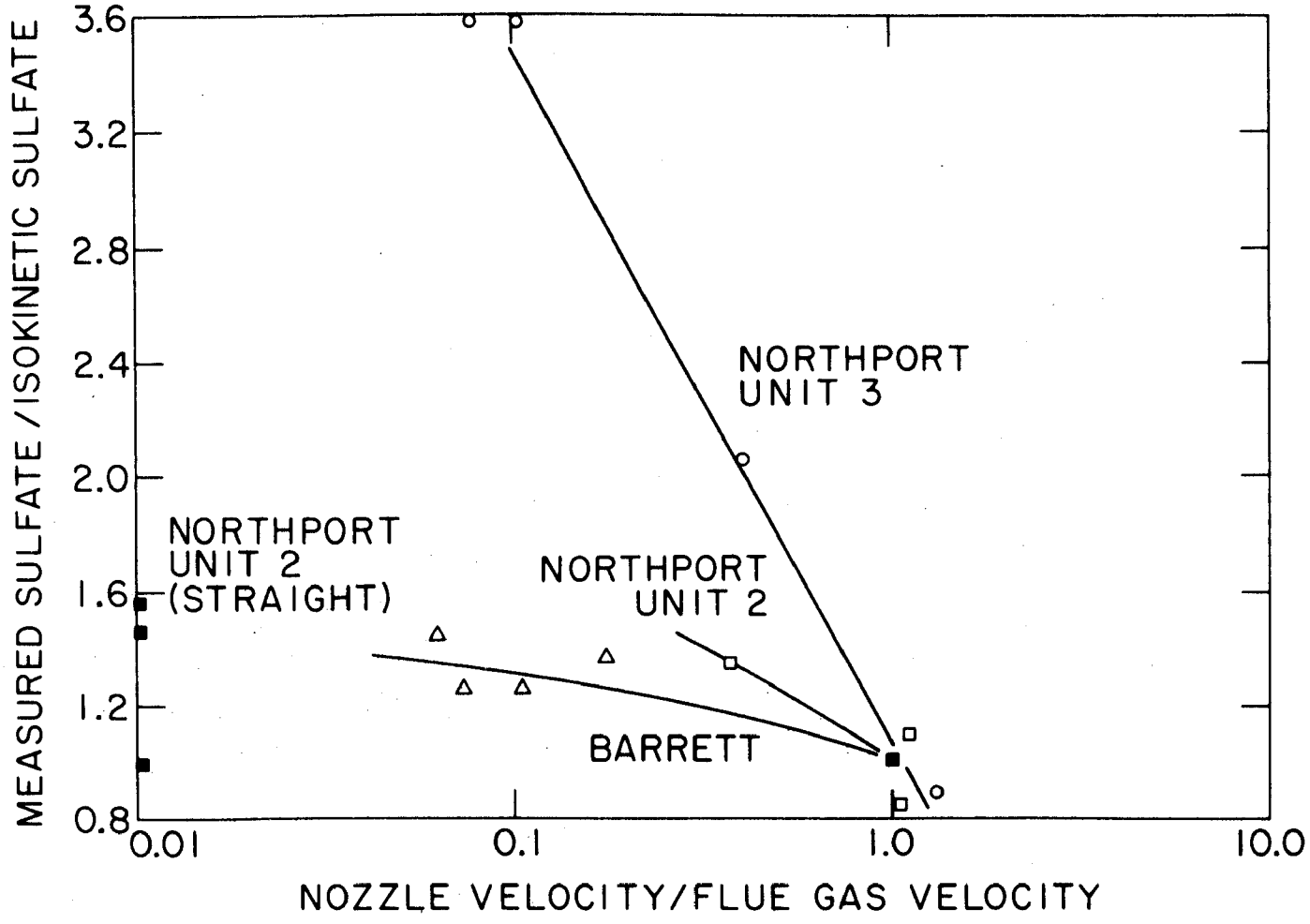

Figure 6. Effect of sub-isokinetic flue gas sampling on measured particulate metal sulfates.

BM6 Field Utilization--Sulfuric Acid (High Emissions)

As discussed earlier, the sulfuric acid from the sampled flue gas was expected to be recovered from the various sections of the Brookhaven Method 6 apparatus including the nozzle filter, the probe, the first midget bubbler, and the bubbler filter; the second midget bubbler was not expected to have measurable amounts of H_2SO_4 because of the absolute filtering capabilities of the bubbler filter.

The results of seven sampling runs at Northport Unit 2, at high H_2SO_4 emissions conditions because of high furnace oxygen levels (1.2% to 2.7% O_2), are shown in Table 2. The H_2SO_4 collected in the different portions of the sampling apparatus was determined primarily by titration with 0.02 N NaOH with a few comparisons by ion chromatography sulfate determination (the values in parentheses).

Neglecting the previously established problems of residual dissolved SO_2 and oxidant in the IPA (the IPA used in these measurements was shown to be oxidant-free both before and after the field experiments), the flue gas H_2SO_4 was determined from the sum of the milliequivalents found in the nozzle filter, the probe, the direct (nonevaporated) solution of midget bubbler 1, and the bubbler filter. For example, for run 76, a flue gas H_2SO_4 direct value of 31.1 ppm (26.5 ppm by ion chromatography) was determined. However, it was apparent that the significant difference between the direct determination of midget bubbler 1 by titration versus that by ion chromatography was indicative of a significant amount of a volatile acid in addition to H_2SO_4. Indeed, after evaporation of midget bubbler 1, the H_2SO_4 determined by both methods was nearly identical (the samples of each bubbler were always split equally so that half could be measured directly and half after evaporation)--indicating that the dissolved SO_2 and any other volatile acid were removed by the evaporation.

That there were substantial amounts of residual dissolved SO_2, even after the recommended stripping volume of 15 ℓ of air, was evident from the significant amounts of SO_2 milliequivalents found in the directly measured midget bubbler 2. Even after evaporating midget bubbler 2, a not-insignificant amount of acid (sulfate) still remained. Since it was shown conclusively that the IPA prior to use contained no oxidant, that the bubbler filter would allow no H_2SO_4 aerosol to penetrate to the second bubbler, and that evaporation was a quantitative method for removing all dissolved SO_2, it was also concluded that the

Table 2. Brookhaven Method 6 Field Results
(Northport Unit 2 - High H_2SO_4)

Run No.	Acid Concentration, milliequivalents[a]							Flue Gas H_2SO_4, Vol. ppm		
	Nozzle Filter	Probe	Midget Bubbler 1		Bubbler Filter	Midget Bubbler 2		BM6		CCS[d]
			Direct	Evap.		Direct	Evap.	Direct[b]	Corr.[c]	
PR-75	0.0032	0.0186	0.0344	0.0132	0.0124	0.0228	0.0008	29.7	20.2	--
76	0.0008	0.0404	0.0364 (0.0224)	0.0192 (0.0205)	0.0088 (0.0099)	0.0220 (0.0211)	0.0028 (0.0055)	31.1 (26.5)	23.9 (23.8)	26.6
77	0.0016	0.0588	0.0400 (0.0283)	0.0200 (0.0235)	0.0074 (0.0080)	0.0240 (0.0163)	0.0040 (0.0069)	40.3 (36.2)	31.4 (31.8)	--
78	0.0032	0.0526	0.0584	0.0184	0.0098	0.0268	0.0036	53.3	34.5	--
79	0.0036	0.0714	0.0328	0.0160	0.0090	0.0204	0.0040	48.0	39.5	--
80	0.0028	0.0702	0.0372	0.0060	0.0036	0.0288	0.0012	52.8	37.8	--
81	0.0048	0.0768	0.0300 (0.0169)	0.0092 (0.0146)	0.0044 (0.0064)	0.0240 (0.0157)	0.0024 (0.0061)	49.2 (44.4)	39.3 (40.9)	--

[a]Milliequivalents determined by titration with 0.02 N NaOH or by ion chromatography (in parentheses).

[b]Direct BM6 results are based on the nozzle, probe, direct midget bubbler 1, and bubbler filter acid (sulfate).

[c]Corrected BM6 results are based on the nozzle, probe, difference of Evap. 1 minus Evap. 2, and the bubbler filter acid (sulfate).

[d]CCS are the controlled condensation system results.

flue gas contained a volatile constituent which dissolved in the IPA solution and which caused the oxidation of dissolved SO_2 either during the sampling or, more likely, during the evaporation step. Thus, these flue gas sampling results using the Brookhaven procedure and apparatus have uncovered another problem associated with the utilization of IPA solution in the presence of flue gas.

Assuming that the oxidized SO_2 after evaporation of the residual dissolved SO_2 was the same in both bubblers, the amount of H_2SO_4 that truly originated in the flue gas could be estimated by subtracting the contents of evaporated bubbler 2 from evaporated bubbler 1. The results, when added to the acid from the nozzle filter, probe, and bubbler filter, were reported as corrected flue gas H_2SO_4. For run 76, the corrected H_2SO_4 determination was 23.9 ppm, in close agreement with the CCS value sampled about two hours earlier. (Unfortunately, only one port was available for sampling at this temporary ducting location.)

On the average, the directly determined H_2SO_4 flue gas concentrations were either about 35% or 11% higher than the corrected levels depending on the method of determination. One could conclude that either with or without the correction, this version of the IPA procedure gave results comparable with the CCS at these high acid levels.

BM6 Field Utilization--Sulfuric Acid (Low Emissions)

When the BM6 approach was used at two low acid emission sources--Northport Unit 3 and Barrett Unit 1--the latter of which had H_2SO_4 levels less than 0.2 ppm, the direct determination of H_2SO_4 was obviously erroneous as shown in Table 3.

In these runs, multiple ports were available enabling the controlled condensation system to be used side by side with the BM6. The IPA used in all these runs with the exception of run 71 was shown to contain oxidant comparable to the amounts found in U1 and U2 of Table 1; that for run 71 was oxidant free.

Before considering the results obtained from the bubblers, a case can be made for the efficacy of the controlled condensation approach for reliably sampling H_2SO_4 at very low levels (less than 0.2 ppm). There was no trace of acid on the bubbler filters, indicating that the H_2SO_4 was in all cases removed prior to reaching the filter. Since the average on the bubbler filters in Table 2 was 0.0080 meq, it would intuitively be expected that the H_2SO_4 in the flue gas was on the order of about 50-fold less--i.e., less than 1 ppm. That, of course, was shown to be

Table 3. Brookhaven Method 6 Field Results
(Northport Unit 3 and Barrett Unit 1 - Low H_2SO_4)

Run[b] No.	Acid Concentration, milliequivalents[a]							Flue Gas H_2SO_4, Vol. ppm		
	Nozzle Filter	Probe[c]	Midget Bubbler 1 Direct	Midget Bubbler 1 Evap.	Bubbler Filter	Midget Bubbler 2 Direct	Midget Bubbler 2 Evap.	BM6 Direct[d]	BM6 Corr.[e]	CCS[f]
PR-44-B	0.0002	0.0000 (390°F)	0.0150	0.0050	0.0000	0.0240 (0.0373)	0.0133	2.41	0.03	0.03
46-B	0.0004	0.0000 (475°F)	0.0160	0.0080 (0.0124)	0.0000	0.0280	0.0180 (0.0267)	2.79	0.07	0.15
48-B	0.0004	0.0004 (365°F)	0.0170	0.0080 (0.0121)	0.0000	0.0310	0.0200 (0.0279)	3.19	0.15	0.12
51-B	0.0002	0.0000 (350°F)	0.0190 (0.0175)	0.0076 (0.0132)	0.0000	0.0260 (0.0259)	0.0166 (0.0243)	3.79	0.04	0.05
55-O	0.0010	0.0060 (480°F)	0.0364	0.0156	0.0000	0.0172	0.0156	10.0	1.6	4.8
57-O	0.0006	0.0000 (430°F)	0.0744	0.0620	0.0000	0.0784	0.0780	12.5	0.10	1.30
59-O	0.0006	0.0000 (405°F)	0.0320	0.0172	0.0000	0.0208	0.0188	6.9	0.13	1.41
63-I	0.0006	0.0000 (370°F)	0.0340	0.0200	0.0000	0.0240	0.0180	5.8	0.10	0.08
71-I	0.0003	0.0022 (300°F)	0.0156	0.0064	0.0000	0.0124	0.0060	6.0	0.82	0.29

[a] Milliequivalents determined by titration with 0.02 N NaOH or by ion chromatography (in parentheses).

[b] B after the run number represents sampling performed at Barrett; O, the electrostatic precipitator (ESP) outlet at Northport; I, the ESP inlet at Northport.

[c] Probe temperature in parentheses.

[d] Direct BM6 results are based on the nozzle, probe, direct midget bubbler 1, and bubbler filter acid (sulfate).

[e] Corrected BM6 results are based on the nozzle and probe acid content only; midget bubbler contents were not used.

[f] CCS are the controlled condensation system results.

the case as confirmed by the CCS values, which, at Barrett (runs with B), varied from 0.03 ppm to 0.15 ppm H_2SO_4. Taking just the acid recovered in the nozzle filter and the probe, the corrected H_2SO_4 levels were computed as shown in Table 2 under the BM6 heading labeled corrected--i.e., the bubbler contents were disregarded. The agreement with the CCS values was remarkably good, indicating that at very low acid levels, the controlled condensation approach was quantitatively reliable.

Run 44 had just a slight amount of acid on the nozzle filter (0.0002 meq) and none in the probe (probe temperature was 390°F); yet that amount of acid was precisely the total amount in the sampled flue gas, as indicated by the comparison between the corrected BM6 level and that from the CCS. For run 46, the probe temperature was much hotter (475°F), and no H_2SO_4 was retained in the probe. The corrected BM6 value of 0.07 ppm was less than that by the CCS (0.15 ppm), indicating that some H_2SO_4 did pass through the probe into the bubbler system. That this was the case was substantiated by run 48 in which the probe temperature was lower (365°F). In that case an equivalent amount of acid was found in the probe and the nozzle filter, giving a corrected BM6 H_2SO_4 value of 0.15 ppm in good agreement with the CCS value (0.12 ppm).

At the Northport Unit 3 ESP inlet (runs 63-I and 71-I), the H_2SO_4 was also quite low. For run 63, just the acid found on the nozzle filter (none in the probe) accounted for the total flue gas H_2SO_4. Significant acid was found in the probe of run 71 which, when combined with the nozzle filter, gave a corrected BM6 H_2SO_4 of 0.82 ppm--significantly higher than the CCS H_2SO_4 of 0.29 ppm. The exact reason for the discrepancy was not evident.

The remaining runs performed at the ESP outlet of Unit 3 (Northport) occurred during somewhat higher acid emissions (1 ppm to 5 ppm). Because of the high probe temperature for those three runs (55, 57, and 59), a major portion of the flue gas acid passed through the probe into the bubbler system, as evidenced by the low values for the corrected BM6 H_2SO_4 compared to the CCS acid. Unfortunately, the problems previously described concomitant with the utilization of IPA bubblers were significant enough to preclude the corrective procedure of the subtractive technique that was used in the high acid cases. Thus, there was no way to adequately determine that portion of the acid in those three runs that entered the midget bubblers.

Run 71 represents the best attempt to utilize correctly the subtractive procedure. First, it should be indicated that the CCS gave an H_2SO_4 concentration of 0.34 ppm at noon and then 0.29 ppm at 1430--the same time the BM6 run 71 was performed. Since all of the acid in the flue gas was removed by the nozzle filter and probe, the difference between evaporated bubbler 1 and evaporated bubbler 2 should have been near zero. That this was the case confirms the philosophy of the approach. The amount of acid found in each evaporated solution of run 71 could only have been formed from the oxidation of SO_2 by an unknown volatile flue gas oxidant simultaneously collected by the IPA. Thus, even if the subtractive procedure did work, the error associated with the small difference between two large numbers could be appreciable. Using the total amount of acid found in midget bubbler 1, which for run 71 could only be comprised of dissolved SO_2 and flue gas oxidized SO_2, an acid level of 6.0 ppm H_2SO_4 would have been recorded--a substantial error.

For almost all of the runs in Table 3, the H_2SO_4 values, determined by including the directly measured acid in midget bubbler 1 with the probe and nozzle filter washings, were from one to two orders of magnitude higher than the correct values. Thus, the utilization of an IPA midget bubbler approach without any regard for residual dissolved SO_2, oxidant in the IPA, or oxidant in the flue gas, can lead to gross positive errors in H_2SO_4 determination.

CONCLUSIONS

Laboratory and field experiments conclusively showed that several problems involving the utilization of the IPA methodology for the collection of flue gas sulfuric acid could be minimized when proper precautions were taken during field sampling at high acid emission sources (>10 ppm H_2SO_4). Under those conditions, the effects of residual dissolved SO_2, oxidant in the IPA reagent (a successful method for neutralizing that oxidant was devised), and a volatile oxidant in the flue gas could be reduced to probably less than 10% positive errors by using the Brookhaven Method 6 (BM6) with the two midget bubbler evaporative subtractive correction. Using the presently recommended Modified EPA Method 6 (1), with a single midget bubbler, positive errors at high acid sources of as much as 10% to 30% were demonstrated.

At low acid sources (H_2SO_4 <1 ppm), the direct Modified EPA Method 6 could result in demonstrated 10- to 100-fold positive biased errors for sulfuric acid. Even the subtractive approach was not reliable because of the need to determine a

small difference between two significantly larger numbers and because the exact amount of residual dissolved SO_2 was variable and generally larger in the second midget bubbler.

If only limited qualitative measurements of the H_2SO_4 emissions at fossil-fueled combustion sources were desired, the IPA methodology might be adequate. For example, if the actual H_2SO_4 level was 20 ppm, measured values of 22 ppm to 24 ppm might be expected by the IPA methodology. At 1 ppm H_2SO_4, actual measurements might give values of 2 ppm to 4 ppm H_2SO_4. And at 0.1 ppm H_2SO_4 levels, measurements with the IPA methodology would still give H_2SO_4 values of 2 ppm to 4 ppm.

Normally, that performance might be adequate from an emissions inventory standpoint, since only the largest sources would be the most significant. However, from a controls standpoint, the actual behavior of sources even at low H_2SO_4 concentration might be very important. If the absolute emission of sulfuric acid were directly dependent on: (1) the sulfur content of the fuel, (2) the vanadium content of the fuel, and (3) the furnace oxygen level, significant reductions in each of those three variables could result in a magnitude of H_2SO_4 reduction not measurable by the IPA methodology. For example (9), at Northport Unit 2 during one set of measurements, the fuel S content was 2.1%, the vanadium was 390 ppm, and the average furnace O_2 was 2.0%; the corresponding average H_2SO_4 was 32 ppm. At Barrett Unit 1, the fuel S content was 0.3% (7-fold reduction), the vanadium averaged about 15 ppm (26-fold reduction), and the furnace oxygen about 1% (2-fold reduction). The total reduction in H_2SO_4 might be expected to be 7 x 26 x 2 or about 360-fold, corresponding to an expected H_2SO_4 level of 32/360 or 0.09 ppm. The actual average acid emissions at Barrett were 0.10 $\pm$ 0.07 ppm, in excellent agreement (9). These low levels could only have been measured by the controlled condensation system. And yet, from the viewpoint of understanding the factors affecting those emissions, the results were very meaningful.

Since there is a better alternative to the IPA methodology, the recommendation is made here that the reference method for H_2SO_4 determination be replaced by a miniaturized version of the Brookhaven CCS (3). Conceptually, the same miniature nozzle and filter assembly designed for the BM6 would be used. But the flue gas, on leaving the probe (maintained electrically at about 350°F), and heated Teflon line (maintained electrically at 140°F), would pass directly into a version of the midget bubbler filter (also maintained electrically at 140°F) for removal of the last traces of H_2SO_4 aerosol. A research study aimed at designing

and validating the midget controlled condensation system should be implemented.

Errors associated with the sub-isokinetic sampling of particulate metal sulfates while sampling normal to the direction of flue gas flow should be quantified at several other combustion sources. Tentatively, the right angle approach appears to produce positive biased errors of about 30%.

ACKNOWLEDGMENTS

We would like to thank Bob Gergley and Bob Wilson for their help in performing the field experiments, as well as Lance Warren and Fred Glaser at Northport and Ted Kempf and Ken Abrams at Barrett for helping with arrangements and supplying field data, Harold Cowherd and Fred Lipfert of LILCO for special arrangements and B. T. Hagewood of LILCO for fuel analyses. A special appreciation goes to the BNL Analytical Group for the sulfate, carbon, and elemental analyses and to Irv Meyer of the BNL glass shop for fabrication of components. Several discussions with Jim Homolya and John Nader of EPA were very helpful.

REFERENCES

1. Cheney, J. L., W. T. Winberry, and J. B. Homolya. Evaluation of a Method for Primary Sulfate Emissions from Combustion Sources. J. Environ. Sci. Health, A12 (10): 549-566, 1977.

2. U.S. Environmental Protection Agency. Standards of Performance for Stationary Sources. Federal Register 41(111), June 1976. 23083-5.

3. Dietz, R. N., and R. F. Wieser. Sulfate Emissions from Fossil Fueled Combustion Sources. Brookhaven National Laboratory, Progress Report No. 5, September 1977.

4. Maddalone, R. F., S. F. Newton, R. G. Rhudy, and R. M. Statnick. Laboratory and Field Evaluation of the Controlled Condensation System (Goksoyr/Ross) for SO_3 Measurements in Flue Gas Streams. 70th Annual Meeting of the Air Pollution Control Assoc., Toronto, June 1977.

5. Homolya, J. U.S. Environmental Protection Agency. Personnel Communication, August 1977.

6. Dietz, R. N. Gas Chromatographic Determination of Nitric Oxide on Treated Molecular Sieve. Anal. Chem., 40:1576-8, 1968.

7. Dietz, R. N., and R. W. Garber. Power Plant Flue Gas and Plume Sampling Studies. Brookhaven National Laboratory, Progress Report No. 1, November 1977.

8. Dietz, R. N., and R. F. Wieser. Sulfate Emissions from Fossil Fueled Combustion Sources. Brookhaven National Laboratory, Progress Report No. 6, March 1978.

9. Dietz, R. N., R. F. Wieser, and L. Newman. Operating Parameters Affecting Sulfate Emissions from an Oil-Fired Power Unit. Proceedings of Workshop on Measurement Technology and Characterization of Primary Sulfur Oxides Emission from Combustion Sources, Southern Pines, North Carolina, April 1978.

Measurements of Sulfur Trioxide at Tennessee Valley Authority Coal-Fired Power Plants Using the Condenser Method

Elizabeth M. Bailey
H. A. Ruddock
Tennessee Valley Authority

ABSTRACT

Previous and recent measurements of sulfur trioxide (SO_3) in the flue gas at several coal-fired generating plants in the TVA system will be presented. Collection of sulfur trioxide was conducted using the condenser method of Lisle and Sensenbaugh. Investigations were conducted on the effects of various plant operating parameters on the SO_3 content of the flue gas. The SO_3 content measured varied from approximately 1 ppm to over 30 ppm depending on plant operating parameters. Some of the sulfur dioxide measurements were determined at one plant using impingers containing dilute solutions of H_2O_2.

Tests were conducted to determine the efficiency of SO_3 collection using the condenser method. The optimum operating parameters that should be used in sample collection were also investigated, and study results will be presented.

INTRODUCTION

The sulfur trioxide (SO_3) content of power plant flue gas is of interest for both operational and environmental reasons. Sulfur trioxide combines with water to form sulfuric acid (H_2SO_4), which causes problems in coal-fired power plant operation due to its corrosive nature. Sulfuric acid is believed to affect human health adversely (1)(2) and to damage both forest and lake ecosystems (3)(4). Most sulfuric acid aerosol in ambient air is formed by oxidation of sulfur dioxide (SO_2) emitted from stationary sources. However, flue gas from coal-fired power plants contains some pri-

mary sulfuric acid aerosol, which is emitted directly from the power plants into the atmosphere.

The Tennessee Valley Authority (TVA) conducted three studies to characterize the SO_3/H_2SO_4 in flue gases. The first study was designed to examine the effects of furnace type and two plant operation conditions, excess oxygen content and temperature of the flue gas, on the SO_3/H_2SO_4 content of flue gas. Measurements were taken at four power plant units of different furnace types over ranges of excess oxygen content and at one plant over a range of flue gas temperature during this study. In the second study, the emission levels of SO_3/H_2SO_4 and SO_2 were characterized at one power plant by sampling flue gas at the base of the stack, and in the third study, the efficiency of the SO_3/H_2SO_4 collection system was evaluated.

EFFECT OF FURNACE TYPE AND PLANT OPERATING CONDITIONS ON THE SULFUR TRIOXIDE CONTENT OF FLUE GAS

The TVA Division of Power Production conducted measurements at four coal-fired power plant units to determine the effect of excess oxygen content, furnace type, and temperature on the SO_3/H_2SO_4 content of flue gas.

Methodology

The condenser method, in which the gas is cooled to a temperature between the acid dewpoint and the water dewpoint to allow collection of the SO_3/H_2SO_4 in a condenser, was used to obtain samples The sampling apparatus, identical to that of Lisle and Sensenbaugh (5), is shown in Figure 1. A glass-lined probe, containing a glass wool plug for removing particulate matter, was used to draw flue gas from the ducts. The temperature of the probe was held at 290°C, and the temperature of the condenser was held between 60°C and 90°C. Sulfur dioxide was collected in two gas-washing bottles, each containing a solution of 1.5% hydrogen peroxide (H_2O_2). The gas sample was then passed through a drying tower containing silica gel, and volume was measured with a wet test meter.

Samples for studying the effects of excess oxygen were collected at the air preheater inlet, whereas those for studying the effects of temperature were collected at the air preheater outlet. Temperature of flue gas at the air preheater inlets was typically 315°C to 370°C, except at Allen 1 where it was 400°C. Because of this high temperature, slow flow rates of 2 ℓ/min were used to maximize the residence time of the flue gas in the condenser. Isokinetic sampling was not possible at these flow rates.

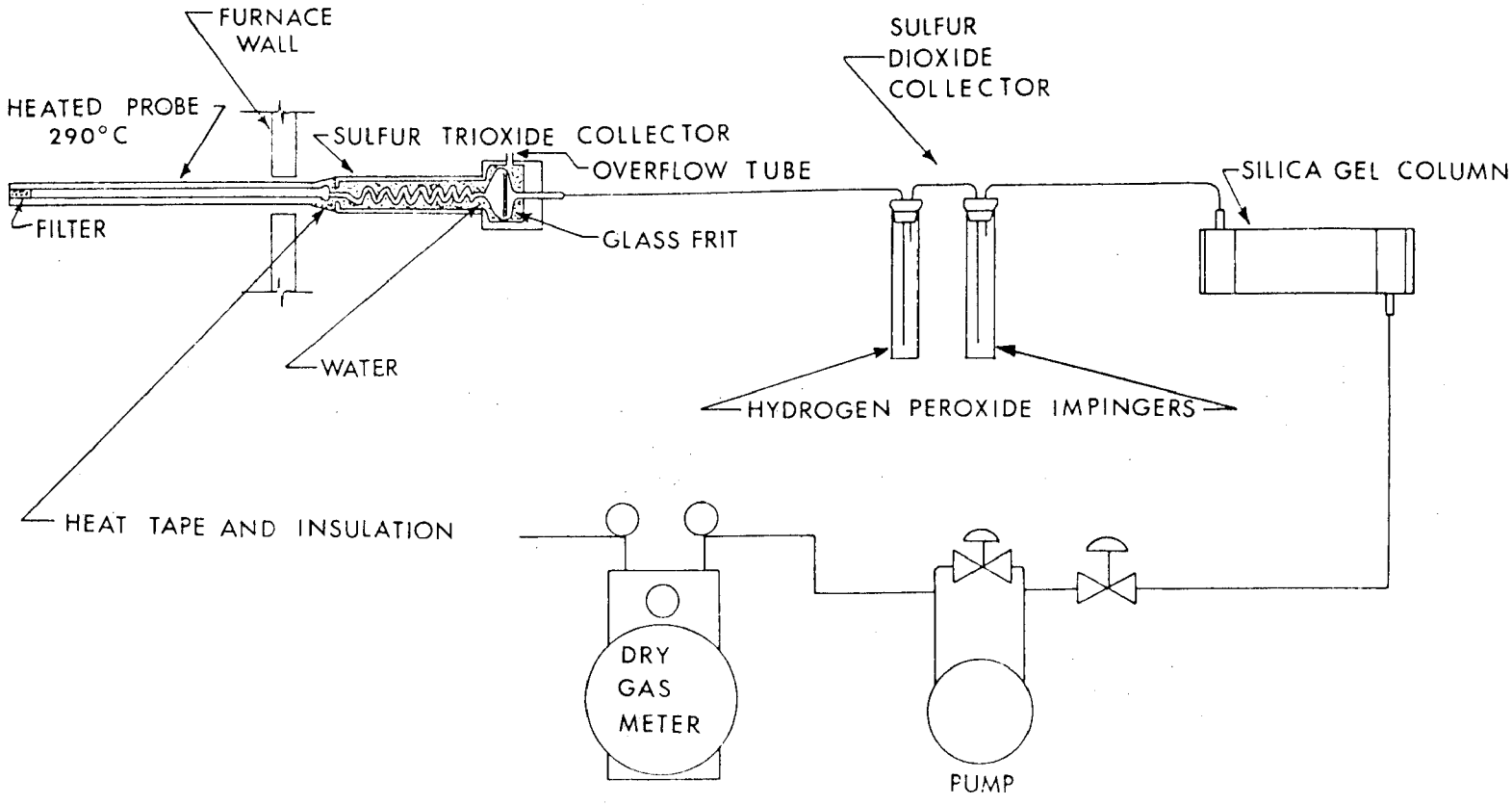

Figure 1. Apparatus used to investigate effects of plant operating parameters on the SO_3 content of flue gases.

The condenser was rinsed with a solution of 5% isopropanol in water after each sample was collected. The rinse solution was titrated with 0.02 N sodium hydroxide (NaOH), and bromphenol blue was used as the indicator. To analyze for SO_2, the H_2O_2 solutions were boiled to destroy excess H_2O_2, and then titrated with 0.1 N NaOH. Bromphenol blue was used as the indicator.

Results and Discussion

Samples were collected at four TVA power plant units to determine the effect of excess oxygen, varying from 2.7% to 5.9% on SO_3/H_2SO_4 content of flue gas. The units investigated and their furnace configurations were Shawnee Unit 3--a 175-MW front-wall unit located in Paducah, Kentucky; Widows Creek Units 7 and 8--tangential units of 575 and 550 MW, respectively, located in Stevenson, Alabama; and Allen Unit 1--a 330-MW cyclone unit located in Memphis, Tennessee. Results of these tests, shown in Table 1 and Figure 2, demonstrated the dependence of the $[SO_3/(SO_2 + SO_3)]$ fraction on the excess oxygen content of the flue gas. A simple linear regression analysis was applied to the data from each unit to obtain the fitted equations:

Shawnee Unit 3 $[SO_3/(SO_2 + SO_3)]$ (%) =
0.12(% excess oxygen) - 0.09 ($R^2 = 0.76$)

Widows Creek Unit 8 $[SO_3/(SO_2 + SO_3)]$ (%) =
0.35(% excess oxygen) - 0.50 ($R^2 = 0.98$)

Widows Creek Unit 7 $[SO_3/(SO_2 + SO_3)]$ (%) =
0.263(% excess oxygen) ($R^2 = 0.84$)

Allen Unit 1 $[SO_3/(SO_2 + SO_3)]$ (%) =
0.27(% excess oxygen) - 1.44 ($R^2 = 0.83$)

Results of these tests also indicated that cyclone furnaces may emit greater percentages of SO_3/H_2SO_4 than do front-wall and tangential furnaces. For all levels of excess oxygen tested, the values of the $[SO_3/(SO_3 + SO_2)]$ ratio, expressed as percent, clustered near or below 1% for all units except Allen Unit 1 (a cyclone furnace), which showed ratios greater than 2%.

The effect of temperature on the SO_3/H_2SO_4 content of flue gas was determined in a series of tests conducted at TVA's Cumberland Unit 2, a horizontally opposed, 1275-MW unit located in Cumberland City, Tennessee. At least five tests were conducted at

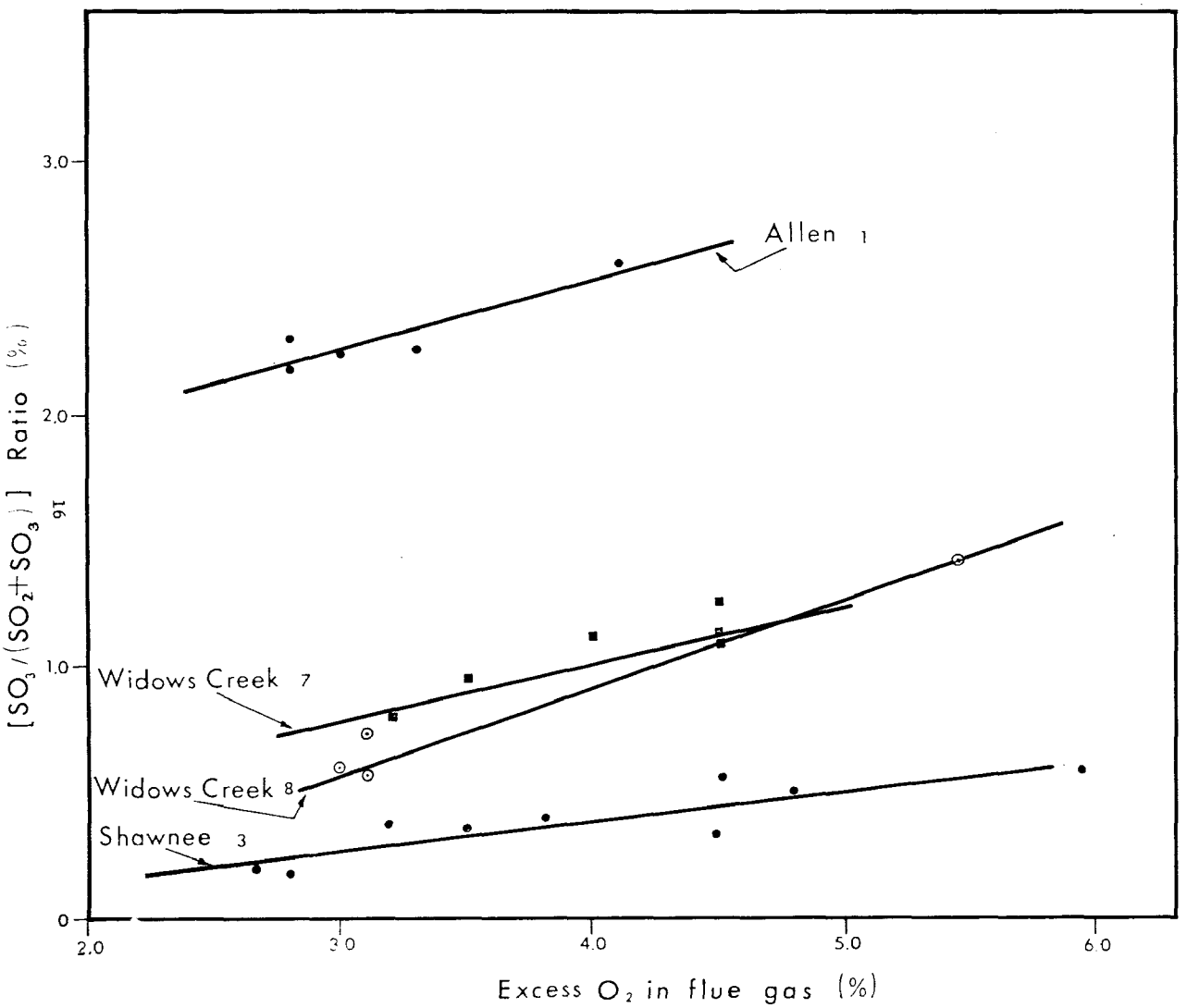

Figure 2. Variation in conversion of SO_2 to SO_3 with excess oxygen content of flue gas.

each temperature range. Results of these series (Table 2) indicated that the SO_3/H_2SO_4 content depends on the flue gas temperature and decreases sharply when the temperature is lowered. This effect may be a result of condensation; it is possible that the SO_3/H_2SO_4 content in a coal-fired unit is highest at the boiler, and as the gas progresses through the unit and cools off, a fraction of the SO_3/H_2SO_4 condenses. The greatest amount of condensation would probably occur in the air preheater, where there is a substantial temperature drop.

Table 1. Sulfur Trioxide Content at TVA Power Plant vs. Excess Oxygen in Flue Gas

Plant	Unit	Capacity (MW)	Furnace Design	Excess O_2 (%)	$[SO_3/(SO_2 + SO_3)]$ (%)
Allen	1	330	Cyclone	2.8	2.3
				2.8	2.2
				3.0	2.3
				3.3	2.3
				4.1	2.6
Shawnee	3	175	Front Wall	2.7	0.19
				2.8	0.18
				3.2	0.38
				3.5	0.35
				3.8	0.40
				4.5	0.56
				4.5	0.34
				4.8	0.50
				5.9	0.58
Widows Creek	7	575	Tangential	3.2	0.80
				3.5	0.95
				4.0	1.1
				4.5	1.3
				4.5	1.2
				4.5	1.1
Widows Creek	8	550	Tangential	3.0	0.60
				3.3	0.70
				3.3	0.57
				4.1	1.5

Table 2. Sulfur Trioxide Content vs. Flue Gas Temperature at Air Preheater Outlet of Cumberland Steam Plant Unit 2

Experiment Series	Flue Gas Temperature Range (°C)	SO_3 Concentration Range (ppm)
1	152-154	2-5
2	162-167	6-7
3	168-173	9-10

MEASUREMENT OF THE EMISSION OF SULFUR TRIOXIDE AND SULFUR DIOXIDE FROM A TVA COAL-FIRED POWER PLANT

The TVA Division of Environmental Planning has conducted two plume chemistry studies at Cumberland Units 1 and 2, both horizontally opposed 1275-MW units located in Cumberland City, Tennessee, to investigate the oxidation rate of SO_2 in the plume. Data on the $[SO_3/(SO_2 + SO_3)]$ fraction in flue gas were needed to determine the fraction of sulfur dioxide that was already oxidized when the gas was emitted to the atmosphere. To obtain these data, flue gas samples, drawn from ports located about 4 m from the base of the stack, were analyzed for SO_3/H_2SO_4 and SO_2.

Methodology

A modified Lisle and Sensenbaugh apparatus (Figure 3) was used to collect samples. The probe used in the first field study was Teflon-lined and contained a Pyrex wool plug; the portion of the probe between the duct wall and condenser was heated. The condenser (Figure 4) was positioned in a waterbath held at 60°C to 70°C. Sulfur dioxide was collected in two midget impingers, each containing a solution of 5% H_2O_2; these impingers were followed by an impinger containing Drierite. Volume was measured by monitoring a calibrated vacuum gauge positioned in front of the pump. The samples were not collected isokinetically; typical flow rates were about 1.4 l/min. After sample collection, the probe and condenser were rinsed with 80% isopropanol. The probe rinse solution was filtered, and both solutions were titrated with 0.005 barium perchlorate $[Ba(ClO_4)_2]$ in 80% isopropanol; thorin was used as the indicator. To analyze for SO_2, the H_2O_2 solutions were boiled to destroy the excess H_2O_2 and then titrated with 0.2 N NaOH. Bromphenol blue was used as the indicator.

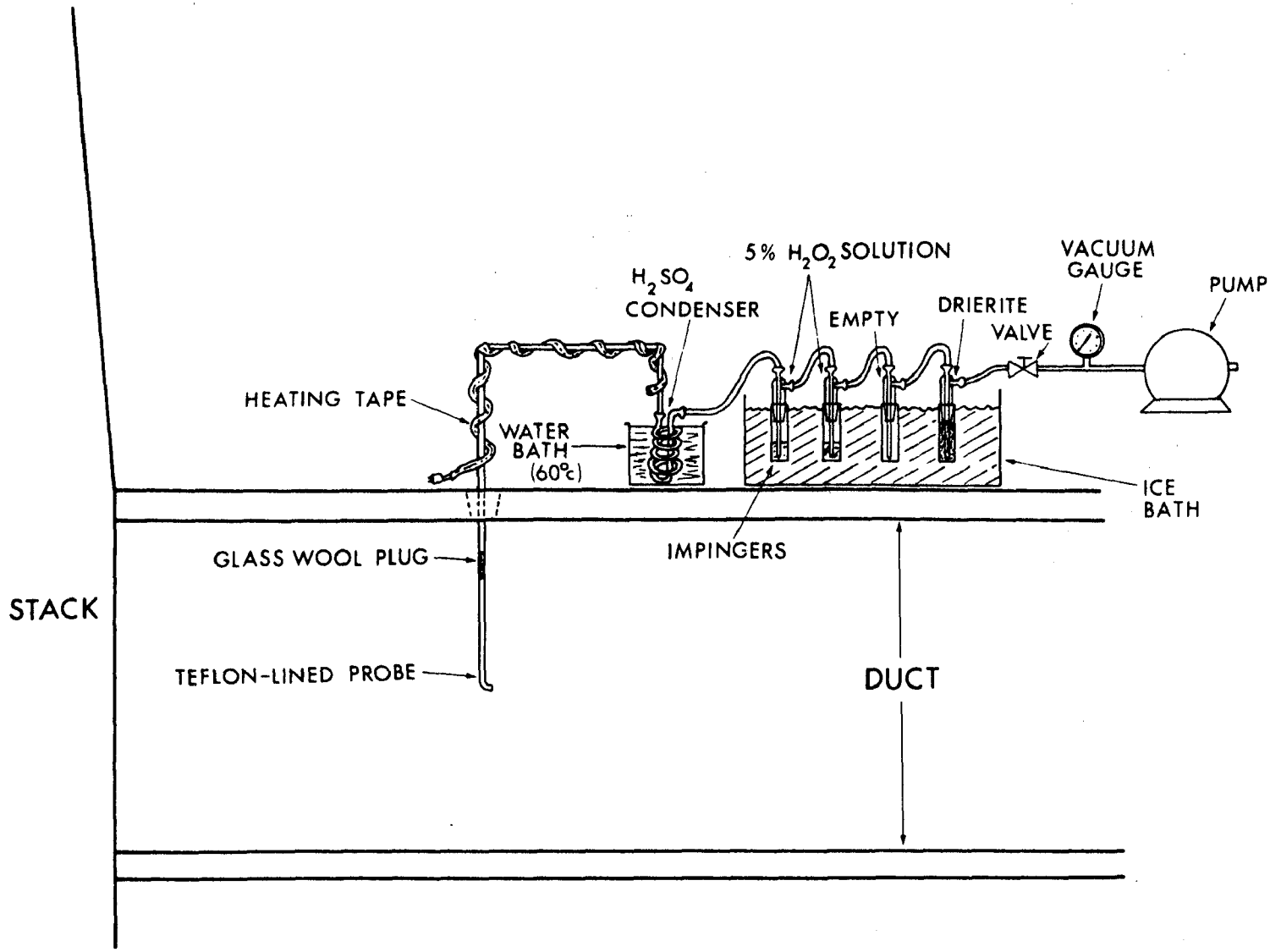

Figure 3. Apparatus used in first study of SO_2 and SO_3 emissions from Cumberland Steam Plant.

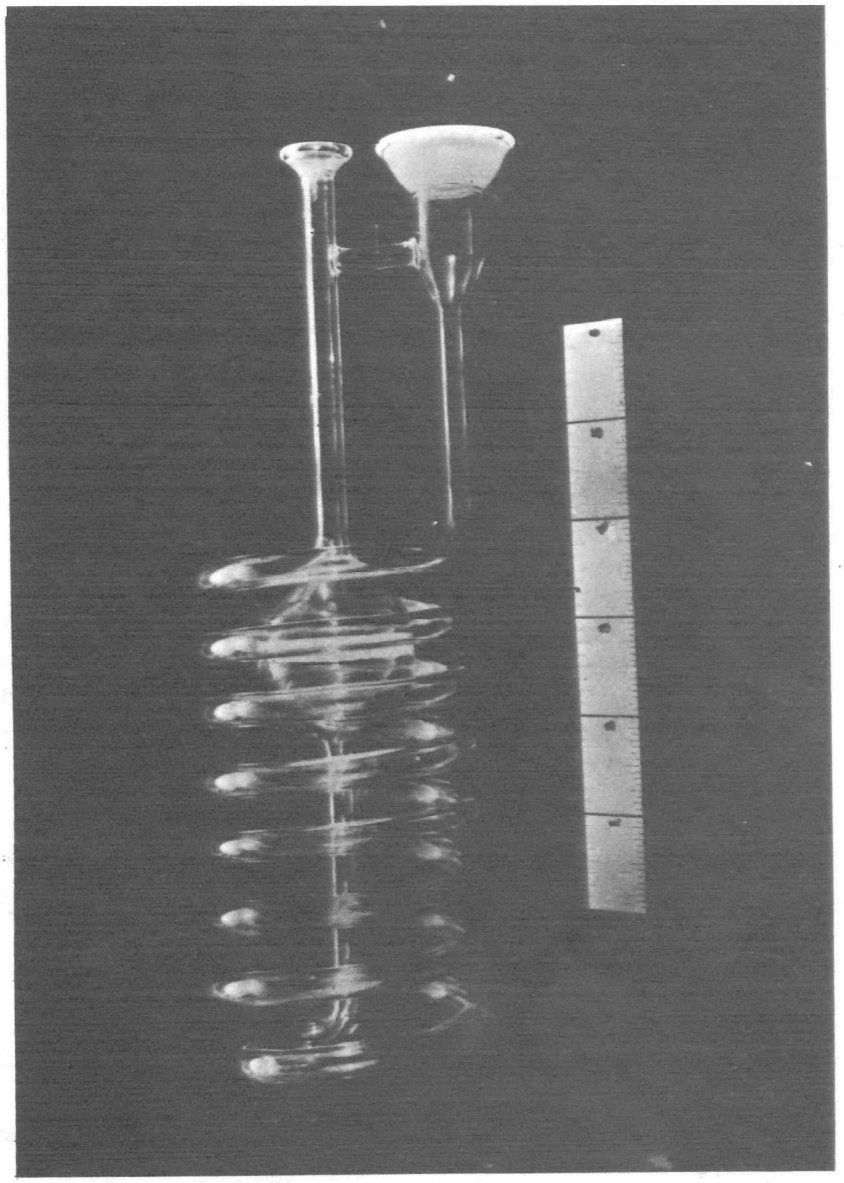

Figure 4. Condenser used in studies of SO_2 and SO_3 emissions from Cumberland Steam Plant.

In the second field study, mass loading data were also collected. For this reason a Research Appliance Company (RAC) isokinetic stack sampling apparatus was modified so that it could be used for collection of either mass loading or SO_3/H_2SO_4 and SO_2 samples. When set up to obtain SO_3/H_2SO_4 and SO_2 data, the RAC apparatus differed from the Lisle and Sensenbaugh apparatus in four ways: (1) The condenser was positioned in a heated compartment instead of in a waterbath, (2) modified Greenberg-Smith impingers containing 100 ml of 3% H_2O_2 solution were used instead of the midget impingers, (3) a dry test meter was used to measure volume, and (4) the samples were collected at flow rates ranging from 4.5 to 20.0 ℓ/min. The analytical procedure was the same as for the first study.

Results and Discussion

The results of these two studies are presented in Table 3. In the first study, the average values for the $[SO_3/(SO_2 + SO_3)]$ fractions (percent) were 0.26 for Unit 1 and 0.22 for Unit 2. The corresponding average excess oxygen contents were 5.9% and 4.1%. In the second study, the $[SO_3/(SO_2 + SO_3)]$ fractions (percent) were 0.19 for Unit 1 and 0.59 for Unit 2: the excess oxygen contents were 5.5% and 6.7%. These data support trends which were previously discussed. The values of the $[SO_3/(SO_2 + SO_3)]$ fraction at Cumberland, like those for Shawnee Unit 3 and Widows Creek Units 7 and 8, are low compared with the fraction found for the cyclone furnace at Allen Unit 1. For both units, the $[SO_3/(SO_2 + SO_3)]$ fraction increased with increasing excess oxygen content, similar to the behavior observed at Shawnee Unit 3, Widows Creek Units 7 and 8, and Allen Unit 1.

Table 3. Sulfur Trioxide and Sulfur Dioxide Emissions Measured at Cumberland Steam Plant

Unit	Capacity (MW)	Furnace Design	Field Study	Excess O_2 (%)	SO_3 (ppm)	SO_2 (ppm)	$\left[\frac{SO_3}{SO_2 + SO_3}\right]$ (%)
1	1275	Horizontally opposed	1	5.9	5.4	2790	0.26
			2	5.5	7.0	3470	0.19
2	1275	Horizontally opposed	1	4.1	7.5	2720	0.22
			2	6.7	18.0	3020	0.59

STACK APPARATUS EFFICIENCY TESTS

Two experiments were conducted to determine the efficiency of the modified RAC stack sampling apparatus for collecting SO_3/H_2SO_4.

Methodology

In the first experiment, as part of the field study procedure, the probe and Pyrex wool plug were rinsed separately from the condenser; the probe and plug rinse solution was titrated separately from the condenser rinse to determine the fraction of SO_3/H_2SO_4 that remained in the probe. In the second experiment, the efficiency of the condenser for collecting SO_3/H_2SO_4 was determined. Two condensers were connected in series in the modified RAC apparatus and the temperature was maintained between 60°C and 70°C for both condensers. Flue gas was then sampled from the base of the stack at TVA's Colbert Unit 1, a 200-MW front-wall unit located near Pride, Alabama. Both condensers were rinsed after sample collection, and the rinse solutions were analyzed for SO_3/H_2SO_4 using the $Ba(ClO_4)_2$ titration procedure.

The results of the first experiment (Table 4) showed that on the average 68% of the SO_3/H_2SO_4 was found in the probe for flow rates ranging from 0.0057 to 0.020 m^3/min. Results of the second experiment (Table 4) indicate that on the average the first condenser was 83% efficient for flow rates ranging from 0.0051 to 0.0014 m^3/min. Combining the efficiencies of the probe and first condenser gives a total system efficiency for SO_3/H_2SO_4 collection of 95%.

CONCLUSION

The results of these studies suggest that the SO_3/H_2SO_4 content of power plant flue gas depends on the excess oxygen content of the flue gas, furnace design, and temperature of the flue gas. Cyclone furnace units may produce higher percentages of SO_3/H_2SO_4 in their flue gases than do tangential and front-wall furnaces. However, this should be verified by sampling at other cyclone units. The SO_3/H_2SO_4 content of flue gas was found to increase with increasing excess oxygen content of the flue gas and to decrease with decreasing flue gas temperature. Because the temperature of the flue gas decreases as the gas passes through a unit, it is possible that SO_3/H_2SO_4 condenses inside the unit, particularly in the air preheater, where a significant temperature drop occurs.

Table 4. Efficiency Tests for SO_3 Collection System

Determination of Fraction of SO_3 Found in the Probe and in the Condenser			
Sample No.	Fraction in Probe	Fraction in Condenser	Flow Rate (m^3/min)
1	0.63	0.37	0.011
2	0.66	0.34	0.0082
3	0.73	0.27	0.014
4	0.71	0.29	0.020
5	0.68	0.32	0.020
6	0.65	0.35	0.0057
7	0.67	0.33	0.020
8	0.70	0.30	0.0068
Average	0.68*	0.32*	

Determination of Fraction of SO_3 Found in the Condenser			
Sample No.	Fraction in 1st Condenser	Fraction in 2nd Condenser	Flow Rate (m^3/min)
1	0.82	0.18	0.0051
2	0.88	1.12	0.0054
3	0.91	0.09	0.0085
4	0.76	0.24	0.010
5	0.82	0.18	0.013
6	0.78	0.22	0.014
Average	0.83*	0.17*	

*Therefore, total collection efficiency of the system is 0.68 + 0.83(0.32) = 0.95.

Sampling of emitted flue gases at one power plant showed that the emission rate for SO_3/H_2SO_4 was about 0.3% of that for SO_2. The efficiency of the method of sampling for SO_3/H_2SO_4 was found to be satisfactory.

REFERENCES

1. Office of Air Quality Planning and Standards. Position Paper on Regulation of Atmospheric Sulfates. EPA-450/2-75-007, U.S. Environmental Protection Agency, Research Triangle Park, North Carolina, 1975. 87 pp.

2. Science Applications, Inc. Effects of Sulfur Oxides on the Lung: An Analytic Base. EPRI 205 (SAI-75-566-LA), Electric Power Research Institute, Palo Alto, California, 1975. 206 pp.

3. Hutchinson, T. C., and L. M. Whitby. The Effects of Acid Rainfall and Heavy Metal Particulates on a Boreal Forest Ecosystem Near the Sudbury Smelting Region of Canada. Water, Air and Soil Pollution, 7:421-438, 1977.

4. Braekke, F. H. Impact of Acid Precipitation on Forest and Fresh-water Ecosystems in Norway. SNSF Fagrapport FR6. Aas-NLH, Norway, 1976. 111 pp.

5. Lisle, E. S., and J. D. Sensenbaugh. The Determination of Sulfur Trioxide and Acid Dew Point in Flue Gas. Combustion, 36(7):12-16, 1965.

Measurement of SO_3/H_2SO_4 Concentration in Kraft Recovery Furnace Stack Gas Using Controlled Condensation

Ashok K. Jain
R. O. Blosser
Howard S. Oglesby
National Council for Air and Stream Improvement

ABSTRACT

Tests were conducted to determine the effects of sample flow rate, condenser temperature, and frit porosity upon the efficiency of controlled condensation equipment to measure parts per million levels of SO_3/H_2SO_4 in a gas stream containing up to 30% moisture. Further laboratory studies were conducted using particulate from several kraft recovery furnaces to study the effect of particulate upon the passage of H_2SO_4 vapors through a quartz filter loaded with particulate. The results showed that H_2SO_4 losses in the filter ranged from 10% to 60% of the inlet concentration and depended upon particulate characteristics.

INTRODUCTION

The recovery of chemicals from spent kraft cooking liquor (black liquor) involves combustion of concentrated black liquor, which consists of wood components, inorganic chemicals, and sulfur compounds in kraft recovery furnaces. The presumed similarity of sulfur-containing fossil fuels and black liquor has raised the question of the possible presence of sulfur trioxide (SO_3) and sulfuric acid (H_2SO_4) in kraft recovery furnace flue gas, although liquor is burned in a manner to minimize SO_2 generation.

This paper describes the results of laboratory studies carried out to date to develop a technique to measure SO_3/H_2SO_4 levels in kraft recovery furnace stack gas using controlled condensation.

DESCRIPTION OF EXPERIMENTAL APPARATUS AND METHODS

Sulfuric Acid Evaporator

A sulfuric acid evaporator, as shown in Figure 1, was used in the laboratory to generate test gases containing desired concentrations of moisture and H_2SO_4. The evaporator was a quartz tube packed with glass beads and wrapped with a heating element and insulation. A coarse quartz frit was installed inside the evaporation tube to provide uniform concentrations of H_2SO_4. Sulfuric acid was added to the evaporator with a low flow rate Masterflex pump manufactured by Cole-Parmer Instrument Co. The temperature of the evaporator was maintained at 650°F.

In those tests in which the performance of particulate filter was evaluated, an additional quartz conditioning tube was added to the evaporator as shown in Figure 1. The conditioning tube was wrapped with a heating element and insulation and allowed the sample stream to be split into two fractions. One fraction went to the filter holder (sample train), and the other went to impingers (reference train) for determining sulfuric acid concentration in the sample stream.

Controlled Condensation Coil

The SO_3 condenser is shown in Figure 2. The inside diameter of the glass tubing for condensing sulfuric acid was 5 mm, and the frit diameter was 45 mm. Three different condensers were evaluated during the study. The first condenser had approximately three feet of glass tubing and a coarse frit (Ace Glass Type B); whereas the second and third condensers had approximately six feet of glass tubing and Ace Glass Type C and D frits, respectively. During the tests the condenser was filled with water, and its temperature was maintained at 175°-185°F with a heating mantle.

Filter Holder Design and Particulate Loading

Filter holders typically used in EPA Method 5 sampling trains were used initially. However, these filter holders are not designed for use above 400°F. For higher temperatures a quartz filter holder shown in Figure 3 was used. The details of the design are specified elsewhere (1).

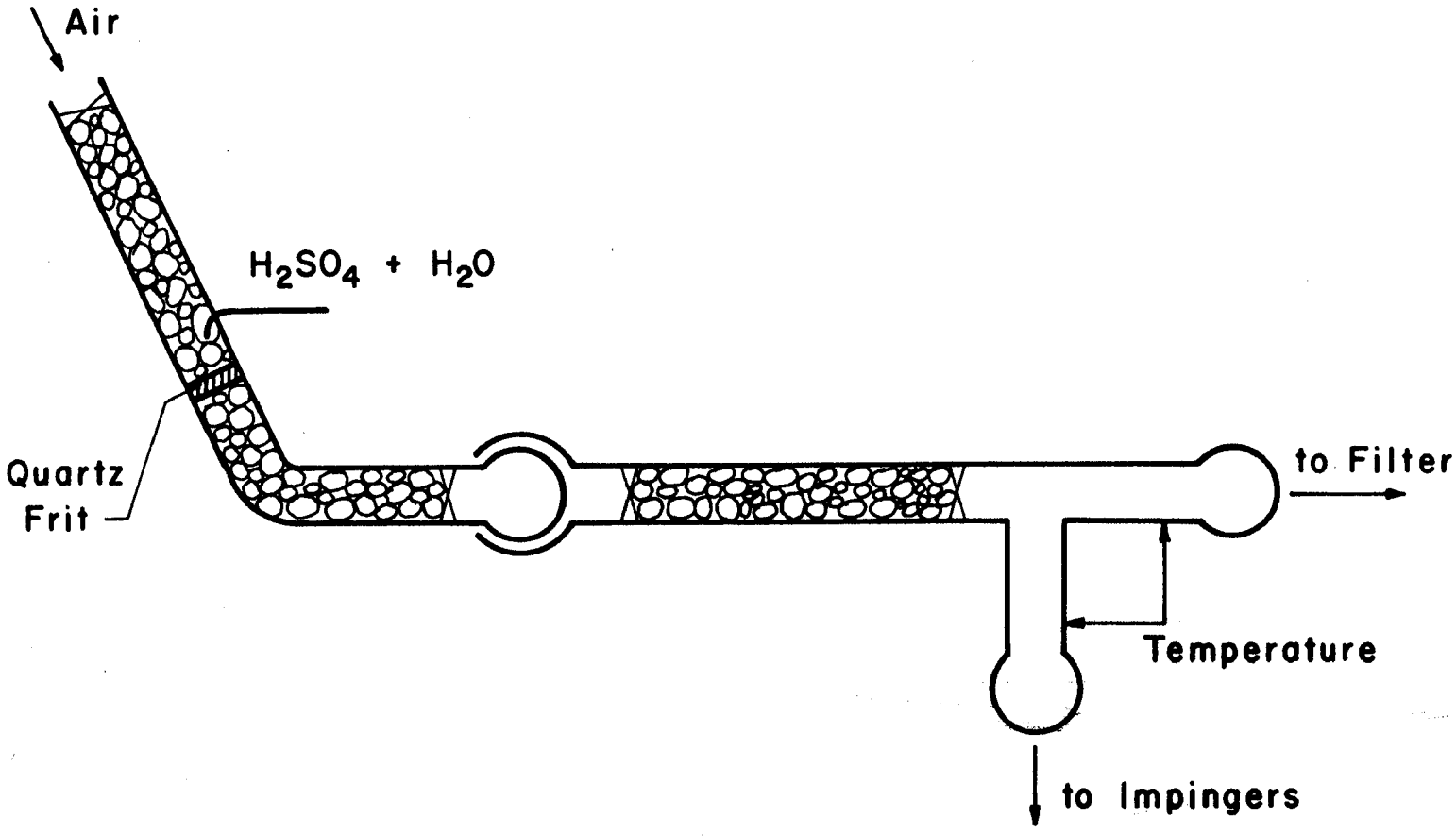

Figure 1. H_2SO_4 evaporation assembly.

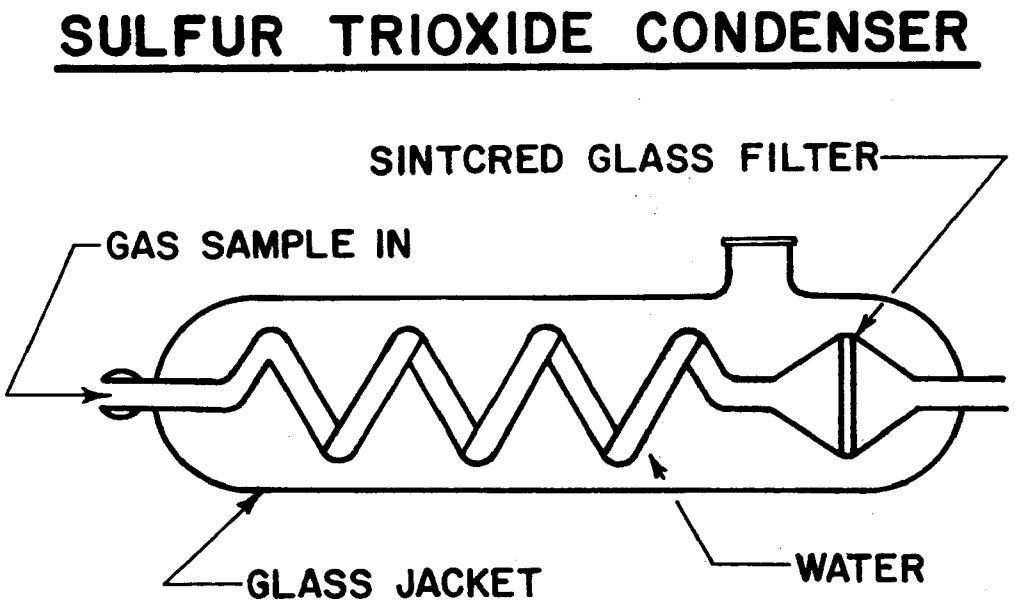

Figure 2. Sulfur trioxide condenser.

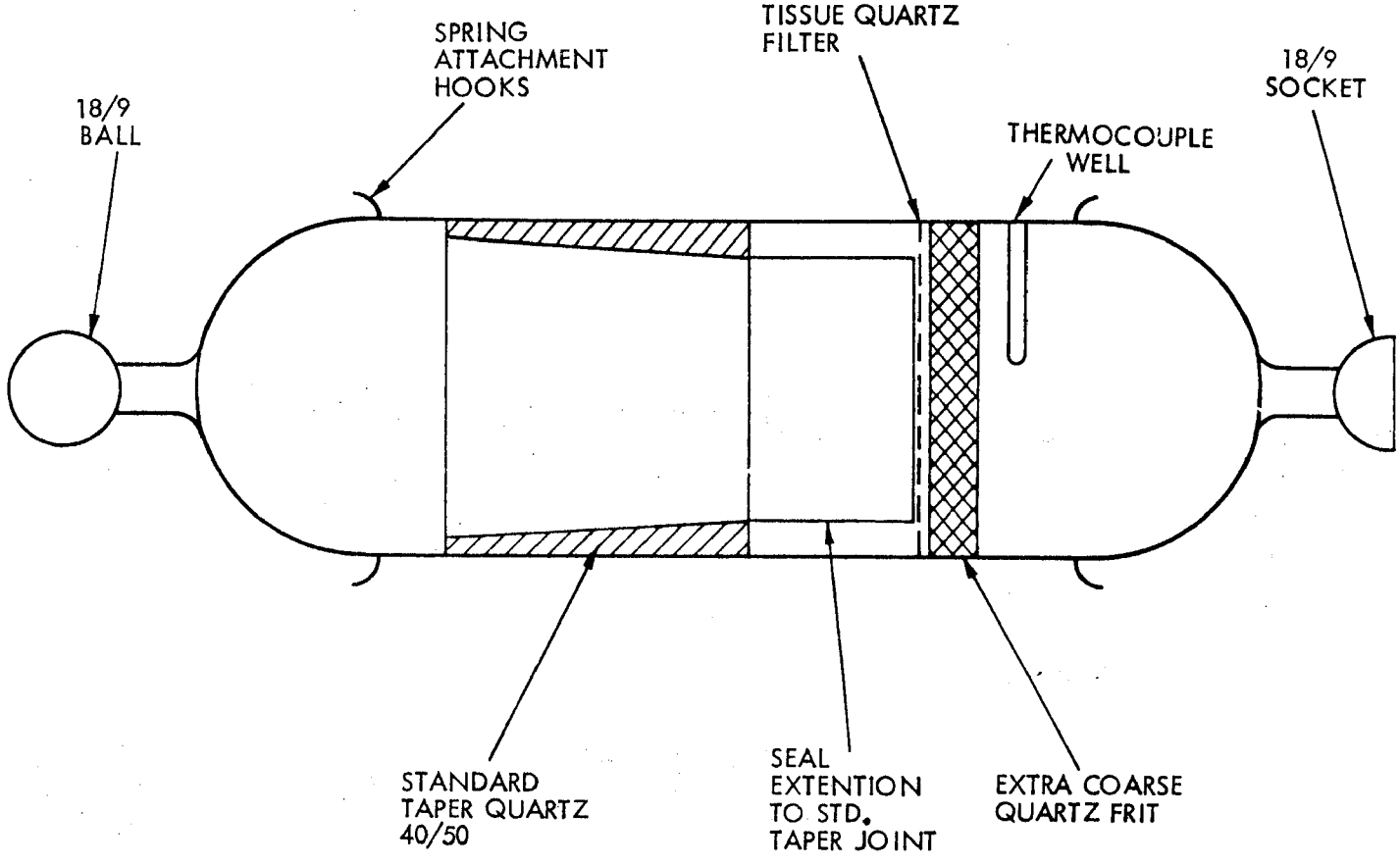

Figure 3. Quartz filter holder.

The filter medium used in all tests was Tissuequartz 2500 QAO, manufactured by Pallflex Products Corporation, Putnam, Conn. In those tests in which the effect of recovery furnace particulate upon H_2SO_4 loss was to be determined, the filter was loaded with measured amounts of particulate by slowly adding particulate directly to the filter while drawing air through the filter at a high rate.

H_2SO_4 Sampling Train

The sampling train for determining sulfuric acid concentration in the gas stream consisted of two Greenberg Smith impingers containing isopropyl alcohol, an impinger containing water, a column of silica gel, a leakproof vacuum pump, a rotameter, and a calibrated dry gas meter.

Method of Sulfate Analysis

The samples were analyzed for their sulfate content by titrating them with barium perchlorate and using Thorin indicator (2). Interference of sodium ions in Thorin titration was also investigated.

Determination of SO_3 Condenser Efficiency

Figure 4 shows the schematic of the sampling system used for determining the efficiencies of H_2SO_4 capture in SO_3 condensers. Tests were conducted at different flow rates through the condensers and with various H_2SO_4 concentrations in the gas stream. Each test lasted approximately 30 minutes. At the end of the test the condenser was washed and analyzed for sulfuric acid retained in the condenser. The impinger solution was also analyzed to determine the amount of H_2SO_4 passing through the condenser.

Determination of H_2SO_4 Losses in Filter Holders

Initial tests to determine the retention of H_2SO_4 vapors in filter holders were conducted at 350°-400°F, and filter holders used in EPA Method 5 sampling trains were used. The schematic of the sampling system was the same as used for condenser evaluation, except that the filter holder was installed in the sampling train in place of the SO_3 condenser.

The tests with quartz filter holders used the schematic shown in Figure 5. Tests were conducted to determine H_2SO_4 loss in the filter holder when (1) there was no particulate filter holder in the sample train, (2) there was quartz filter holder in the sample train, and (3) the quartz filter holder was loaded with particulate samples from different recovery furnaces. The amount of particulate on the filter paper was equivalent to an average particulate concentration of approximately 0.2 gm/1000 liters dry gas.

RESULTS AND DISCUSSION

Method of Sulfate Analysis

Thorin titration was found satisfactory in our studies and gave sharp end points at low concentrations. However, since sodium constitutes a large fraction of recovery furnace particulates, tests were conducted to determine sodium ion interference with Thorin titration. The results are recorded in Table 1 and show that sodium ion increased the volume of titrant required and caused a positive interference in sulfate analysis.

Table 1. Sodium Interference with Thorin Titration

No.	Vol 0.01 N $NaNO_3$ (ml)	Vol 0.022 N $Ba(ClO_4)_2$ Titrant (ml)
1	0	9.10
2	10	9.15
3	20	9.30
4	30	9.45
5	40	9.65

Efficiency of SO_3 Condensation Coil

Effect of Frit Porosity and Coil Length on Condenser Efficiency--The results of tests aimed at determining the effect of frit porosity upon the efficiency of the SO_3 condenser are recorded in Table 2. During these tests the temperature of the condenser was maintained between 175°-185°F. The low efficiency of H_2SO_4 capture with the Type B frit may partially be due to smaller length of the condensing coil. The Type D frit gave very high capture efficiency

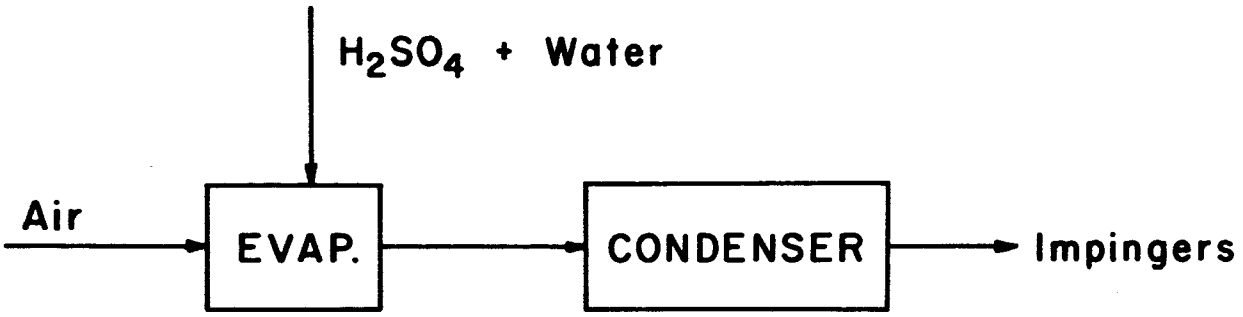

Figure 4. Schematic for determining condenser efficiency.

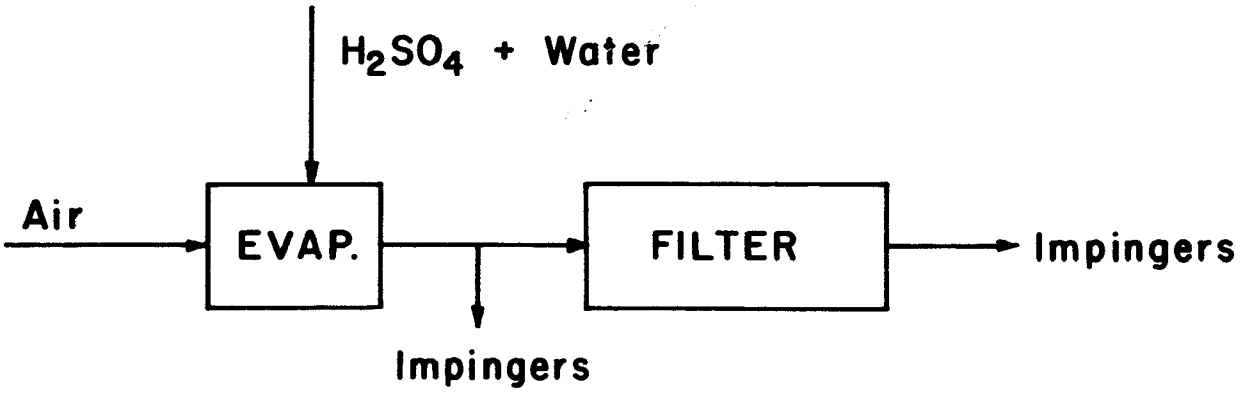

Figure 5. Schematic for determining filter losses.

but did not allow sample flow rates higher than 2 lit/min. The Type C frit was found to be most acceptable from the point of view of sample flow rate and efficiency of H_2SO_4 capture.

Table 2. Effect of Frit Porosity Upon Condenser Efficiency

No.	Frit Type*	Max. Pore Dia. Range (μM)	Length of Condensing Coil (ft)	Flow Rate (lit/min)	% H_2SO_4 Capture
1	B	70-100	3	2	20-40
2	D	10-20	6	2	99
3	C	25-50	6	2-8	90-99

*Ace Glass

Effect of Flow Rate on Condenser Efficiency--The results of tests aimed at determining the effect of flow rate on the efficiency of SO_3 condenser are summarized in Table 3. The results show that the efficiency of H_2SO_4 capture varied from 90.0% to 99.4% during these tests, and the average efficiency of H_2SO_4 capture was slightly higher during high flow rate tests.

Table 3. Effect of Flow Rate on Efficiency of SO_3 Condenser

Flow Rate (lit/min)	No. of Runs	% H_2SO_4 Capture		
		Max.	Min.	Avg.
3.5	7	96.8	90.0	93.3
9.5	13	99.4	91.1	95.4

Effect of H_2SO_4 Concentration on Condenser Efficiency--Tests were conducted in the concentration range of 1 ppm to 50 ppm to determine if there was any effect of H_2SO_4 concentration on its efficiency of capture. The results are summarized in Table 4. All tests were made at flow rates of approximately 9 lit/min. The

results show that the efficiencies of capture were generally higher than 95%, except when 50 ppm H_2SO_4 was present in the gas stream. However, only two runs were made at high H_2SO_4 concentration.

When a "t" test was performed to test the hypothesis that the me efficiencies of capture were different for 1 ppm and 50 ppm H_2SO_4 samples, it was concluded that there was insufficient evidence to indicate that the two efficiencies of capture were different at the 0.05 level of significance.

Table 4. Effect of H_2SO_4 Concentration on Capture Efficiency

H_2SO_4 Conc. (ppm)	No. of Runs	% H_2SO_4 Capture		
		Max.	Min.	Avg.
1	6	99.2	92.0	95.0
5	4	99.4	94.7	97.8
20	1	95.9	95.9	95.9
50	2	91.7	91.1	91.4

Loss of H_2SO_4 in Filter Holders

EPA Method 5 Type Filter Holders--Tests with EPA Method 5 filter holders were conducted by maintaining the filter holders in the temperature range of 390° to 440°F. The results of six tests showed that on an average 45% of the H_2SO_4 present in the gas stream was retained in the filter holder. These results indicated the need to maintain the filter holder at higher temperatures, which was not possible with this type filter holders.

Quartz Filter Holder--The results of tests to determine the effect of the quartz filter assembly upon the passage of H_2SO_4 are recorded in Table 5. A comparison of the tests with and without the filter support assembly indicates that there was no significant loss in the filter assembly, and most of the variability was in the sampling and analytical technique itself.

Table 5. Effect of Quartz Filter Assembly Upon Sample Recovery

No. of Runs	Ref. Train H_2SO_4 Conc. Range (ppm)	Filter Assembly Present	% Error[a] Max.[b]	Min.[c]	Avg.[d]
9	5.8-18.2	No	11.4	1.7	0.0
12	5.6-18.0	Yes	14.9	1.8	1.8

[a] $\% \text{ Error} = \frac{(\text{Ref.} - \text{Sample})}{\text{Ref.}} \times 100$

[b] Max. Error = Max. Abs. (% Error)

[c] Min. Error = Min. Abs. (% Error)

[d] Avg. Error = Abs. (Σ (% Error)/No. Runs)

Filter Holder H_2SO_4 Losses in the Presence of Particulate

The data in Table 6 show a summary of the tests to determine H_2SO_4 losses in the filter holder when the filter was loaded with particulate samples from different recovery furnaces. During the tests the amount of particulate on the filter was approximately 0.2 gm/1000 lit dry gas. The results showed large variations in H_2SO_4 loss in the particulate holder with average losses varying from 7% to 55%. The particulate samples were also analyzed for their alkalinity to determine if the filter loss could be correlated to alkalinity. However, no such correlation was observed in Table 6.

Table 6. Filter Holder Losses for Different Particulate Samples

Source	Part. Alkalinity gm $CaCO_3$/kg	No. of Runs	% H_2SO_4 Loss Max.	Min.	Avg.
A	32.4	7	13	2	7
B	9.4	1	27	27	27
C	45.0	3	62	45	55
D	39.0	12	62	29	48
E	0	3	38	23	32
F	8.4	3	15	3	8
G	6.3	1	19	19	19

SUMMARY

1. Thorin titration was found acceptable for sulfate analysis. However, sodium ions caused a positive interference.

2. The efficiency of H_2SO_4 capture in SO_3 condensers was found to be dependent upon the frit porosity and coil length.

3. The flow rate and concentration of H_2SO_4 did not significantly affect the efficiency of H_2SO_4 capture in the condenser with Ace Glass Type C frit.

4. The quartz filter assembly did not cause any loss of H_2SO_4 when it was maintained at 600°-650°F.

5. In the presence of particulate, H_2SO_4 losses in the filter holder varied from 7% to 55% for different particulate samples and could not be correlated with particulate alkalinity.

ACKNOWLEDGMENT

The authors acknowledge the contribution of Mr. John Ruppersberger of the Environmental Protection Agency. Work is being partially supported by USEPA Industrial Environmental Research Laboratory under Contract R-804644-01-0.

REFERENCES

1. Process Measurement Procedures Sulfuric Acid Emissions. Prepared for: Industrial Environmental Research Laboratory, U.S. Environmental Protection Agency, Research Triangle Park, North Carolina, Contract No. 68-02-2165, February 1977.

2. Method 8 - Determination of Sulfuric Acid Mist and Sulfur Dioxide Emissions from Stationary Sources. Federal Register 36, December 23, 1971. 247.

Characterization of Combustion Source Sulfate Emissions with a Selective Condensation Sampling System

James L. Cheney
James B. Homolya
U.S. Environmental Protection Agency

ABSTRACT

Present studies of sulfate emissions include an examination of both the formation of sulfate during the combustion of sulfur-containing fuels and the long-range impact of sulfates on the atmosphere. Like any attempt to inventory source emissions, confirmation of the sulfate emissions relies heavily on the measurement methodology used. Our work has emphasized not only the measurement of total sulfate emissions, but also the characterization of these sulfates. Using this approach, a reliable impact can be determined by predicting the mass emission rates of individual sulfate components.

A substantial number of current source sulfate measurements involve the separation of unassociated H_2SO_4 from particulate-related sulfate and the subsequent recovery and quantitative determination of the separate components. At present, most of these efforts involve high temperature gas-solid separation by filtration, followed by collection of the acid in a temperature-controlled Goksoyr-Ross coil. We have performed controlled sampling experiments using the selective condensation method to determine its reliability in characterizing sulfate emissions.

The design of the manual sampling equipment and experiments will be described, including studies of collection efficiency, separation, and isolation of the sulfate components. The collected data will be presented, and

in-depth examination of the data collected as sampling variables were changed will be discussed, along with suggestions for possible future efforts using this sampling approach.

INTRODUCTION

A considerable amount of effort is currently in progress to establish the correlation between sulfates emitted from combustion sources and those measured in the atmosphere. In addition to efforts (1) to relate sulfate emissions to local and long-term atmospheric impact, further efforts involve sulfate emission measurements for evaluating the effectiveness of current control technology. During the course of the past few years, a need has developed (2) for a sulfate characterization method. The particular emphasis in sulfate characterization studies, both with respect to atmospheric effect as well as the emission control studies, has been to determine sulfuric acid (H_2SO_4) as a separate entity from total sulfate. For the high temperature combustion source, the H_2SO_4 which is unassociated with particulate matter usually behaves (3) as a gaseous emission, in contrast to the inorganic sulfate or particle-absorbed acid.

Ideally, then, a sulfate measurement method is desired that will simultaneously provide the concentration of both particulate sulfate and the concentration of H_2SO_4. For the purpose of clarification, particulate sulfate is defined here as all metal sulfates as well as H_2SO_4 absorbed on the particles. For such a method, emphasis has been placed most recently on the Shell (4) selective condensation approach. The method involves the extractive sampling of the flue gas, followed by high temperature separation of the particulate fraction, with a subsequent collection of H_2SO_4 in a temperature-controlled Goksoyr-Ross condensation coil. Problems have been encountered with this approach, however, which include the usual problem of using bulky glassware for field sampling, high pressure drops across the backup aerosol collection frit in the Goksoyr-Ross coil, and an inadequate gas-particle (2) separation during sampling.

Prior evidence indicates that an apparent equilibrium between H_2SO_4 in the gas phase and particulate matter can exist in flue gases. The equilibrium between the gaseous acid component and the particles is dependent on, among many variables, contact time, concentration of acid and particles, and temperature. The difficulty of characterizing the sulfates by this method is in sampling so as not to disturb the gas-solid equilibrium.

Furthermore, in order to provide an accurate measure of particulate concentration, isokinetic sampling will be necessary. As stack gas velocities vary with fuel, excess O_2, load, and other parameters, different sampling velocities would be necessary.

As there appeared to be minimal available data which pertained to the effects of sampling rates, acid collection efficiency, and possible alternatives to the selective condensation approach, a study was undertaken to establish such data. This work presents the effects of sampling rates on the gas-particulate sulfate distribution in a selective condensation sampling system. Also addressed in this study are the collection efficiency of the Goksoyr-Ross condensation coil and a potential alternative method for isolating gaseous H_2SO_4.

EXPERIMENTAL

All of the sulfate measurements were performed on a 100,000 lb./ hr. oil-fired steam boiler which operates solely as a heat source for a local college campus. Throughout the tests, an excess oxygen of 4% to 5% was utilized to burn a nominal 2.2% sulfur and 350 ppm (w/w) vanadium residual fuel oil. The sampling was conducted just subsequent to the last boiler pass but prior to the preheater and stack.

The manual selective condensation sampling system used during the measurements is depicted in Figure 1. A standard 10.2 cm (4 inch) port cap with a centered 2.54 cm (1 inch) Swagelok* fitting holds a .9 M (3 foot) long, 2.54 cm (1 inch) O.D. heated quartz probe. Following the probe is a high-temperature, all-quartz filter holder. Both the probe and filter holder are heated and temperature controlled with separate variable voltage controls located in the sampling module. Also located in this module are four thermocouple readouts which provide temperature readings for the flue gas, probe, filter, and condenser.

The filters used for the sulfate measurements were fabricated from high-purity quartz and were shown (5) to be 99.9% effective for collecting particle sizes down to 0.3 μm. During the study the filter was maintained between 265°C and 288°C during sampling.

Following the high temperature filter is the Goksoyr-Ross acid condensation coil which utilizes a medium porosity frit. The purpose of the frit is for the collection of any acid aerosol which has not been collected by impaction in the preceding temperature-controlled

---

*Mention of brand names does not imply EPA endorsement.

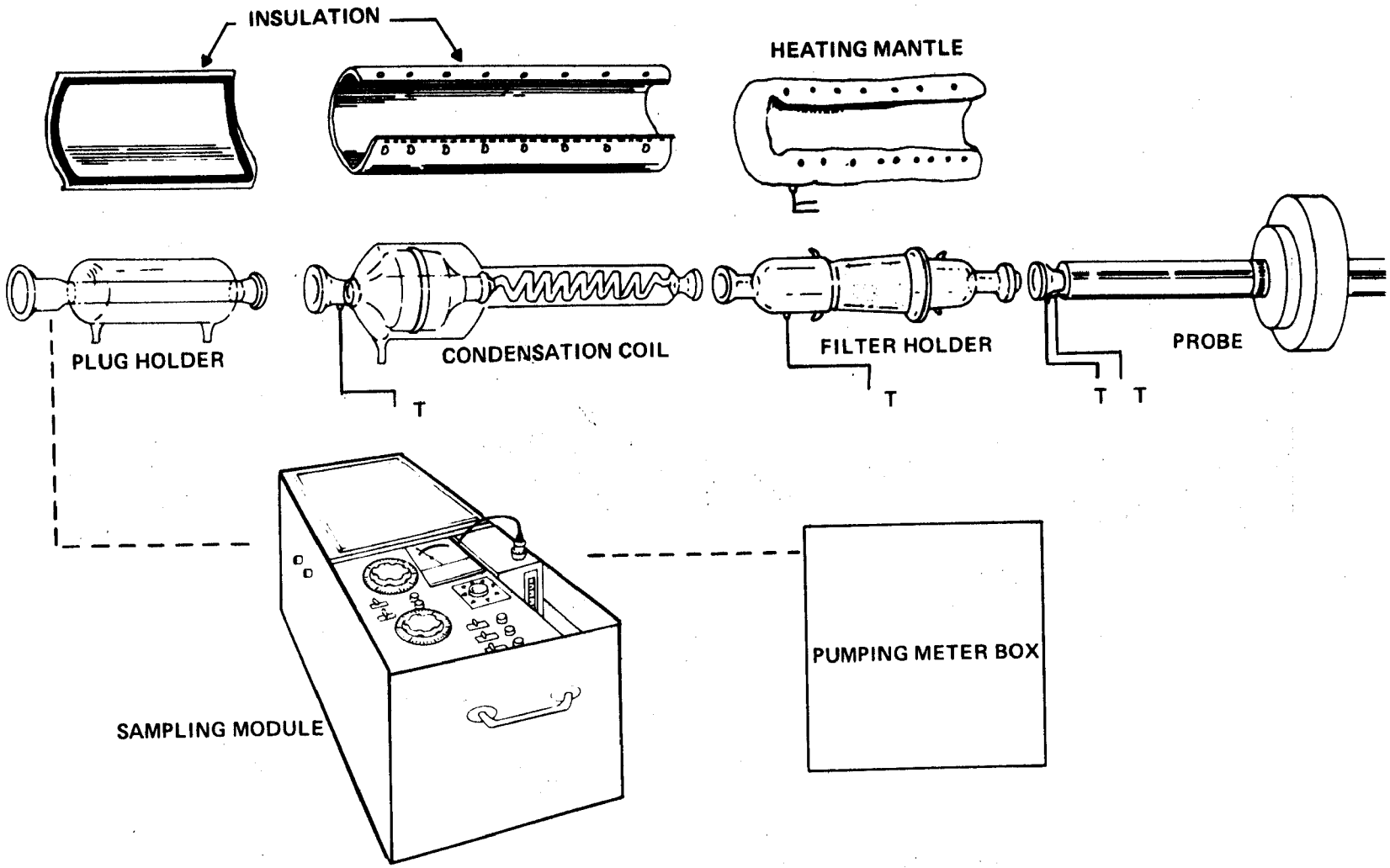

Figure 1. Schematic drawing of manual acid condensation system.

spiral coils. During some of the measurements, a specially constructed glass wool plug holder (also shown in Figure 1) was used either as a backup or substitute acid collector to the condenser. As with the condenser, the plug holder was temperature controlled by circulating water from the water bath in the sampling module.

Following the temperature-controlled acid collection devices is an ice bath with isopropanol (IPA) and peroxide (3% H_2O_2) impingers for collecting any acid penetrating the previous devices as well as the sulfur dioxide (SO_2).

After the impingers is a gas meter-gas pump box. Sampling rates were determined by timing the gas meter revolutions with the second-hand of a stopwatch.

Each sample run consisted of separate fractions collected from the probe, filter, condenser, backup filter plug, IPA, and H_2O_2. Analysis of each fraction was accomplished by a Barium-Thorin titration (6). It was necessary to pass the sample fractions recovered from the probe wash and filter through a mixed bed resin to avoid cation interference to the titrations.

RESULTS

Three basic series of measurements were performed:

1. a series of measurements to establish sampling rate effects on sulfate distribution in the sampling train

2. a series of sulfate measurements to evaluate the collection efficiency of the Goksoyr-Ross coil

3. a series of measurements to establish if the condenser approach to acid collection could be substituted with a more simple approach.

Sampling was conducted over a sampling rate interval of 2 to 16 l/min. The results of the sulfates collected, in terms of total sulfate and percent occurrence of total sulfate in three fractions, are presented in Table 1.

A second series of tests were performed to establish the collection efficiency of the Goksoyr-Ross condenser. The results of these measurements are presented in Table 2. The sulfate concentrations are presented as ppm on a vol/vol basis.

Table 1. Sulfate Distribution and Sampling Rate

Sample Rate(1)	T-SO_4(2)	%-P(3)	%-F(3)	% "Acid"(4)
16	36.3	10.7	9.9	79.3
12	38.6	13.9	7.8	78.4
8.3	35.8	12.3	13.9	73.8
7.5	31.6	13.6	16.8	69.6
6.5	27.2	15.8	17.8	66.4
5.1	41.9	18.3	10.6	71.1
4.7	37.8	36.0	12.2	51.8
3.8	32.8	19.1	30.0	50.9
2.3	50.1	23.9	36.9	39.2

(1) In l/min.
(2) Total sulfate collected, expressed as ppm (vol/vol)
(3) Percent of total sulfate collected in probe (P) and filter (F), respectively, in ppm (vol/vol)
(4) Percent of total sulfate passing probe and filter

Table 2. Total Sulfate With and Without Plug

Sample >	PW	Filt	Cond	Plug	SO_2	%-T(c)	%-T(wp)
1	4.4	5.0	25.6	0.4	824	4.12	4.16
2	4.3	5.3	21.2	0.7	745	3.98	4.16
3	6.9	5.4	26.5	0.7	944	4.21	4.28
4	8.4	3.5	26.8	1.6	805	4.72	4.90
5	8.9	4.1	21.7	2.7	768	4.49	4.81
6	4.2	6.9	21.2	2.8	717	4.37	4.73

PW = probe wash; Filt = filter; Cond = Goksoyr-Ross condenser; plug = glass wool plug; and SO_2 = H_2O_2 catch. %-T(c) and %-T(wp) = Total SO_4/Total SO_4 Δ SO_2) x 100% for condenser and for condenser and wool plug, respectively, using ppm (v/v).

The sampling arrangement used to obtain the data in Table 2 consisted of a Goksoyr-Ross condensation condenser followed by the glass wool plug as a backup acid collector. For samples involving glass wool, untreated, reagent grade Pyrex wool which showed no sulfate blank was used. Both the condenser and glass plug were maintained at 60°C during sampling. A slight increase in acid collection is apparent when including the plug catch as the average SO_2 conversion factor (%-T) increased from 4.37% to 4.74%.

The final series of sulfate measurements involved the substitution of the Goksoyr-Ross condensation condenser with the temperature controlled glass plug holder. During these measurements, the glass plug was maintained at 60°C during sampling. The results of several measurements utilizing the two sampling train arrangements are presented in Table 3.

Table 3. Acid Collection with Condenser and Glass Wool Plug

Condenser			Glass Plug		
Sulfate(1)	SO_2(1)	%-T(2)	Sulfate(1)	SO_2(1)	%-T(2)
35.5	824	4.17	31.5	707	4.27
31.6	745	4.07	37.8	896	4.05
42.2	944	4.28	58.5	858	6.38
41.5	805	4.90	33.7	777	4.16
38.8	768	4.81	30.7	649	4.52
35.6	717	4.73	31.3	728	4.12

Averages:	Sulfate(1)	SO_2(1)	%-T(2)
Condensation	37.6 ± 3.4	801 ± 57	4.49 ± 0.32
Glass Plug	37.4 ± 7.4	769 ± 58	4.58 ± 0.43

(1) In ppm (v/v)
(2) %-T = Total SO_4/(Total SO_4 + SO_2) x 100%

Within experimental error, there appears to be no difference in sulfate collection. The average standard deviation of ±0.32 to ±0.43 represents a 7.13% to 9.39% deviation for condenser and glass plug sulfate conversion, respectively.

DISCUSSION

A very significant effect on sulfate measurements (in terms of differentiating gaseous H_2SO_4 from particulate related sulfate) occurs as the sampling rate varies. For combustion source measurements of sulfates, the flue gas stream velocity can vary two or threefold from one source to another, and this effect on acid-particle separation presents a special problem. For example, for a flue gas at 300°F (150°C) and 10% moisture, a variation from 25 to 75 ft/sec. (7.6 to 22.8 m/sec.) in velocity will result in isokinetic sampling rates from 5 to 15 l/min. when using a 3/16 inch nozzle. From the data in this study, the resulting fraction of the total sulfate collected as acid beyond the filter would be from 61% to 75%. While isokinetic sampling using this procedure would result in a correct total sulfate value, the ability of the procedure to serve as a characterization method appears quite limited.

Apparently little acid penetrated the coil and frit during the backup plug collections during this study. A slight increase in calculated SO_2 conversion to sulfate does occur, and, as the data are presented in the chronological order of collection, the possibility of some phenomena involving acid retention and acid carryover from the frit may be occurring. This, however, is highly speculative with the limited amount of data presented here.

This study has also shown that in the sampling procedure presented an equivalent acid collection component can be used to replace the awkward condensation condenser. While the temperature of the glass plug holder must be maintained above the H_2O dewpoint and below the acid dewpoint, requiring the waterbath or some type of heat source, it offers a simpler method of acid collection than the condenser. For sources with high negative pressures, the additional pressure drop in the sampling system (12 in. Hg for the medium frit) makes high sampling rates difficult to achieve. During the study a different glass plug was used in the plug holder for each sample collected. To be a convenient method, the plug should be able to collect acid on a repeatable basis. Whether this is possible has yet to be determined.

In conclusion, while the selective condensation approach appears to be the best sulfate measurement method available at present, it must be used with caution, particularly with respect to interpretation of results. Since the problem involves the filtration process, placing the filter on the sample inlet end of the probe (in the stack) would eliminate acid-particulate association in the probe; however, the same problem of acid retention

at the filter interface would still remain. Use of the condensation procedure for sulfate measurements should, therefore, be performed by a well-defined procedure if comparisons of results either from separate sources or by separate sampling personnel are to be meaningful.

REFERENCES

1. Homolya, J. B., and J. L. Cheney. A Study of the Local Ambient Air Impact of Primary Sulfate Emissions from the Combustion of Residual Oil. Presented at the 175th Annual ACS, March 1978.

2. Cheney, J. L., J. B. Homolya, and H. M. Barnes. Measurement and Identification of Primary Sulfates Emitted from Combustion Sources. 70th Annual AICHE, New York, Nov. 1977.

3. Cheney, J. L., C. R. Fortune, J. B. Homolya, and H. M. Barnes. The Application of an Acid Dewpoint Meter for the Measurement of SO_3/H_2SO_4 Emissions. Proceedings of the Fourth Annual Conference on Energy and the Environment, Cincinnati, Ohio, 1976.

4. Goksoyr, H., and K. Ross. Shell Report No. M-211, Thornton Research Center, 1962.

5. Benson, A. L., P. L. Levins, A. A. Massucco, and J. R. Valentine. Development of a High Purity Filter for High Temperature Particulate Sampling and Analysis. EPA-650/2-73-032, Nov. 1973.

6. Cheney, J. L., W. T. Winberry, and J. B. Homolya. Evaluation of a Method for Measuring Primary Sulfate Emissions from Combustion Sources. J. Environ. Sci. Health, A12(10):549, 1977.

A Specific Method for the Determination of Sulfuric Acid Emissions from Combustion Sources

Paul Urone
University of Florida

Robert A. Lucas
Employers Insurance of Wausau

ABSTRACT

The sampling and analysis of sulfur trioxide and sulfuric acid in emission sources continue to be a source of difficulty. Various standardized and proposed alternate testing methods are under study, ranging from simple acid-base and colorimetric techniques to advanced instrumented methods. Most of the difficulties in sampling and analysis are related to the high concurrent concentrations of sulfur dioxide, other acids, and particulate sulfates.

A colorimetric reagent was investigated for the specific determination of sulfuric acid emissions. The method utilizes a sulfone dye precursor, which reacts with the sulfuric acid or sulfur trioxide to form the sulfone dye. At a given pH, the color of the dye is specific for the sulfonation reaction and independent of other acids or sulfate compounds present. Three dye precursors, phenolphthalein, thymolphthalein, and acid orange A have been studied; each reacts specifically with sulfuric acid aerosols and strong ($\geq$5M) sulfuric acid solutions. Filters impregnated with the dye precursors develop the specific colors, but the colors fade with time. Additional studies are being undertaken to prevent reversal of the reaction and to determine its sensitivity limits.

INTRODUCTION

The sampling and analysis of sulfur trioxide and sulfuric acid in emission sources continue to be a source of difficulty. At present, a number of methods are used to determine sulfuric acid mist in either emission sources or ambient air. These methods can generally be divided into two basic operations: (1) the sampling or collection of the aerosol; and (2) the analysis or measurement of the collected aerosol (1).

The major methods of collection of sulfuric acid aerosols are absorption into isopropyl alcohol or alkaline solutions, controlled and uncontrolled condensation, impaction, and filtration.

The major methods of measurement and their chemical basis for the analysis of H_2SO_4 at present are:

a) Sodium Hydroxide Titration (1). This is a simple and direct method; however, it is not specific and depends upon the assumption that the only acid present is H_2SO_4 and that no basic substances are present to interfere.

b) Barium Ion Titration (2). This is the method specified by EPA's Method 8. The reaction is specific for any soluble sulfate. Thorin is used as the indicator.

c) Chloranilate Method (1). This method depends on the release of the colored chloranilate ion from the insoluble barium chloranilate salt. Sulfate reacts with the barium chloranilate to form insoluble barium sulfate and release the chloranilate ion to color the solution in a quantitative manner.

d) Turbidimetric Method (1). In this method barium ion is used to precipitate the sulfate as a uniformly distributed suspension. The turbidity of the solution is measured spectrophotometrically.

e) Flame Photoluminescent Detector (1). This method relies on the principle that all sulfur compounds fluoresce in hydrogen-rich flames at a wavelength that is relatively specific for sulfur. The fluorescent light is measured by means of a photomultiplier tube.

f) Vanadium Method (3). The sulfuric acid is determined by ammonium vanadate aqueous solution which forms a yellow

color. The intensity of this color is a linear function of sulfuric acid concentration.

g) Bromphenol Blue Method (4). This is a simple method and depends on a color change due to sulfuric acid in an aqueous solution of isopropanol and bromphenol blue. It is a measure of total acidity and assumes no basic substances are present to interfere.

h) Coulometric Method (5). This is a simple method and nonspecific and provides a measure of the effective hydrogen ion concentration only.

The major difficulties encountered by the presently available methods are due generally to the sampling methods with their inherent interferences from co-pollutants and sampling efficiency. The various analytical methods have been shown to be reliable enough, considering the limitations of the sampling methods.

Formation of H_2SO_4 Aerosol

During combustion of a fossil fuel, a small fraction (1%-5%) of the sulfur is oxidized to SO_3. This can result in a yield of 5 ppm to 50 ppm in the flue gas as SO_3, depending upon such factors as sulfur content, excess air, and combustion temperature (6). Since most of the sulfur in power plant flue gases appears as SO_2, reactions may occur on filter and collection surfaces as well as combustion aerosols. Aerosol formation may also be initiated by homogeneous gas phase reactions, with subsequent clustering reactions leading to the formation of new particles (7).

New sulfuric acid particle formation may be viewed as being a three-step process (8)(9):

1. Oxidation of SO_2:
   $SO_2(g) + 1/2\ O_2(g) \xrightarrow[cat]{} SO_3(g)$
   The gas phase oxidation of SO_2 to SO_3 is assumed to be the rate determining step in the production of H_2SO_4.

2. Reaction of SO_3 with water to form H_2SO_4:
   $SO_3(g) + H_2O(g) + M \rightarrow H_2SO_4(g)$
   At temperatures below 400°F, essentially all the SO_3 present is converted to H_2SO_4 at equilibrium. In contrast to the formation of SO_3, the formation of H_2SO_4 occurs rapidly in the thermodynamically feasible temperature range.

3. Clustering of H_2SO_4 and H_2O molecules to form prenucleation embryos, followed by the heteromolecular nucleation process:

$$H_2SO_4 + X(H_2O) \rightarrow (H_2SO_4)(H_2O)_x \text{ (cluster)}$$

$$(H_2SO_4)(H_2O)_x + H_2O \text{ particles} \rightarrow \text{larger particle}$$

There are several conditions that regulate the two possible reaction channels for the conversion of SO_3 to H_2SO_4. One involves a direct gas phase reaction with H_2O and the other involves a surface reaction as SO_3 is scavenged by a pre-existing aerosol particle. In general, in an environment with higher relative humidity, less total surface area of suspended particles, lower temperature, and a higher production rate of SO_2 molecules, more secondary new sulfuric acid aerosols will be generated.

Sulfonation

A specific analytical technique for the analysis of sulfuric acid is possible due to the sulfonating ability of sulfuric acid with aromatic and heterocyclic compounds. By definition sulfonation is the process of replacement of a hydrogen atom in an organic compound with the sulfonic group (SO_3H^+). The replaced hydrogen atom and the hydroxyl ion (OH^-) from sulfuric acid form a water molecule (10), (Figure 1).

There is no clear cut guideline to follow when considering reaction temperatures, concentrations, percent product recovery, and reaction rates when considering sulfonation of species not generally dealt with in industrial applications. However, sulfonation of rings which are substituted with electron withdrawing groups (-CL , $-Br^-$, $-SO_3H$, $-CO_2H$, $-NO_2$) proceeds with difficulty since the ring is already electron poor. Electron donating groups ($-NH_2$, -OH, -OR, $-O^-$) attached to the ring aid sulfonation and are ortho and para directing.

Kinetic and mechanistic studies of the sulfonation of aromatic compounds have led to the conclusion that it is an S_E^2 reaction with monomeric SO_3 as the effective reacting species, not only with SO_3 itself, but also when sulfuric acid or oleum is used. It has been proposed that in sulfuric acid an acid solvate of SO_3 is the active species. This is considered possible, but less likely than free SO_3 (10).

Aromatic compounds can be sulfonated with concentrated H_2SO_4 , but as the concentration of the water increases during reaction, the rate of sulfonation steadily decreases, the reaction rate being

SULFONATION REACTION

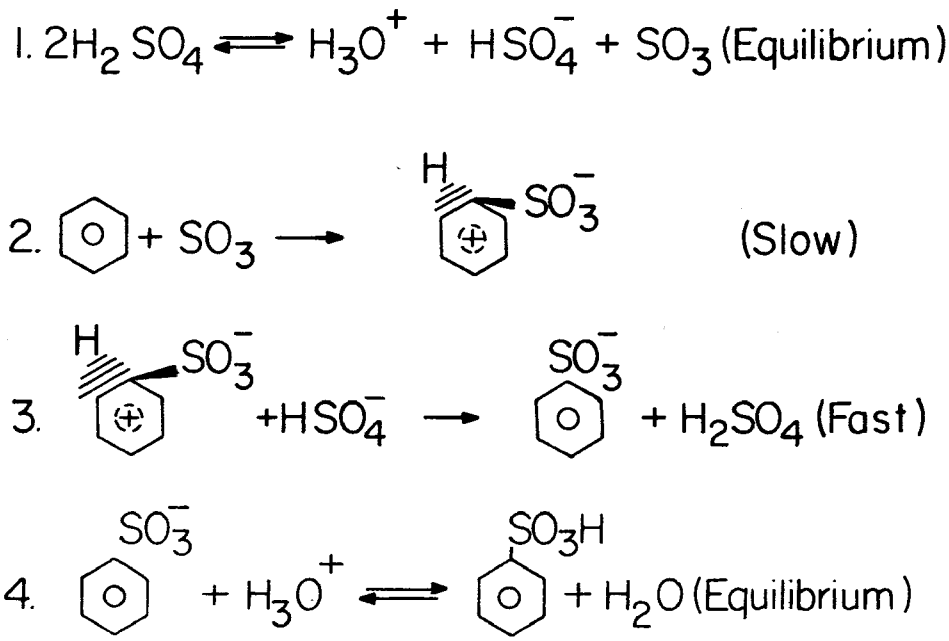

DESULFONATION REACTION

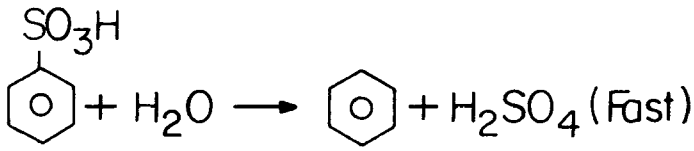

Figure 1. Sulfonation reactions.

inversely proportional to the square of the water concentration. The reaction ceases when the acid concentration reaches a level characteristic of each compound. Sulfonation differs from most other types of electrophillic substitution in that the process is readily reversible under mild conditions (11). Desulfonation of some aromatic compounds proceeds rapidly and in good yield by simple dilution in aqueous medium. Therefore, to carry sulfonation reaction to completion, the removal of water formed from the reaction is essential. However, the hydrolysis of sulfonated aromatics will not occur if the acid strength is kept high.

Filter Material and Pretreatment--The type of filter used to collect the sulfuric acid aerosol was the Gelman Type A/E glass fiber filter. Glass fiber filters combine the desirable features of high retention efficiency with high flow rates. They have been shown to have the tear resistance and wet strength necessary to enable them to withstand being submersed into the precursor solution followed by drying and filtration (12).

These filters are devoid of any organic binders and have a minimum retention efficiency of 99.7% for 0.3 μm particles as measured by the dioctyl phthalate penetration test. Various researchers have found that glass fiber filters can react with atmospheric sulfur dioxide and sulfuric acid catalytically on the glass surface and thus seriously interfere with the determination of sulfuric acid aerosols (13-15). Barton and McAdie developed a method of treatment of the glass fiber filters by soaking in 20% sulfuric acid followed by gentle boiling for 10 minutes, rinsing with distilled water, 80% isopropanol, and finally acetone. The filters are then dried in a desiccator (16). This method of filter treatment was selected for this study.

Materials and Methods--Acid orange A, phenolphthalein, and thymolphthalein (Figure 2) were selected as the indicator precursors. To prepare a 0.4% solution of both compounds, 0.4 g of each was dissolved in a slightly alkaline solution of sodium hydroxide in a 100 ml volumetric flask. Because both compounds are acid base indicators, a color change occurred in the basic solution. To bring the pH to a neutral range, concentrated HCl was applied drop-wise until a clear solution resulted. The solution was then diluted with distilled water to the desired final volume.

The filters were treated by submersing them into the precursor indicator solutions and allowing them to soak for five minutes. The filters were then removed and allowed to dry in a desiccator.

ACID ORANGE A

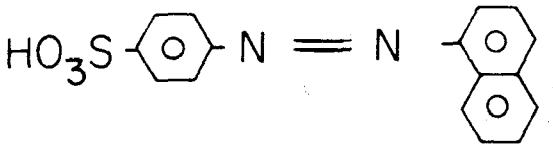

PHENOLPHTHALEIN

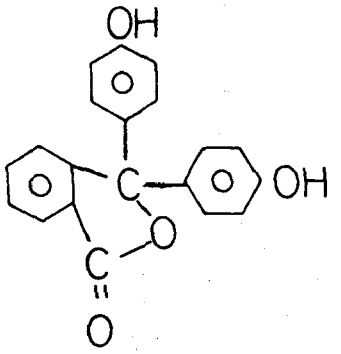

THYMOLPHTHALEIN

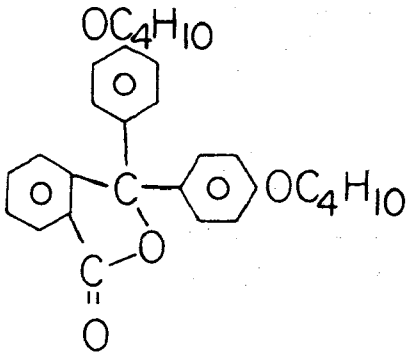

Figure 2. Dye substrates selected for sulfonation reactions.

To test the precursor indicators for color change, two methods were used to apply the sulfuric acid. The first method was simply the addition of various concentrations of H_2SO_4 directly onto the treated filters with an eye dropper. The second method consisted of a compressed air supply filtered through a silica gel bed followed by flow measurement in a rotameter. After the rotameter the air was used to generate a sulfuric acid aerosol by the use of a DeVilbiss model atomizer. The aerosol generated was then equilibrated in a 4 ℓ glass chamber. The air flow was separated at the top of the glass chamber with excess air going to a hood for removal and the remaining fraction going to a filter holder followed by a critical orifice, silica gel trap, and air pump (Figure 3). The air flow was held at 3.8 ℓ/minute through the rotameter and 0.9 ℓ/minute through the filter holder.

An absorbance curve was run on a Bausch and Lomb Spectronic 20 for the reaction products from the addition of 20 ml of concentrated H_2SO_4 to 20 ml of phenolphthalein and thymolphthalein solutions in an ice bath. The absorbance curves obtained are shown in Figures 4 and 5.

The next procedure was to see if the sulfonated products could be easily removed from the filter material. The various extracting solutions used were: distilled water, 6 N hydrochloric acid, methanol, 20% nitric acid, triethylene glycol, benzene, and hexane.

Based on previous work of Joseph Griffiths (17), acid orange A was selected as a possible precursor dye. Published results (18) indicate that this dye in a solution of concentrated H_2SO_4 would sulfonate easily and result in a very noticeable color change. Acid orange A was prepared in the lab by relatively simple chemical procedures. Its structure, along with the structure of phenolphthalein and thymolphthalein, appears in Figure 2.

A 0.15% solution of acid orange A was prepared by dilution of 0.15 g acid orange A in 50 ml of distilled water and 50 ml of methanol. The same procedure of filter treatment and testing was used as for the indicator precursors.

Three absorbance curves were run on the acid orange A: one on the solution itself without any reaction, the second on the reaction product of 20 ml of concentrated H_2SO_4 added slowly to 20 ml of acid orange A in an ice bath, and the third on the solution produced from rinsing a filter that collected sulfuric acid aerosol from the atomizer, with 6 N hydrochloric acid. The results of these data can be seen graphically in Figure 6.

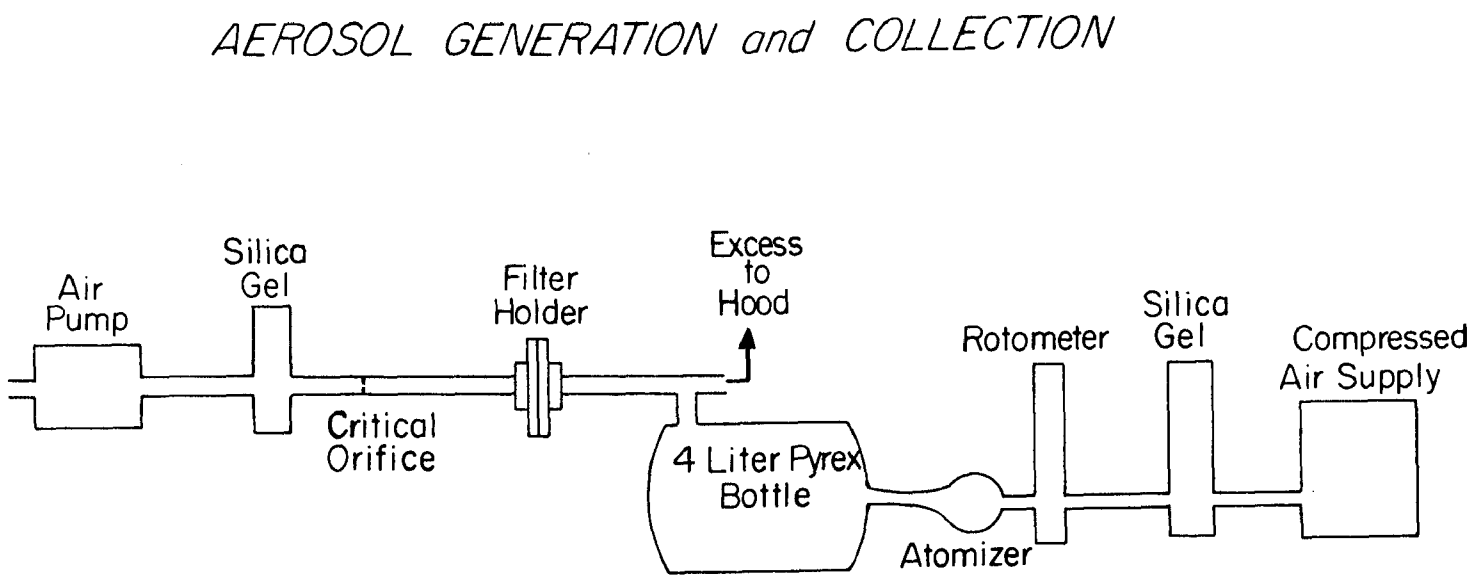

Figure 3. Apparatus for the generation and collection of sulfuric acid aerosol.

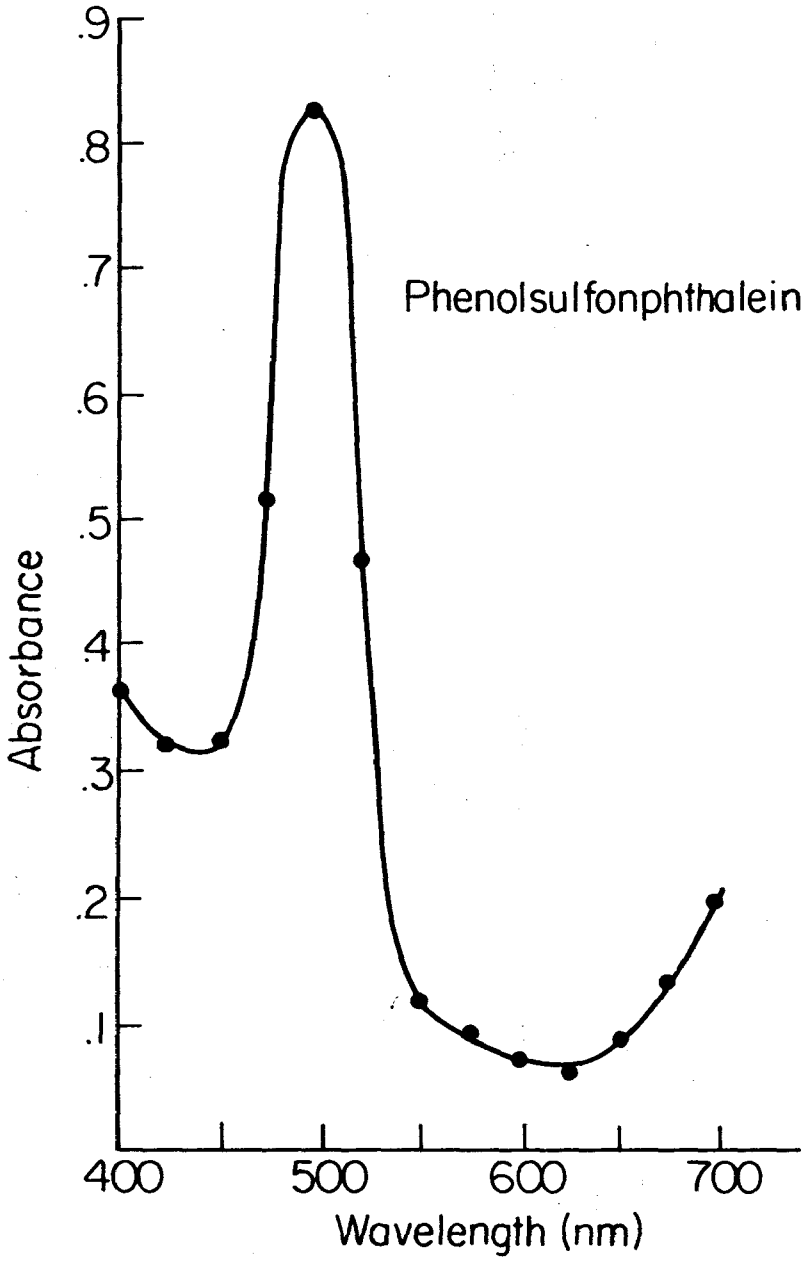

Figure 4. Phenolsulfonphthalein absorbance curve.

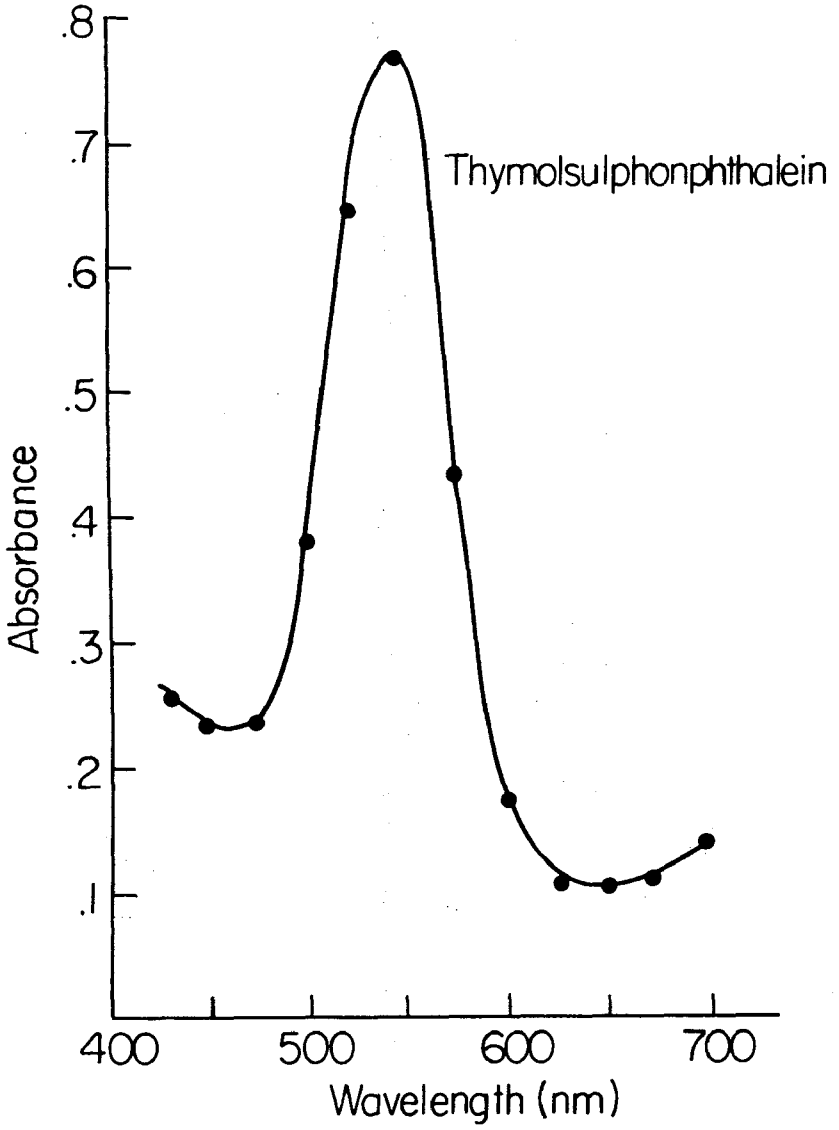

Figure 5. Thymolsulfonphthalein absorbance curve.

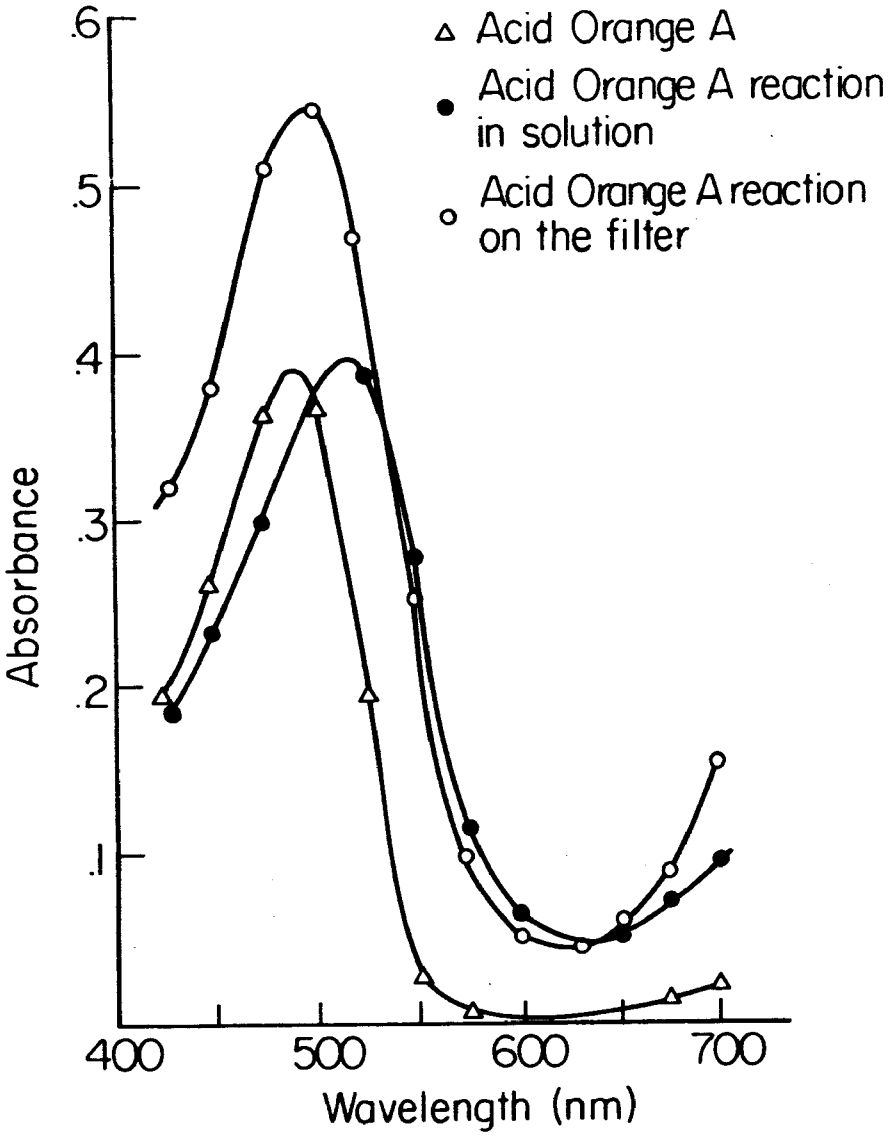

Figure 6. Acid orange A absorbance curves.

RESULTS AND DISCUSSION

Phenolphthalein and thymolphthalein reacted with 5 M H_2SO_4 and stronger solutions to produce noticeable color developments on the white filters. The phenolphthalein filters turned from yellow to orange as the concentration applied increased. Thymolphthalein filters turned various shades of pink as the concentration was varied. The products from both indicators reacted in solution showed strong absorbance peaks, phenolphthalein at 500 nm and thymolphthalein at 550 nm.

The removal of the colored products by the various extracting solutions resulted in a reversal of the sulfonation reaction, and a clear solution was produced in all cases. This reversal could be expected in distilled water due to sulfonation reactions being reversible in excess water; however, the several alcohols and organic solutions were not expected to give such results. After observing this fact, filters treated with sulfuric acid were allowed to stand exposed to room air for several minutes after treatment. The color on the filters gradually faded until after about one hour no color development remained. This implies that the reaction is not only readily reversible in aqueous solution but also when exposed to room air. Heating at 100°, 150°, and 200°C failed to fix the product on the treated filters. In fact, instead of fixing the product, it aided the reversal rate.

Acid orange A changed in color from a light orange to magenta red for sulfuric acid concentrations greater than 5 M. The reaction on the filter from the application of 6 M H_2SO_4 from an eye dropper was observed in one hour at room temperature.

The extraction of the colored product from the filter material resulted in a reversal of the sulfonation reaction of acid orange A in all cases except one. With 6 N (normal) hydrochloric acid as the extracting solution, the red color was retained, whereas all the other extracting solutions turned the product back into an orange solution. This indicates that hydrolysis of the sulfonated acid orange A did not occur in the presence of low acidity.

The absorbance curves in Figure 6 show the various absorbance peaks for acid orange A before and after sulfonation. Acid orange A absorbs strongly at 490 nm compared to acid orange A reacted with H_2SO_4 in solution absorbing strongly at 515 nm. When acid orange A was reacted with H_2SO_4 on the filter and then rinsed off with 6 N hydrochloric acid, the absorption peak occurred at 500 nm.

The absorbance of the solution extracted from the filter shows an intermediate absorbance peak due to the partial reacted and unreacted filter areas.

Filters were then placed in the aerosol generating system as shown in Figure 3. Sulfuric acid was collected until most of the filter surface became reacted. After removing the filter, the color developed faded slowly back to the original color of the precursor dye. This was unexpected, due to the fact that the coated filter which had reacted with H_2SO_4 from an eye dropper had remained relatively stable for one hour or more. The aerosol generated from the atomizer reacted only on the surface of the filter and showed no signs of penetration due to the original orange color appearing on the backside of the filter immediately after removal. The filter in which the sulfuric acid was applied with an eye dropper soaked clear through the filter. This soaking prevented the immediate reversal by the room air. Heating at various temperatures again did not result in dye fixation.

At present, measures are being taken to prevent reversal of the sulfonation products from these three dye and indicator precursors. Sulfonated dyes are used in industry and have been shown to be stable under mild conditions (19). Whether or not any of these dyes can be sulfonated with H_2SO_4 under experimental conditions in air sampling is still a question. If the determination of the sulfuric acid aerosols is to be accomplished by spectrophotometric analysis of sulfonated dyes or indicators, they must be stable and react in a quantitative manner.

ACKNOWLEDGMENT

This work was supported by grants from the Environmental Protection Agency and the Smelter Environmental Research Association.

REFERENCES

1. Urone, P. Source and Ambient Air Analysis of SO_3 and H_2SO_4: State of the Art Report. Health Lab. Sci., 11:246, July 1974.

2. Barton, S. C., and H. G. McAdie. An Automated Instrument for the Specific Determination of Ambient H_2SO_4 Aerosol. Presented before the Division of Water, Air and Waste Chemistry, ACS, New York, 1972.

3. Baviha, C. J., and L. S. Shinkararenka. Determination of Sulfuric Acid in Air by a Vanadate Method. Neftepererab Neftehhim, 9:40-41, 1971.

4. Barrett, W. J., H. C. Miller, J. E. Smith, and C. H. Guin. Development of a Portable Device to Collect Sulfuric Acid Aerosol. Interim Report from EPA, February 1977.

5. Scaringelli, F. P., and K. A. Rehme. Determination of Atmospheric Concentrations of Sulfuric Acid Aerosol by Spectrophotometry, Coulometry and Flame Photometry. Anal. Chem., 41:707-713, June 1969.

6. Crumley, P. H., and A. W. Fletcher. Fuel Combustion Characteristics. Inst. Fuel, 29:322, 1956.

7. Robinson, E., and R. C. Robbins. Sources Abundance and Fate of Gaseous Atmospheric Pollutants. Stanford Research Institute Project PR 6755, February 1968.

8. Kiang, C. S., and D. Stauffer. Chemical Nucleation Theory for Various Humidities and Pollutants. Faraday Sym., 7:26, University Press, Aberdeen, N.D., 1973.

9. Middleton, P., and C. S. Kiang. A Kinetic Aerosol Model for the Formation of New Sulfuric Acid Particles. Submitted for publication, 1976.

10. Gilbert, E. E. Sulfonation and Related Reactions. Interscience Publishers, New York, 1965.

11. Butler, G. B., and K. D. Berlin. Fundamentals of Organic Chemistry Theory and Application. Ronald Press Company, New York, 1972.

12. Gelman Instrument Company Catalog, 1975.

13. Scaringelli, F. P., and K. A. Rehme. Anal. Chem., 41:707, June 1969.

14. Byers, R. L., and J. W. Davis. Sulfur Dioxide Adsorption and Desorption on Various Filter Media. Air Poll. Control Assoc., 20:236.

15. Pate, J. B., B. E. Ammons, G. A. Swanson, and J. P. Lodge, Jr. Nitrite Interference in Spectrophotometric Determination of Atmospheric Sulfur Dioxide. Anal. Chem., 37:942, 1965.

16. Barton, S. C., and H. G. McAdie. Preparation of Glass Fiber Filters for Sulfuric Acid Aerosol Collection. Env. Sci. Tech., 4:769-770, September 1970.

17. Griffiths, J. F. Colorimetric Determination of Sulfuric Acid Aerosol. Paper presented to the Graduate Council at the University of Florida, October 1975.

18. Green, A. G. The Analysis of Dyestuffs. 3rd ed., Griffin and Company, London, 1920.

19. Lubs, H. A., ed. The Chemistry of Synthetic Dyes and Pigments, Reinhold Publishers, New York, 1955.

Measurements of Sulfuric Acid Vapor by Infrared Spectroscopy

Roosevelt Rollins
U.S. Environmental Protection Agency

ABSTRACT

Recent investigations were directed toward the development of an in situ method of measuring gaseous sulfuric acid emissions in flue gases. This presentation summarizes the results of two EPA-sponsored studies conducted to determine the feasibility of measuring sulfuric acid vapor using infrared spectrophotometric techniques. These studies primarily involved the generation and analysis of absorption spectral data in the 7-12 microns region.

Two regions, 8.2 microns (wave number 1220) and 11.4 microns (wave number 880), were identified as being most promising for spectroscopic monitoring purposes. Spectral measurements did not reveal any fine absorption line structure for the sulfuric acid vapor at atmospheric pressure conditions although it was observed that sulfuric acid vapor absorbs rather strongly in both regions. Absorption co-efficients of 6.4/atm-cm and 6.8/atm-cm were obtained at wave numbers 1222 and 880, respectively. The maximum percentage change in absorption strength occurred on the side of the peak at wave number 1222.

As a result of these spectral studies, it is believed that gaseous sulfuric acid emissions can be monitored spectroscopically. A high-resolution system would most likely be required because of the lack of fine absorption line structure for gaseous sulfuric acid. For a tunable diode laser system, it is estimated that a 2 ppm-m sensitivity would be possible.

INTRODUCTION

Recent studies (1) have shown the need for a dependable and reliable method for measuring the concentration of sulfuric acid vapor in flue gases. All of the present analytical methods require some type of sample collection. As a result, measurement errors are likely to occur because of the probable change in the chemical or physical composition of the gas sample during the sampling. The problem of measuring sulfuric acid emissions is further complicated by the highly reactive properties of this vapor and the many substances in the effluent with which it may react.

Because of the inherent problems of maintaining sample integrity in extractive methods, recent activities have been directed toward the development of a non-extractive, instrumental method for measuring sulfuric acid vapor emissions. An in situ method, employing optical techniques, would not disturb the sample and, thus, would provide an indication of the true characteristic of the gas stream.

Infrared absorption spectroscopy is an effective optical technique for detecting a variety of gases. Several investigators (2)(3)(4) have published low-resolution, qualitative spectra which indicate that sulfuric acid vapor absorbs infrared radiation in bands centered at 2.8, 6.9, 8.2, and 11.3 microns. Since water vapor is known also to absorb very strongly in the first two bands, only the last two bands offer promises for stack monitoring purposes.

This paper summarizes the efforts and experimental results of two EPA-sponsored studies involving spectral measurements on laboratory-generated sulfuric acid vapor. These studies were conducted for the purpose of determining the feasibility of measuring sulfuric acid vapor in flue gases by infrared spectroscopy. The initial investigation was performed under EPA Contract 68-02-1774 by Burch and co-workers at Aeronutronic Ford Corporation. Under EPA Contract 68-02-2482, further studies were conducted by R. Eng at Laser Analytics, Inc.

DISCUSSION OF RESULTS

The spectral measurements made at Aeronutronic Ford (5) resulted in low-resolution spectra for H_2SO_4 vapor absorption over the 8-12 microns region. The measurements were made using a grating spectrometer with a spectral resolution that varied from approximately 2 cm^{-1} at 12 microns to 4 cm^{-1} at 8 microns. Figure 1 shows spectral curves of transmission obtained for three samples of hot H_2SO_4 vapor.

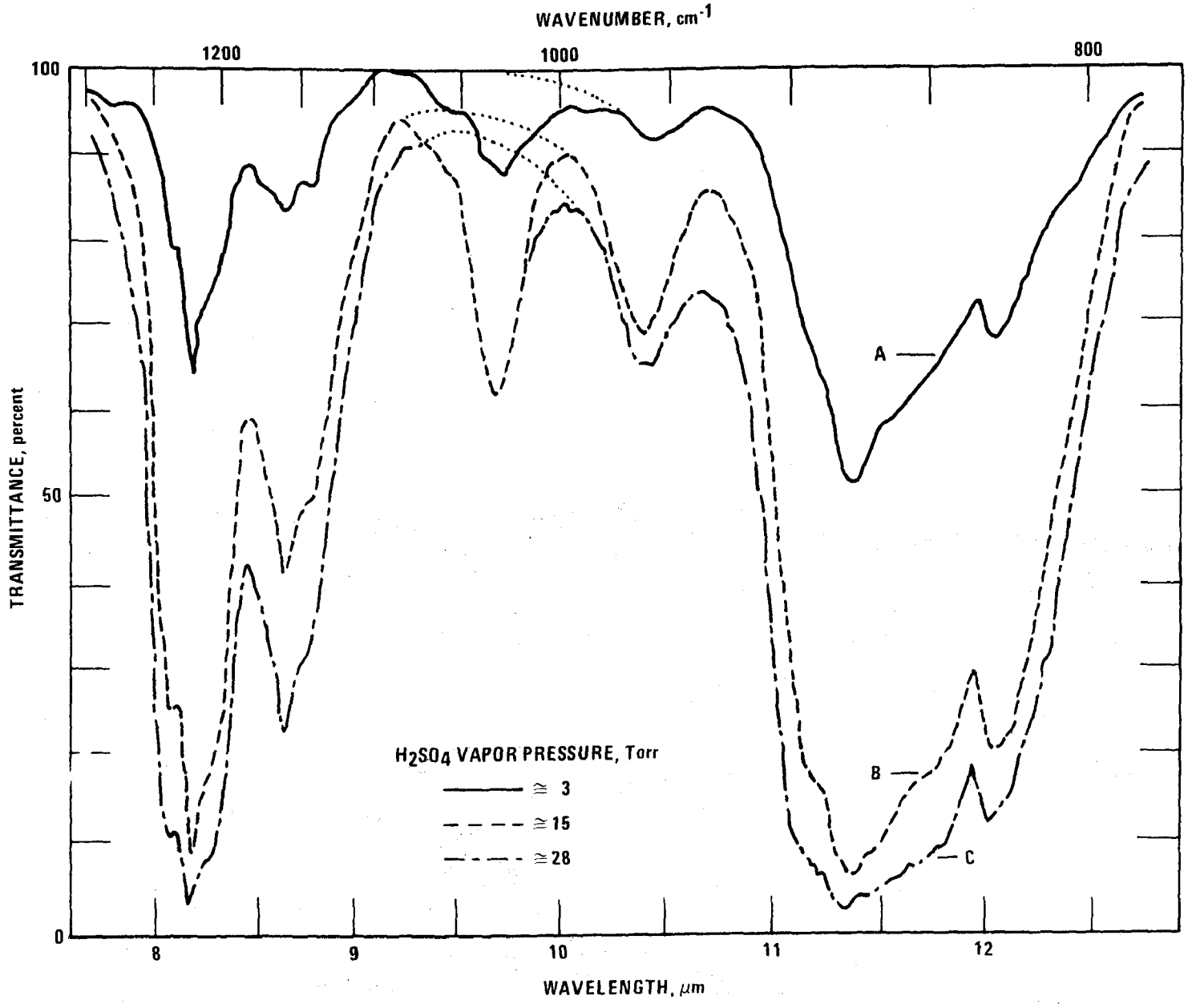

Figure 1. Spectral curves of transmittance for three samples of H_2SO_4. Path length = 52 cm. Vapor temperature = 235°C. The spectral slitwidth varies from approximately 4 cm^{-1} at 8 μm to 2 cm^{-1} at 12 μm.

47

The partial pressures given for H_2SO_4 are estimates based on thermodynamics tables. Two regions, 8.24 and 11.4 microns, were identified as having absorption strengths adequate for monitoring purposes. At wavelengths of maximum absorption, the absorption coefficient is approximately 4.0 $atm^{-1} cm^{-1}$.

Although the absorption by H_2SO_4 vapor is relatively strong, the spectral curves do not show any line absorption features. Alpert (6) has published high-resolution spectral data which indicate many individual H_2SO_4 absorption lines in the infrared region from 1312 cm^{-1} to 1549 cm^{-1}. Based on his data, it was concluded that there might be similar individual absorption lines in the 8.2 μ and 11.3 μ bands. To answer this question, high resolution (<0.1 cm^{-1}) measurements became necessary.

The high-resolution measurements were performed by Laser Analytics (7) utilizing a tunable diode laser spectrometer. Spectral scans were made for the central portions of the H_2SO_4 absorption bands at 8.2 μ (1222 cm^{-1}) and 11.3 μ (880 cm^{-1}). Measurements were made for several H_2SO_4 vapor samples at both low pressure (< 1 torr) and atmospheric pressure conditions. Figure 2 shows typical recorder tracings for a low pressure H_2SO_4 absorption near 1223 cm^{-1}. The traces show some fine structure as well as smooth absorption. Except in this spectral region, there was no fine structure observed anywhere else in the 1222 cm^{-1} and 880 cm^{-1} bands. As expected, the smooth part of the total absorption shows a large variation with H_2SO_4 partial pressure. Figure 3 is a summary of the low pressure scans for the 1210-1240 cm^{-1} region. This plot was obtained by combining a large number of scans like those shown in Figure 2. Similar measurements were made for the 880 cm^{-1} region and the results are shown in Figures 4 and 5. For the H_2SO_4 vapor at low pressure conditions, absorption coefficients are 7.2 and 7.0 $atm^{-1} cm^{-1}$ at 1222 cm^{-1} and 880 cm^{-1}, respectively.

Using a flowing-gas cell with dry nitrogen as the carrier gas, spectral measurements were made for H_2SO_4 vapor at atmospheric pressure. After identifying prominent absorption locations, scans at atmospheric pressure were performed for 2 cm^{-1} intervals in both regions. Figure 6 shows a summary of the atmospheric spectral data and the location of the 2 cm^{-1} interval for the 1222 cm^{-1} region. Similarly, Figure 7 shows a summary for scans in the 880 cm^{-} region. For H_2SO_4 vapor at atmospheric pressure conditions, absorption coefficients of 6.5 and 6.9 $atm^{-1} cm^{-1}$ were obtained at 1222 cm^{-1} and 880 cm^{-1}, respectively.

To determine the severity of possible interferences, high resolution measurements were made for the interferants H_2O, SO_2,

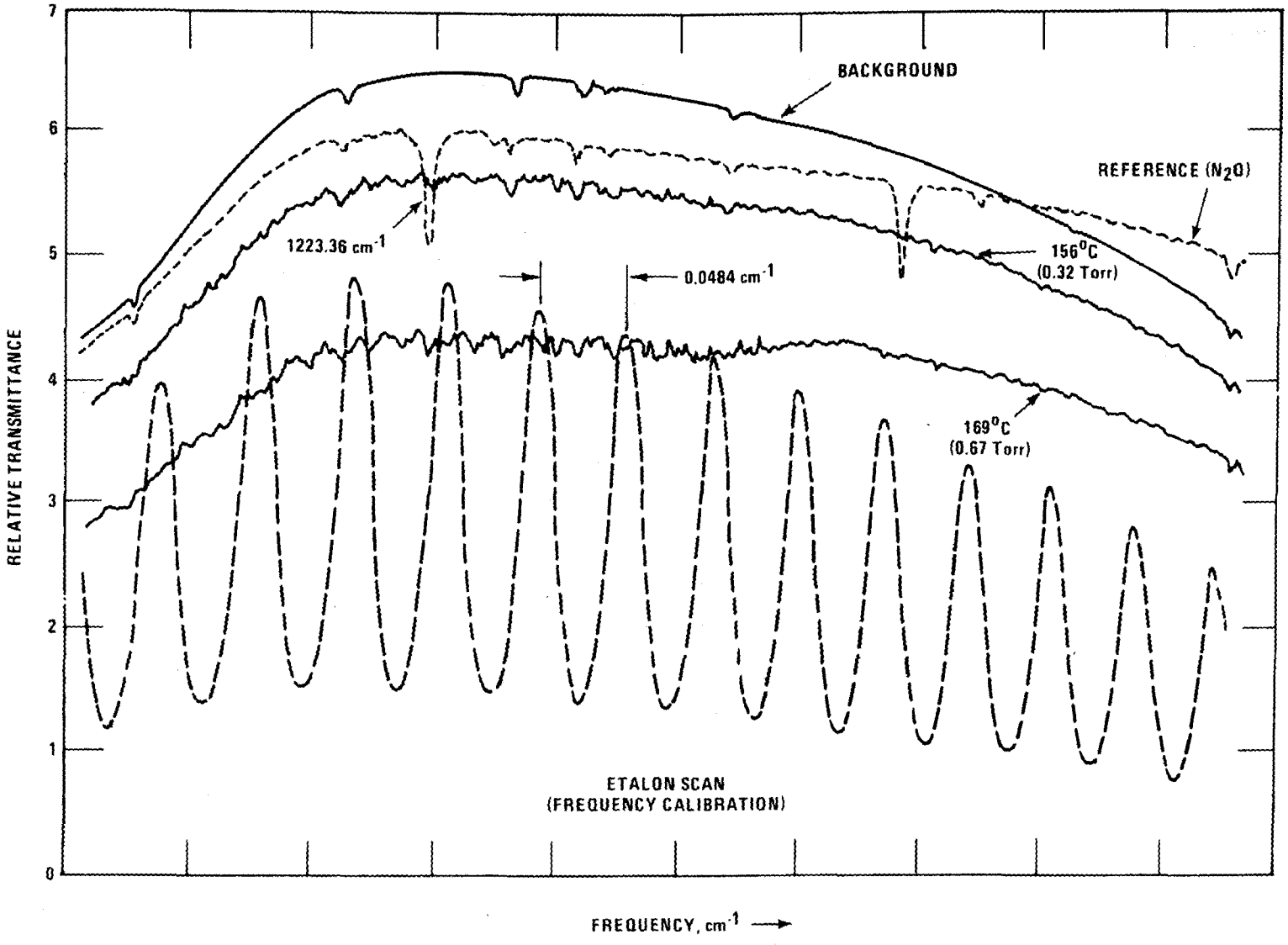

Figure 2. H_2SO_4 absorption near 1223 cm^{-1}.

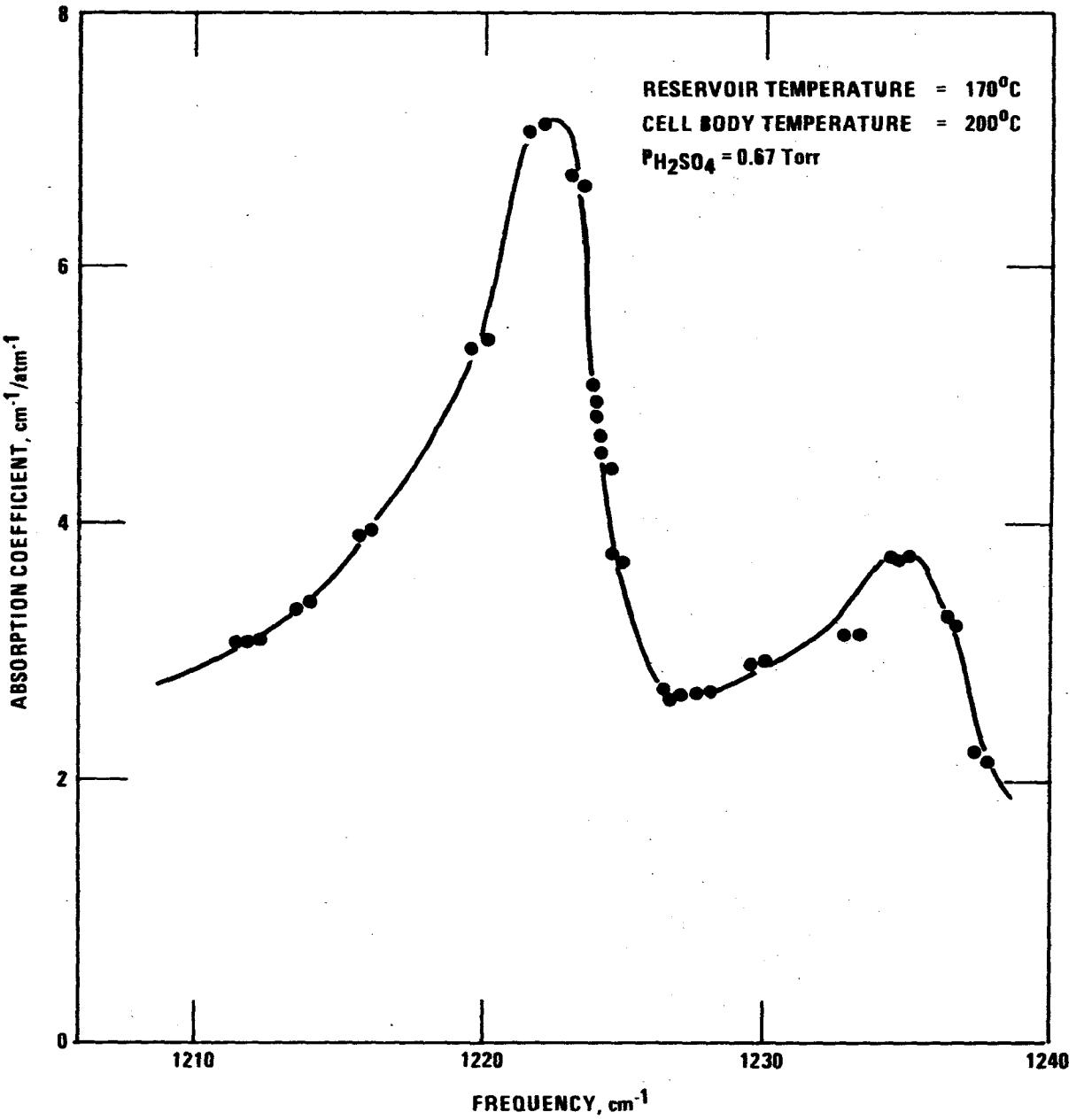

Figure 3. Low pressure H_2SO_4 absorption (P ~ 0.67 Torr, T = 170°C).

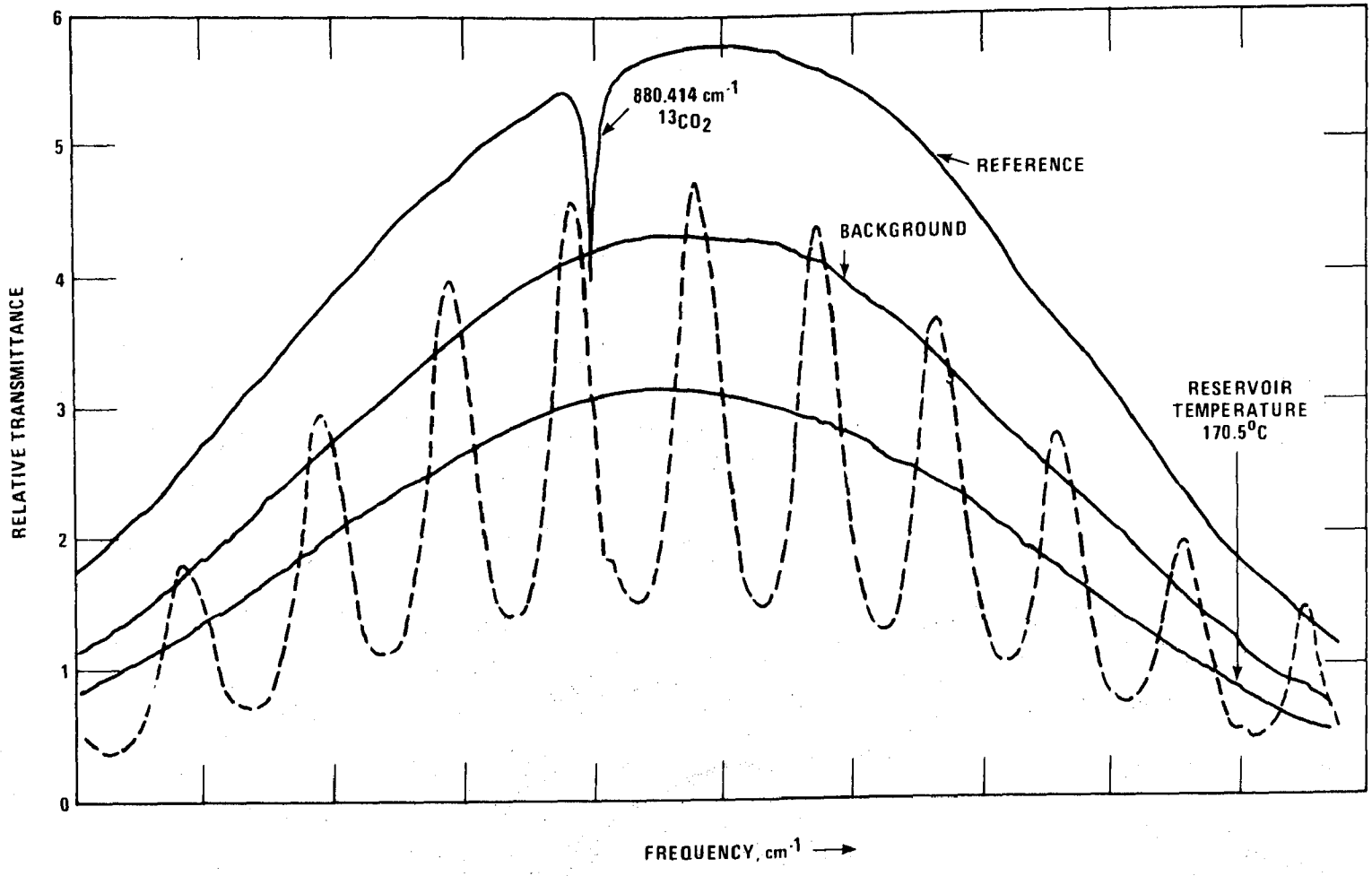

Figure 4. Low-pressure H_2SO_4 absorption near 880.5 cm^{-1}.

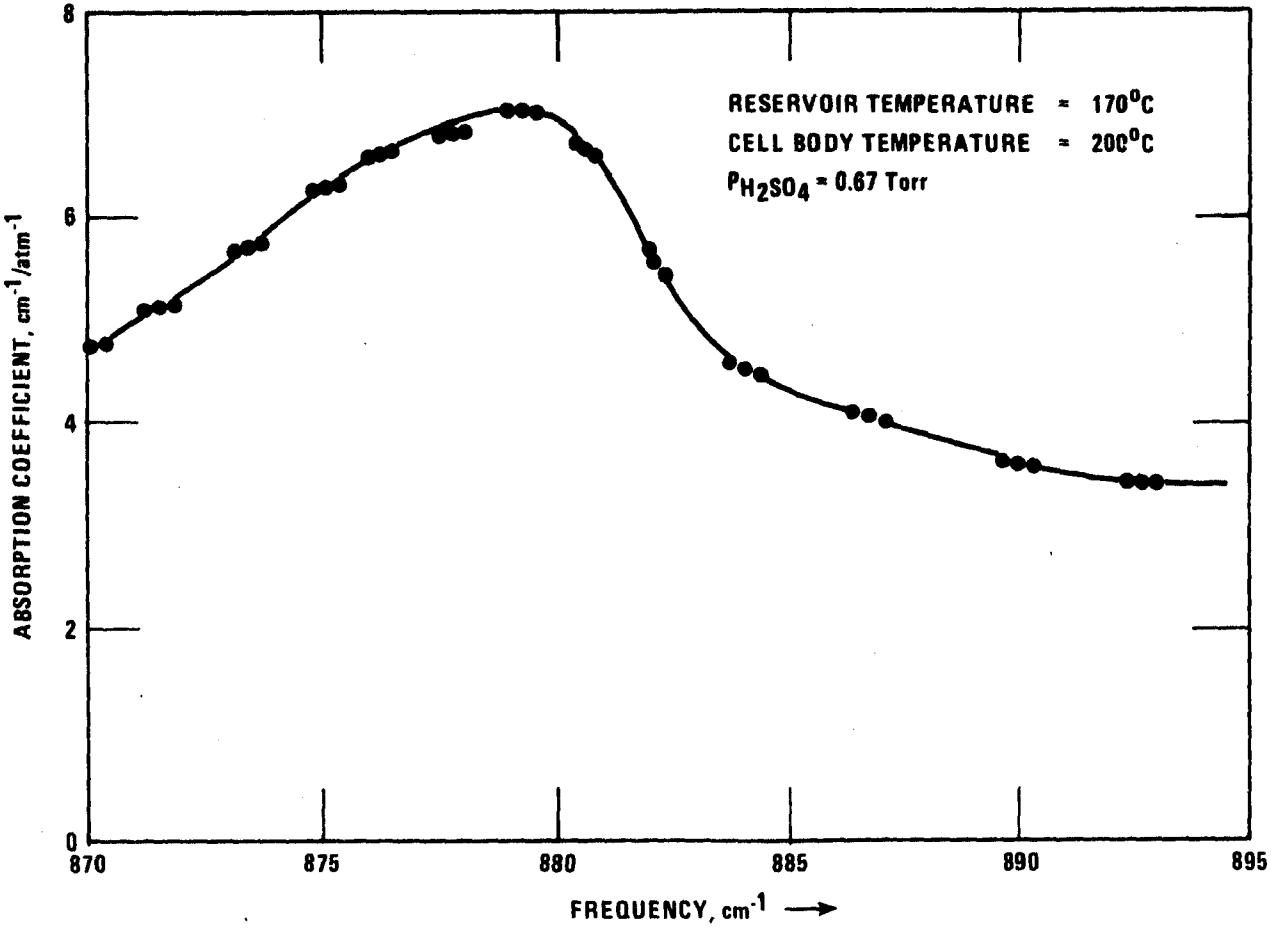

Figure 5. Low pressure H_2SO_4 absorption (P ~ 0.67 Torr, T = 170°C).

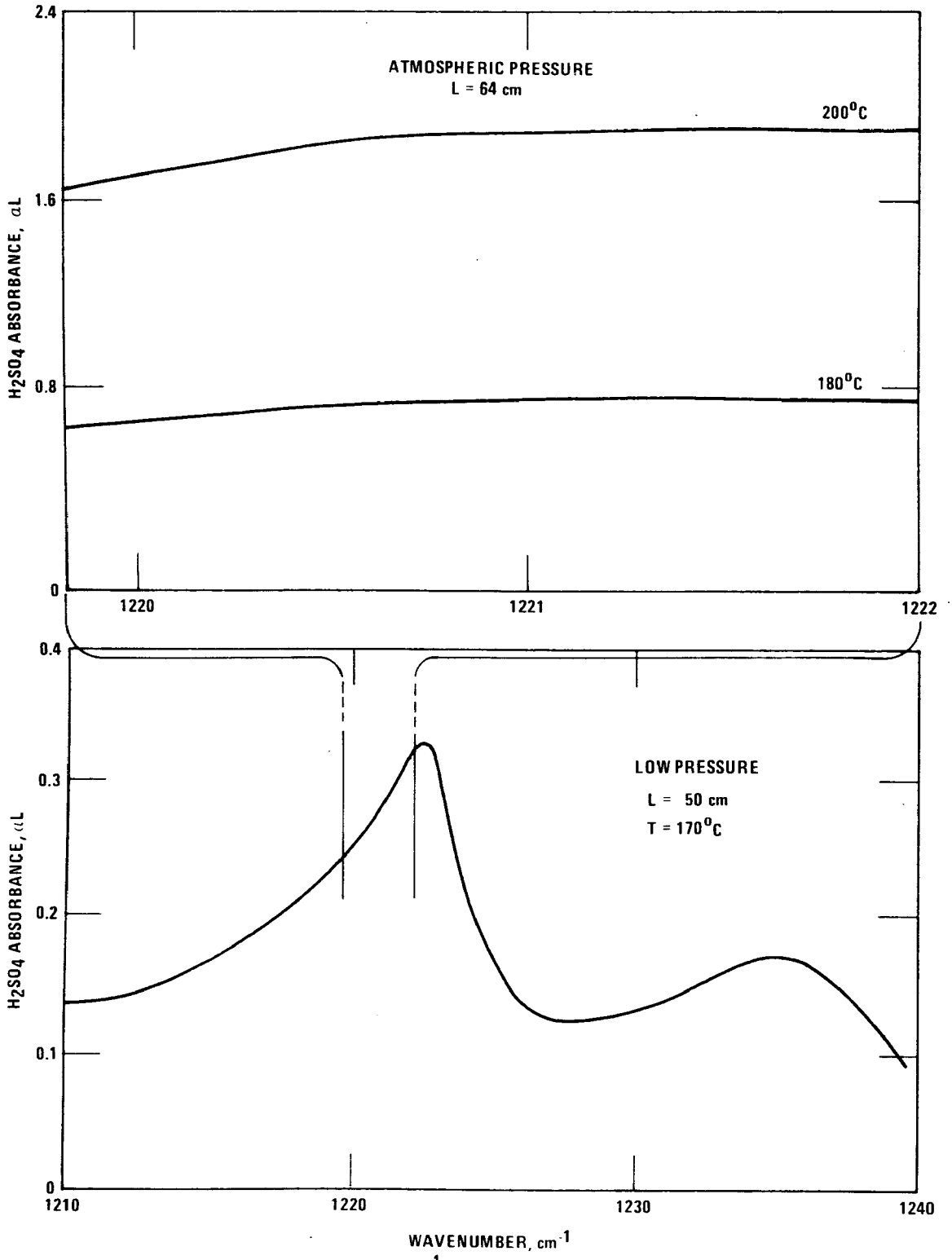

Figure 6. Location of the 2 cm^{-1} atmospheric scan region with respect to the 1210-1240 cm^{-1} low pressure scan.

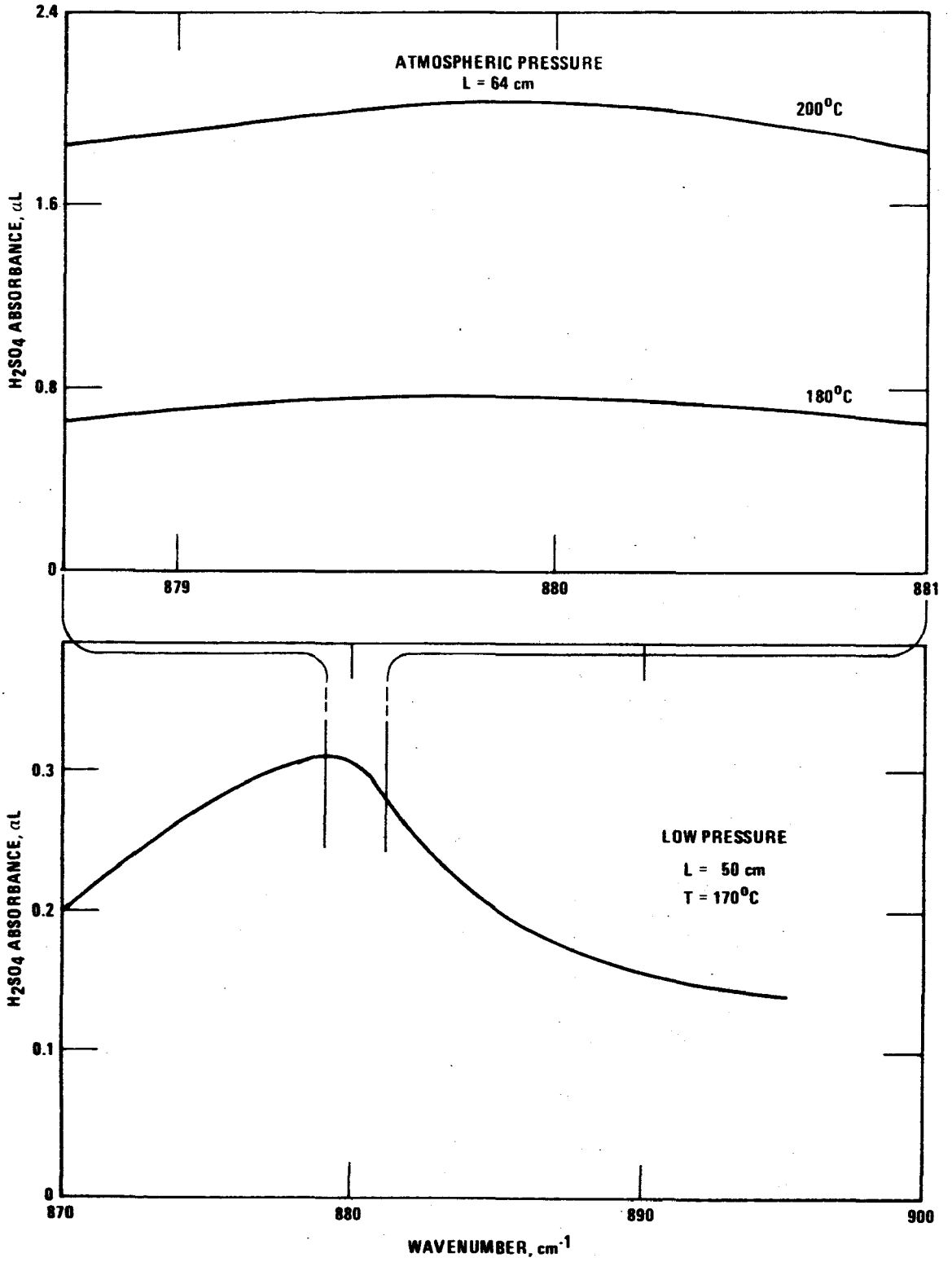

Figure 7. Location of the 2 cm^{-1} atmospheric scan region with respect to the 870-895 cm^{-1} low pressure scan.

and CO_2. These absorption measurements were made over the same 2 cm^{-1} intervals as those used for the H_2SO_4 vapor. Figures 8 and 9 show the SO_2 and H_2O vapor absorption lines between 1219 and 1222 cm^{-1}. Figures 10 and 11 show the absorption lines for CO_2 and H_2O from 878 to 881 cm^{-1}. In the 1222 cm^{-1} region, the SO_2 exhibits a very high line density. The H_2O absorption is much stronger at 1222 cm^{-1} than at 880 cm^{-1}. In the 880 cm^{-1} region, CO_2 absorption was not detectable for a 100 torr sample in a 1.1 meter path.

A spectroscopic technique was also employed to determine the partial pressures of H_2SO_4, SO_3, and H_2O above hot azeotropic H_2SO_4 solutions. This was done by measuring the partial pressures of H_2O and SO_3 directly using known and calibrated absorption strengths. The total vapor pressure was then measured using a "U" tube manometer. The partial pressure of H_2SO_4 vapor was calculated as the difference between the total pressure and the sum of the SO_3 and H_2O partial pressures. Table 1 shows the results of the partial pressure measurements. The numbers in the parentheses are from Luchinski's published data (8) for the atmospheric azeotrope (98.3% H_2SO_4). The H_2SO_4 partial pressures determined in this program are about 30% smaller than those reported in the literature. Therefore, as a result, the absorption coefficient for H_2SO_4 vapor is correspondingly higher. The effect of H_2SO_4 dissociation could account for the discrepancy.

Table 1. Partial Pressure vs. Temperature of H_2SO_4 Azeotrope

Temp. (°C)	Partial Pressure (Torr)		
	H_2O	SO_3	H_2SO_4
107	0.024 ± 0.002 (0.01)	0.022 ± 0.002 (0.005)	0.034 ± 0.02 (0.04)
150	0.023 ± 0.07 (0.145)	0.21 ± 0.02 (0.086)	0.32 ± 0.08 (0.45)
200	2.3 ± 0.2 (1.7)	2.0 ± 0.2 (1.3)	3.5 ± 0.8 (4.4)

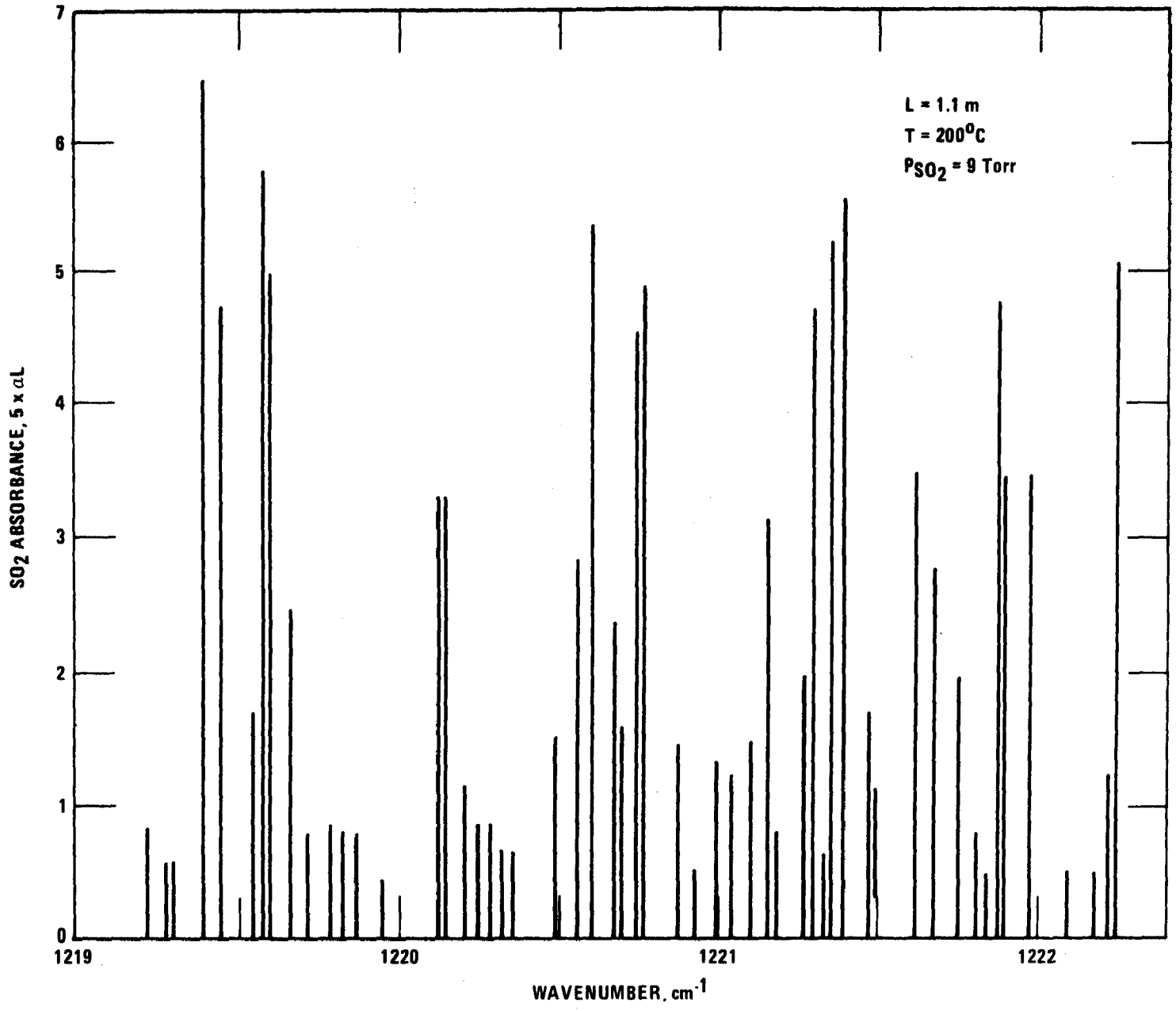

Figure 8. SO_2 absorption.

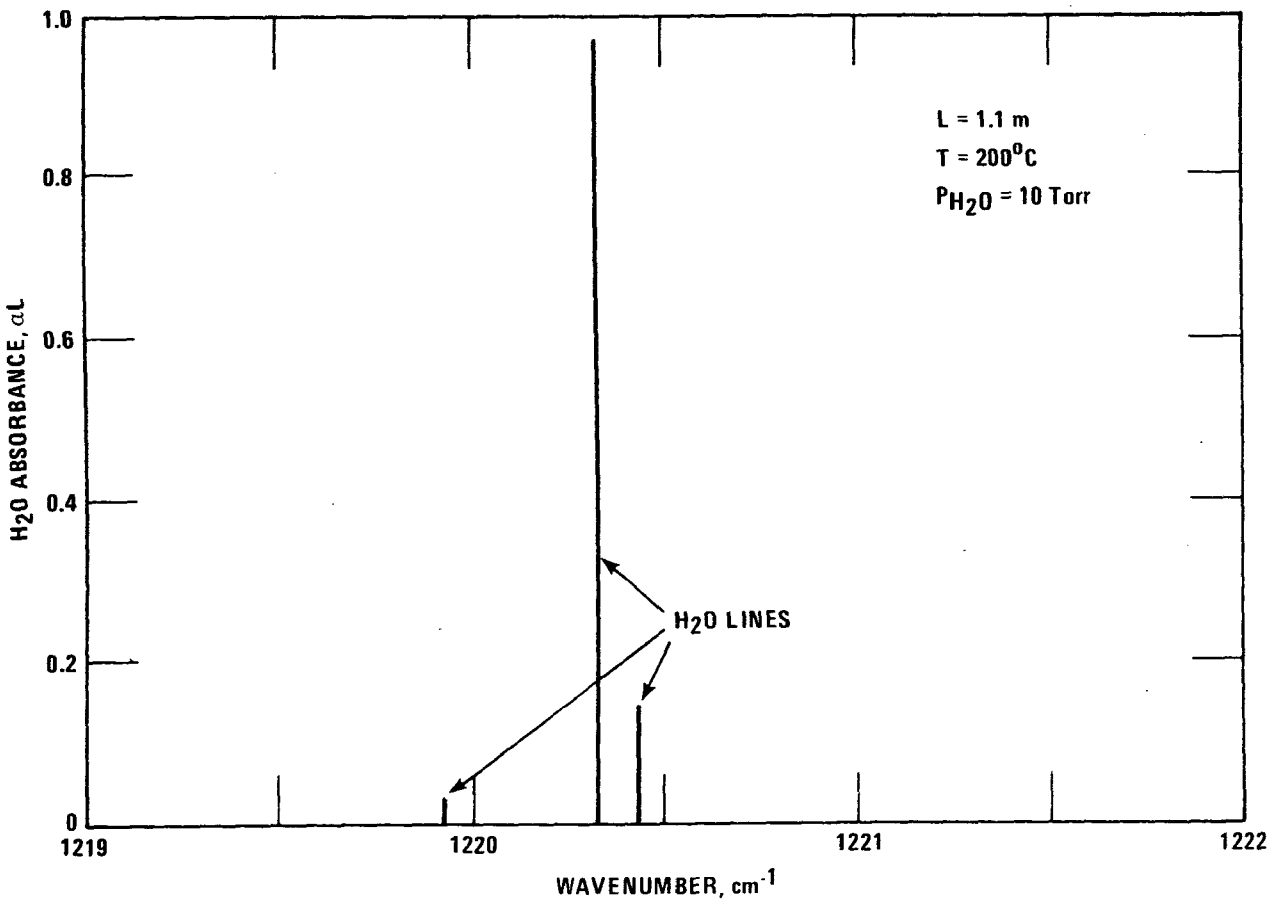

Figure 9. H_2O absorption.

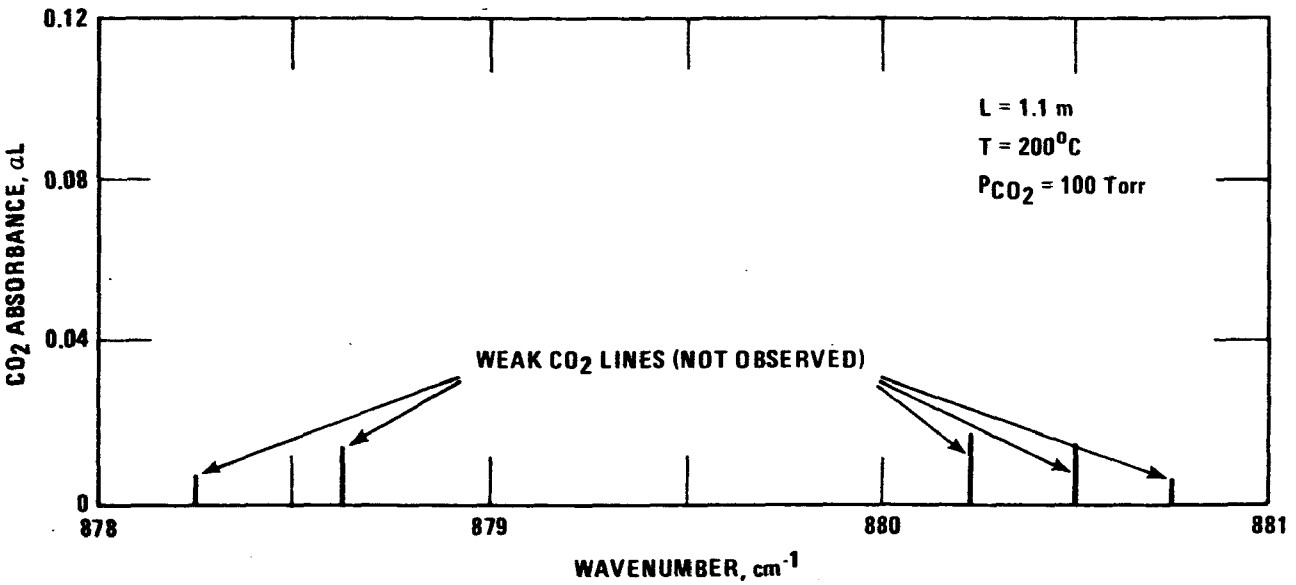

Figure 10. CO_2 absorption.

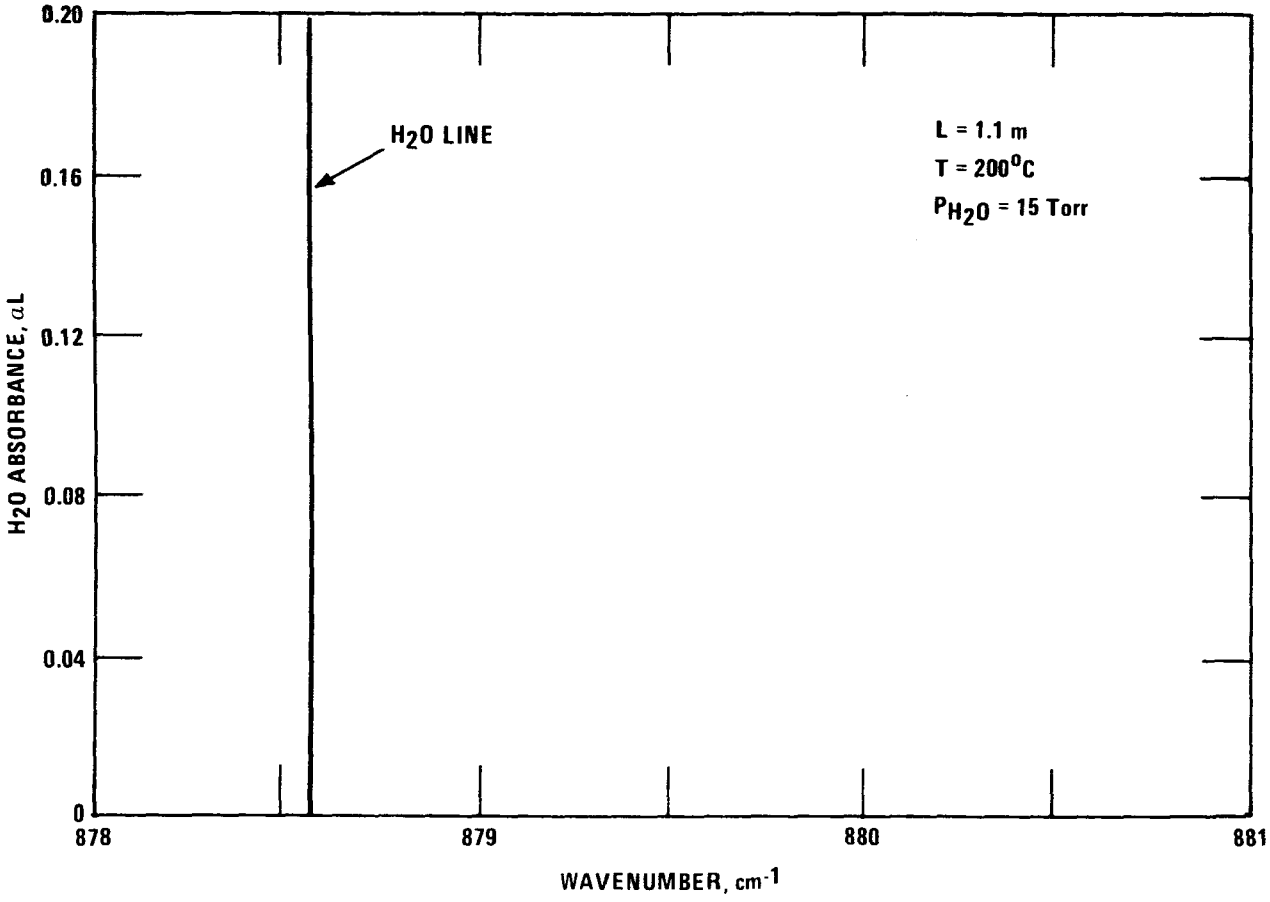

Figure 11. H_2O absorption.

CONCLUSIONS

Laboratory studies have shown that sulfuric acid vapor absorbs quite strongly, but rather broadly, at 880 cm^{-1} and 1222 cm^{-1}. The maximum percentage change in absorption strength occurs on the high frequency side of the peak at 1222 cm^{-1}. The absorption in the 880 cm^{-1} region exhibits a smaller change but is less subject to interference. For H_2SO_4 vapor at atmospheric conditions, absorption coefficients of 6.5 and 6.9 $atm^{-1} cm^{-1}$ have been measured for the 1222 cm^{-1} and 8880 cm^{-1} bands, respectively.

Even though H_2SO_4 vapor at atmospheric pressure apparently has no line absorption structure, it appears that H_2SO_4 can be monitored spectroscopically by utilizing the broad absorption features. The best choice of spectral regions will depend on possible interfering gases and the absorption features for H_2SO_4 vapor. It seems likely that a high-resolution system will be required for the monitoring task. Several measurement approaches seem feasible, including differential absorption spectroscopy using diode lasers, derivative spectroscopy, and Fourier transform interferometry. For an H_2SO_4 monitor utilizing diode lasers, a sensitivity of 2 ppm-meters would probably be possible.

REFERENCES

1. Cheney, J. L., J. B. Homolya, and H. M. Barnes. Measurement and Identification of Primary Sulfates Emitted from Combustion Sources. 70th Annual AICHE, New York, November 1977.

2. Stopperka, K. The Infrared Spectrum of the Water-free H_2SO_4 and the Composition of the H_2O-H_2SO_4 System. Zeit fur Anorgan und Alleg. Chem., 344:263-278, 1963.

3. Chackalackal, S. M., and F. E. Stafford. Infrared Spectra of the Vapors Above Sulfuric and Deuteriosulfuric Acids. Journ. Amer. Chem. Soc., 88:4, 723-728, February 20, 1966.

4. Stopperka, K., and F. Kilz. Die Zusammersetzung der Gasphase über dem flüssigen System H_2SO_4 in Abhängigkeit von der Temperature. Z. Anorg. u Allgem. Chem., Band 270, 49-66, 1969.

5. Burch, D. E., D. E. Gates, and N. Potter. Infrared Absorption by Sulfuric Acid Vapors. Final Report No. EPA-600/2-76-191, July 1976.

6. Alpert, B. D. Studies in High Resolution Infrared Spectroscopy. Ph.D. Dissertation (Appendix B contains H_2SO_4 data), Ohio State University, Columbus, Ohio, 1970.

7. Eng, R. E., K. W. Nill, and J. R. Butler. Spectral Measurements of Gaseous Sulfuric Acid Using Tunable Diode Lasers. Final Report No. EPA-600/2-78-019, February 1978.

8. Luchinski, G. P. Zhur, F12 Khem, 30:1207, 1956.

Chemical Speciation and Concentration Monitoring of Sulfur Oxides by Laser-Raman Scattering

Richard K. Chang
Robert E. Benner
Yale University

ABSTRACT

By the laser-Raman scattering technique, we have measured directly, without filter collection, the concentration of sulfate ions (40 $\mu g/m^3$ level) in laboratory-generated aerosol particles of less than 2 μm in diameter. Our new tabletop design, consisting of an argon laser, multiple-pass cell, concave grating spectrograph, and TV camera detector, should give increased sensitivity. Details of such a laser-Raman monitoring system will be discussed, along with the possibility of using Raman shifts and Raman line widths to distinguish and to monitor various phases (gas, liquid, or solid) and types of sulfur oxides (H_2SO_4, SO_3, SO_2, HSO_4, SO_4, and metal sulfates) in the presence of other atmospheric molecules. In addition, recent results on the angular distribution of inelastic radiation (fluorescence and Raman) from small monodispersed spherical particles will be compared with elastic Lorenz-Mie scattering and fluorescence from a continuum medium. These data, which are dependent on the particle-air index of refraction interface, are pertinent to the conversion of detected photon signals to molecular concentrations contained within aerosols.

INTRODUCTION

Since the vibrational-rotational energies are characteristically distinct for different types of molecules, chemical speciation of a multicomponent mixture can be achieved using Raman light

scattering techniques. In the Raman method, photons with energy $h\nu_i$ are incident on the mixture, and a very small fraction of the light is inelastically scattered, resulting in Raman photons with energy $h\nu_s$. The photon energy difference ($h\nu_i - h\nu_s$) is precisely equal to the vibrational-rotational energy of the scattering molecule. Raman scattering is describable by a second-order perturbation process in which the absorption of an incident photon causes an electron to make a virtual transition to an intermediate state. The final state occurs with the emission of a Raman photon, and the electron is left in the excited vibrational-rotational state [Figure 1(a)]. Consequently, by using monochromatic incident radiation from a laser and by spectrally analyzing the Raman scattered radiation with a spectrograph or a spectrometer, the chemical species present in the scattering volume can be determined from the known vibrational-rotational energies of different molecules. In addition, since the intensity of the radiation scattered by a molecular species is linearly proportional to its concentration, the amount of a particular constituent can be determined from measured Raman scattering cross sections.

An alternative means of probing molecular energy levels utilizes infrared absorption of photons with photon energy $h\nu_{IR}$ which involves a real transition of an electron from its ground state to the excited vibrational-rotational state [Figure 1(b)]. For molecules that do not possess a center of inversion, the vibrational-rotational state probed by infrared absorption is identical to that reached by the Raman scattering process. Both the infrared absorption and the Raman scattering processes distinguish different types of molecules by the uniqueness of their vibrational-rotational energies. In general, infrared spectroscopy does not require a laser source, but the use of lasers in Raman spectroscopy greatly enhances signal/noise ratios. The vibrational state energies are influenced significantly by the phase (gas, liquid, or solid) of the sample. Furthermore, additional vibrational peaks become observable when the molecular species changes from the gaseous to the liquid phase and from the liquid to the solid phase.

Both the infrared and the Raman processes are affected by the finite lifetimes of the excited vibrational-rotational states which result in a broadening of the infrared absorption and Raman scattering peaks. In the gaseous phase, the major contributions to a broadened linewidth are collisions among the molecules ($\simeq .01$ cm^{-1} at 1 atm) and the Doppler effect ($\simeq .005$ cm^{-1}). For the liquid phase, the typical collisioned broadened linewidth (1-10 cm^{-1}) can be further broadened (5-50 cm^{-1}) by proton

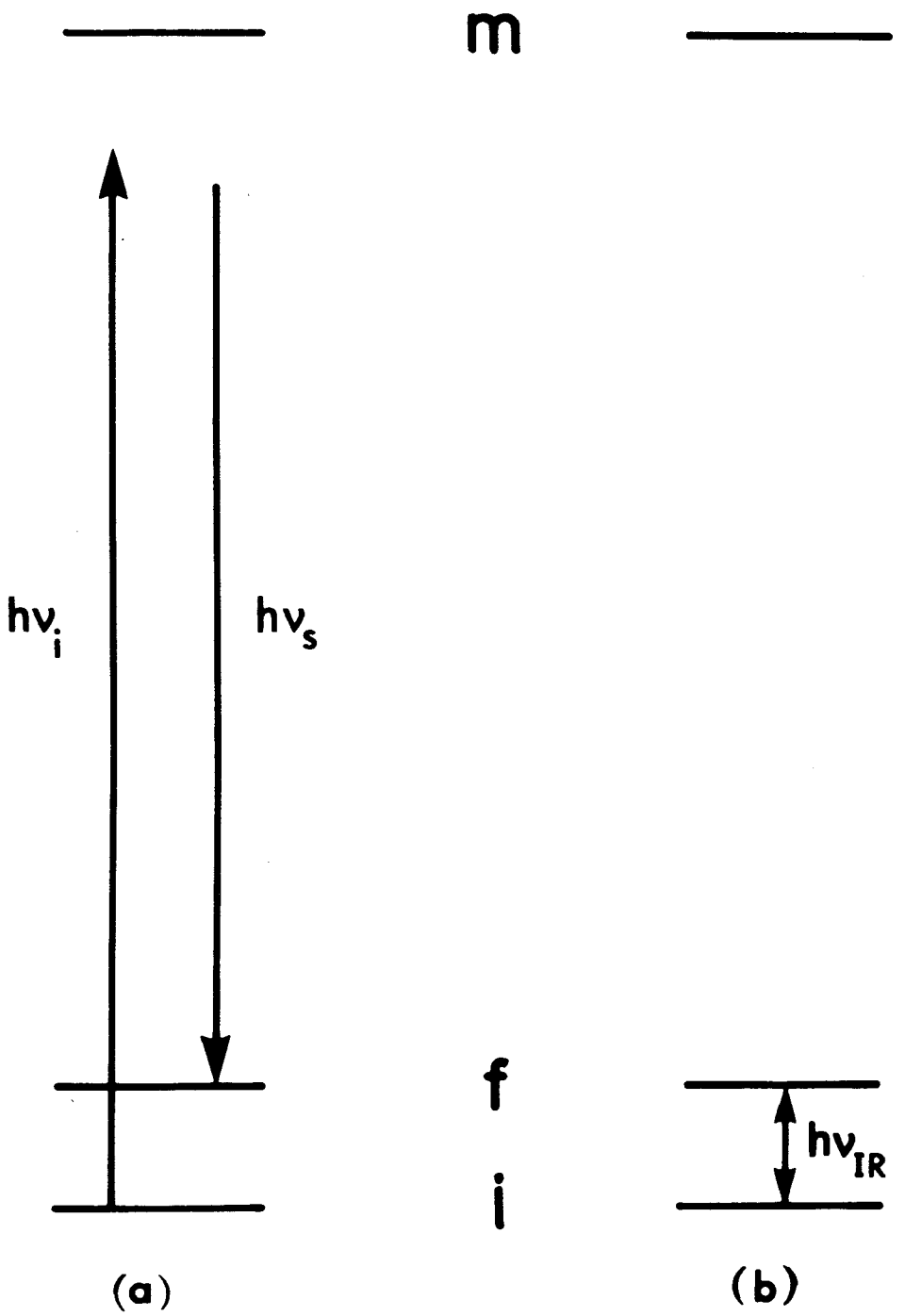

Figure 1. Schematic representation of the Raman scattering process (a) and the infrared absorption process (b). Initial, intermediate, and final states are labeled i, m, and f, respectively.

(H_3O^+) exchange if the pH is low (1). In the solid phase, the linewidths generally lie between those of the gaseous and liquid phases because of the momentum selection rule ($K \simeq 0$) imposed by the periodicity of the crystalline structures. The major contribution to the phonon linewidth (0.5-10 cm^{-1}) is due to anharmonic lattice effects which can cause a phonon to decay into different vibrational modes. In principle, the phase of the molecular scatterer can be deduced not only from the precise energy of the vibrational state but also from the linewidths of the infrared and Raman peaks.

There are three significant differences between infrared and Raman spectroscopy: (1) Since Raman scattering is considerably weaker than infrared absorption, higher power laser sources are required for the Raman technique as compared with those needed for infrared absorption. (2) The Raman approach is better suited for point-sampling (cylindrical focal volume of 100 μm x 1 cm), while the infrared approach can average over a much longer path length. (3) Using one laser source, the Raman scattered radiation contains chemical speciation and concentration information on all the molecules present in the cylindrical focal volume, whereas high resolution infrared differential absorption requires a tunable laser source for each type of molecule. With regard to these differences and the difficulties inherent in using optical techniques to monitor emissions inside a stack or downstream outside the stack, the infrared and Raman techniques have complementary attributes. Which technique is more viable, particularly in situations in which the simultaneous monitoring of several emissions is desirable, remains unclear.

In this paper we shall review what is known about the Raman effect in sulfur-containing molecules in their gaseous, liquid, and aerosol forms. Although much is already known, much important information is still missing. It is, therefore, not yet possible to estimate the sensitivity or the degree of specificity of the Raman technique when it is applied to stack emission analysis where gaseous H_2SO_4, SO_3, SO_2, and H_2S can coexist with liquid H_2SO_4 and H_2SO_3, as well as with solid metal sulfates/sulfites, $(NH_4)SO_4$, and $(NH_4)HSO_4$ in the presence of other atmospheric gases and aerosols.

GASEOUS PHASE

The Raman shifts, $\Delta\nu = \nu_i - \nu_s$ (in cm^{-1} units), and the relative Raman cross sections of common atmospheric gases are listed in Table 1. For these gases, using standard laboratory Raman systems,

Table 1. Raman Shifts and Cross Sections for Common Atmospheric Gases

Molecules	Raman shifts in cm^{-1} Numbers in [ ] denote relative cross sections						Ref.
SO_3	1330		1069		652	532	a
	1380		1065		-	536	b
SO_2	1151	[5.5]	519	[0.11]			c,d
H_2S	2611	[6.6]					c
N_2	2331	[1]					c
O_2	1556	[1.2]					c
O_3	1103	[4.0]					e
H_2	4160	[2.2]					e
CO	2145	[0.9]					c
CO_2	1388	[1.5]	1286	[1.0]			c
NO	1877	[0.55]					e
N_2O	2223	[0.53]	1287	[2.7]			e
NH_3	3334	[3.1]					f
H_2O	3652	[2.5]					g
CH_4	3020	[0.79]	2914	[8.0]			e,f

References

a. Wright, M. L., and K. S. Krishman. EPA-R2-73-219, 1973.
b. Tang, Sheng-Yuh, and Chris W. Brown. J. Raman Spectry, 3:387, 1975.
c. Fouche, D. G., and R. K. Chang. Appl. Phys. Lett., 18:579, 1971.
d. Inaba, H. Topics in Applied Physics, Vol. 14. Laser Monitoring of the Atmosphere. E. D. Hinkley, Springer-Verlag, Berlin, Heidelberg, 1976. p. 153.
e. Fouche, D. G., and R. K. Chang. Appl. Phys. Lett, 20:256, 1972.
f. Murphy, W. F., W. Holzer, and H. J. Bernstein. Appl. Spectry, 23:211, 1969.
g. C. M. Penney, L. M. Goldman, and M. Lapp. Nature, 235:110, 1972.

there is no difficulty in uniquely identifying and measuring trace molecular concentrations of less than one part-per-million (ppm). If the absolute value of the differential cross section for Raman scattering ($\partial\sigma/\partial\Omega$) is known, the detectable amount of scattered light intensity can be easily calculated, as follows:

$$W_s = (\partial\sigma/\partial\Omega)\partial\Omega c\eta\ell W_i, \qquad [1]$$

where

$(\partial\sigma/\partial\Omega)$ = the differential Raman cross section in units of cm^2/sr. For N_2 gas molecules measured with 514.5 nm laser excitation, the value is 4.4×10^{-31} cm /sr (2).

$\partial\Omega$ = the solid angle of the collection optics in units of sr. For an f/1 lens, the solid angle is 0.67 sr.

c = the gas concentration in units of number of molecules per cc.

η = the overall efficiency of the Raman spectrometer, including lens reflection losses, spectrometer throughput, and the quantum efficiency of the photodetector. Typical values are 0.5 for lens losses, 0.1 for spectrometer throughput, and 0.15 for detector quantum efficiency. Thus, η is approximately 8×10^{-3}.

ℓ = the focal length of the incident laser beam in units of cm. The typical length for f/1 collection optics and an f/8 spectrometer of 2 cm slit height is 0.25 cm.

W_i, W_s = the incident and scattered power, respectively, in units of Watts. Conversion of Watts into photons per second requires multiplication by 6.3×10^{18} $(h\nu_s)^{-1}$, where $h\nu_s$ is the scattered photon energy in eV.

If the incident photon energy is below the energies of any excited electronic levels of the sample, the Raman scattering cross section increases proportionally as $(h\nu_s)^4$. When the $(h\nu_s)^4$ law is obeyed, the inelastic scattering process is known as the ordinary Raman effect (ORE). In contrast, the resonance Raman effect (RRE), resonance fluorescence (RF), and broad

fluorescence (BG) processes depicted in Figure 2 offer means of enhancing inelastic light intensity. For example, the resonant Raman scattering cross section of I_2 molecules is known to be 10^6 times greater than the ordinary Raman cross section (3). The resonant Raman cross sections for O_3, OH^-, and SO_2 have also been reported (4)(5)(6). Rousseau et al. (7) recently made explicit the distinction between RRE and RF in I_2 molecules by observing the variations in the time decay of inelastic emission as the laser photon energy was tuned through an absorption peak. Fouche et al. (3) further clarified the distinction between RRE and RF in I_2 molecules by measuring the pressure quenching coefficient of the inelastic emission as the photon energy was tuned through resonance. RF and BF emission have been observed (8) for NO_2. The inelastic emission cross section was 10^2 times greater than the Raman cross section of N_2 at 514.5 nm.

In spite of the obvious gain in the scattering cross section that can be achieved with RRE, RF, and BF, utilization of these processes sacrifices a principal attribute of the ordinary Raman technique--that is, with ORE one monochromatic incident laser source can provide chemical species and concentration information on all of the molecular constituents contained within the focal volume. With RRE, RF, and BF, different laser wavelengths must be used to achieve resonance for each type of molecule. Thus similar to the infrared absorption approach, a tunable source is required. Coherent anti-Stokes Raman spectroscopy (CARS) also requires specific adjustment of source wavelengths, depending upon the species under investigation. While the CARS technique may be preferable for determining the major component of a gas mixture, ORE gives greater sensitivity in detecting the minor components (9).

Several approaches have been devised to increase the ORE signal from a gas. Hill et al. (10) discussed construction of a multipass light trap employing an ellipsoidal mirror and a flat spherical mirror assembly which, when used to study Raman scattered light from atmospheric N_2, provided an experimental gain of 93 relative to the scattering obtained with one beam. A simplified configuration consisting of two spherical mirrors positioned so that their common radii of curvature were coincident was used by Stafford et al. (11) to obtain an effective W_i 49 times greater than the single pass laser power. In the latter system, a third concave mirror was used to redirect Raman scattered photons that would normally be lost back toward the collection optics. In a single pass scheme with 340 mW of power at the 488 nm line of an argon laser and a double spectrometer of 1 mm slit width and 10 mm slit height, the Raman signal from atmospheric N_2 was found (11) to be 5700 counts per second.

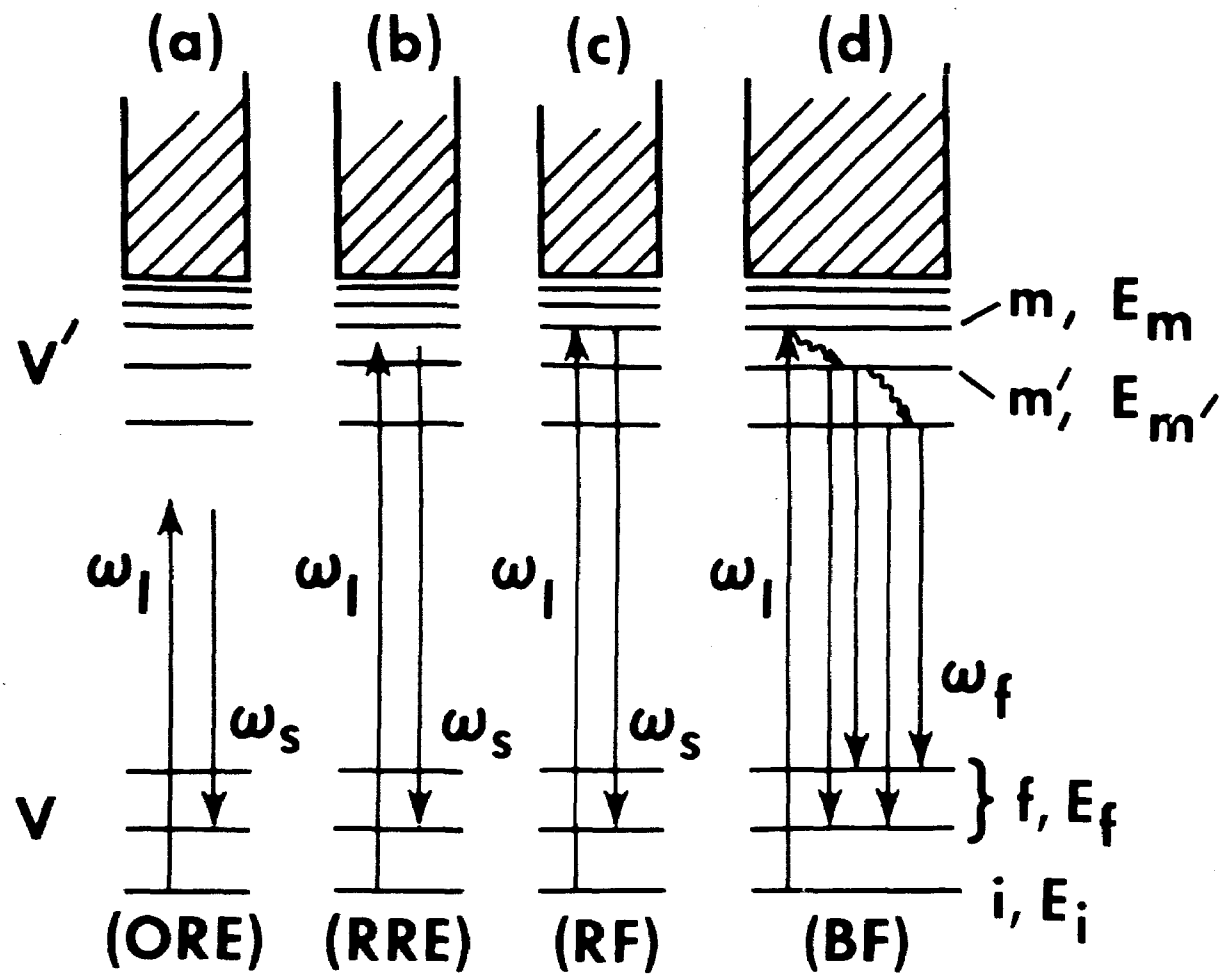

Figure 2. The possible ways in which a laser photon may be scattered inelastically by a molecule. Ordinary Raman effect (ORE) is shown in (a). Resonance Raman effect (RRE) and resonance fluorescence (RF) are depicted in (b) and (c). Processes (a)-(c) all give rise to discrete energies for the scattered emission ($h\omega_s$). Broad fluorescence emission (BF) at ($h\omega_f$) is shown in (d). The wavy arrows indicate nonradiative transitions caused by collisions (8).

Including the multipass light trap and the third mirror, the atmospheric N_2 signal increased to 5.22×10^5 counts per second, a gain of approximately 92. Use of larger mirrors in this configuration can be expected to further increase ORE signal/noise ratios.

It should be noted from Table 1 that the cross section of SO_3 is unknown and that the Raman shift and cross section of H_2SO_4 (gaseous) are yet to be determined.

LIQUID STATE

The Raman effect also can be exploited in investigating the constitution of acid solutions at varying concentrations (pure liquid acid to aqueous solutions of acids). Changes in the molecular configuration or constitution of the acid caused by dilution or concentration will cause corresponding changes in the Raman shifts, linewidths, and intensities. Figure 3 shows the distribution of Raman shifts from pure acid H_2SO_4 at varying concentrations (12). The shifting of some of the principal Raman peaks in H_2SO_4 versus concentration (12) is shown in Figure 4. The absolute cross section of pure acid H_2SO_4 is unknown.

By dissolving SO_3 in 100% sulfuric acid, the characteristic lines of H_2SO_4 gradually disappear and new lines develop. This effect has been attributed (12) to the formation of $H_2S_2O_7$, S_2O_6, or S_3O_9. The Raman shifts from fuming sulfuric and sulfuric acids are summarized in Table 2.

Sulfuric acid in the dilute state dissociates into HSO_4^- and $SO_4^=$. The corresponding spectra (11) for 1M H_2SO_4, 1M $(NH_4)HSO_4$, and 1M $(NH_4)_2SO_4$ are shown in Figure 5. Note that $(NH_4)HSO_4$ also dissociates into HSO_4^- and $SO_4^=$. The absolute Raman cross section for $SO_4^=$ in the aqueous state is 6.3×10^{30} cm^2/sr with 514.5 nm excitation, which is 14 times the N_2 cross section. The broad linewidth associated with the HSO_4^- and $SO_4^=$ peaks is due mainly to proton transfer (1). Raman spectra for $KHSO_4$ and $NaHSO_4$ dissolved in water are shown in Figure 6 along with those for H_2SO_4 and $(NH_4)HSO_4$. Once these molecules are dissociated, their Raman spectra are insensitive to the cations. The results of Stafford et al. (11) established that the vibrational frequency of $SO_4^=$ is the same for all solutions because of its independence on cations when freely dissociated. The HSO_4^- anion has two vibrational frequencies near the 981 cm^{-1} line of $SO_4^=$. The first is at 895 cm^{-1}, which is very near the 910 cm^{-1} line of an undissociated H_2SO_4 molecule (13). However, the H_2SO_4 contribution

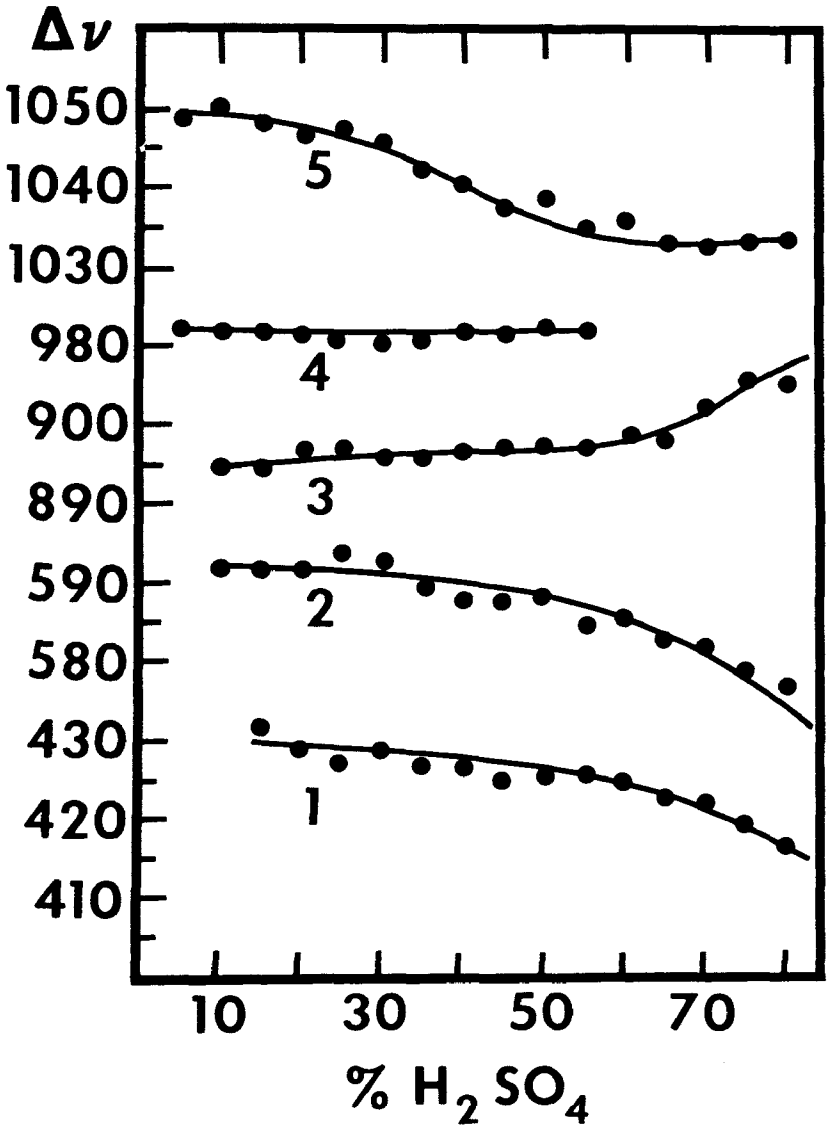

Figure 3. The change in the principal Raman shifts Δ_ν in units of cm^{-1} for various concentrations of H_2SO_4 (13).

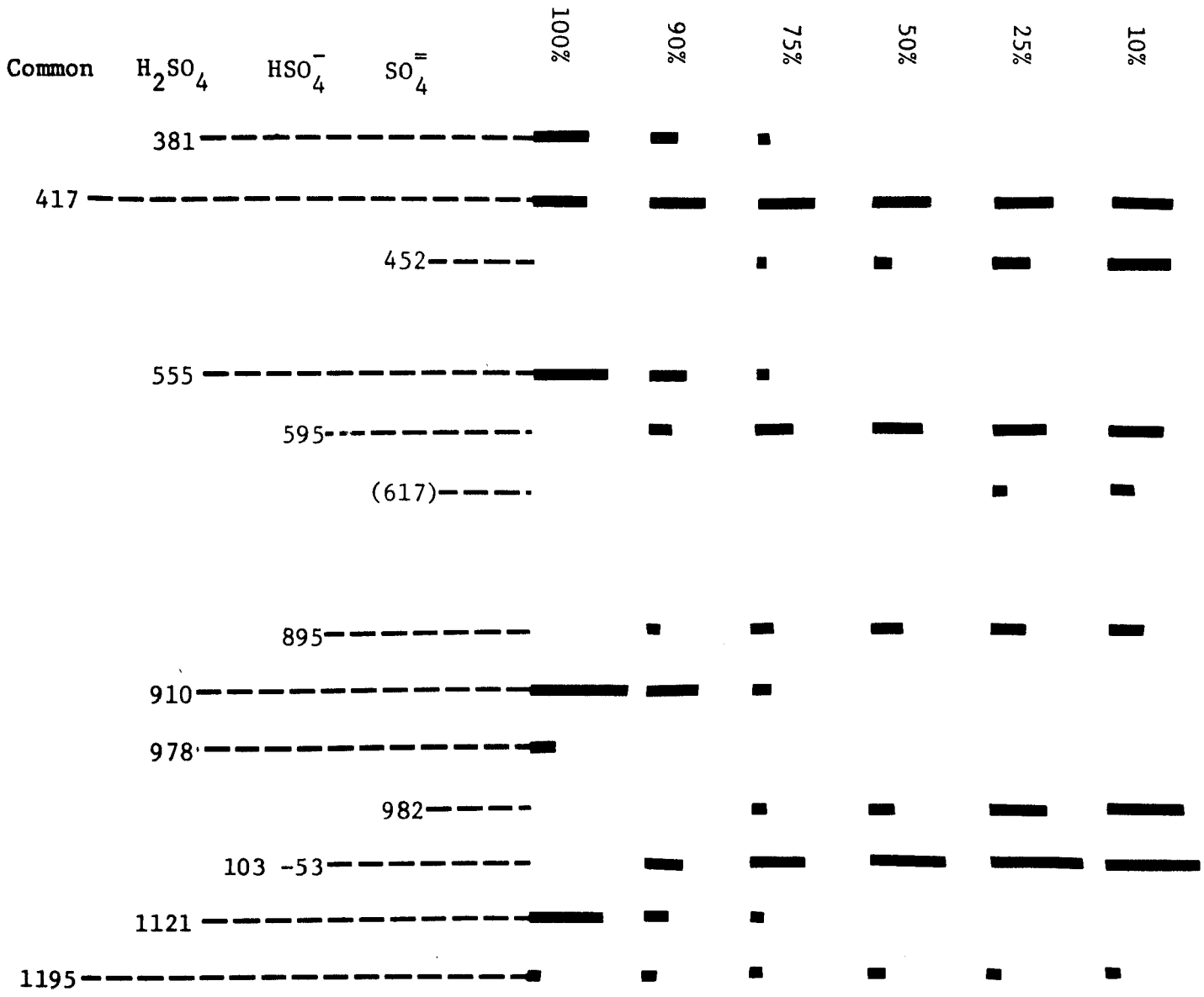

Figure 4. The distribution of Raman shifts (cm^{-1}) from H_2SO_4 at varying concentrations (12).

Table 2. Raman Shifts from Fuming Sulfuric and Sulfuric Acids*

Raman shifts in cm^{-1}								
Fuming sulfuric acid (Free SO_3 given in percent)					Sulfuric acid			
68%	51%	36%	23%	10%	100%	90%	80%	70%
245	246							
295	297	300	305	315				
330	331	325	327					
			390	388	395			
484	480	480	427	427	430	412	414	424
536	535	525						
		565	565	562	560	566	580	583
688	688							
737	740	735	740	735				
		904	915	915	917	915	907	902
957	960	957	975	970	972			
1075	1075					1045	1040	1040
		1160	1160	1140	1140	1148		
1252	1250	1250	1240					
1450	1450	1440	1420	1393	1370			

*Hibben, James H. The Raman Effect and Its Chemical Applications. Reinhold Publishing Corp., New York, 1939. p. 364.

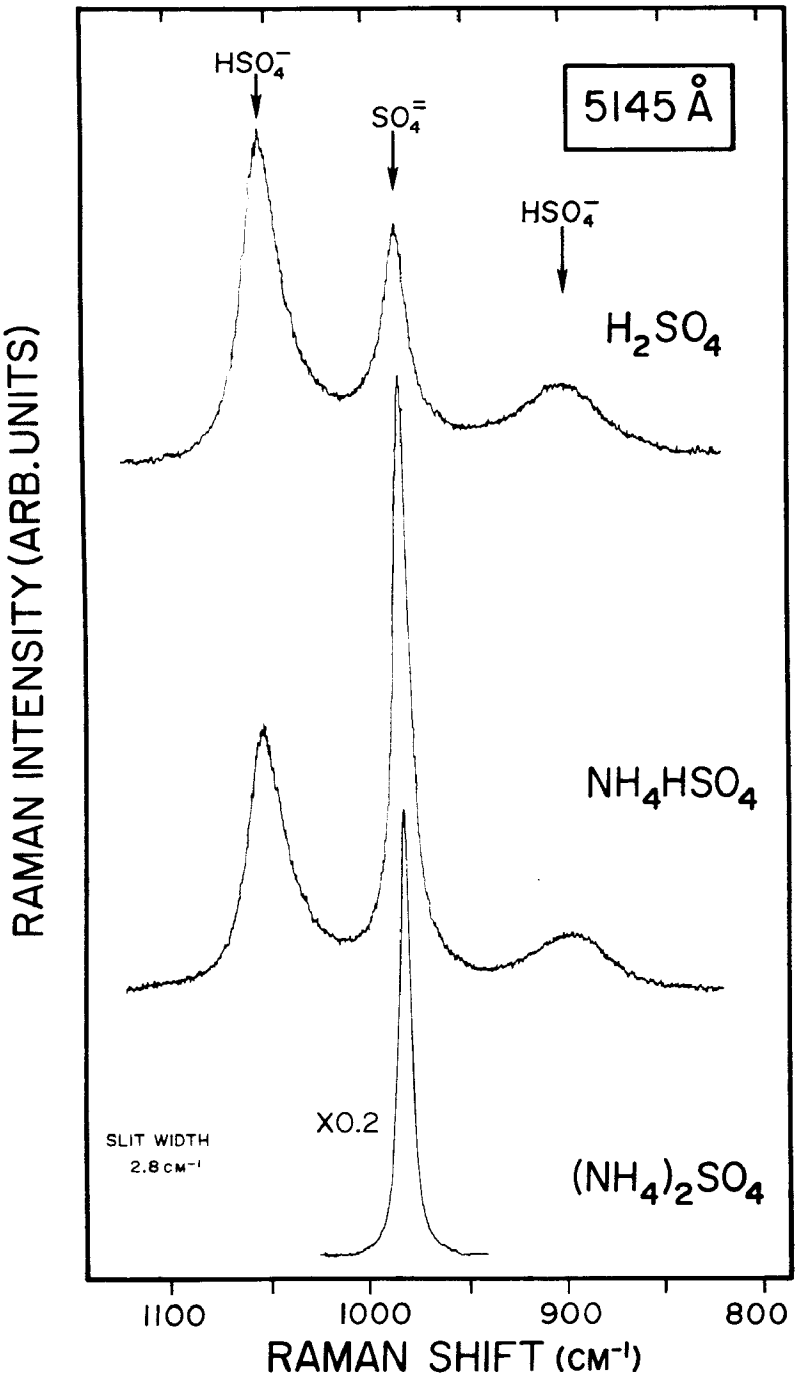

Figure 5. Raman spectra of 1M solutions containing sulfate and bisulfate anions. The $(NH_4)_2SO_4$ ordinate has been decreased by a factor 0.2. Spectra are restricted to the region about ν_1, vibration of the free $SO_4^{=}$ anion at 981 cm^{-1} (11).

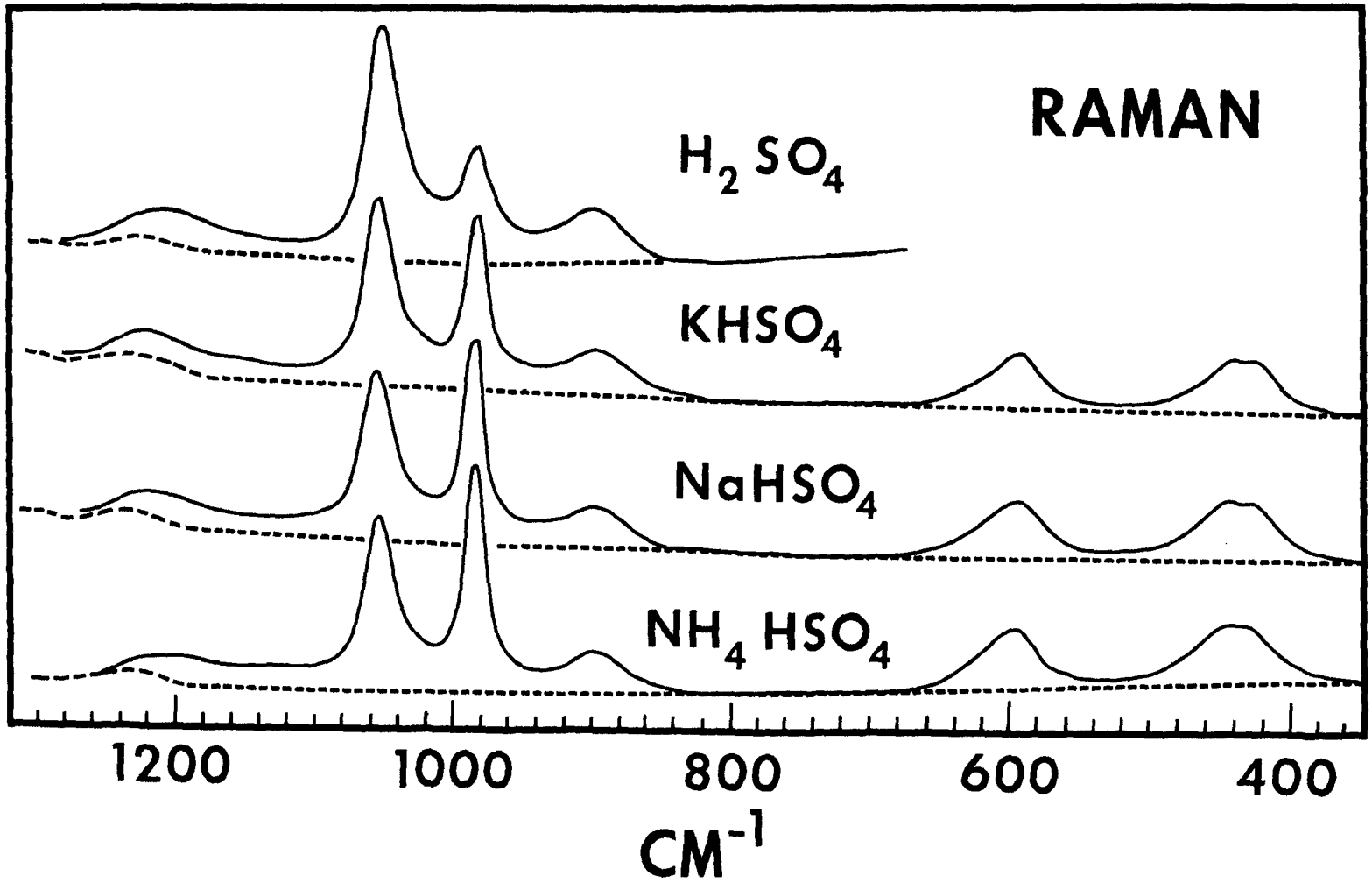

Figure 6. Raman spectra of 2M H_2SO_4, $KHSO_4$, $NaHSO_4$, and NH_4HSO_4 solutions (1).

is negligible for 1M H_2SO_4 and is practically nonexistent in 1M NH_4HSO_4. The second frequency is concentration dependent and varies from 1055 cm^{-1} to 1030 cm^{-1} as the concentration of HSO_4^- increases (1)(13). These lines are also much broader than the 981 cm^{-1} line and overlap to form a complex spectrum. Unfolding this complex spectrum to accurately determine $d\sigma/d\Omega$ for HS_4^- requires making assumptions about the lineshapes. Zarakhani (14) has attempted this approach with H_2SO_4 and attained a ratio of $SO_4^=$ to HSO_4^- integrated strength of approximately 2/1 for the 981 cm^{-1} and 1040 cm^{-1} lines. This ratio is compatible with a simple deconvolution of the spectra in Figure 5 using the 1m dissociation constant of HSO_4^- (1) (15). The absolute cross section of HSO_4^- is therefore approximately 1/2 that of $SO_4^=$.

It would be desirable to obtain an integrated Raman intensity that is linear with total sulfate and bisulfate concentration. However, it has been shown that respective concentrations of $SO_4^=$ and HSO_4^- are not linear with the total concentration of H_2SO_4 (16). Since the cross sections of the 1040 cm^{-1} and 981 cm^{-1} lines are not equal, an integrated Raman intensity of the two would not be linear with total concentration. This causes a problem since the two lines must be integrated. The reason for this is that the concentrations of sulfate pollutants in the atmosphere are sufficiently small that the Raman signal would be too weak to obtain an accurate spectrum that would allow an unfolding of the two overlapping lines. However, because of this latter point, the 895 cm^{-1} line of HSO_4^- must also be included in the integrated intensity, since it strongly overlaps with the 981 cm^{-1} line of $SO_4^=$. By taking the sum of the integrated intensities of these three lines (1040 cm^{-1}, 981 cm^{-1}, 895 cm^{-1}), the following is found: for one molar concentrations of $(NH_4)_2SO_4$, NH_4HSO_4, or H_2SO_4, the Raman spectra of which are shown in Figure 5, the sums, normalized to $(NH_4)_2SO_4$, are 1, 0.98, and 1.03, respectively. These sums are approximately equal within the experimental accuracy of $\pm 10\%$. If one takes the deconvoluted integrated intensities of Zarakhani et al. (14) for H_2SO_4 and also performs the same sum, for molar concentrations between 0.4 and 5M, the total sum is approximately linear with total concentration. For H_2SO_4, Stafford et al. (11) checked and extended this approximate linearity from 5M down to 0.01M for total integration without deconvolution. Over this concentration range, the peak height ratio of the Raman intensities of the 981 cm^{-1} and 1040 cm^{-1} line reverses, indicating the complexity of the superimposed spectra. A 1M solution of $NaHSO_4$ was also analyzed with results confirming those of NH_4HSO_4 and H_2SO_4. Thus, by using a spectral slit width that encompasses the lines 1040, 981, and

895 cm^{-1}, the resulting integrated Raman intensity will be approximately linear with total sulfate and bisulfate concentration in aqueous solutions over the range 0.01-5M. The absolute concentration can then be determined from the integrated Raman intensity and the absolute differential cross section of $SO_4^{=}$ given above.

LIQUID MIST FORM

Should the sulfur-containing liquid be in mist form, then it is important to know the size distribution of the droplets. When the droplet size is comparable to the wavelength of the infrared light, elastic Mie scattering and the electric field inside distorted by the droplet boundary can affect the infrared absorption coefficient. Similarly, when the droplet size is comparable to the excitation wavelength in the visible region, the Raman scattering intensity will be affected by the droplet size, shape, and refractive index (17)(18)(19). However, the Raman shifts will not be influenced by the droplet character of the scatterer.

The Raman signature of $(NH_4)_2SO_4$ mist (size less than 2 μm) flowing past the cylindrical focal volume of the incident laser has been measured recently (20). As indicated in Figure 7, eight parts-per-billion (ppb) of $SO_4^{=}$ were detected with a counting period of 1000 second using the experimental arrangement shown in Figure 8. The $(NH_4)_2SO_4$ must have been dissociated totally as the observed Raman shift coincides with that of free $SO_4^{=}$ ions in the liquid phase (981 cm^{-1}) and not with that in the solid phase (976 cm^{-1}). Significantly, the Raman intensity seems to indicate that the relative cross section of $SO_4^{=}$ is 20 times larger than that of $SO_4^{=}$ dissolved in aqueous solution. This result implies a large enhancement caused by the droplet size, shape, and index of refraction. Further confirmation of this enhancement is desirable.

The Raman shifts from other common ions are listed in Table 3. However, the cross sections other than for $SO_4^{=}$ are not known.

SOLID PHASE

Sulfates in the solid phase are numerous. Table 4 summarizes representative species along with reported Raman shifts of sulfates in the solid form. The corresponding shifts (21) (in cm^{-1}) for free $SO_4^{=}$ are ν_1 = 981, ν_2 = 451, ν_3 = 1104, ν_4 = 613. Raman cross sections for bulk sulfate crystals are unknown. However, Blomer et al. (22) and Wright et al. (23) have reported some preliminary results on the absolute cross sections of sulfates in powder form.

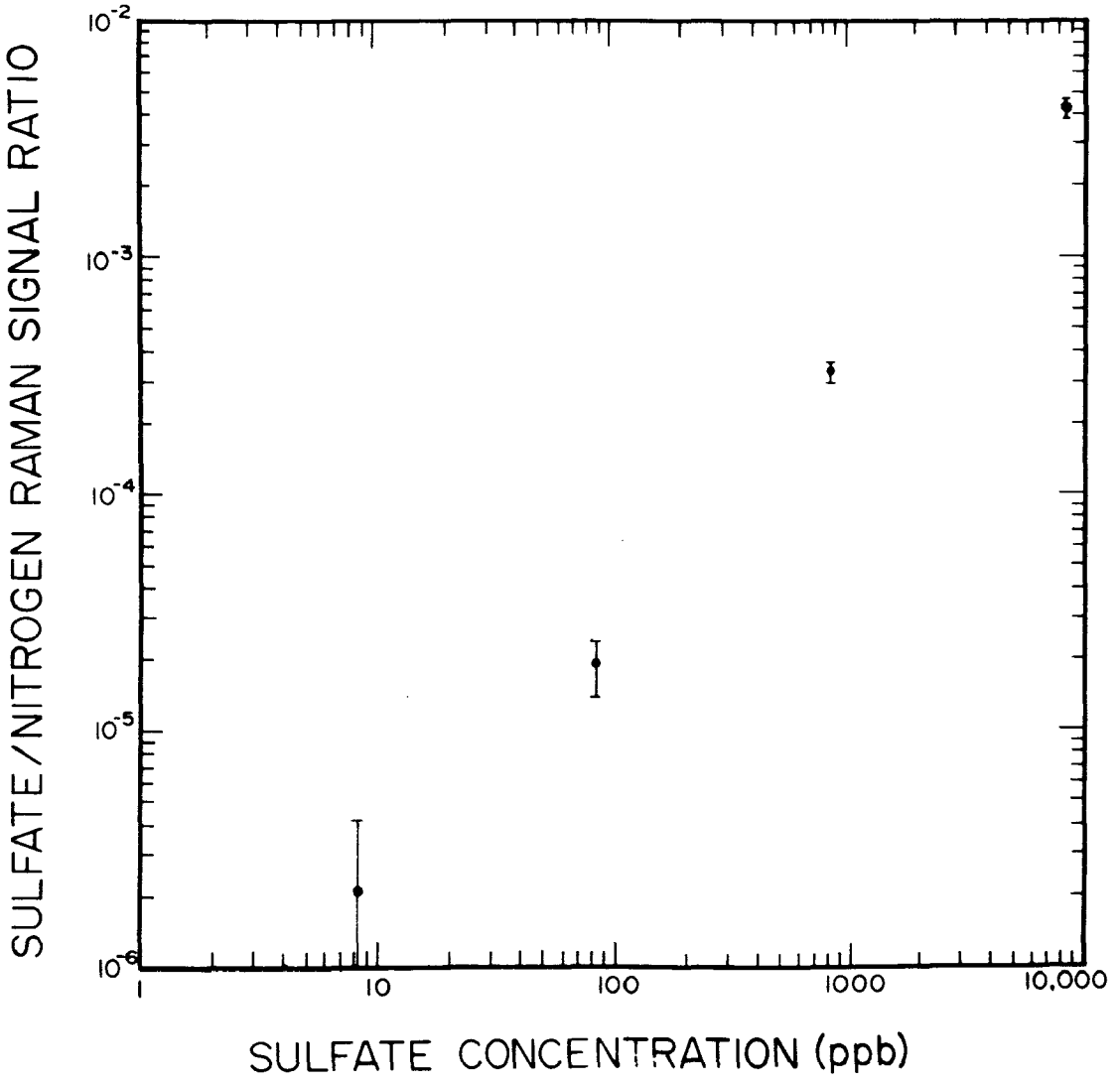

Figure 7. Graph of the sulfate Raman signal versus sulfate concentration, normalized to the Raman signal of ambient N_2. The accuracy in the sulfate concentration calibration measurement was $\pm$ 50% (20).

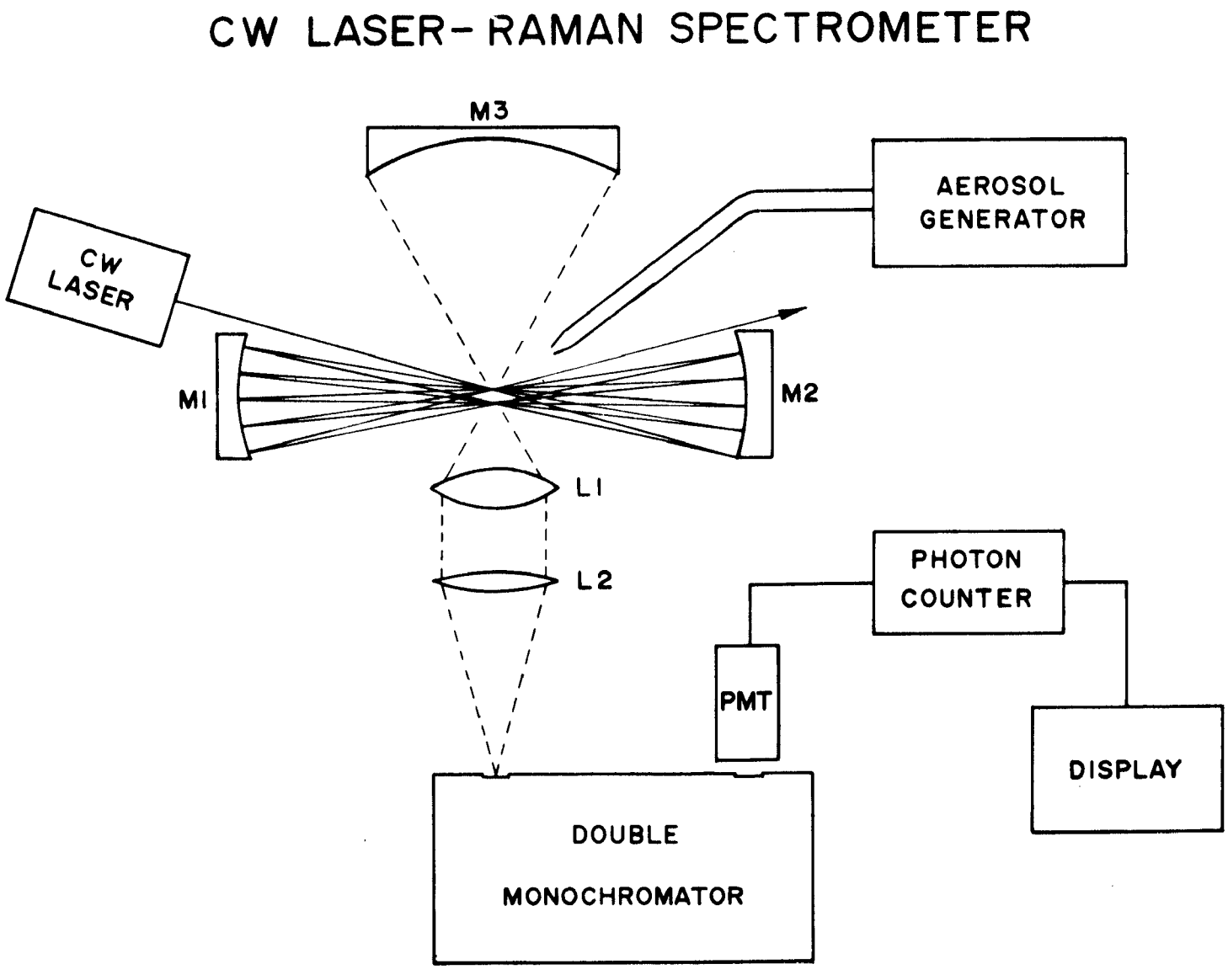

Figure 8. Schematic of a laser-Raman scattering experiment used for the detection of laboratory generated sulfate aerosols. The Raman signal is enhanced by a multipass optical assembly (20).

Table 3. Raman Shifts from Various Ions*

Ions	Raman shifts in cm^{-1}			
SO_4^{2-}	1104	981	613	451
ClO_4^{2-}	1102	935	628	462
PO_4^{3-}	1082	935	515	363
NH_4^+	3134	3033	1685	1397
CO_3^{2-}	1415	1063	680	
NO_3^-	1390	1050	720	

*Wright, M. L., and K. S. Krishnan. EPA-R2-73-219, 1973.

Table 4. Raman Shifts of Sulfates in the Solid Phase

Cation	Mean $SO_4^{=}$ frequencies, cm^{-1}				Ref.
	ν_1	ν_2	ν_3	ν_4	
Li_2	1017	518	1118	722	a
	997	440	1104	595	b
LiK	1010	-	1110	-	b
Na_2	995	459	1110	637	a
	990	460	1115	615	b
KH	980	427	-	593	b
K_2	985	451	1119	624	a
	986	454	-	617	b
$(NH_4)_2$	978	449	1091	621	a
	977	453	1108	616	b
	976	450	1090	613	c
Rb_2	976	454	1073	600	a
	976	453	-	-	b
Cs_2	972	442	1066	606	a
Be_2	1061	528	1193	850	a
	990	450	1108	620	b
Cu_2	983	448	1108	612	b
Mg_2	1029	-	-	-	a
	985	456	1108	613	b
Ca_2	1015	456	1132	638	a
	1013	415	1108	609	b
(Anhydrite)	1015	425	1150	620	c
Ca_2 (Gypsum)	1005	415	1113	620	b
Sr_2	999	456	1140	637	a
	999	460	1106	628	b
Ba_2	989	458	1126	633	a
	989	451	-	625	b
Zn_2	1051	-	-	-	a
	980	450	1108	620	b

Table 4 (continued)

Cation	Mean $SO_4^{=}$ Frequencies, cm^{-1}				Ref.
	ν_1	ν_2	ν_3	ν_4	
Cd_2	1027	-	-	-	a
	1010	462	1108	621	b
	1000	497	1050	658	c
Hg_2	1014	499	-	-	a
	986	499	-	-	b
	987	495	1125	660	c
$A\ell_2$	981	457	-	612	b
	1000	480	-	620	c
$KA\ell$	984	461	-	600	b
$T\ell_2$	963	-	-	-	d
Pb_2	978	445	1105	624	a
	-	-	-	668	b
	978	443	1065	608	c
Mn_2	990	448	-	606	b
Fe_2	978	-	-	673	b
$FeNH_4$	992	-	-	-	b
Ni_2	980	460	-	620	b

References

a. Ananthanarayanan, V. Indian J. Pure Appl. Phys., 1:58, 1963.

b. Hibben, J. H. The Raman Effect and Its Chemical Applications. Reinhold, New York, 1939.

c. Wright, M. L., and K. S. Krishnan. EPA-RE-73-219, 1973.

d. Blomer, F., and H. Moser. Z. Angew. Phys. 27:302, 1969.

To obtain more precise cross section values, the effect of size, shape, and index of refraction of sulfate particulates should be investigated further.

Particulate matter is present (24) in the atmosphere at a level of about 100 $\mu g/m^3$. Sulfate particulates represent approximately 10% (5 $\mu g/m^3$-15 $\mu g/m^3$). A quantity of 1 $\mu g/m^3$ represents 0.25 ppb of $SO_4^{=}$ and 0.38 ppb of SO_2. Thus, analytical techniques capable of detecting ambient concentrations of sulfur-containing molecules require sensitivities to levels of less than 1 ppb. Particle sizes range from 0.1 μm to several microns in diameter.

Raman scattering techniques are capable of detecting sulfur compounds in the low ppb range. For example, as noted above, Stafford et al. (20) detected 8 ppb of $SO_4^{=}$ in a mist of ammonium sulfate flowing past the laser focal volume. Rosasco et al. (25) have developed a Raman microprobe technique to study individual micron size particles positioned on a substrate and have collected spectra from small sulfate salt particles. A principal result of this work is that the Raman shifts from a micron size particle do not differ from those of the bulk material. In addition, Rosen and Novakov (26) have identified $(NH_4)_2SO_4$ as a major constituent of filter collected ambient and source-enriched aerosol particulates by observing the Raman spectra from the particulate laden filter.

An attribute of the Raman method is its ability to characterize the chemical constituents of an aerosol as it flows past the laser focal volume without prior filter collection which might alter the chemical nature of the species being identified. However, using optical techniques to probe micron-size particulates dispersed in air requires consideration of the spatial distribution of excitation electric field intensity within the particle, as well as the angular profile of emitted radiation. This information is essential if molecular concentrations are to be inferred from measured Raman signal intensities and bulk scattering cross sections. The angular distribution of elastic (Lorenz-Mie) scattering from monodispersed spherical particles having diameters comparable to the incident light wavelength has undergone extensive investigation both theoretically and experimentally (27)(28). Furthermore, Chew et al. (17) have recently presented a theoretical model for inelastic (Raman and fluorescent) scattering by molecules embedded in small particles. Their treatment describes the angular distribution of radiation from a dipole located at an arbitrary position within a dielectric sphere of given refractive index after excitation by a plane wave and can be extended easily to a large number of such dipoles dispersed within the sphere. Experimental deter-

minations of the angular distribution of fluorescence intensity from monodispersed spherical particles having dye molecules dispersed throughout the sphere have also recently been reported (18)(19). Figure 9 summarizes results obtained with 0.81 μm diameter polystyrene particles and 0.488 μm laser excitation (19). The value of $m = 1.195$ is defined as the ratio of the particle's refractive index to that of the surrounding medium and provides a measure of optical index mismatch. In Figure 9(a), the observed elastic Mie scattering structure, which can be related to the sphere size, is shown along with the angular profile of fluorescence measured at a wavelength of 0.525 μm. The letters V-V and H-H refer to the incident and scattered light being polarized perpendicular and parallel to the observation plane, respectively. The interference structure observed in the elastically scattered light is completely absent in the fluorescence profile. This observation is consistent with the fact that Mie scattering requires a coherent sum of polarizations within the particle, while fluorescence entails an incoherent sum since the phase associated with each emission center is random in time. Figure 9(b) represents the difference in fluorescence intensity from dye molecules contained within 0.81 μm diameter particles relative to dye molecules dispersed in a liquid for the two polarization cases. The plotted quantity, a percentage deviation, Δ, was obtained by first normalizing the particle and liquid case intensities to be equal at an observation angle of 10°. The percentage deviation was then defined as the difference between the normalized particle and liquid fluorescence intensity values divided by the liquid intensity and multiplied by 100 to obtain a percentage. The observed deviations were largest for the backward direction (near 180°) and at 90° for H-H polarization.

At 168°, Δ for both V-V and H-H polarization approached 0% as the refractive index ratio, $m = n_p/n_\ell$, between the particle ($n_p = 1.59$) and the surrounding fluid was made nearly equal to one by adding glycerol ($n_\ell = 1.476$) to water ($n_\ell = 1.33$). It can be concluded that Δ near the backward direction is a result of distortion of the planes of constant phase and electric field amplitude within the particle caused by the particle-medium index of refraction mismatch. This result, when applied to aerosols for which $n_\ell = 1$, predicts a large signal enhancement in backscattering, and the conversion of fluorescent LIDAR data (29) to molecular concentrations within aerosols must account for the particle-air index mismatch, as well as the size and shape of the particle. The observation by Stafford et al. (20) that the apparent cross section of $SO_4^{=}$ in liquid mist form is approximately 20 times greater than its bulk value is likely to be a manifestation of this effect.

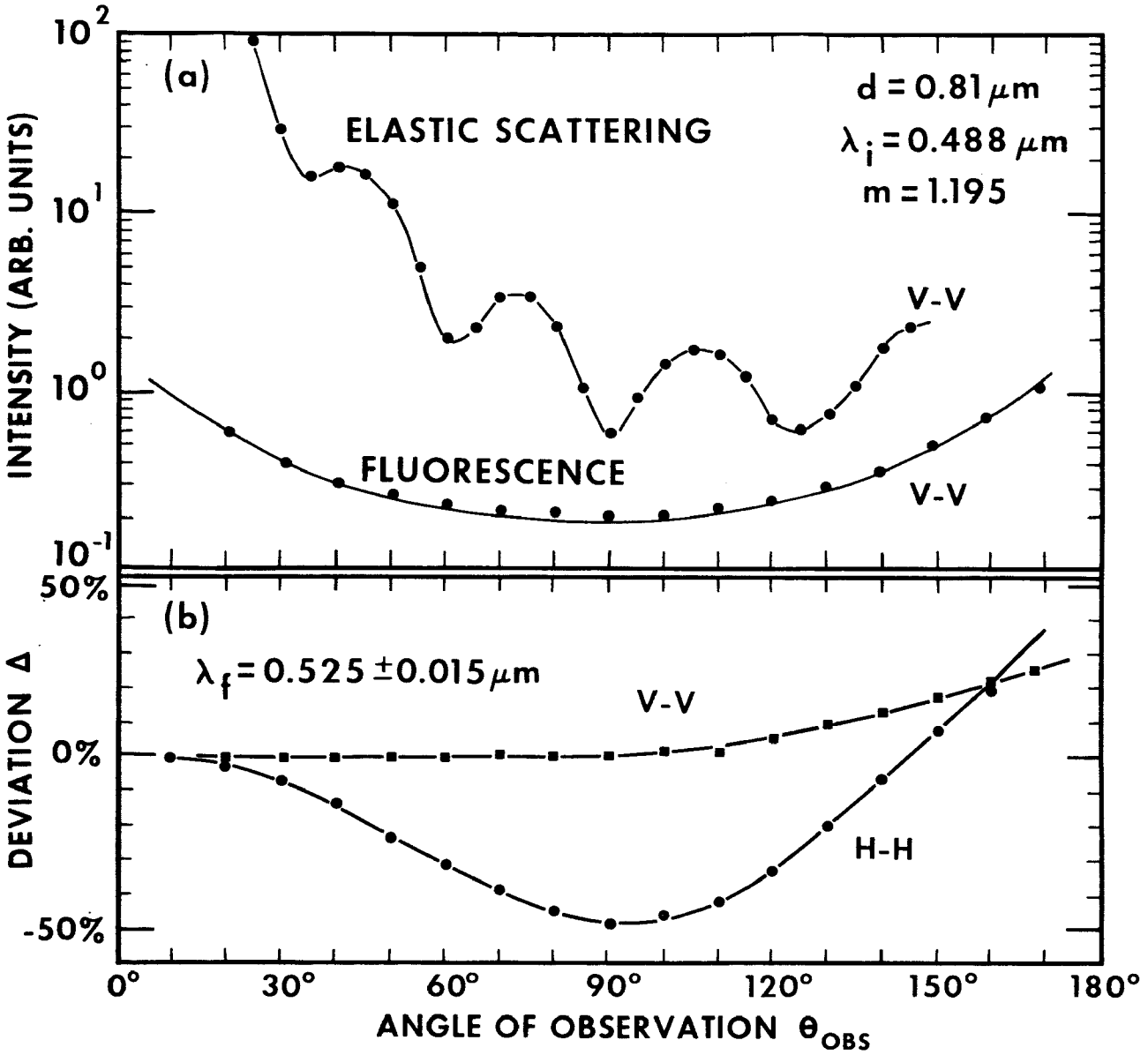

Figure 9. (a) Angular distribution of elastic scattering (top) and fluorescence (bottom) from 0.81 μm diameter particles with 0.488 μm excitation. (b) Deviation, Δ, of 0.81 μm particle fluorescence from dye solution fluorescence. The interference filter used to isolate the fluorescence wavelength, λ_f, was centered at 0.525 μm and has a half-width of 0.015 μm. The incident wavelength is λ_i (19).

The large Δ for H-H polarization at 90° did not vanish even when n_ℓ approached n_p. In the theoretical approximation (17) of a single electric dipole located at the center of the sphere which is fixed in space (not tumbling), the fluorescence intensity at 90° and H-H polarization should be identically zero. The observed deviation is ascribed to random orientation of dye molecules with anisotropic polarizability within the particles, which are assumed not to tumble during the fluorescent re-emission time τ_F. For aerosols, however, the tumbling frequency may approach τ_F^{-1}.

A configuration in which dye molecules were incorporated only on the surface of monodispersed spherical particles was also investigated. The characteristic interference structure was observed in the elastic scattering, and the fluorescence distribution was again a smooth curve. The deviations for V-V and H-H polarizations were slightly smaller than for the corresponding volume distributed dye molecules.

The fluorescence results can be applied directly to spontaneous Raman scattering from monodispersed spherical particles with diameters comparable to the incident and Raman shifted wavelengths. The Raman process also requires an incoherent sum of polarizations within the particle since the phase associated with each scattering site is related to the arbitrary and random phase of the molecular vibration. The angular distribution of Raman scattering from such particles can be expected to be featureless and to deviate from the gaseous and liquid cases in direct analogy with the reported fluorescence results.

For applications requiring chemical analysis and concentration information on a sample containing numerous molecular species existing in different phases, including particulates of varying diameters and shapes, it may not be sufficient to record in situ a single composite Raman spectrum. While identification of the different molecular species may be possible since the probed characteristic vibrational frequencies are not distorted by the particulate nature of the sample, extraction of concentration data would be extremely difficult because of the superposition of varying linewidths and effective cross sections associated with the different phases. In such a situation, prior filter collection of the particulates may be required in order to separate the phases, to confine the range of size, or to concentrate the particulate density.

In choosing an appropriate scattering geometry to obtain spectra from a collected particulate sample, factors to be considered include maximizing the collected Raman signal, minimizing the amount of elastically scattered light which enters the spectrometer, and

isolating any contributions from the supporting substrate. Rosasco et al. (25), in recording spectra from single micron-size particles, have demonstrated that heating effects caused by the high excitation laser power densities associated with extreme focusing of the probing light beam can be minimized if the particle is in good thermal contact with a substrate, such as sapphire or LiF_2. Thus, to characterize a distribution of particles with a single Raman scan, the particulate sample should be distributed as a monolayer on a substrate to maximize the thermal contact so that high field intensities can be employed to increase the Raman signal. An obvious approach is to use a relatively high power laser focused directly on the collected sample and a conventional spectrometer which could probe a sample area having a diameter of 100 μm or larger. However, adaptation of the techniques of internal reflection spectroscopy (30) to enhance the excitation electric field intensity at the particulate-substrate interface may provide significant advantages.

Carniglia et al. (31) have investigated, both theoretically and experimentally, the excitation of a monolayer of fluorescent molecules by evanescent or exponentially decaying waves generated upon total internal reflection as well as the emission of light by the excited molecules. They find that absorption is proportional to the square of the exciting field whether the incident light is homogeneous or evanescent and that the emission process follows a reciprocity principle. Lee et al. (32) recently have completed similar experiments to determine the polarization and angular dependence of fluorescence from a thick liquid dye layer in contact with the substrate excited by evanescent waves in the configuration shown in Figure 10. Light entered a hemicylindrical sapphire prism at an angle of incidence, θ_{INC}, which exceeded the critical angle for the prism-dye solution interface; thus, excitation of the dye molecules was by an evanescent wave. The emitted fluorescence was observed with an angular resolution of 0.3° upon its passing through the prism at an observation angle, θ_{OBS}, as defined in Figure 10. The observed fluorescence intensity as a function of θ_{OBS} for the different polarization cases (as defined above) for an angle of incidence of 60° is shown in Figure 11. In good agreement with the work of Carniglia et al. (31), as well as with Fresnel theory, the fluorescence in all cases was observed to peak at a specific angle which is equal to the critical angle had the light of the fluorescence wavelength been incident from the prism to the dye solution. It should be noted that, because of dispersion in the prism refractive index, the fluorescence does not peak at the critical angle corresponding to the excitation wavelength. The fluorescence intensity dependence on θ_{INC} is shown in Figure 12, which indicates that the largest fluorescence intensity is observed when the excitation and fluorescence radiations are at their respective critical angles.

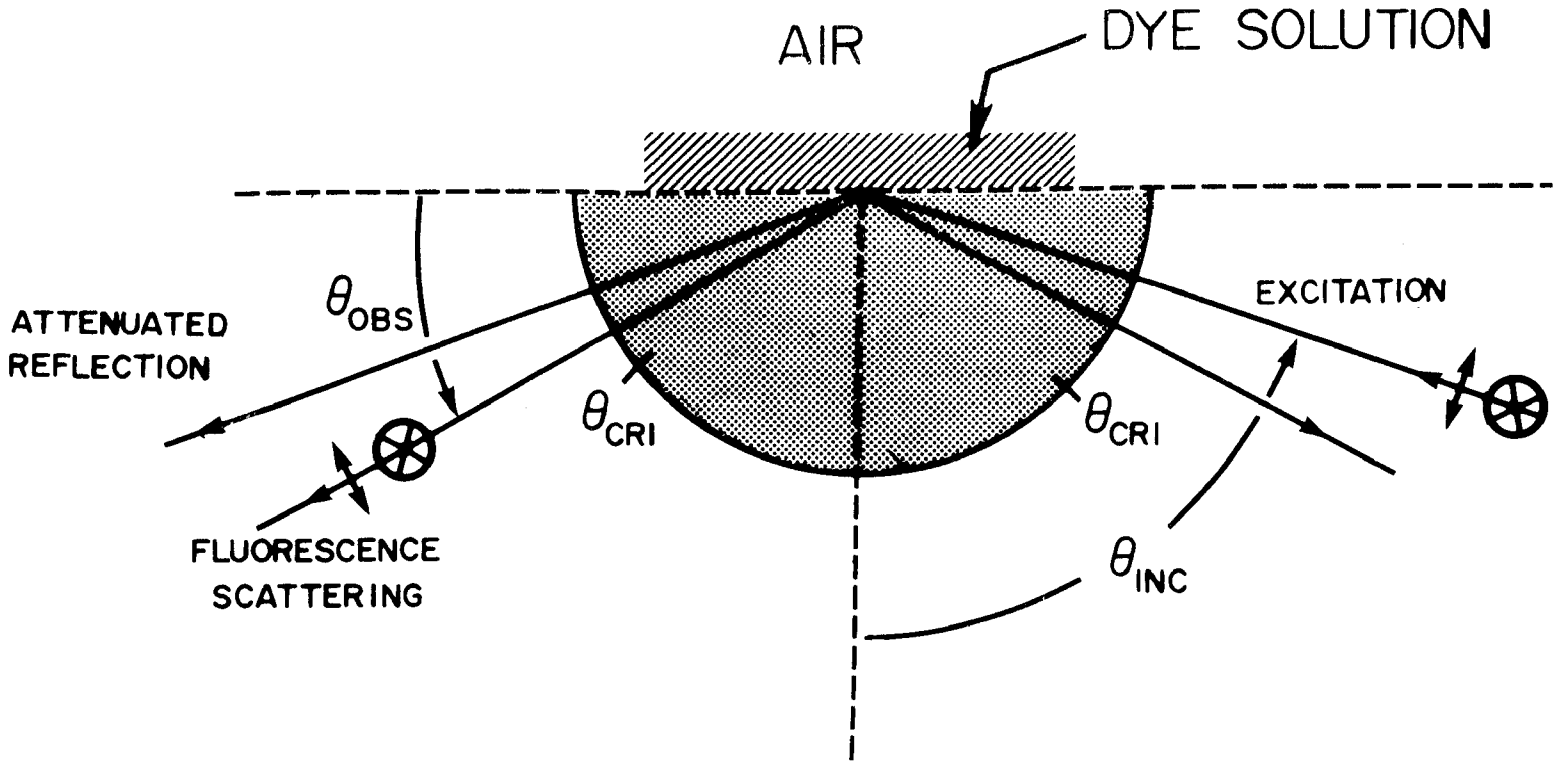

Figure 10. Hemicylindrical sapphire prism with dye solution on top. The angle of incidence, θ_{INC}, exceeds the critical angle for the prism-dye solution interface, causing the evanescent wave in the dye solution. The fluorescence scattering is detected as a function of θ_{OBS}. Different combinations of polarization for incident and scattered radiation can be selected with polarizers.

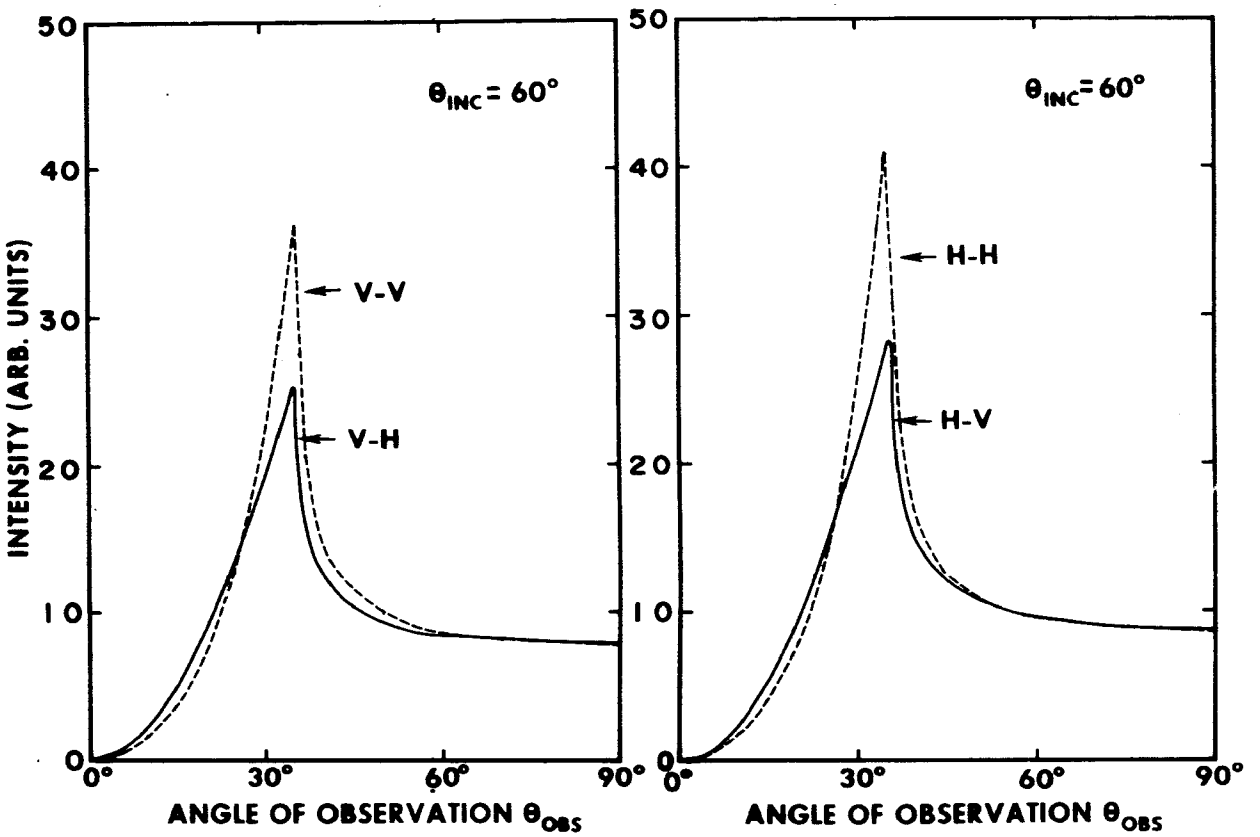

Figure 11. The observed fluorescence intensity as a function of θ_{OBS} for different polarization combinations. V and H designate vertical and horizontal polarization directions, respectively, with regard to the scattering plane shown in Figure 10. θ_{INC} was greater than the critical angle. The fluorescence intensity peaked at the prism-dye solution interface critical angle for fluorescence wavelength.

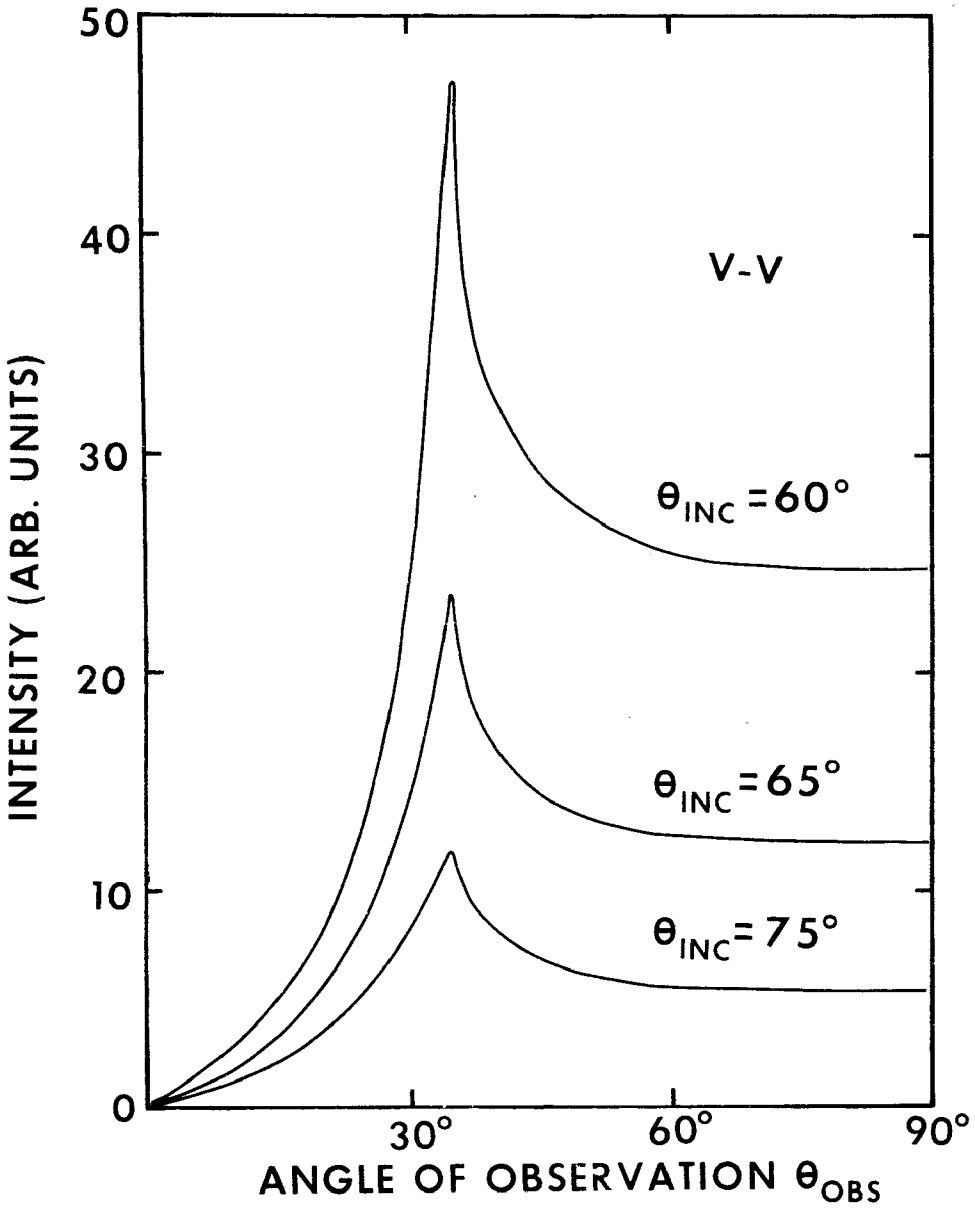

Figure 12. The fluorescence intensity as a function of θ_{OBS} for several θ_{INC}. Note that the largest fluorescence intensity is observed when θ_{INC} and θ_{OBS} are at their respective critical angles. The polarization combination is V-V.

This internal reflection configuration applied to observing Raman scattering from a monolayer of particulates offers several advantages. First, the electric field amplitude at the interface can be enhanced by a factor two because of superposition of the incoming and reflected field amplitudes (30), which causes a factor 4 increase in the excitation intensity. Correspondingly, utilizing the reciprocity of the emission process, an additional factor 4 enhancement (at maximum) can be attained when the evanescent fluorescence is converted to a homogeneous wave upon entering the prism. Second, because of the prism dispersion, the reflected incident light is spatially separated from the angular peak in the Raman signal intensity and need not enter the spectrometer. In addition, localization of the laser amplitude within the monolayer can be achieved since the penetration depth of the evanescent wave can be on the order of the monolayer thickness, depending upon the refractive index ratio of the substrate and particulate, the excitation wavelength, and the angle of incidence. However, isolation of the desired Raman signal from fluorescence, elastic, and Raman scattering initiated within the substrate may be difficult to obtain.

By replacing the liquid dye layer in the configuration of Figure 10 with a layer of monodispersed spherical particles containing dye molecules, the fluorescence angular distributions (32) given in Figure 13 were obtained. The packing density of particles on the substrate was found to affect the fluorescence profile. With a layer of particles on a substrate, there are effectively two interfaces, one defined by the contact area between the prism and the spheres and another formed in the space between neighboring particles as an air-prism boundary. A dense packing of particles led to the angular distribution of curve (c) shown in Figure 13, which peaked at an effective critical angle corresponding to the particle-prism interface. In curve (a), for which the spheres were sparsely packed, the air-prism critical angle dominated the distribution. Curve (b) represents an intermediate packing density. Otherwise, the results obtained were analogous to those of the liquid dye configuration.

The preliminary data obtained utilizing internal reflection techniques to enhance the signal are encouraging and indicate that additional studies should be completed. Application of resonant internal-reflection prism approaches, as recently reviewed by Hjortsberg et al. (3), should result in much larger signal enhancements than achieved in the ordinary internal reflection geometry. For example, utilizing a surface plasmon enhancement in the geometry of Simon et al. (34) could increase the effective interface excitation intensity by a factor 50 or greater. By choosing the observation angle to be at resonance, a similar additional enhancement

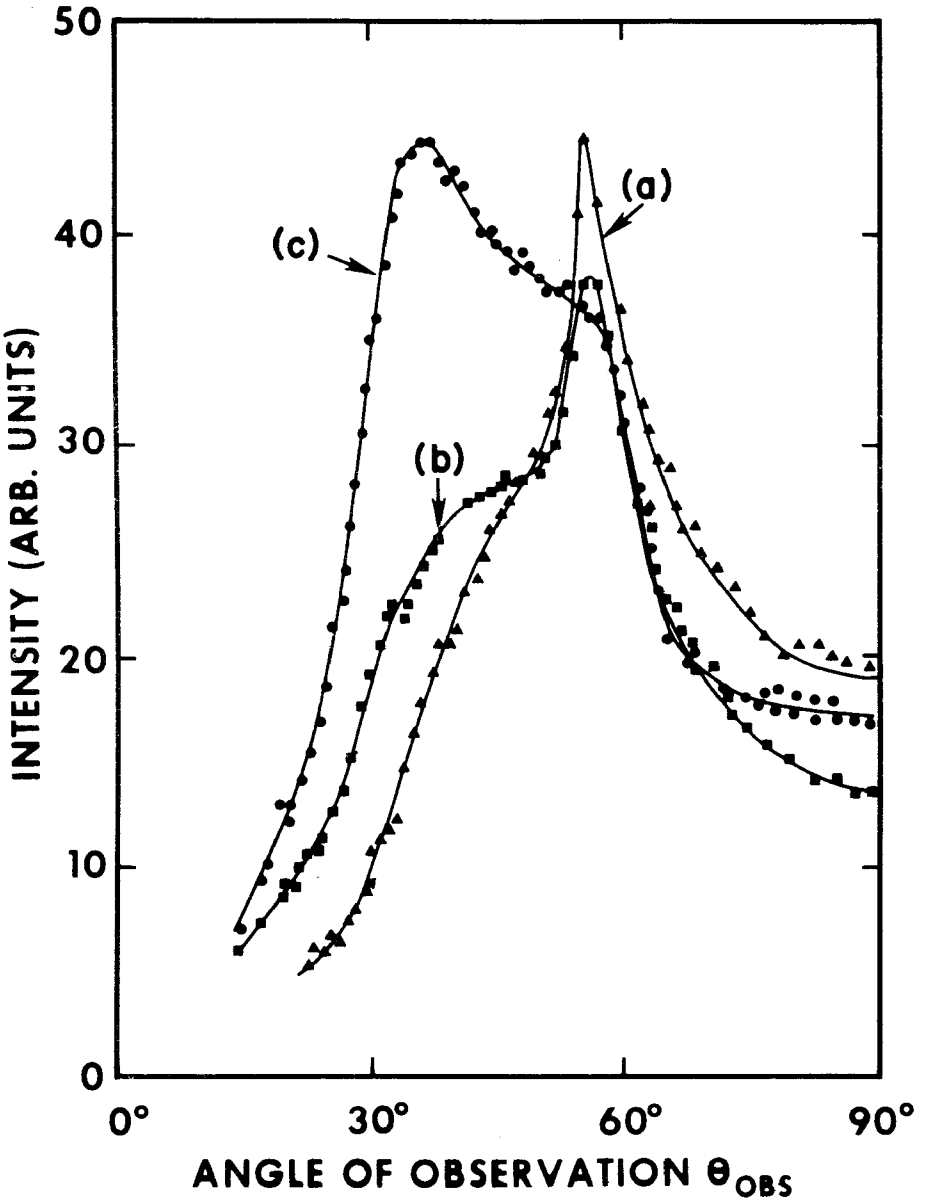

Figure 13. By replacing the dye-solution shown in Figure 10 with monodispersed spherical particles (0.81 μm) containing dye molecules, the fluorescence intensity as a function of θ_{OBS} is shown. Dense packing of particles is shown in (c), while the sparsely packed case is shown in (a). Curve (b) represents an intermediate packing density. Two effective interfaces (prism-air and prism-particle) are present, and thus the fluorescence emission is expected to peak at the corresponding critical angles.

should be achievable in coupling the Raman signal back to the prism. Furthermore, the pronounced dip in elastically reflected light intensity associated with excitation of the surface plasmon mode should yield excellent isolation from the laser wavelength. Although the optimum configuration will depend largely on the difficulty of minimizing unwanted signals generated in the substrate materials, these resonance methods offer a prospective means of increasing the sensitivity of the Raman method in analyzing sulfur-containing particulates.

INSTRUMENTAL TECHNIQUES

While laboratory Raman systems similar to that depicted in Figure 8 have become highly refined since the advent of the laser, specialization of equipment to the problem of obtaining spectra from atmospheric gases, aerosols, and particulates could yield improvement in signal/noise ratios. Figure 14 is a schematic representation of a Raman system currently being developed in our laboratory to investigate atmospheric constituents. In common with the apparatus of Figure 8, the new system will use a 3W continuous argon laser for excitation and employ a multipass optical light trap to increase the total excitation intensity within the focal volume. Two concave mirrors with dielectric coatings will be mounted with multiple degrees of freedom to insure optimum alignment. Collection optics include the lens L_2, and an f/1.2 camera lens in conjunction with a third spherical mirror. After collection, the Raman scattered light passes through an interference filter (IF) chosen to block light at the laser wavelength (5145 Å) with a rejection of 10^{-4} and pass Raman shifted signals ($\Delta\upsilon \simeq$ 500-3050 cm^{-1}) with an average transmission exceeding 70%. The scattered light is focused, commensurate with an f/8, 1 meter focal length diffraction grating, onto the spectrograph entrance slit. To determine the frequency components present in the scattered light, the system uses a single concave holographic grating which has a high rejection ($\simeq 10^{-8}$) and requires no additional components inside the spectrometer. Use of a single grating of high rejection rather than the usual double grating approach significantly improves system throughput. As indicated in Figure 14, the instrument can be used as a conventional spectrometer with an exit slit, photomultiplier, and photon-counting electronics or as a Raman spectrograph by imaging a selected portion of the entire diffracted spectra (about 500 cm^{-1}) on a silicon intensifier target (SIT) vidicon having approximately 500 channels of resolution.

The parallel-channel approach to detection (35) offers many advantages. It provides the capability of simultaneously detecting numerous constituents having different Raman shifts within

RAMAN SPECTROGRAPH

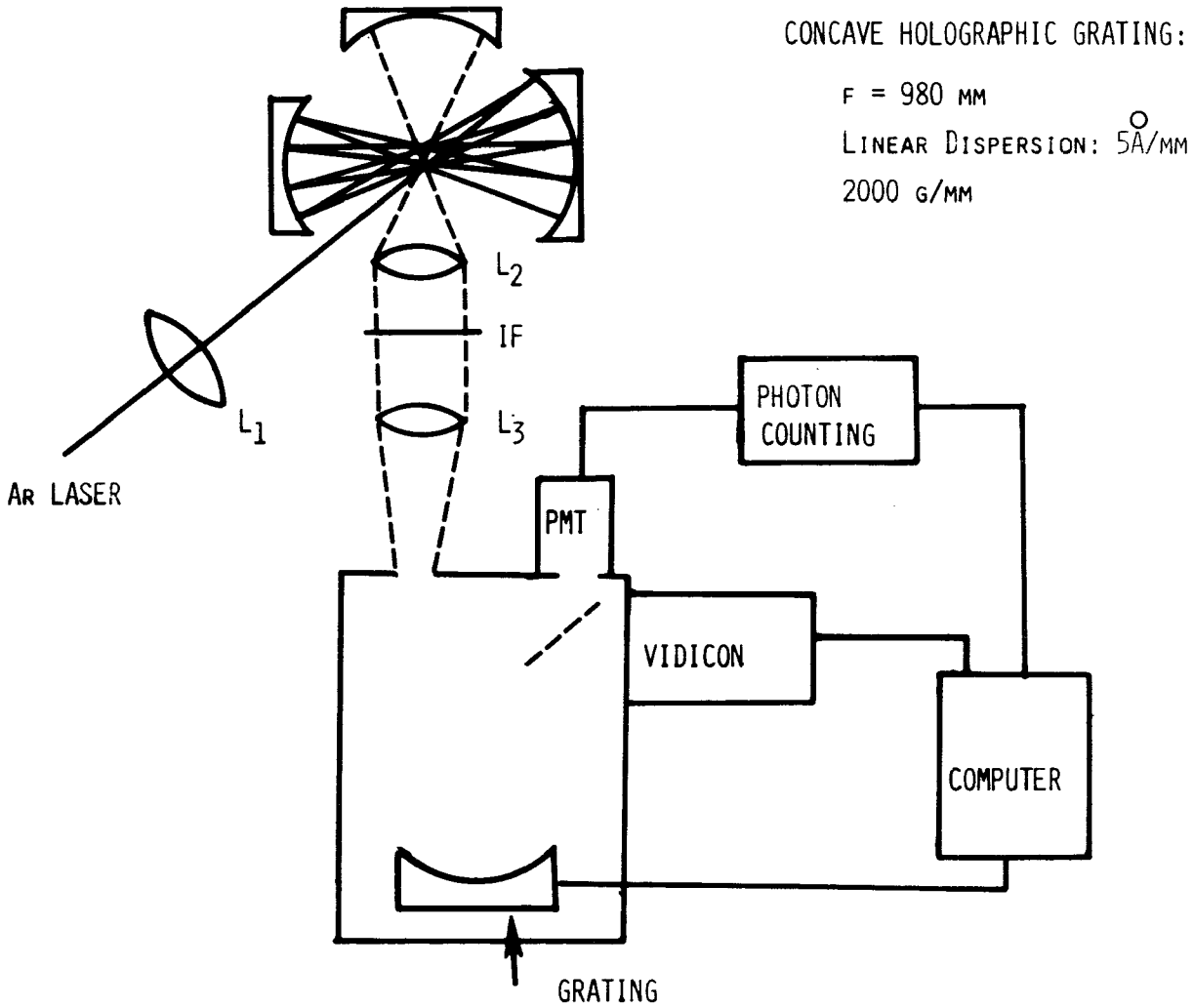

Figure 14. Schematic diagram of a high throughput spectrometer/spectrograph containing a single concave holographic grating. For single-channel detection, a specific Raman wavelength is passed through the slit and then onto the photomultiplier. For parallel-channel detection, a range of Raman wavelengths is deflected by a mirror onto the front face of a vidicon camera.

an interval of 500 cm^{-1} and therefore decreases recording time by a factor 500. More important, since the dark count rate is comparable to that of a conventional photomultiplier, shorter collection times result in larger signal/noise ratios. In addition, spectral anomalies and relative peak height variations caused by fluctuations in laser power and ambient concentration levels which occur as a spectrometer is scanned through wavelength can be minimized by parallel-channel detection. Camera scanning and grating rotation (in order to diffract other intervals of 500 cm^{-1}) are controlled by a minicomputer, which can also perform molecular concentration calculations based on recorded Raman intensities.

A disadvantage of the ORE approach to characterizing sulfur containing molecules is its inability to probe a wide geographic area. Unlike LIDAR, which can probe samples distant from the spectrometer, ORE requires that the species of interest be contained within the focal volume of the multipass light trap. As a partial solution, the feasibility of using fiber optic cables to guide excitation laser light to a remote scattering cell and to return the Raman scattered light to the spectrometer is also being investigated in our laboratory. A multipass light trap can be used with each pair of fiber cables to increase the Raman signal. The low transmission losses ($\simeq$10 dB/km) of present optical fibers should, at the least, enable remote sensing using ORE with sufficient sensitivity to detect toxic species in hostile environments. For these applications, a single laser and spectrometer could be used with many pairs of fiber cables to sample numerous locations with the ultimate sensitivity being limited mainly by the ability to couple light into and out of the fibers and by the background scattered signals generated in the transmitting light cables.

CONCLUSION

The Raman effect of sulfur oxides in gaseous, liquid, solid, and aerosol forms has been summarized, and recent developments in the understanding of inelastic scattering from small particles have been discussed. Many specific values of the Raman cross sections, lineshifts, and linewidths of some important sulfur oxides are still undetermined. Consequently, it is not possible at this time to state unequivocally that the Raman technique can be used to distinguish the chemical species and their phases or to measure the concentration of each species contained in the emission from combustion sources. The Raman technique does have the potential of being a viable approach for monitoring simultaneously and in situ many chemicals in their various phases.

This work was supported in part by the American Gas Association Grant No. GRI 5009-362-0044/AGA BR-142-1, by the National Science Foundation Grant No. ENG77-07157, and by the Northeast Utilities Service Company, Hartford, Connecticut.

REFERENCES

1. Irish, D. E., and H. Chen. Equilibria and Proton Transfer in the Bisulfate-Sulfate System. J. Phys. Chem., 74(21): 3796-3801, 1970.

2. Fouche, D. G., and R. K. Chang. Relative Raman Cross Section for O_3, CH_4, C_3H_8, NO, N_2O, and H_2. Appl. Phys. Lett., 20(7):256-257, 1972.

3. Fouche, D. G., and R. K. Chang. Observation of Resonance Raman Scattering Below the Dissociation Limit in I_2 Vapor. Phys. Rev. Lett., 29(9):536-539, 1972.

4. Penney, C. M. Remote Measurement of Ozone by Resonance Raman Scattering and Differential Absorption. IEEE J. Quantum Electron., QE-11:36D, 1975.

5. Wang, Charles C., and L. I. Davis, Jr. Measurement of Hydroxyl Concentrations in Air Using a Tunable UV Laser Beam. Phys. Rev. Lett., 32(7):349-352, 1974.

6. Penney, C. M., W. W. Morey, R. L. St. Peters, S. D. Silverstein, M. Lapp, and D. R. White. Study of Resonance Light Scattering for Remote Optical Probing. NASA Report No. CR-132363, 1973.

7. Rousseau, D. L., and P. F. Williams. Resonance Raman Scattering of Light from a Diatomic Molecule. J. Chem. Phys., 64(9):3519-3537, 1976.

8. Fouche, D. G., A. Herzenberg, and R. K. Chang. Inelastic Photon Scattering by a Polyatomic Molecule: NO_2. J. Appl. Phys., 43(9):3846-3851, 1972.

9. Tolles, W. M., and R. D. Turner. A Comparative Analysis of the Analytical Capabilities of Coherent Anti-Stokes Raman Spectroscopy (CARS) Relative to Raman Scattering and Absorption Spectroscopy. Appl. Spectry., 31(2):96-103, 1977.

10. Hill, R. A., and D. L. Hartley. Focused, Multiple-Pass Cell for Raman Scattering. Appl. Opt., 13(1):186-192, 1974.

11. Stafford, Richard G., and Richard K. Chang. Absolute Raman Scattering Cross Sections of Sulfate and Bisulfate and Their Application to Aqueous Aerosol Monitoring. In: International Conference on Environmental Sensing and Assessment, Vol. 2, IEEE, New York, 1976. pp. 23-5/1-4.

12. Woodward, L. A., and R. G. Horner. Changes in the Raman Spectrum of Sulphuric Acid on Dilution. Proc. Roy. Soc. (London), 144A(851):129-143, 1934.

13. Hibben, James H. The Raman Effect and Its Chemical Applications. Reinhold Publishing Corp., New York, 1939. 544 pp.

14. Zarakhani, N. G., N. B. Librovich, and M. I. Vinnik. Homogeneous Catalytically Active Solutions. VII. The Equilibrium Compositiion of the Sulphuric Acid-Water System. J. Phys. Chem., 45(7):981-983, 1971.

15. Lindstrom, Richard E., and Henry E. Wirth. Estimation of the Bisulfate Ion Dissociation in Solutions of Sulfuric Acid and Sodium Bisulfate. J. Phys. Chem., 73(1):218-223, 1969.

16. Young, T. F., and G. E. Walrafen. Raman Spectra of Concentrated Aqueous Solutions of Sulphuric Acid. Trans. Faraday Soc., 57(1):34-39, 1961.

17. Chew, H., P. J. McNulty, and M. Kerker. Model for Raman and Fluorescent Scattering by Molecules Embedded in Small Particles. Phys. Rev., A 13(1):396-404, 1976.

18. Kratohvil, J. P., M.-P. Lee, and M. Kerker. Angular Distributior of Fluorescence from Small Particles. To be published, Appl. Opt., 1978.

19. Lee, El-Hang, R. E. Benner, J. B. Fenn, and R. K. Chang. Angular Distribution of Fluorescence from Monodispersed Particles. To be published, Appl. Opt., 1978.

20. Stafford, R. G., R. K. Chang, and P. J. Kindlmann. Laser-Raman Monitoring of Ambient Sulfate Aerosols. In: Methods and Standards for Environmental Measurement, Proceedings of the 8th Materials Research Symposium. NBS Special Publication 464. William H. Kirchoff, ed. U.S. Government Printing Office, Washington, D.C., 1976. pp. 659-667.

21. Anathanarayanan, V. A Comparative Study of the Raman Spectra of Anhydrous Sulphates and Estimation of Crystalline Forces. Indian J. Pure Appl. Phys., 1(2):58-61, 1963.

22. Blomer, F., and H. Moser. Absolute Intensitätsmessungen an Raman-Kristallpulverspektren von Nitraten und Sulfaten. Z. angew. Phys., 27(5):302-306, 1969.

23. Wright, M. L., and K. S. Krishnan. Feasibility Study of In-Situ Source Monitoring of Particulate Composition by Raman or Fluorescence Scatter. EPA-R2-73-219, U.S. Environmental Protection Agency, Washington, D.C., 1973. 117 pp.

24. Radian Corp. Literature Evaluation of Methods Available for the Collection and Measurement of Sulfur Dioxide, Sulfur Trioxide, Sulfuric Acid, and Particulate Sulfate in Ambient Air. RC No. 200-077. Austin, Texas, 1974. 80 pp.

25. Rosasco, G. J., E. S. Etz, and W. A. Cassatt. The Analysis of Discrete Fine Particles by Raman Spectroscopy. Appl. Spectry., 29(5):396-404, 1975.

26. Rosen, H., and T. Novakov. Identification of Primary Particulate Carbon and Sulfate Species by Raman Spectroscopy. Topical Meeting of the Optical Society of America. Aerosols: Their Optical Properties and Effects. Williamsburg, Va., 1976.

27. Van de Hulst, H. C. Light Scattering by Small Particles. John Wiley & Sons, New York, 1962. 470 pp.

28. Kerker, Milton. The Scattering of Light and Other Electromagnetic Radiation. Academic Press, New York, 1969. 666 pp.

29. Byer, R. L. Review, Remote Air Pollution Measurement. Optical & Quantum Electron., 7(3):147-177, 1975.

30. Harrick, N. J. Internal Reflection Spectroscopy. Interscience Publishers, New York, 1967. 327 pp.

31. Carniglia, C. K., L. Mandel, and K. H. Drexhage. Absorption and Emission of Evanescent Photons. J. Opt. Soc. Am., 62(4):479-486, 1972.

32. Lee, El-Hang, R. E. Benner, J. B. Fenn, and R. K. Chang. Angular Profile of Fluorescence from Monodispersed Spheres by Evanescent Wave Excitation. To be published.

33. Hjortsberg, A., W. P. Chen, and E. Burstein. Resonant Internal-Reflection Prism Spectroscopy Using Surface, Guided, and Fabry-Perot EM Waves. Appl. Opt., 17(3):430-434, 1978.

34. Simon, H. J., R. E. Benner, and J. G. Rako. Optical Second Harmonic Generation with Surface Plasmons in Piezoelectric Crystals. Opt. Commun., 23(2):245-248, 1977.

35. Black, P. C., and P. J. Kindlmann. Parallel-Channel Detection System for Low Light Level Spectroscopy. In: Proceedings of the Technical Program, Electro-Optical Systems Design Conference-1973, New York, 1973. pp. 206-215.

Report of the Working Group on Measurement of Gaseous Sulfur Oxides Emissions

Russell N. Dietz, *Reporter*

This working group, charged primarily with the responsibility for examining the pertinent aspects of sampling and analysis for the gas phase sulfur constituents in flue gas, made recommendations in the following areas:

- Definition of terms
- Essential measurements
- Units for data presentation
- Sampling methodology
- Specific research needs

DEFINITION OF TERMS

Molecular Formulation

Correct molecular formulation for the presentation and reporting of constituents is essential. For example,

- sulfur dioxide - SO_2
- sulfur trioxide - SO_3
- sulfate salts or sulfates - MSO_4
  (do <u>not</u> use SO_4 only)

Sulfuric Acid

H_2SO_4 can exist as a vapor, adsorbed vapor, or liquid aerosol. The H_2SO_4 vapor exists as a gas in the flue gas with a certain fraction existing in the adsorbed state on particulate matter in the flue gas. If the temperature of the flue gas is below the dewpoint temperature for the sulfur acid (not the usual case), some of the H_2SO_4 could be present as liquid aerosol.

Sulfate Salts

The balance of sulfate material collected on a filter medium is considered to be comprised of sulfate salts. Some of the remaining sulfate fraction on the particulate matter may be chemisorbed H_2SO_4, but there would be no simple means for distinguishing that from true sulfate salts.

Total Sulfates

Sulfuric acid and sulfate salts may be referred to collectively as total sulfates. But in every case of usage, the authors should explicitly define their meaning.

Artifact Sulfate

Sulfate that is generated by the measurement technique, and that is determined as sulfate because of either an interference problem or because of conversion of SO_2 to sulfate during the collection and/or determination, may be considered to be artifact sulfate and is, in fact, a measurement error.

ESSENTIAL MEASUREMENTS

Separation of H_2SO_4 and Sulfate Salts

A filter should be utilized to adequately separate the flue gas particulate matter from the sulfuric acid in the vapor phase. The filter should first be extracted with an appropriate solvent (e.g., anhydrous acetone, isopropyl alcohol) for the recovery of adsorbed H_2SO_4 or liquid aerosol H_2SO_4. This is followed by extraction with water for recovery of the water soluble sulfate salts. The vapor phase fraction of the H_2SO_4 should be appropriately collected downstream of the filter.

Sampling Location, Temperature, Water Vapor, and Oxygen Level

The location of the sampling point should be clearly indicated. In addition, the temperature and water vapor content at the sampling location should be specified in order to determine the physical and chemical state of the sulfuric acid (i.e., vapor H_2SO_4, liquid aerosol H_2SO_4, or gaseous SO_3). Sampling location of the oxygen level should also be determined in order to correct for leaks in the flue gas ducting downstream of the boiler.

Furnace Oxygen

The furnace or boiler O_2 level has been shown to directly affect the levels of H_2SO_4 and sulfate salts formed within the combustion unit. It is essential that the amount of furnace or boiler oxygen be determined and that this quantity not be confused with the oxygen level existing at the sampling location.

UNITS FOR DATA PRESENTATION

Gaseous Species

Volumetric units such as ppm (parts per million), denoted by vol. ppm or by vol. %, may be used for reporting the concentration of gaseous species.

Liquid or Solid Species

Mass units reported as mass per unit volume of flue gas is preferred for liquid and solid species. The formula name of the specie being reported must be specified since units of mass are being used. In addition, the conditions at which the gas volume is being reported must be indicated (i.e., temperature and pressure).

In both cases above, the other conditions of the flue gas such as wet or dry basis, and whether or not corrections were made for flue gas ducting leaks, should be reported.

SAMPLING METHODOLOGY FOR H_2SO_4

Isopropyl Alcohol Methodology

With regard to the application of methods utilizing isopropyl alcohol (IPA) for the determination of sulfuric acid, there are problems associated with the use of a small static amount of IPA in contact with a significant volume of flue gas. At sulfuric acid concentrations in flue gas less than 3 to 5 vol. ppm, significant errors in H_2SO_4 determination can occur because of H_2SO_4 aerosol collection inefficiency, residual dissolved SO_2, or oxidation of SO_2 to H_2SO_4. It is not possible to measure H_2SO_4 concentrations less than 1 vol. ppm in flue gas using IPA methodology (e.g., EPA Modified Method 6 or Method 8).

If utilizing IPA methodology, an appropriate reagent grade, free of oxidant, should be used.

Controlled Condensation Methodology

The controlled condensation methodology is the preferred approach for manual determination of H_2SO_4. There is a critical need for the specification of equipment design and sampling practice, including approaches addressing the problems of pre-filtering, final condenser filtering, and pressure drop considerations.

Acid Dewpoint Methodology

Such monitors have limited application; other direct methods such as controlled condensation are preferred.

SPECIFIC RESEARCH NEEDS

Particulate and Vapor Separation

Research must be directed towards separation methods for adequately distinguishing between the H_2SO_4 vapor and the sulfate salts. Potential separation techniques include filtering, electrostatic precipitation, and cyclone separation.

Optical Methods

Research should be directed towards studying optical techniques because of their potential for in-stack determinations for multiple compounds.

Continuous IPA H_2SO_4 Monitor

The continuous automatic analyzer for H_2SO_4 developed by the Central Electricity Generating Board in England, based on co-current absorption in IPA solution followed by reaction with barium chloranilate for colorimetric determination as 535 nm, should be tested and evaluated.

Automatic Controlled Condensation

The EPA approach should be studied in more detail.

Validation of Methods

There should be a continual examination of reference and field methods for latest improvements and up-dating of these techniques as field experience is acquired.

Section 2

Particulate Sampling and Analysis

Collection Methods for the Determination of Stationary Source Particulate Sulfur and Other Elements

Kenneth T. Knapp
Roy L. Bennett
Robert J. Griffin
Raymond C. Steward
U.S. Environmental Protection Agency

ABSTRACT

The growing concern over the chemical composition of the particulate emissions from stationary sources has led to the improvement of sampling methods, so that representative samples compatible with chemical analysis can be obtained. Improvements include the development of techniques for obtaining particle-sized samples. Analytical techniques used should be sensitive; require minimal sample preparation and small samples, and work quickly. One technique that offers these qualities is x-ray fluorescence spectrometry (XRF). Some XRF systems can determine 30 elements in less than 10 minutes. In addition, these systems are non-destructive and require little preparation for filter samples. For light elements such as sulfur, the best results are obtained using samples collected uniformly on the surface of thin substances with a low mass, such as filters made of organic polymers.

The collection of samples on thin membranes at many sources has been the source of several major problems. The most severe problems are related to the temperature limitation of the filters and their degradation by hot sulfuric acid emissions. However, good samples for chemical analysis can be obtained in the field using temperature controls and careful handling. Since, in general, only small amounts of material are collected, the samples must be handled carefully in the laboratory to avoid sample loss, contamination, and moisture effects.

The use of impactor-sized samples for XRF analysis creates additional problems, including non-uniform collection, many small piles of material, and substrates that usually are not compatible with the XRF spectrometer. Several techniques are presently being used to transfer these types of samples to compatible substances. Another approach being pursued is the development of a new system that will yield uniform-sized samples on compatible substrates.

INTRODUCTION

The growing concern for information on the chemical composition of particulate emissions from stationary sources has resulted in research to improve sampling methods so that representative samples are compatible with the analytical techniques. The information sought includes the chemical analysis of both bulk and sized particulate emissions. The analytical techniques used should have good sensitivity, require small samples, and need only minimal sample preparation. X-ray fluorescence spectrometry (XRF) is one technique that offers these qualities. It is fast and non-destructive, and filter samples require little or no preparation. The XRF system used by the Particulate Emissions Research Section (PERS) of the Environmental Sciences Research Laboratory of EPA can determine 30 elements including sulfur in a filter sample in less than ten minutes. Since XRF analysis of source emissions and the PERS system have been described in several publications, no detailed discussion of them will be presented in this paper (1)(2)(3).

The sampling techniques described in this paper have been designed for optimum XRF analysis of the emissions from stationary sources. Special attention has been given to sulfur analysis. Two types of sample collection techniques are discussed, those for bulk or total sample analysis and those for particle-sized sample analysis.

METHODS

Systems that are used to obtain samples for chemical or other analysis from stationary sources have basically three parts. The first part transfers the emitted sample from the source to the collecting device. This transfer section, sometimes referred to as the sampling interface, can be a simple nozzle or a complex boundary layer quantitative transport system. The collecting device, the second part of the sampler, can be open cups, impaction surfaces or filters. Filters have several advantages over the other

devices, including low cost, ease of handling, and efficiency. The final part of the sampler is the gas flow section which contains the gas pump and a flow measuring device. For particle-sized samples, the collecting device generally performs the sizing.

Obtaining a gas flow system that will provide a reasonably accurate flow over a wide range is no major problem. Therefore, no further discussion of it will be given. Many investigators have worked on the problems of sample transport, and several publications are available on this subject (4)(5)(6); therefore, it too will not be discussed further.

Filters

One of the most critical problems in measuring the particulate emissions from sources is getting a truly representative sample to the measuring device. Of equal importance, when the chemical composition of the emissions is to be determined, is the proper selection of the collecting surface or device. Filters are generally used to collect the samples. They are usually simple to use and are compatible with many analytical techniques such as XRF. Listed in Tables 1 and 2 are the filters which PERS has used for chemical analysis of source emissions. Table 2 is a list of fluorinated polymer filters tested. Figure 1 shows the pressure drop at various flows for these filters.

The most commonly used filter for air pollution work is the glass fiber filter. While it has several advantages for measuring total particulate mass such as low pressure drop, high capacity, ease of weighing, and cost, it has several major drawbacks for XRF analysis. Even the best grade of glass fibers has high x-ray backgrounds due to trace element contamination. The filters also scatter large amounts of x-rays. In addition, these filters are depth filters where the particles penetrate deep into the filters and cause attenuation of the characteristic x-rays from the light elements such as sulfur. This makes corrections necessary. Theoretical corrections are hard to determine; therefore, empirical corrections are generally used.

In an attempt to obtain a filter with a lower background, EPA contracted for the development of a filter made of quartz fibers. Such a filter was developed and is described in an EPA report (7). However, the filters made of quartz fibers are not strong enough to be useful in general field sampling.

Table 1. Characteristics of Filters Used for Source Sampling

Filter (pore size)	Composition	Upper Temp. Limit °C	Ease of Weighing	Ease of Handling	Remarks
Glass fiber	Glass fiber	>250	Good	Good	High capacity, good extractive filter, poor for XRF, poor for in-stack
Quartz	SiO_2 fibers	>250	Fair	Poor	Too fragile for general field use
Millipore AA (0.8 μm)	Mixed esters of cellulose	105	Poor to good (high static change)	Good	Good for XRF, decomposed by hot H_2SO_4
Nucleopore (0.8 μm)	Polycarbonate	130	Good	Poor	Excellent for XRF, high pressure drop, low capacity
Gelman HT 650 (0.65 μm)	Unknown sulfur containing polymer	135	Good	Good	Not usable for sulfur-sulfate analysis by XRF

Table 2. Polytetrafluoroethylene* and Other Fluorinated Polymer Filters

Filter (pore size)	Composition	Upper Temp. Limit °C	Ease of Weighing	Ease of Handling in Field	Remarks
Fluoropore (1 μm)	PTFE on polypropylene (PP)	150	Fair	Poor-Fair	Low capacity, backing changes shape in hot gases
Millipore FSLW (3 μm)	PTFE on non-woven PP	150	Good	Poor	Hard to center in filter holder, low pressure drop
Ghia Dual Teflon (1 μm)	PTFE on PTFE	>250	Good	Poor	Hard to center in filter holder, low capacity
S&S TE36 (0.5 μm)	PTFE on non-woven PP	150	Good	Poor	Pressure drop too high
S&S TE37 (1 μm)	PTFE on non-woven PP	150	Good	Poor	Hard to center in filter holder, low capacity
Mitex LC (10 μm)	PTFE	>250	Good	Fair	Filter efficiency too low
Millipore 457-55 (1 μm)	Unknown fluorinated polymer	200	Good	Fair	Pressure drop too high

*PTFE

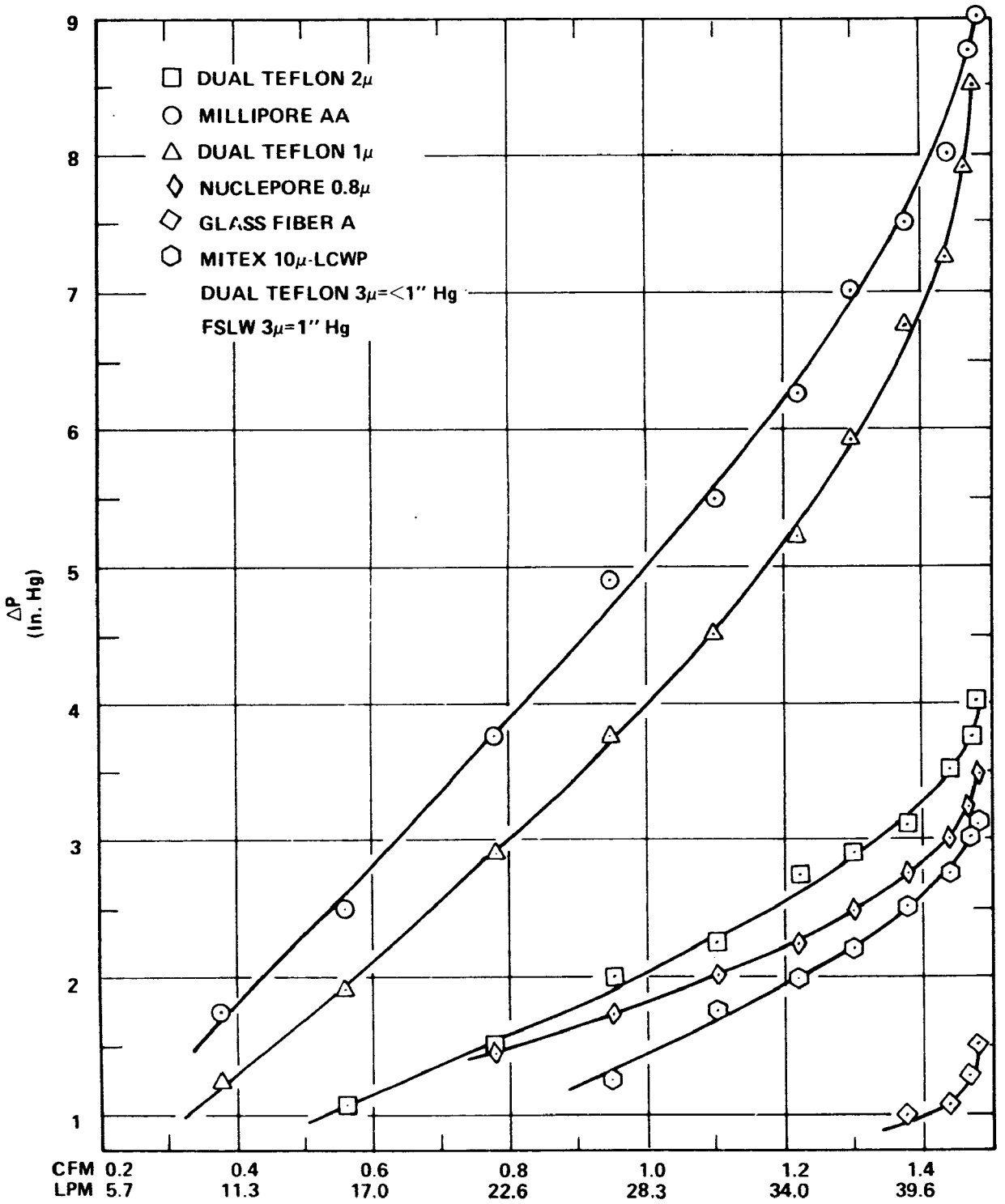

Figure 1. Pressure drop vs. flow for 47 mm filters.

Many of the synthetic polymeric fiber filters have low levels of trace element contamination and low x-ray scattering. In addition, some of these filters collect the material on their surfaces and minimize the x-ray absorption problem. The Nucleopore filters have these qualities but have the drawback of high pressure drop for the high efficiency filters. They also have a temperature limitation of 130°C and have low capacity for particulate loading. These filters are used for collecting extractive samples where the temperature can be maintained below 130°C and when low loading is desired such as for microscopy.

The polymeric fiber filter used most extensively in the past field work by PERS for collecting samples for chemical analysis by XRF is Millipore. Generally, the 47 mm 0.8 μm pore size AA filters were used because of their ease of handling in the field, low XRF background, and adequate capacity for particulate loading. However, several major problems have been discovered with these filters in source sampling. One problem is their thermal instability. The filters will totally disintegrate at temperatures above 125°C. At most sources, this limits the use of these filters to carefully controlled extractive sample systems. Exposure of these filters to gas streams with large amounts of hot sulfuric acid (temperature above 100°C) results in the saponification of the acetate esters and the loss of filter weight. These filters are sensitive to the moisture content of the air and, therefore, give different and sometimes changing weights with different air moisture content. These weight changes may be as high as 100 micrograms. The static charge of these filters presents a problem that affects weighing them on microbalances. Weighing in a carefully controlled balance room has minimized these weighing problems. Even with these serious disadvantages, the AA filters are the most frequently used for source characterization by PERS, since no known good replacement is currently available.

The Gelman HT 650 filter was considered since it has good temperature stability, ease of weighing and handling, and sufficient capacity. However, the filter cannot be used in the PERS source characterization work since it contains sulfur and gives too high an XRF sulfur background.

The fluorinated polymeric fibers have good temperature stability and low XRF background. However, because these fibers do not hold together well, good filters of only fluorinated polymers have been difficult to make. Most fluorinated polymer filters are made with

some type of backing, usually polypropylene. Both woven and non-woven backings are used. Several new filters which have the fluorinated polymer backing have become available and have a high (>250°C) temperature limit. All the fluorinated polymer filters are hard to handle in the field, and most have low capacity for particulate loading and high pressure drop. The 10 μm Mitex LC filter has too low efficiency to be useful. With improved handling techniques, the fluorinated polymer filters may emerge as the best overall filter for source characterization.

Table 3 gives the element sensitivity for the PERS XRF system. The background counts for selected elements of three filters are given in Table 4.

Sizing Device

The two types of sizing devices used in the source characterization work at PERS are the cascade impactors and series cyclone. The series cyclone was used to get bulk-sized material that was not deposited on some surface. This material was used for carbon and other analyses that are done by methods other than XRF. The system used consisted of a three-cyclone unit with cut points at 3.3, 1.8, and 0.8 μm. This cyclone unit could be used in-stack; however, it was more practical to use it with the same extractive probe used with the extractive impactor described below. Several investigators have continued to work on the development of series cyclones for analytical use and a group at Southern Research Institute has developed a five-series in-stack system (8).

Good in-stack impactors are available. However, all of them collect the samples on surfaces that are not compatible with the PERS XRF system. Two approaches have been developed that present the sized particles in a suitable form for x-ray analysis. One approach is to use the Andersen Model 0203, one-cfm ambient sampler with polycarbonate films for collection surfaces as an extractive impactor. The other approach is to redeposit the collected material of the in-stack impactors on a suitable substrate for XRF analysis. The sample in the Andersen System is extracted from the sources with a heated probe into the impactor which is held in a special heated sampling box. The collected sized samples are analyzed by XRF on the collection films. Besides the drawbacks of losing material in the probe, the results suffer from the non-uniformity of the material deposits. Not only are the deposits not uniform, but each impactor stage gives a different material deposit

Table 3. Emissions Characterization Data for Coal-Fired Power Plants with ESP's

Date	Time	Part. (mg/Nm^3)	SO_2 (mg/m^3)	$SO_4^=$ (mg/m^3)	$SO_4^=/SO_x$ (%)	Plume[a] Opac. (%)	In-Stack[b] Opacity (%)	Remarks
Plant P[c]								
7/19/77	1551-1636	840	7,200	250	3.4	27	21	2 fields off
7/20/77	1020-1120	1,100	6,000	330	5.2	23	28	2 fields off
7/22/77	0939-1039	360	7,300	180	2.4	32	31	2 fields off
Plant MC[d]								
7/26/77	1430-1545	330	5,900	210	3.4	18	21	1 field off
7/27/77	0915-1015	2,800	5,900	190	3.1	86	81	3 fields off
7/28/77	0900-1000	2,100	6,500	240	3.6	80	72	3 fields off
7/28/77	1110-1210	450	6,500	240	3.6	20	17	Normal operation

[a]Observer measurements.

[b]Transmissometer measurements.

[c]8% Ash, 3.3% S, 99 ppm V, 100 MW.

[d]14% Ash, 3.9% S, 35 ppm V, 330 MW.

Table 4. Magnitude and Uniformity of Background Count for Three Types of Membrane Filters (2)

	Nucleopore 0.8 μ (Mass = 1.1 mg/cm²)		Fluoropore Type FA (Mass = 2.7 mg/cm²)		Millipore Type AA (Mass = 5.0 mg/cm²)	
	$\overline{N}$[a]	σ[b]	$\overline{N}$	σ	$\overline{N}$	σ
F	1.32	0.09	549.78	28.20	1.96	0.13
Na	0.22	0.06	0.15	0.05	0.28	0.05
Mg	0.64	0.08	0.75	0.10	1.43	0.16
Si	66.22	4.44	1.25	0.25	2.29	0.27
P	17.77	0.62	17.63	2.16	16.34	0.35
S	48.54	0.82	40.21	2.23	54.52	0.63
Cl	86.49	3.18	54.44	4.81	200.24	5.59
K	64.48	2.67	63.49	2.46	212.40	2.40
Ca	4.43	1.17	8.85	3.15	333.84	7.13
Ti	2.91	0.56	7.67	1.20	12.74	1.62
V	7.95	0.80	16.10	1.93	25.71	1.65
Fe	44.28	4.21	50.41	4.86	62.51	4.79
Ni	2.10	0.36	3.51	0.67	5.52	1.12
Cu	553.46	9.03	567.36	14.13	577.69	21.61
Zn	12.14	0.81	26.31	3.49	41.34	6.82
Cd	1.87	0.08	2.12	0.11	3.18	0.17
Ba	2.35	0.35	5.00	0.57	8.27	0.94

[a] $\overline{N}$ is the mean value in cps for ten blank specimens.
[b] σ is the standard deviation in background for ten blank specimens.

distribution, i.e., there are different sizes and numbers of piles of material. In spite of these problems, usable results based on elemental ratios have been obtained. The results from some of the PERS studies are given in another paper of this workshop (9).

Since better sizing of source-emitted particles is obtained with the in-stack impactors due to the elimination of probe losses and collection of the material at stack conditions, a technique for obtaining XRF analysis on these sized materials was desired. An extraction redeposition technique has been developed which removes the material from the impactor collection plates and redeposits it on suitable substrates. In this technique, the collected sized material is washed from the impactor plates into glass evaporation chambers with suitable substrates at the bottom. The extraction solvent is then evaporated under a stream of dry nitrogen. During the evaporation step, the sides of the chambers are frequently washed with clean solvent. Good transfer of the sized material can be obtained; however, much care must be used in the removal of the material from the impactor plate, the washing down of the chamber walls, and the handling of the redeposited sample. The results from three runs of sulfur distribution among sized material from an oil-fired power plant by the redeposition technique are given in Table 5. Table 6 shows the results for all the important elements detected in one of these samples. The data given in these two tables illustrate the type that can be obtained by this technique. The vanadium is enriched in the fine particles with iron, calcium, silicon, and aluminum present in higher percentages in the larger particles.

SUMMARY

When sulfur and other elemental analyses are needed on emissions from stationary sources, the collection substrate must be carefully chosen. Each of the filters now in use has some drawback such as temperature limitation, low capacity, or poor XRF background; therefore, compromises must be made in filter selection. In spite of all the problems, good chemical analysis can be obtained from XRF analysis of samples collected on Nucleopore, Millipore AA, and some of the fluorinated polymer filters.

As with filters, compromises must be made in selecting devices for analysis of sized particulate emissions. With in-stack impactors, the sized material must be transferred to a suitable substrate. Extractive impactors suffer from probe losses and non-uniform deposits.

With careful work, good representative samples can be obtained that will yield good chemical analysis of emissions from sources.

Table 5. Percent Sulfur in Sized Fractions
Oil-Fired Power Plants

Stage D_{50}, μm	Boiler Excess O_2 Levels 0.2%	0.25	0.6%
23	-	2.1	5.3
10	1.6	2.9	3.6
4.7	2.0	3.5	1.9
1.9	-	3.2	4.6
1.0	3.9	5.3	3.5
0.52	8.9	3.1	4.9
0.27	2.6	1.3	2.4
Filter	2.4	2.4	1.7

Table 6. Distribution of Important Elements in Sized Fractions - Oil-Fired Power Plant

Stage D_{50}, μm	Elements, Weight Percent						
	S	V	Ni	Fe	Ca	Si	Al
23	5.3	2.8	0.3	2.7	0.4	0.2	0.1
10	3.6	2.0	0.2	1.4	0.1	0.3	0.03
4.7	1.9	0.4	0.03	0.2	0.05	0.6	0.009
1.9	4.6	0.6	0.02	0.2	0.04	0.6	0.008
1.0	3.5	0.5	0.03	0.3	0.1	0.3	0.02
0.52	4.9	0.3	0.02	0.2	0.02	0.6	NF
0.27	2.4	0.007	NF	0.02	0.009	0.1	NF
Filter	1.7	5.1	0.8	0.1	NF	NF	NF

REFERENCES

1. Bennett, R. L., J. Wagman, and K. T. Knapp. The Application of a Multichannel Fixed and Sequential Spectrometer System to the Analysis of Air Pollution Particulte Samples from Source Emissions and Ambient Air. In: Advances in X-ray Analyses, Vol. 19, Kendall/Hunt Publishing Company, Dubuque, Iowa, 1976. pp. 393-402.

2. Wagman, J., R. L. Bennett, and K. T. Knapp. X-ray Fluorescence Multispectrometer for Rapid Elemental Analysis of Particulate Pollutants. EPA-600/2-76-033, U.S. Environmental Protection Agency, Research Triangle Park, North Carolina, 1976. 44 pp.

3. Wagman, J., R. L. Bennett, and K. T. Knapp. Simultaneous Multi-wavelength Spectrometer for Rapid Elemental Analysis of Particulate Pollutants. In: X-ray Fluorescence Analysis of Environmental Samples, T. G. Dzubay, ed. Ann Arbor Science Publishers, Inc., Ann Arbor, Mich., 1977. pp. 35-55.

4. Ranade, N. B. Sampling Interface for the Quantitative Transport of Aerosols, Field Prototype. EPA-600/2-76-157, U.S. Environmental Protection Agency, Research Triangle Park, North Carolina, 1976. 68 pp.

5. Lundgren, D. A., and M. D. Durham. Aerosol Sampling in Turbulent or Tangential Flow. EPA Report to be published, U.S. Environmental Protection Agency, Research Triangle Park, North Carolina, 1978.

6. Lundgren, D. A., M. D. Durham, and K. W. Mason. Sampling Tangential Flow Streams. J. of Am. Industrial Hygiene Association, Summer 1978 (in press).

7. Benson, A. L., P. L. Levins, A. A. Massucco, and J. R. Valentine. Development of a High-Purity Filter for High Temperature Particulate Sampling and Analysis. EPA-650/2-73-032, U.S. Environmental Protection Agency, Washington, D.C. 1973. 71 pp.

8. Smith, W. B., and R. Wilson, Jr. Development and Laboratory Evaluation of a Five-Stage Cyclone System. EPA-600/7-78-008, U.S. Environmental Protection Agency, Washington, D.C., 1978. 66 pp.

9. Bennett, R. L., and K. T. Knapp. Sulfur and Trace Metal Particulate Emissions from Combustion Sources. In: Measurement Technology and Characterization of Primary Sulfur Oxides Emission from Combustion Sources, Southern Pines, North Carolina, April 1978.

A Stack Gas Sulfate Aerosol Measurement Problem

Dale A. Lundgren
Paul Urone
University of Florida

Thomas Gunderson
Los Alamos Scientific Laboratory

ABSTRACT

Measurement of the emission of sulfur-containing particulate matter from a combustion source is complicated by the presence of high concentrations of relatively reactive sulfur gases, namely, SO_2, SO_3, and H_2SO_4. As stack gas temperature changes, the gases may react, change phase (condense), or adsorb out on surfaces -- especially particulate collection surfaces such as filters. If appropriate precautions are not taken, it is not uncommon or improbable for gaseous sulfur compounds to contribute more sulfur to a particulate catch than the "precollection" stack gas particulate matter.

This problem can be magnified when attempts are made to determine the in-stack particle size distribution of a sulfur-containing aerosol. Gas sorption-reaction on surfaces such as glass fiber filter-covered impaction plates can be a major source of error in measuring particles at in-stack conditions. Particle size measurements made out-of-stack frequently require cooling of the extracted gas stream, which, in turn, can cause reaction-condensation of SO_3-H_2SO_4 to particulate or sorption of water vapor by hygroscopic sulfate particles causing size change.

These problems will be discussed as they relate to sulfate particle concentration and size distribution measurement.

INTRODUCTION

A major problem in stack gas sampling and analysis is how to classify gases which condense or react in the sampling train or on the particle collection medium to form what may be considered particulate matter. One substance which falls into this category is sulfur trioxide (SO_3), formed in equilibrium with sulfur dioxide (SO_2) when sulfur-containing fossil fuels are burned. Up to 5% of the total sulfur in the fuel is converted to SO_3, yielding from 5 ppm to 50 ppm SO_3 in the flue gas (1)(2). The SO_3 is in equilibrium with water (H_2O) vapor in the flue gas, and, depending on temperature and gas component concentrations, various amounts of sulfuric acid (H_2SO_4) vapor will be formed. This H_2SO_4 can be collected on filters and weighed as particulate.

The importance of establishing whether or not condensed SO_3/H_2SO_4 is to be considered particulate matter is pointed out by a 36% average contribution of this material to total measured particulate grain loading (oil-fired boiler emissions) as reported by Jaworowski (3). As fly ash emission levels are reduced by air pollution control equipment, this amount of condensed SO_3/H_2SO_4 may equal or surpass the dry particulate sulfate contribution.

SO_x, H_2O AND H_2SO_4 EQUILIBRIA IN FLUE GAS

Most sulfur in power plant flue gases appears as SO_2 (Table 1) (4), with typical SO_3 levels ranging from 1.0% to 2.5% of the SO_2. However, as Figure 1 shows, the equilibrium constant for the reaction:

$$SO_2 + 1/2\ C_2 \rightleftharpoons SO_3$$

strongly favors the formation of SO_3 at temperatures below about 540°C (1000°F). This graph was calculated from data cited by Hedley (5). Kinetics of the reaction are unfavorable in the absence of a catalyst, but thermodynamically the SO_3 concentrations could exist at levels much greater than those normally encountered. Ratios of SO_3 to SO_2 as high as 0.1 have been reported (6). Since formation of SO_3 is controlled by catalytic effects as well as amount of excess air present, concentration of SO_3 resulting from combustion of a particular fuel can only be estimated in absence of direct measurements.

Reaction between H_2O vapor and SO_3 is given by:

$$H_2O + SO_3 \rightleftharpoons H_2SO_4 .$$

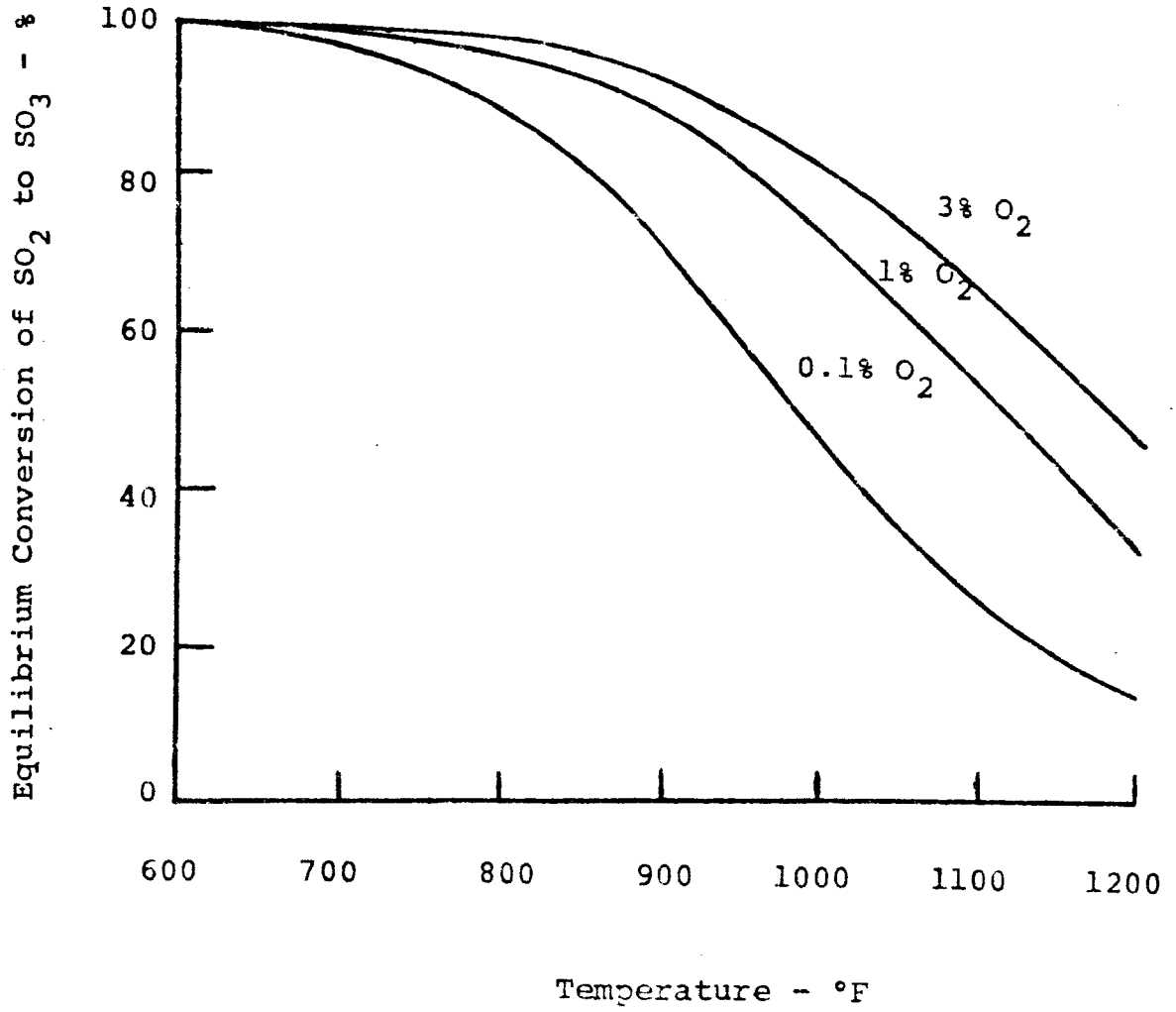

Figure 1. Equilibrium conversion of SO_2 to SO_3 [from Hillenbrand, Engdahl, and Barrett (4)].

Figure 2 shows equilibrium conversion of SO_3 to H_2SO_4 as a function of temperature for a typical flue gas H_2O vapor concentration of 8 vol%. At temperatures below 204°C (400°F), essentially all SO_3 present is converted to H_2SO_4 at equilibrium. In contrast to formation of SO_3, formation of H_2SO_4 occurs rapidly in the thermodynamically feasible temperature range (7).

Table 1. Typical Exhaust-Gas Composition from Coal-Fired Boiler [From Hillenbrand, Engdahl and Barrett (4)]

Component	Concentration	
	Volume Percent	g/m^3 [a]
H_2O	4.0	30
CO_2	15.0	273
Fly ash before precipitator		9.16 (4 gr/ft^3)
Fly ash after precipitator		0.458 (0.2 gr/ft^3)
NO	0.050	0.63
SO_2	0.20	5.3
SO_3	0.0030 (30 ppm)	0.10
Hydrocarbons	(0.0010)	<0.1

[a] At 21°C (70°F), 1 atmosphere.

DETERMINATION OF H_2SO_4 DEWPOINT

Fly ash particles can influence the apparent dewpoint (saturation temperature of H_2SO_4 in flue gas), but one commits practically no error by neglecting the presence of other gases and considering only the H_2SO_4-H_2O system (8). Thermodynamic

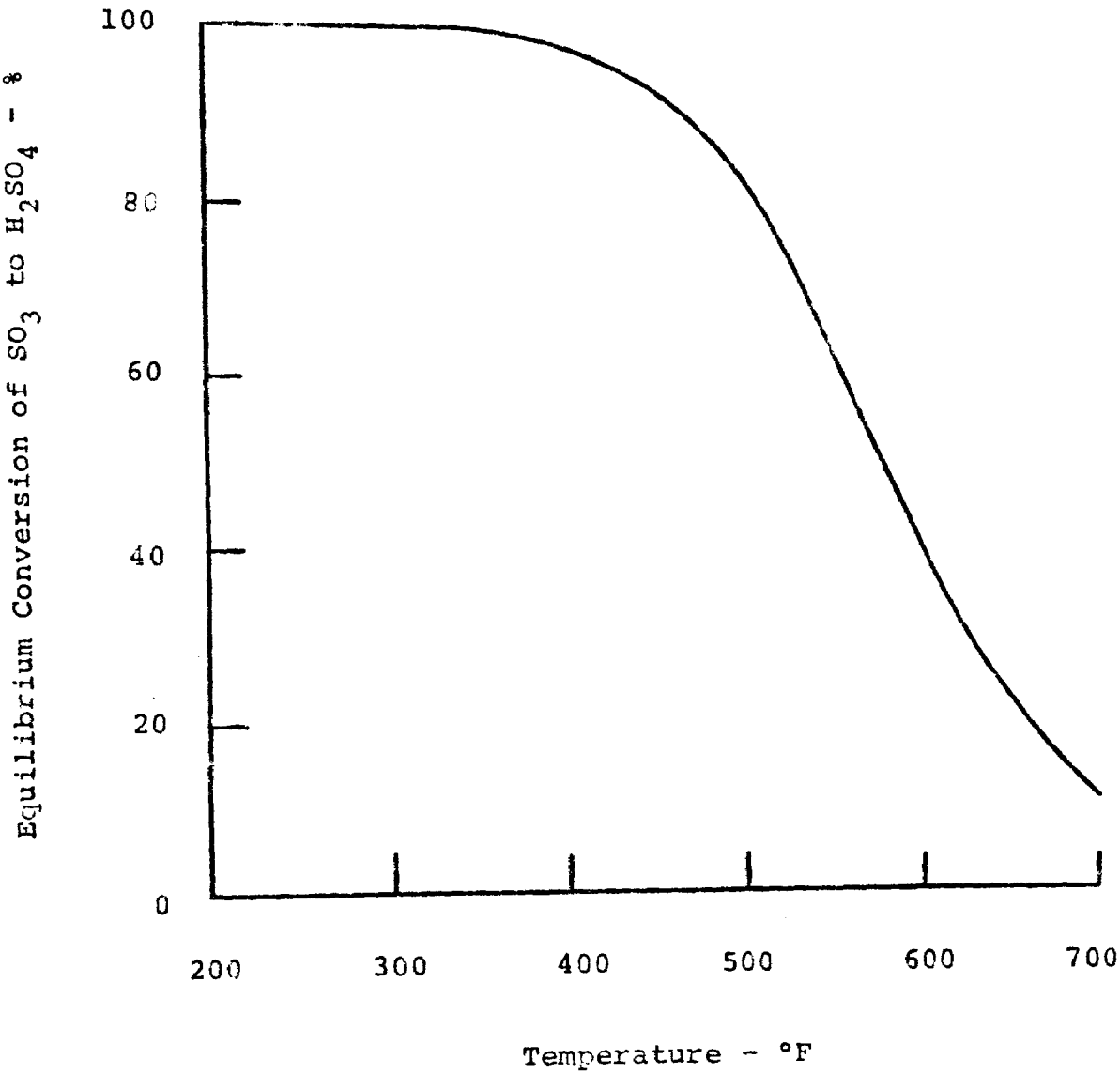

Figure 2. Equilibrium conversion of SO_3 to H_2SO_4 at 8.0 vol% in flue gas [from Hillenbrand, Engdahl, and Barrett (4)].

analysis of the H_2SO_4-H_2O flue gas system, ignoring fly ash effects, provides a theoretical basis for predicting acid dewpoints and condensate composition from vapor-liquid equilibria data.

Abel (9) was the first to derive a relationship enabling calculation of H_2SO_4, H_2O and SO_3 partial pressures from enthalpy, entropy, free energy, and heat capacity values. From his H_2SO_4 partial pressures and Greenewalt's H_2O partial pressures over H_2SO_4 solutions, H_2SO_4-H_2O dewpoint charts were prepared (Figures 3 and 4). The range of uncertainty indicated by Abel is on the order of 5°C (9°F) at 10 vol% H_2O vapor.

Information contained in Figure 3 can be used to predict dewpoint temperature from an analysis of H_2SO_4 and H_2O vapor content. If gas is cooled below its dewpoint, condensate equilibrium concentration and mass can be obtained. Condensate mass predicted from use of the dewpoint chart is actually a prediction of the amount available for condensation. The actual amount of condensate depositing on a fiber or metal surface may differ from the chart prediction because of mass transfer considerations.

As an example of the use of the chart, consider a flue gas containing 10 ppm H_2SO_4 and 10 vol% H_2O vapor. Condensation would occur at about 135°C (275°F), and condensate composition at that point would be about 79 wt% H_2SO_4. If the gas were cooled to 121°C (250°F), 85% of the H_2SO_4 would be removed from the gas phase and an insignificant amount of H_2O vapor would also condense. Condensation, therefore, follows the 10 vol% water line, resulting in a condensate which would be the equilibrium composition of the condensate at 121°C (250°F), assuming the vapor phase is in equilibrium with the total liquid condensed. Composition change of the liquid is small over the temperature interval given in this example, ranging from 79 vol% at 135°C (275°F) to 75 vol% at 121°C (250°F).

Large changes in H_2O vapor content of flue gases cause only slight changes in acid dewpoint. Variation of dewpoint with H_2SO_4 content of gases having different H_2O vapor concentrations is shown in Figure 5, where the range from 0.5% to 15 vol% H_2O vapor changes dewpoint only 17°C (30°F) to 22°C (40°F) for the medium-to-high acid concentrations indicated.

In addition to the procedure based on calculated partial pressure, a number of efforts have been made to determine H_2SO_4 dewpoints from instrumental and chemical procedures. Figures 6 and 7 present results obtained for flue gas dewpoints as a

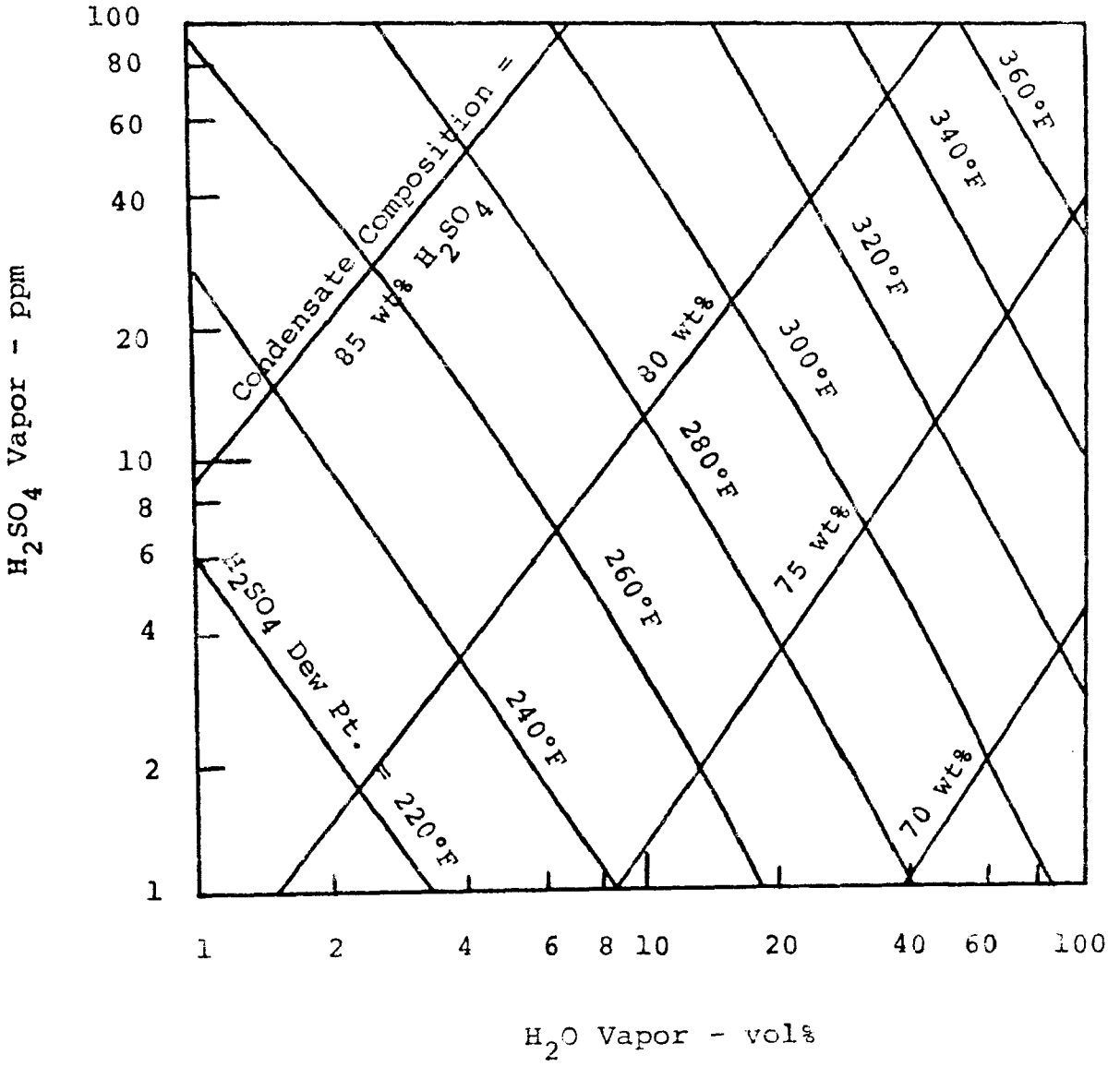

Figure 3. Dewpoint and condensate composition for vapor mixtures of H_2O and H_2SO_4 at 760 mm Hg total pressure [from Abel (9) and Greenewalt (10)].

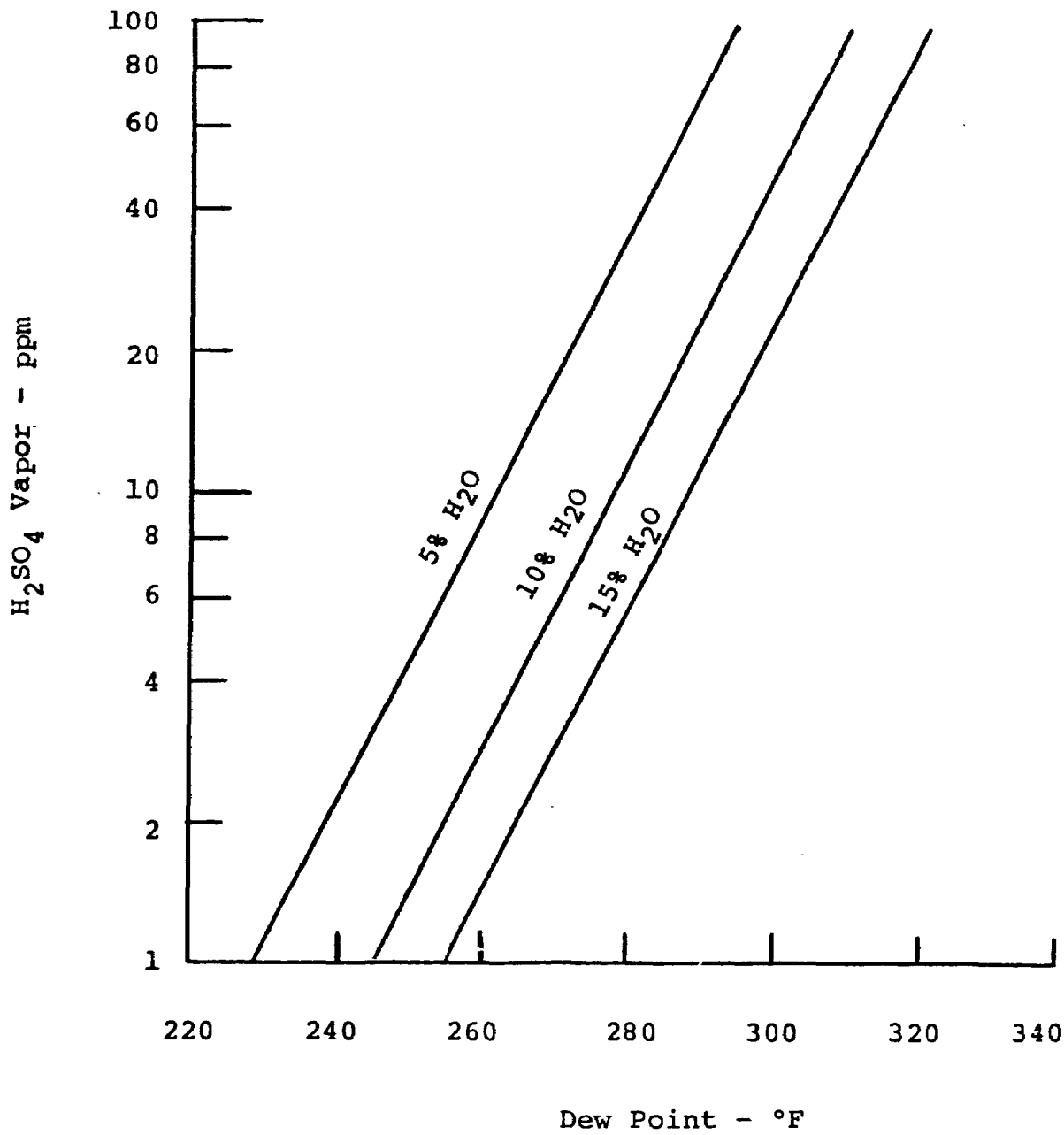

Figure 4. H_2SO_4 dewpoint for typical flue gas moisture concentrations [from Abel (9) and Greenewalt (10)].

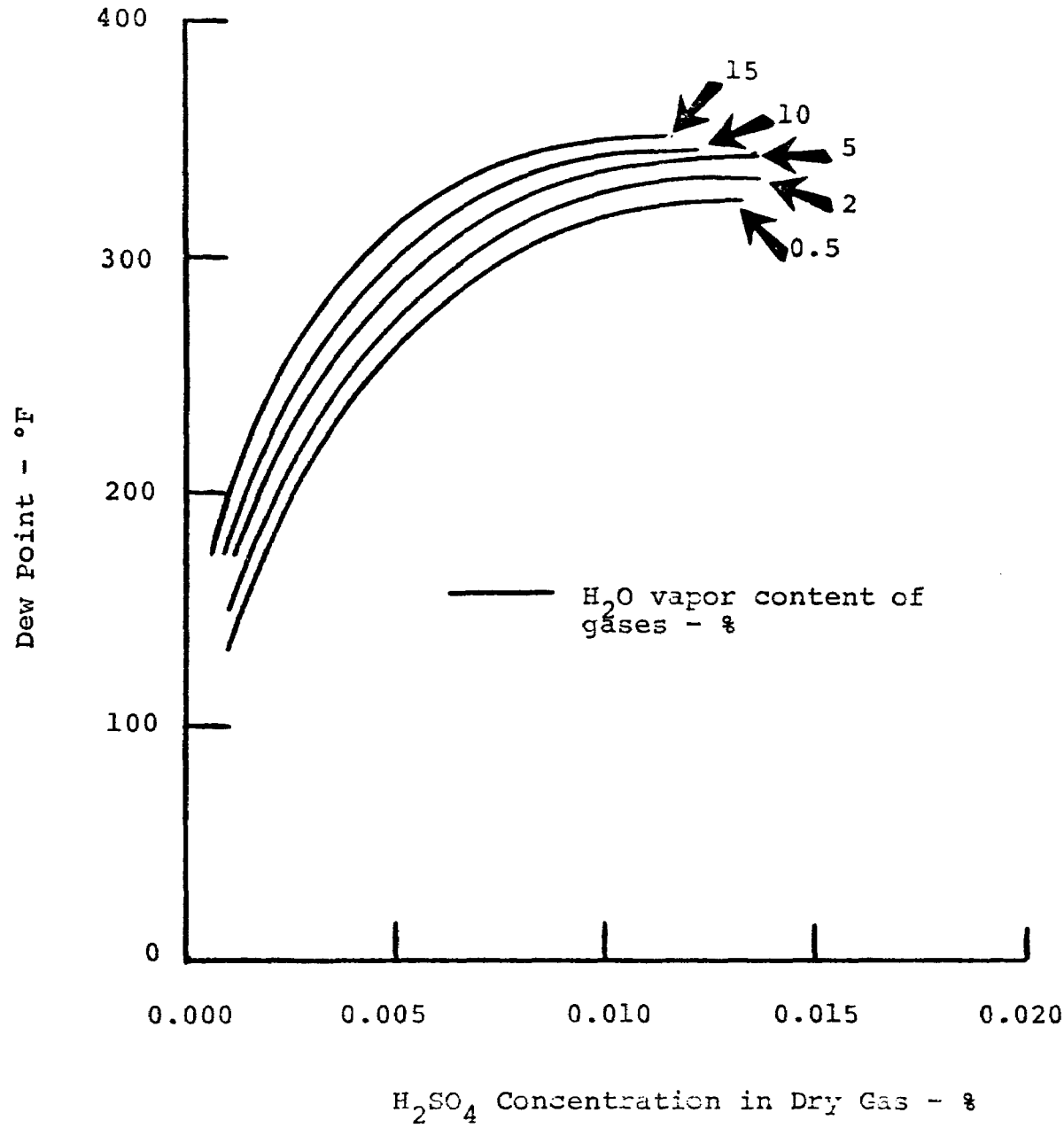

Figure 5. Variation of dewpoint with H_2SO_4 content for gases having different H_2O contents [from Matty and Diehl (11)].

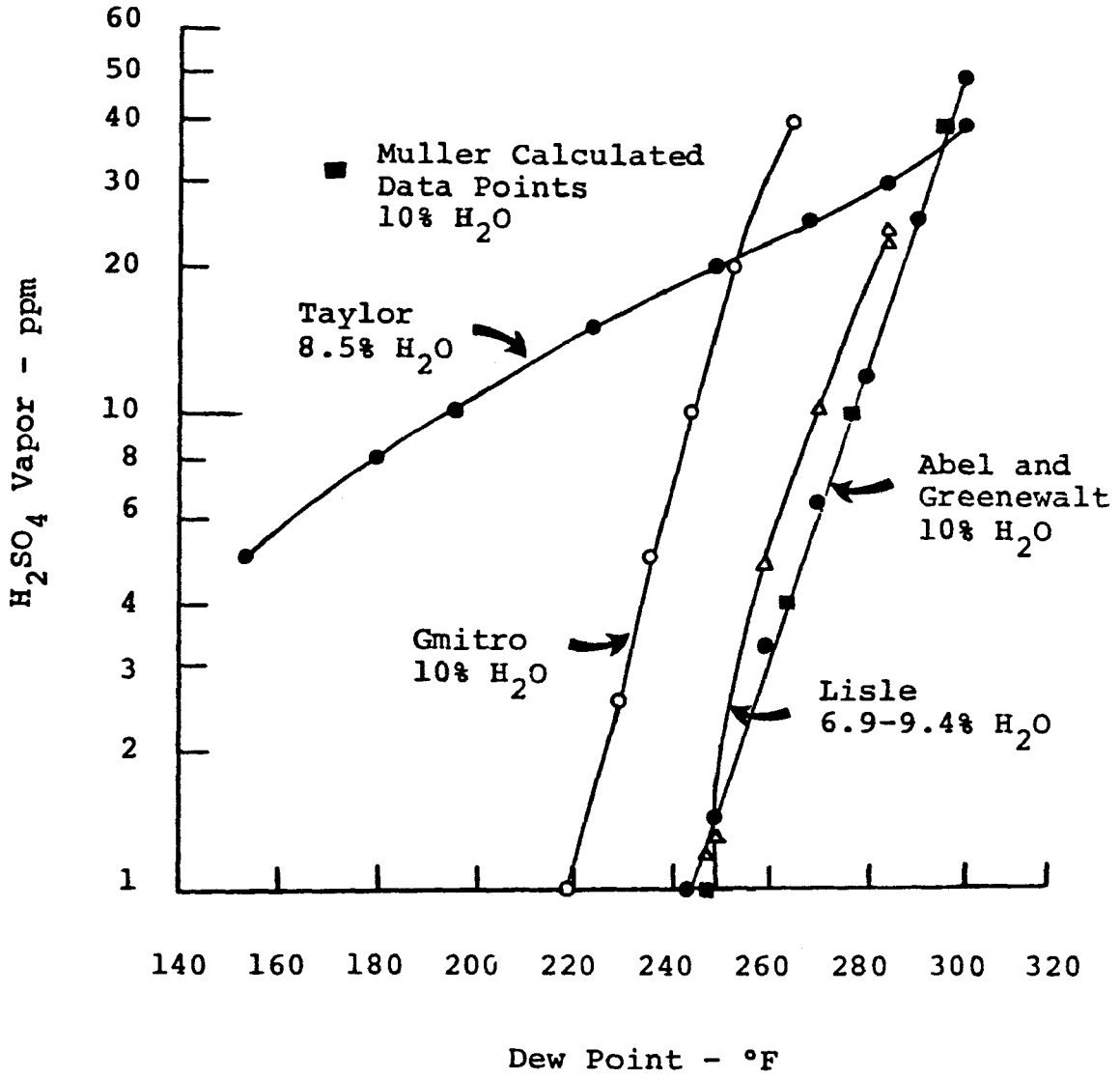

Figure 6. H_2SO_4 dewpoint obtained by various investigators [Abel (9) and Greenewalt (10), Gmitro (14), Lisle (13), Muller (8), and Taylor (12)].

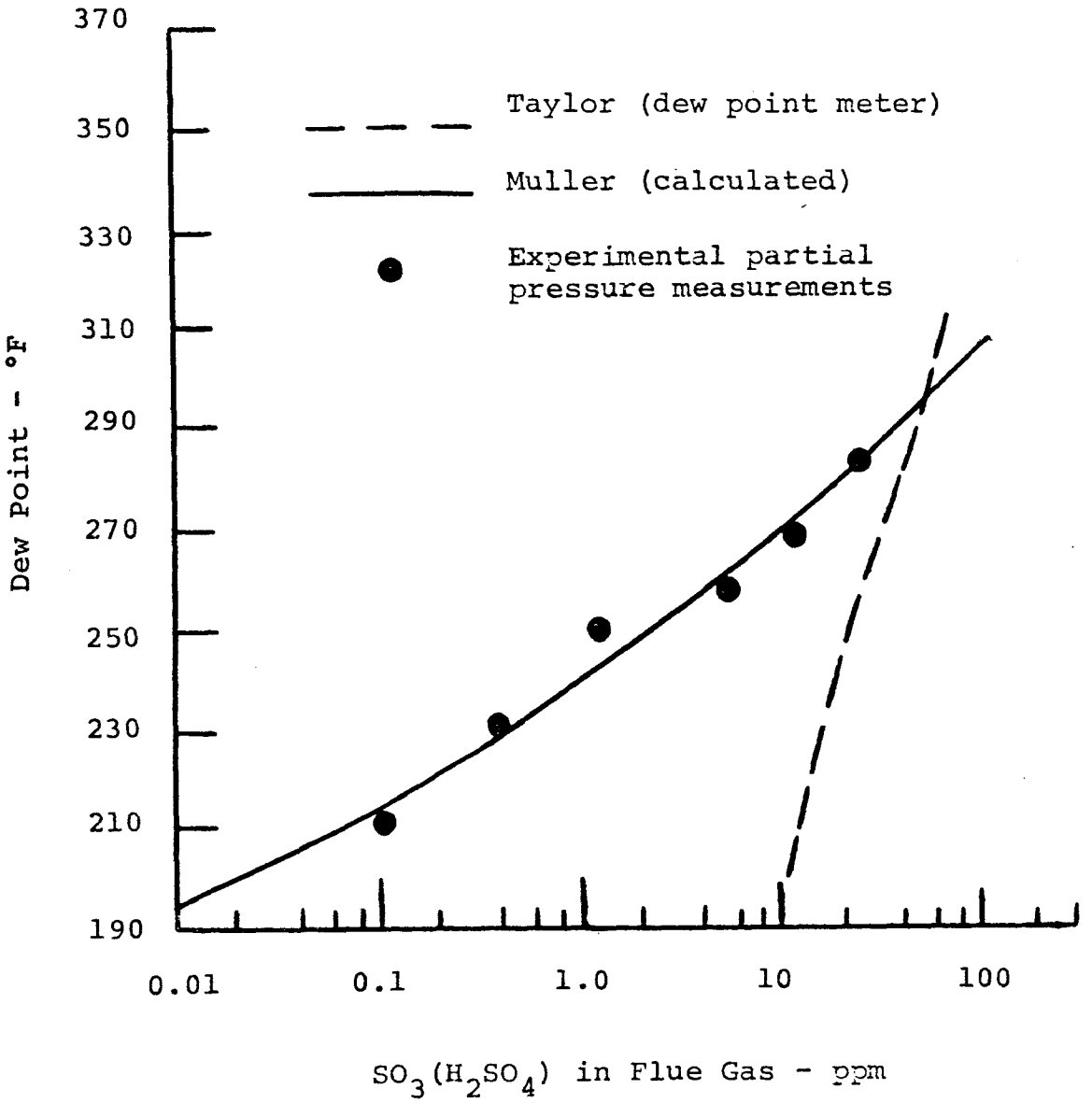

Figure 7. Dewpoint as a function of H_2SO_4 concentration [from Taylor (12) and Mueller (8)].

function of H_2SO_4 content by various investigators. To make an exact comparison, all curves should be for a gas of the same vol% H_2O vapor. However, reference to Figure 3 will indicate that a variation in H_2O vapor concentration from 7 vol% to 10 vol% can cause only about 1°C (2°F) to 2°C (4°F) change in dewpoint. Taylor's (12) results were obtained from an electrical dewpoint meter which is inaccurate at low acid partial pressures. Lisle and Sensenbaugh's (13) data were obtained with a spiral condenser. Dewpoint curves of Gmitro (14), Muller (8), Abel (9), and Greenewalt (10) were based on calculated partial pressures.

In view of the difficulties with calculation based on liquid phase thermodynamic properties and inaccuracy of dewpoint meters at low acid partial pressure, the most reliable method of correlating H_2SO_4 dewpoints with H_2O and H_2SO_4 vapor concentration is the experimental condensation method employed by Lisle and Sensenbaugh (13). Their data correlate best with Muller's calculated dewpoints and are the basis for ASME Power Test Code 19.10.

Rendle and Wilson (15) have also published some data on relation of the SO_3 content of combustion gas and of gas dewpoint to sulfur content of fuel oils (Figure 8). Results of several other investigators have also been plotted. The type of oil, ash content, and combustion conditions differ for the various sets of points. Although the plot of SO_3 content shows considerable scatter, it is apparent that with more than 0.5% sulfur in the oil, SO_3 content of the gas does not increase proportionately to the fuel sulfur %.

Figure 8 indicates the following:

1. There is a rapid initial rise in dewpoint with the first increment of sulfur in the fuel. For an estimated dewpoint of 38°C (100°F) with no sulfur, an increase to 127°C (260°F) (H_2SO_4 dewpoint) is found with 1% sulfur.

2. There is a relatively small rise in dewpoint as sulfur in the fuel oil increases from 1% to 6%.

EXPERIMENTAL DATA

Hillenbrand et al. (4) sampled flue gas from a coal-fired boiler with quartz filters maintained at 205°C (400°F) and 138°C

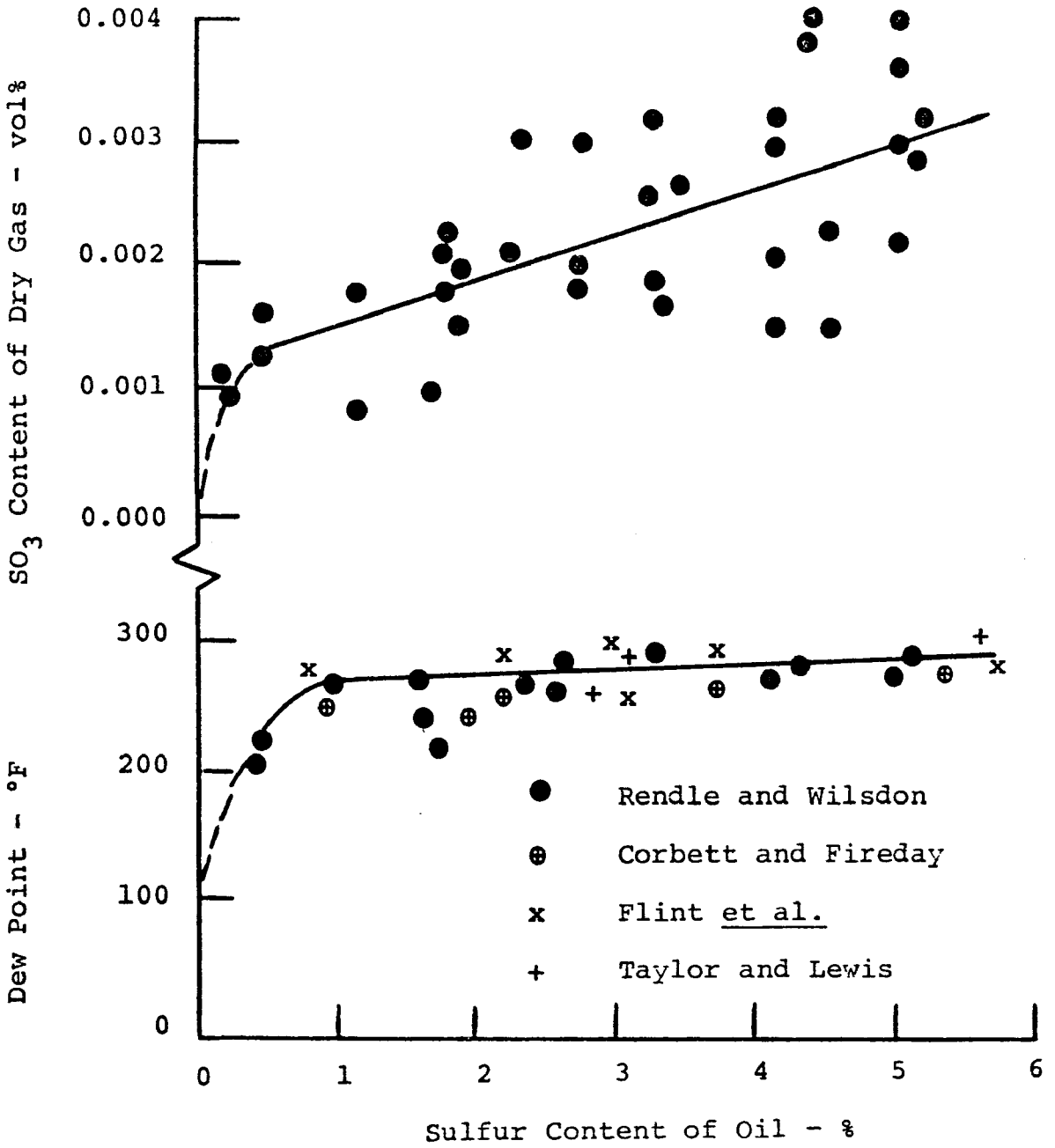

Figure 8. Relation of dewpoint and SO_3 content of combustion gases to sulfur content of oil [from Corbett and Fireday (18), Flint et al. (17), Taylor and Lewis (16), and Rendle and Wilson (15)].

(280°F) and found that filter temperature significantly affected the amount of H_2SO_4 found on the filter. At 138°C (280°F), 45% and 41% of the total H_2SO_4 catch (total H_2SO_4 mass in probe, filter, and impingers) were found on the filter in two trials. At 205°C (400°F), 24% and 8% of the total H_2SO_4 catch were found on the filter in two trials. The greater amount of H_2SO_4 found on the cooler filter was interpreted by them to mean:

1. A considerable portion of H_2SO_4 collected on the filter resulted from both condensation and reaction of particulate with the SO_2 and SO_3.

2. Condensation and consequent reaction is favored at lower temperature.

Jaworowski (3) sampled flue gas from several oil-fired boilers with three different sampling methods: EPA Method 5 sampling train, ceramic thimble apparatus, and a high-volume sampling system. In all three sampling methods, temperature of the filter was kept between 120°C (250°F) and 150°C (300°F). His results (Table 2) show the magnitude of H_2SO_4 contribution to total particulate grain loading ranged from 18% to 78% and averaged 36% of the total measured emissions.

Experiments with H_2SO_4 aerosol were conducted by Lundgren and Gunderson (19) at two temperatures [120°C (248°F), 205°C (401°F)], 25 cm/sec filtration velocity, 8.5 vol% H_2O vapor, and 140 ppm H_2SO_4. At these concentrations of H_2SO_4 and H_2O vapor, the acid dewpoint is about 170°C (338°F). The results in Table 3 show at 120°C (248°F), below the H_2SO_4 dewpoint, most of the H_2SO_4 was found in the coil and on the test filter. At 205°C (401°F), above the H_2SO_4 dewpoint, most of the H_2SO_4 was found after the test filter in the impinger contents and on the backup filter. Simple calculations based on typical stack sampling data from oil-fired boilers and on these experimental data indicate H_2SO_4 could account for more than 50% of the total particulate catch at a 120°C (248°F) sampling temperature (or at a temperature below the H_2SO_4 dewpoint in the stack gas), but only for about 9% at a 205°C (401°F) sampling temperature (or at a temperature above the H_2SO_4 dewpoint in the stack gas).

CONCLUSION

A gas such as H_2SO_4 (SO_3) can condense at normal sampling temperatures and condense out on sampling lines or be collected out by a particulate collection device. It is not improbable

Table 2. Amount of H_2SO_4 Found in Particulate Matter by Various Stock Sampling Methods [From Jaworowski (3)]

Location	Filter	H_2SO_4 ppm	H_2SO_4 gr/SCF	Total gr/SCF	H_2SO_4 % of Total
Plant A	Thimble[a]	8.1	0.0147	0.0694	21
		8.1	0.0147	0.0344	43
		10.8	0.0196	0.107	18
		9.5	0.0172	0.366	47
		9.9	0.0180	0.0645	28
		9.5	0.0172	0.0329	52
		9.5	0.0172	0.0688	25
		9.5	0.0172	0.0405	42
Plant A	Hi-volume[a]	6.9	0.0125	0.0548	23
		6.0	0.0109	0.0540	20
		8.8	0.0147	0.0255	62
		8.1	0.0050	0.0292	50
Plant A	EPA/APCO[a]	14.9	0.027	0.151	18
		13.8	0.025	0.0321	78
		7.5	0.0135	0.0308	44
		11.6	0.021	0.0388	54
		6.1	0.011	0.0242	45
		9.5	0.0172	0.0403	43
		9.5	0.0172	0.0643	27
		8.8	0.0159	0.0659	24
		8.8	0.016	0.033	48
Plant A	EPA/APCO[a]	11.0	0.020	0.033	61
		9.9	0.018	0.077	23
		9.9	0.018	0.0757	24
Plant B	EPA/APCO[b]	5.0	0.0092	0.022	42
		5.0	0.0092	0.023	40
		6.7	0.0123	0.036	34
		5.7	0.0104	0.030	35
		5.9	0.0104	0.031	34
		5.4	0.0098	0.033	30
Plant C	Hi-volume[a]	4.7	0.0085	0.0111	77
		2.8	0.0050	0.0076	66
Plant C	EPA/APCO[b]	3.5	0.0064	0.0212	30
		4.2	0.0076	0.0200	38

[a] $BaCl_2$ precipitation

[b] NaOH titration

Table 3. H_2SO_4 Distribution in Sampling Train (19)

	120°C[a]	205°C[a]
	% of Total H_2SO_4 Catch[b]	% of Total H_2SO_4 Catch[b]
S.S. Coil at Test Temperature	61	8
Filter at Test Temperature	32	11
Two Impingers + Backup Filter	7	81
Total	100	100

[a] H_2SO_4 Dewpoint 170°C
[b] Average of two trials

that this contribution of particulate sulfate is greater than the "dry" particulate sulfate that exists at "pre-collection" conditions--if appropriate precautions are not taken.

ACKNOWLEDGMENT

This work was supported by Environmental Protection Agency Research Grant No. 803126-01-0.

REFERENCES

1. Danielson, J. A. Air Pollution Engineering Manual, Los Angeles County Air Pollution Control District, Los Angeles, California, 1967, p. 536.

2. Hemeon, W. C. L., and A. W. J. Black. Stack Dust Sampling: In-Stack Filter or EPA Train. J. Air Poll. Control Assoc., 22(7):516, 1972.

3. Jaworowski, R. J. Condensed Sulfur: Trioxide Particulate or Vapor? J. Air Poll. Control Assoc., 23(9):791, 1973.

4. Chemical Composition of Particulate Air Pollutants From Fossil-Fuel Combustion Sources. Battelle-Columbus Laboratories, p. II-2, March 1, 1973.

5. Hedley, A. B. In: The Mechanism of Corrosion by Fuel Impurities, H. R. Johnson and D. L. Littler, eds. Butterworth, London, 1963, p. 204.

6. Cuffe, S. T., R. W. Gerstle, A. A. Orning, and C. H. Schwartz. J. Air Poll. Control Assoc., 14:353, 1964.

7. Snowden, P. N., and M. H. Ryan. Sulfuric Acid Condensation from Flue Gases Containing Sulfur Oxides. J. Inst. Fuel, 42:188, 1969.

8. Mueller, P. Study of the Influence of Sulfuric Acid on the DewPoint Temperature of the Flue Gas. Chemie-Ing.-Tech., 31:345, 1959.

9. Abel, E. The Vapor Phase Above the System Sulfuric Acid-Water. J. Phys. Chem., 50:260, 1946.

10. Greenewalt, C. H. Partial Pressure of Water Out of Aqueous Solutions of Sulfuric Acid. Ind. and Eng. Chem., 17:552-553.

11. Matty, R. E., and E. K. Diehl. New Methods for Determining SO_2 and SO_3 in Flue Gas. Power Engineering, 57:87, Dec. 1953.

12. Taylor, A. A. Relation Between Dew Point and the Concentration of Sulfuric Acid in Flue Gases. J. Inst. Fuel, 16:25, 1942.

13. Lisle, E. S., and J. D. Sensenbaugh. The Determination of Sulfur Trioxide and Acid Dew Point in Flue Gases. Combustion, 36(1):12, 1965.

14. Gmitro, J. I., and T. Vermuelen. Vapor-Liquid Equilibria for Aqueous Sulfuric Acid. Univ. of Cal. Radiation Lab., Report 10866, Berkeley, California, June 24, 1963.

15. Rendle, L. K., and R. D. Wilson. The Prevention of Acid Condensation in Oil-Fired Boilers. J. Inst. Fuel, 29:372-380, 1956.

16. Taylor, R. P., and A. Lewis. Sulfur Trioxide Formation in Oil Firing. In: Proceedings of Fourth Inst. Congress on Industrial Heating, Group II, Sec. 24, No. 154, Paris, France, 1952.

17. Flint, D., A. W. Lindsay, and R. F. Littlejohn. The Effect of Metal Oxide Smokes on the SO_3 Content of Combustion Gases from Fuel Oils. J. Inst. Fuel, 26:122-127, 1953.

18. Corbett, P. F., and F. Fireday. The SO_3 Content of the Combustion Gases from an Oil-Fired Water-Tube Boiler. J. Inst. Fuel, 26:92-106, 1953.

19. Lundgren, D. A., and T. C. Gunderson. Filtration Characteristics of Glass Fiber Filter Media at Elevated Temperatures. EPA-600/2-76-192, U.S. Environmental Protection Agency, Research Triangle Park, North Carolina, July 1976, pp. 13-72.

Sulfur Oxide Interaction with Filters Used for Method 5 Stack Sampling

Edward T. Peters
Jeffrey W. Adams
Arthur D. Little, Inc.

ABSTRACT

An experimental program was conducted to study the conditions under which sulfur oxide-containing gases can interact with high efficiency filters to form "false" particulate, e.g., particulate formed as a result of the sample collection process. Evaluation filters were exposed to particulate-free gas streams containing air, water, sulfur dioxide and/or sulfuric acid vapor at elevated temperatures. After exposure, the filters were leached in hot water which was analyzed for sulfate content. Filters tested included two quartz and seven glass compositions corresponding to four classes - high titania, medium titania, high barium, and borosilicate. Sulfate pickup on clean and on Mn^{+2} spiked filters exposed to streams containing 500 ppm or 2000 ppm SO_2 and up to 25 volume percent moisture at 205°C was less than 1 mg/m^3, comparable to sulfate blank analyses for these filters. However, exposures at 205°C with sulfuric acid vapor at 10 ppm to 40 ppm and moisture contents up to 25 volume percent (acid moisture dewpoint of 120°-150°C) lead to collection of 1-40 mg/m^3 sulfate, depending upon steam parameters and stream concentration. As a result, a series of exposures (in triplicate) was carried out with all commonly used stack sampling filters; stream conditions included 10 ppm sulfuric acid vapor and 10% to 15% moisture content at 200°C in simulation of a typical combustion source. Levels of 1 to 14 mg/m^3 were encountered. The results and implication to Method 5 stack sampling will be given.

INTRODUCTION

General

In response to the provisions of the Clean Air Act of 1970, the Environmental Protection Agency has identified stationary sources categories that contribute significantly to air pollution. Standards of performance applicable to new and modified sources within these industrial categories have been promulgated for twenty-four classifications and have been proposed for more. These regulations provide emission limits for various pollutants and specify the reference methods that are to be utilized in determining compliance with the standards.

At present, fifteen of the stationary source categories are regulated with respect to particulate emissions. As defined, particulate matter is "any matter, other than uncombined water, which exists in a finely divided form as a liquid or solid at standard conditions (20°C, 760 mm Hg)." The promulgated standards specify the use of Reference Method 5 to measure the amount of particulate matter in stack emissions. In application, a known volume of stack gas is withdrawn isokinetically from the source, and particulate material is collected in the sampling train by out-of-stack filtration. The particulate collection filter is maintained at a temperature above the dewpoint of water to prevent condensation and filter plugging. Particulate weight is determined gravimetrically after removal of uncombined water.

The objective of stack sampling is to provide a measure of the particulate burden to the atmosphere as it would exist in the dispersed plume. Each industrial category exhibits variations in the properties of the emission, including composition, concentration, gas temperature, residence time, and moisture content. Thus, it is necessary to determine if the assay procedure is influenced by variations in stack conditions. Also, it must be established if the formation or loss of particulate occurs due to the nature of the collection process or the configuration of the sampling train. Mechanisms for particulate formation during sampling include chemical reaction of stack gas components with collected particulate or sampling train components, catalytic conversion and condensation of stack gases, and compound hydration. Such particulate that would not have formed in the atmosphere at 20°C and 760 mm Hg is called false particulate.

With respect to these issues, the EPA has sponsored several studies to evaluate Method 5 particulate measurement as applied to specific industrial categories. The present report describes

a laboratory evaluation of the interaction of sulfur oxides with particulate collection filters.

Interaction of Sulfur Oxides and Particulate Collection Filters

The extraction of a representative sample from an elevated temperature gas stream containing flyash or other process particulate, sulfur oxide constituents, water vapor, and many other chemical species has posed a burdensome problem to chemists and engineers since the inception of standard sampling methodology. Uncertainties regarding the chemistry of the sample within the sampling train, particularly along the length of the probe and across the filter, have often resulted in doubt being placed upon the results obtained from these analyses, leading to the following kinds of questions:

- Are chemical interactions involving transformation from gas phase to particulate taking place on the filter that might influence the measured particulate concentration?

- Does the moisture content, temperature, or chemical composition of the sampled gases influence the results or sampling procedure in any way?

The possibility of forming false particulate (particulate matter formed as a result of the collection process) is of specific concern, as this would result in an overestimate of the true particulate emissions for a source. Such an overestimate could cause an undue burden upon that source in terms of satisfying compliance requirements.

Of special interest are sources containing considerable amounts of sulfur oxides in the stack gas. These sources include fossil fuel combustion and product recovery processes, such as petroleum refinery catalyst regeneration and Kraft pulp mill black liquor recovery. Up to 5% or more of the sulfur in these emissions can be present as SO_3 which, in equilibrium with water vapor, exists as sulfuric acid vapor. The H_2SO_4 - H_2O dewpoint chart is given in Figure 1. As temperature is reduced from stack conditions, generally in excess of 150°C (300°F) for these sources, to 120°C (250°F), the temperature maintained in the collection train, essentially all sulfuric acid in the flue gas is condensed and collected as particulate. No information is available, however, relating to the reaction of sulfuric acid mist vapor with glass fiber filters, as could occur with a particulate sampling train using an in-stack filter. Further, there are no data relating to the oxidation of SO_2 to SO_3 during sampling with collection as

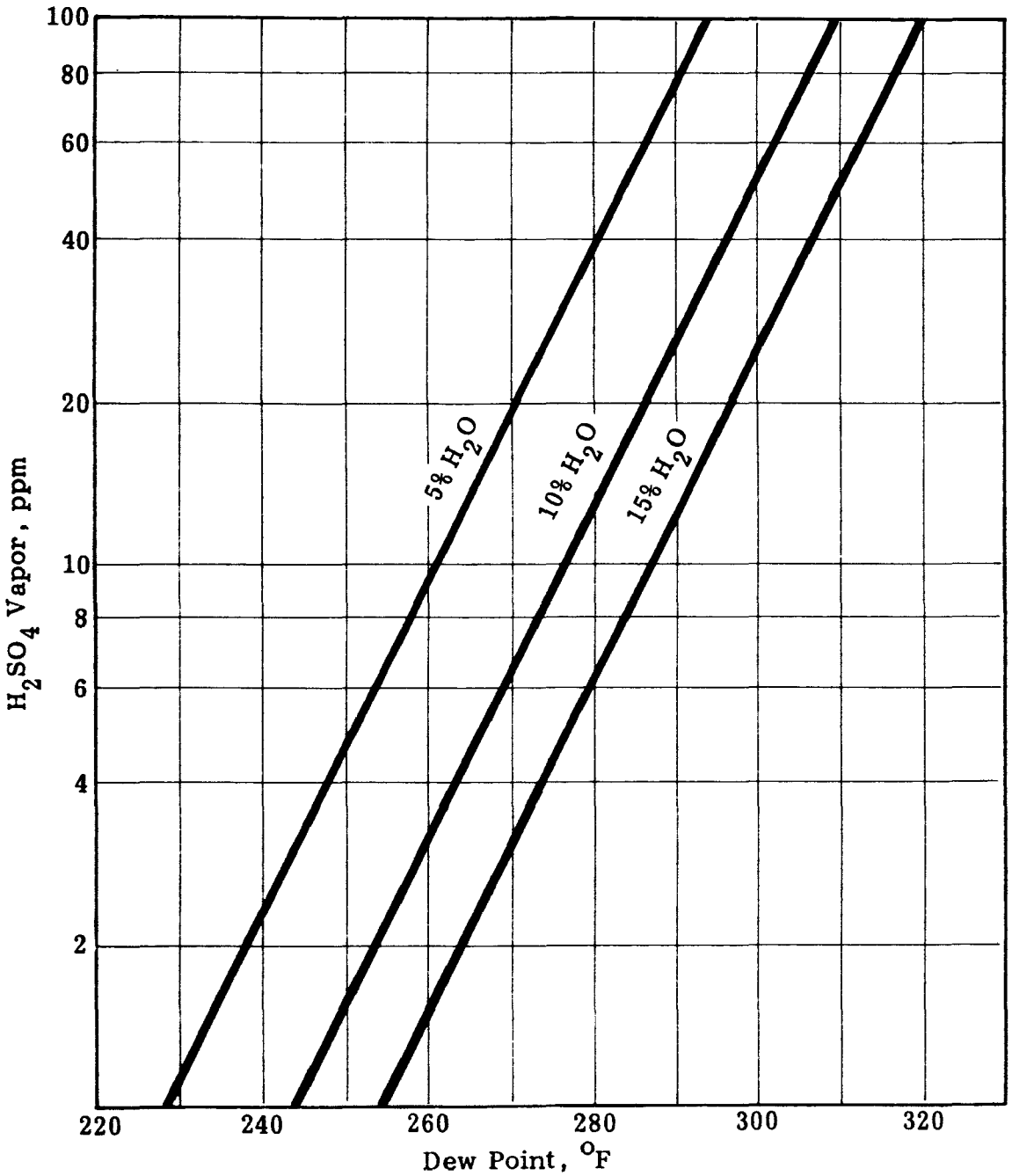

Figure 1. H_2SO_4 dewpoint for typical flue gas moisture concentrations.

sulfate through direct reaction with the filter media or catalytic conversion by components in the collected particulate.

To experimentally determine the presence and extent of these types of false particulate formation, a two-part laboratory investigation was carried out. Part one concentrated on evaluating stream parameters, including sulfur oxide components, their concentrations, moisture content, and temperature. These streams were passed through both clean filters and filters treated with a metal salt to simulate a deposit with cationic properties. Subsequently, part two was carried out to evaluate a variety of flat glass fiber filters under worst-case stream conditions to determine the relationship between glass chemistry and formation of false particulate.

PROGRAM PLAN

The objective of the study was to develop the background and understanding necessary to evaluate the relationship between filter/gas stream chemistry and false particulate formation. Specifically, it was hoped to establish the conditions under which the filter media, gas stream conditions, or combinations of both exhibit reactive or catalytic properties contributing to the collection of sulfur oxide or sulfuric acid vapor as measurable particulate.

To provide best control of experimental parameters, it was decided to carry out filter challenge studies in the laboratory. The experimental plan required the generation of a dust free, SO_x enriched gas stream and the extraction of a known volume of this stream through test filters with subsequent analyzers of the filters to determine the presence and amount of collectable sulfate. The experimental parameters to be tested were selected on the basis of conditions typically encountered in source sampling. Parameters of specific interest and selected for evaluation were:

- Gas stream/filter temperature - 120°C (250°F), typical collection train temperature, and 205°C (400°F), typical stack gas temperature.
- Gas stream moisture content - dry and 25%.
- Sulfur dioxide concentration - 500 ppm and 2000 ppm, typical for low and high sulfur fossil fuel combustion, respectively.

- Sulfuric acid content - 10 ppm and 40 ppm, representing about 2% of the SO_2 concentration.

- Presence of a filter deposit - Does the presence of certain metal ions in the deposit result in the catalytic conversion of SO_2 to collectable sulfate? Filters were immersed in a solution of $MnCl_2$ at a concentration designed to provide loadings of 30 μg Mn^{+2} per filter.

- Filter media - Preliminary studies considered several general classes of filters, including flat glass fiber commercial filters (MSA 1106BH and Gelman A), an experimental flat quartz filter (ADL/Balston Microquartz), and a glass fiber thimble suitable for in-stack collection (Svenska Flakt Jabrikan thimble). Later (Part 2) studies utilized a variety of commercial flat glass filters and both commercial and experimental flat quartz filters.

The initial (Part 1) set of experiments was carried out in three phases, involving the following types of stream challenges:

Phase 1 - Sulfur dioxide - clean filter

Phase 2 - Sulfuric acid vapor (alone or with sulfur dioxide) - clean filter

Phase 3 - Sulfur dioxide (alone or with sulfuric acid vapor) - soiled filter containing Mn^{+2}.

These phases were carried out to address the following types of questions:

Phase 1 - Is there a reaction between sulfur dioxide and a clean filter resulting in collectable particulate and for what stream conditions? The experimental design is shown in Table 1 which also indicates some additional evaluations carried out at a subsequent time or with a different filter media.

Phase 2 - Is sulfuric acid collected under stream where it is in the vapor state and does the co-existence of sulfur dioxide have an influence? The experimental plan for these evaluations is given in Table 2.

After this series of runs, a reaction between the gas stream components and the stainless steel parts of the stream generation apparatus resulted in system pluggage. Therefore, all stainless was replaced by Teflon or glass fittings.

Table 1. Phase 1 Test Grid: Sulfur Dioxide - Clean Glass Fiber Filter Interaction

A. Statistical Experiment Grid

Sulfur Dioxide Content	Moisture Content	Gas Stream/Filter Temperature 120°C	205°C
500 ppm	0	x x	x x
	25%	x x	x x
2000 ppm	0	x x	x x
	25%	x x	x x

x - Simultaneous exposure of MSA1106BH and SFJ Thimble filters

B. Additional Evaluations (Gas Stream/Filter Temperature = 205°C)

Filter	Gas Concentration 500 ppm SO_2 25% H_2O	2000 ppm SO_2 0% H_2O	2000 ppm SO_2 25% H_2O
SFJ Thimble			x x x x
MSA 1106BH	y	x	x
ADL/Balston MQ			x x x

x - Evaluations carried out in stainless/glass apparatus

y - Evaluations carried out in Teflon/glass apparatus

Table 2. Phase 2 Test Grid: Sulfuric Acid Vapor - Clean Glass Fiber Filter Interaction with and without Sulfur Dioxide (Gas Stream/Filter Temperature - 205°C, Moisture Content = 25%)

Filter	Gas Concentration		
	500 ppm SO_2 10 ppm H_2SO_4	2000 ppm SO_2 40 ppm H_2SO_4	40 ppm H_2SO_4
SFJ Thimble		x x x x	x x x
MSA 1106BH	y y y	x x x x, y y y y	x x x
Gelman A		y y	
ADL/Balston MQ		y y	y y y

x - Evaluations carried out in stainless/glass apparatus

y - Evaluations carried out in Teflon/glass apparatus

Phase 3 - Does the presence of a metal catalyst on the filter result in the conversion of sulfur dioxide (alone or in the presence of H_2SO_4 vapor) to collectable sulfate?

For this purpose, Mn^{+2} was selected as being representative of active metal catalysts for SO_2 conversion to SO_3 (and, in the presence of moisture, to H_2SO_4). The experimental plan for evaluating the interaction of sulfur oxide-containing streams with Mn^{+2} spiked filters is given in Table 3.

Subsequent to Part 1 experiments, a second series of experiments was planned to determine the influence of glass fiber composition and filter production variables on reactivity with sulfur oxide-containing streams. A total of nine filter materials was selected on the basis of glass composition (determined by X-ray emission analysis), manufacturer, and usage for stack sampling. The candidate filters, together with classification according to composition, are identified in Table 4 which also presents the relative x-ray interaction for major elements (excluding Si) and sulfate levels. The experimental test grid for the Phase 4 studies are given in Table 5.

Table 3. Phase 3 Test Grid: Sulfur Dioxide and Sulfuric Acid Vapor - Mn^{+2} Spiked Glass Fiber Filter Interaction (Gas Stream/Filter Temperature = 205°C, Moisture Content = 25%)

	Gas Concentration		
Filter	500 ppm SO_2 10 ppm H_2SO_4	2000 ppm SO_2 40 ppm H_2SO_4	2000 ppm SO_2
SFJ Thimble		x x x	x x x
MSA 1106BH	y y y	x x x, y y y	x x x
Gelman A	y y y		
ADL/Balston MQ	y y	y y	

x - Evaluations carried out in stainless/glass apparatus

y - Evaluations carried out in Teflon/glass apparatus

Table 4. Identification of Filters: Qualitative Elemental Analysis and Extractable Sulfate Content

Filter Type	Relative X-ray Intensity							Amount Sulfate
	Ca	K	Al	Ti	Fe	S	Cl	(mg per filter)
Quartz								
ADL/Balston Microquartz	300	30	20	190	5	0	15	0-0.2
Gelman Microquartz	1500	180	30	70	5	0	35	0
High Titanium								
Reeve Angel 934AH	33,600	320	30	4200	40	20	30	0.6
Gelman A	41,800	520	0	2800	35	20	0	0.2-0.35
High Barium								
Watman A	12,500	7100	20	---	20	120	0	0.15
SFJ Thimble	12,800	7000	20	---	20	100	0	0-0.6
Borosilicate								
Gelman Spectrograde	19,900	2600	20	90	10	290	10	NA
Schleicher & Schuell 810	23,800	3100	40	70	20	70	80	0.5
Reeve Angel 900AF	24,400	3300	30	140	20	65	75	0.5
MSA 1106BH	25,300	3500	30	80	20	60	60	0.4-1.0
Gelman AE	26,800	3600	20	90	20	160	35	0.15

Table 5. Phase 4 Test Grid: Filter Reaction with SO_2 + H_2SO_4 Vapor Containing Gas Stream (Gas Stream/Filter Temperature = 205°C, Moisture Content = 10%, SO_2 = 2000 ppm, H_2SO_4 = 10 ppm)

	Filter Position		
Run No.	1	2	3
102	A	SS	AE
103	RA	AE	A
104	Q	Q	RA
105	M	RA	Q
106	SS	M	SS
107	AE	GQ	GQ
108	GQ	A	M
109	K	GF	GF
110	GF	K	K

Q = ADL/Balston Microquartz

GQ = Gelman Microquartz

A = Gelman A

AE = Gelman AE

K = Reeve Angel 934AH

RA = Reeve Angel 900

M = MSA 1106BH

GF = Whatman GF/A

SS = Schleicher and Schuell 810

EXPERIMENTAL METHODS

Filter Exposure Apparatus

The designed program required the construction of a system for generating sulfur oxide-containing streams, exposing test filters, and recovering sulfur oxides from the filtered gas stream within the following design requirements.

Gas stream and filter temperature	120° and 205°C
Flow rate	~2 m^3/hr
Moisture content	0-25%
SO_2 content	0, 500 ppm, 2000 ppm
H_2SO_4 content	0, 10 ppm, 40 ppm

A schematic sketch of the exposure system is given in Figure 2. Metered amounts of compressed air and water are passed through an evaporation coil and into a furnace maintained at the desired test temperature. After introducing SO_2, the stream is passed through a mixing tank. Sulfuric acid mist is then injected into the stream at a controlled rate by means of a syringe drive. During stabilization of conditions, the entire stream is exhausted with a portion of the stream passing through an NDIR gas analyzer to monitor SO_2 levels. For exposure, the pumps on the sampling trains are activated, and a portion of the challenge gas stream is pulled through the filters at a rate of about 0.05 m^3/min., with excess gas being exhausted. The sampling trains were commercial versions of an EPA approved particulate sampling train with the following modifications: 1) the heated sampling probe and nozzle were excluded, and 2) a condenser was incorporated between the filter holder and first impinger to recover the sulfuric acid mist (and water) from the stream. The sampling train impingers were charged with 10% hydrogen peroxide to collect SO_2.

The original stream generation apparatus was constructed with stainless steel tubing and glass. However, during the Phase 2 and 3 evaluations involving the introduction of sulfuric acid mist, very poor sulfuric acid mist recoveries from the system were noted. Inspection of the system revealed substantial corrosion of the stainless in the vicinity of sulfuric acid injection. Therefore, the system was reconstructed with glass tubing and Teflon fittings. The SFJ thimble filter could not be tested during this series of evaluations, as it required the use of a stainless steel holder. The apparatus was reconstructed for the Phase 4 challenge experiments

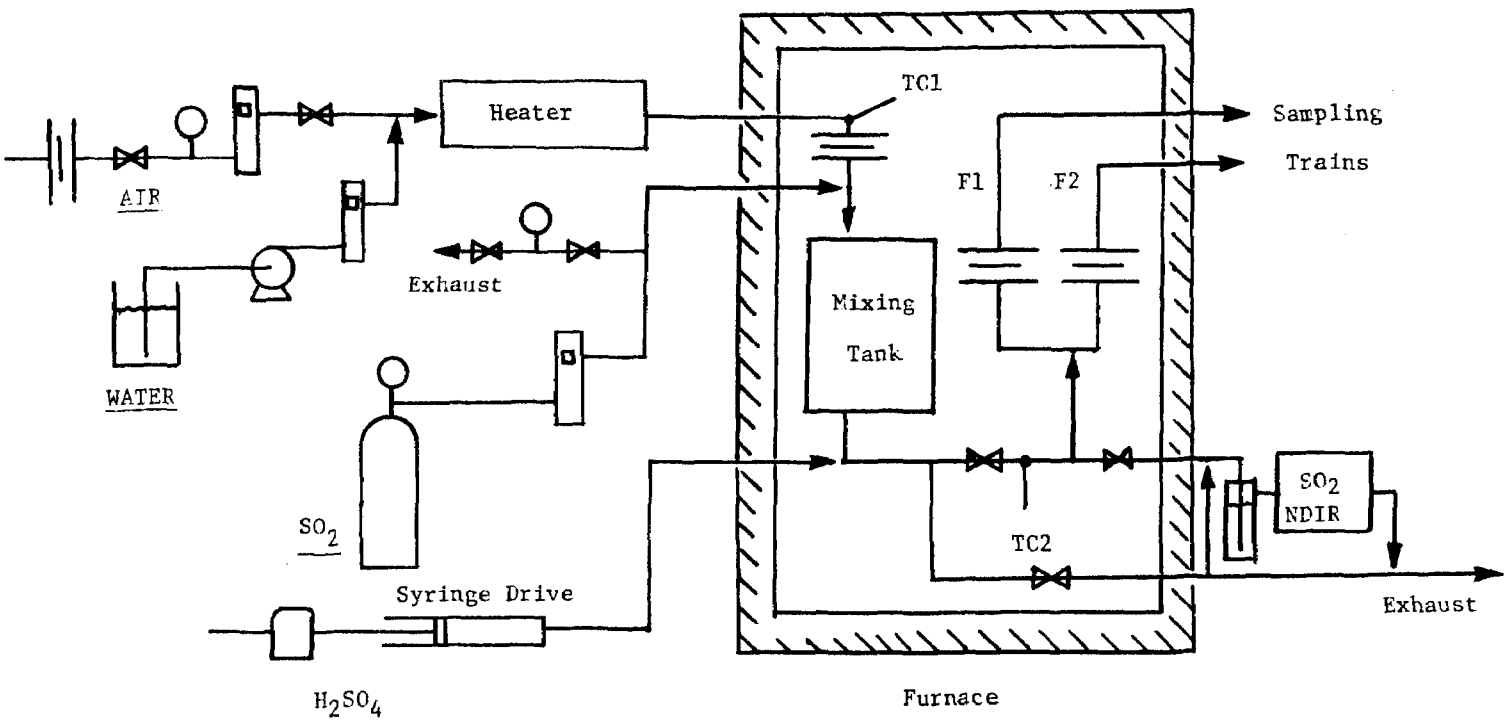

Figure 2. Schematic sketch of filter exposure apparatus.

to achieve a gas stream flow of about 0.15 m^3/min. enabling the simultaneous exposure of three filters.

Characterization and Preparation of Test Filters

All candidate filter materials were analyzed by x-ray fluorescence to determine the relative amounts of major elements, permitting a classification of filters according to glass composition. In addition, x-ray fluorescence was used to make a qualitative estimate of the presence and amount of sulfur and chlorine associated with the filters. Subsequently replicate samples of all filters were analyzed for background sulfate levels, using the barium chloranilate colorimetric procedure.

Prior to gas stream exposure, all filters were pretreated by heating to 500°C for one hour. Filters selected for spiking with Mn^{+2} were soaked in a solution of $MnCl_2$ and oven dried. Several spiked filters of each type were analyzed for Mn^{+2} content by atomic absorption to establish that doping levels were within the desired range of ~30 μg per filter.

Sample Analysis

At the completion of each filter exposure experiment, the following individual samples were obtained from each of the collection trains:

- Filter
- Condenser solutions and rinsings (for experiments with H_2SO_4 injection)
- Impinger solutions and rinsings
- Silica gel

During clean-up, the water gain, attributable to moisture condensation, was measured and recorded in accordance with Method 5 protocol for moisture content determination. The filters were removed from their holders and stored in individually sealed petri dishes until such time as sulfate determinations could be performed. After recovery, all train solutions were immediately analyzed by wet chemical techniques to quantify the level of SO_2 and/or H_2SO_4 and variable amounts of SO_2 entrained within the dropout liquor. To determine this entrained level, an aliquot of the condenser solution was analyzed as sulfite by an iodimetric

titration procedure. A second aliquot was treated with peroxide to oxidize the sulfurous acid to sulfuric acid. This aliquot was then titrated with standard base to determine total acid content. The value obtained by the iodimetric procedure was then subtracted from the total acid value to determine the amount of H_2SO_4 collected in the condenser.

The impinger solutions, which initially had been charged with 7%-10% hydrogen peroxide solutions, were titrated directly with a standardized base for quantitative determination of SO_2. This value was added to the sulfite value previously discussed to calculate the total SO_2 content of the sampled gas stream.

Soluble sulfate was extracted from the collection filters by extraction in boiling water. The amount of sulfate was then determined by the barium chloranilate method.

RESULTS AND DISCUSSION

Phase 1 - Sulfur Dioxide - Clean Filter Evaluations

The exposure of clean filters to streams containing sulfur dioxide did not result in the collection of significant amounts of sulfate. For the statistical grid of experiments considering variation in SO_2 content, moisture content and gas temperature, the measured sulfate values (given in Table 6) averaged 1.3 mg/m^3 for the MSA 1106BH filters and 0.3 for the SFJ thimbles. These values are generally in the range observed for the sulfate content on clean filters.

In summary, the Phase 1 filter challenge experiments involving variation in SO_2 concentration, moisture content, and filter temperature resulted in very low sulfate recoveries from the tested filters. These recoveries were not substantially different than blank sulfate levels for SFJ thimble and AD/Balston MO filters and were less than one mg/m^3 higher than the blank for the MSA 1106BH filter.

Table 6. Results of Phase 1 Sulfur Dioxide Challenge Studies: Statistical Experimental Grid

A. MSA 1106BH

Sulfur Dioxide Content	Moisture Content	Sulfate Gain - mg/m^3 Gas Stream/Filter Temperature 120°C	205°C
500 ppm	0	0.7, 0.9	0.8, 0.8
	25%	1.1, 1.4	1.7, 1.0
2000 ppm	0	1.0, 0.9	1.3, 1.3
	25%	1.8, 1.4	1.7, 2.3

B. SFJ Thimble

Sulfur Dioxide Content	Moisture Content	Gas Stream/Filter Temperature 120°C	205°C
500 ppm	0	0.6, 0.2	0.3, 0
	25%	0.6, 0.5	0.2, 0.2
2000 ppm	0	0.3, 0.2	0.2, 0
	25%	0.5, 0.7	0.4, 0.1

Phase 2 - Sulfuric Acid Vapor - Clean Filter Evaluations

Filters exposed to gas streams containing sulfuric acid vapor (in equilibrium with water), sometimes in coexistence with SO_2, were found in some cases to collect appreciable amounts of sulfate at a test temperature well above the acid dewpoint, i.e., as false particulate. The data for individual experiments are given in Table 7.

For the Teflon/glass system exposures, measurable sulfate is collected by all test filters after exposure to a stream containing 40 ppm H_2SO_4 vapor (corresponding to about 160 mg/m^3) and 2000 ppm SO_2. The level of sulfate is appreciable for MSA 1106BH, being about 40 mg/m^3, with lower levels of 7 and 2 mg/m^3 for Gelman A and ADL/Balston Microquartz, corresponding to 25%, 4%, and 1% of the H_2SO_4 vapor in the stream, respectively. The data for the ADL/Balston Microquartz show equivalent sulfate gains for exposure with and without the coexistence of 2000 ppm SO_2. Therefore, in agreement with the Phase 1 results, SO_2 is not being converted to collectable sulfate. For the MSA 1106BH filter, comparable levels of sulfate (about 40 mg/m^3) are collected from streams with 10 ppm H_2SO_4 and 40 ppm H_2SO_4. This suggests an upper limit to H_2SO_4 vapor collection which, for MSA 1106BH, is about 40 mg/m^3 corresponding to a stream concentration of 10 ppm H_2SO_4.

Phase 3 - Sulfur Dioxide and Sulfuric Acid Vapor - Mn^{+2} Spiked Filter Evaluations

The major purpose of this series of experiments was to determine whether the presence of an appropriate catalyst for SO_2 oxidation on the filter results in sulfate collection. The experimental results for individual experiments are presented in Table 8. Experiments performed with the stainless/glass system yield sulfate values that indicate an influence from system memory. No conclusions can be drawn from these data. For the case of evaluations in the Teflon/glass system, sulfate recoveries are generally comparable to the results for Phase 2 studies for the same conditions of gas composition. It is concluded that the presence of Mn^{+2} on the filter does not result in the conversion of SO_2 to collected sulfate.

Table 7. Results of Phase 2 Sulfuric Acid Vapor - Clean Filter Challenge Studies (Gas Stream/Filter Temperature = 205°C, Moisture Content = 25 volume percent)

Filter	Gas Concentration		
	500 ppm SO_2 10 ppm H_2SO_4	2000 ppm SO_2 40 ppm H_2SO_4	40 ppm H_2SO_4
	Sulfate Gain - mg/m^3		
Stainless/Glass System			
SFJ Thimble		2.4, 8.2, 2.4, 3.3	20.5, 12.6, 44.7
MSA 1106BH		6.1, 6.8, 4.2, 7.0	21.4, 15.8, 40.8
Teflon/Glass System			
MSA 1106BH	45.7, 47.2, 47.3	54.0, 47.1, NA, 17.4	
Gelman A		6.5, 7.7	
ADL/Balston MQ		2.2, 1.7	1.4, 2.0, 2.1
	Average Sulfate - mg/m^3 (Std. Dev. - mg/m^3)		
Stainless/Glass System			
SFJ Thimble		4.1 (2.8)	25.9 (16.7)
MSA 1106BH		6.0 (1.6)	26.0 (13.1)
Teflon/Glass System			
MSA 1106BH	46.7 (0.8)	40.2 (19.9)	
Gelman A		7.0 (0.9)	
ADL/Balston MQ		2.0 (0.4)	2.3 (0.5)

Table 8. Results of Phase 3 Sulfur Dioxide and Sulfuric Acid Vapor - Mn^{+2} Spiked Filter Challenge Studies (Gas Stream/Filter Temperature = 205°C, Moisture Content = 25 volume percent)

Filter	Gas Concentration		
	500 ppm SO_2 10 ppm H_2SO_4	2000 ppm SO_2 40 ppm H_2SO_4	2000 ppm SO_2
	Sulfate Gain - mg/m^3		
Stainless/Glass System			
SFJ Thimble		12.0, 7.3, 5.8	14.2, 10.0, 5.4
MSA 1106BH		13.7, 15.2, 11.7	12.3, 11.9, 15.9
Teflon/Glass System			
MSA 1106BH	35.8 15.8, 40.7	48.0, 69.0, 38.6	
Gelman A	3.7, 3.6, 3.7		
ADL/Balston MQ	0, 0.8	2.9, 2.7	
	Average Sulfate - mg/m^3 (Std. Dev. - mg/m^3)		
Stainless/Glass System			
SFJ Thimble		8.4 (3.2)	9.9 (4.4)
MSA 1106BH		13.5 (1.8)	13.4 (2.2)
Teflon/Glass System			
MSA 1106BH	30.8 (13.2)	51.9 (15.6)	
Gelman A	3.7 (0.1)		
ADL/Balston MQ	0.4 (0.6)	2.8 (0.1)	

Phase 4 - Sulfur Dioxide and Sulfuric Acid Vapor - Clean Filter Evaluations

Phase 1, 2, and 3 studies gave evidence that varying amounts of sulfuric acid vapor were collected on filters as false particulate. The amount collected was apparently associated with the glass composition of these filters and was highest for MSA 1106BH, a borosilicate glass. As a result, a variety of filter materials was evaluated to identify their composition and to determine their susceptibility to sulfuric acid vapor collection. The filters included all commercial grades used for stack sampling and a high purity quartz filter (ADL/Balston Microquartz) developed under EPA Contract No. 68-02-0585. These filters are identified in Table 4.

The ADL/Balston Microquartz material is from a pilot scale run using high purity quartz fibers. Produced on special stainless steel papermaking equipment, it represents the highest purity filter material available. The Gelman Microquartz includes 5% glass fiber (to permit a lower annealing temperature), resulting in higher levels of Ca, K, and Cl. All of the other filters are prepared from glass fibers. The Reeve Angel 934AH and Gelman A represent high titania glasses of somewhat different composition. The Reeve Angel 934AH should be more refractory (i.e., better thermal and chemical stability at elevated temperature than the Gelman A as a result of a higher Ti and lower Ca and K content). The Whatman A and SFJ thimble filters are prepared from the same composition glass, rich in Ba, Zn, and K. This composition is less refractory than the titania glasses or quartz but more refractory than the borosilicate composition found for the other five filters.

The results of triplicate exposures of these filters (excluding the SFJ thimble) to a gas stream at 200°C and containing 2000 ppm SO_2, 10 ppm H_2SO_4 vapor, and 10%-15% moisture are presented in Table 9. As expected from the chemical and thermal inertness of the classes of filters, inferred from the glass compositions, the ADL/Balston Microquartz shows no effect from stream exposure. The Gelman Microquartz and Reeve Angel 934AH materials are very inert, with collected sulfate levels of 0.5 mg/m^3, perhaps slightly above background levels. The Whatman GF/A and Gelman A filters exhibit a moderate amount of sulfate collection, corresponding to 7-8 mg/m^3, and the four borosilicate composition filters tested collect appreciable levels of sulfate, corresponding to 13-14 mg/m^3.

The collected sulfate on these filters is false particulate, for the challenge gas stream was maintained at 200°C, well above

Table 9. Results of Phase 4 Sulfur Dioxide - Sulfuric Acid Mist Challenge Studies (Gas Stream/Filter Temperature = 205°C, Moisture Content = 10%, SO_2 = 2000 ppm, H_2SO_4 = 10 ppm)

Filter	Sulfate Gain - mg/m^3				
	1	2	3	Ave.	Std. Dev.
ADL/Balston Microquartz	0	0.2	0.2	0.1	0.1
Gelman Microquartz	0.6	0.5	0.5	0.5	0.1
Reeve Angel 934AH	0.5	0.5	0.5	0.5	0
Whatman GF/A	6.3	6.8	7.3	6.8	0.5
Gelman A	7.0	7.8	8.5	7.8	0.8
Gelman AE	14.4	9.6	15.0	13.0	3.0
MSA 1106BH	12.7	13.3	11.9	12.6	0.7
Reeve Angel 900	13.3	12.8	15.6	13.9	1.5
Schleicher and Schuell 810	15.2	13.7	14.3	14.4	0.8

the sulfuric acid-water vapor mixture dewpoint of 135°C. As the sulfur oxide content of the test gas stream is not unlike stack emission streams for a number of stationary source categories, the choice of the filter material used in stack sampling can have a profound effect on the apparent level of particulate.

The nature of the reaction between sulfuric acid vapor and the components of borosilicate and other glasses is not known. It is known that components of the glass will partially hydrolyze in the presence of water vapor, yielding acidic boron oxide and alkaline compounds of sodium and potassium. It is probable that these alkaline products react with the acid gas to form collectable compounds. The amount of collected sulfate, therefore, depends both on stream conditions (temperature, moisture content, H_2SO_4 content) and on the presence, form, and amount of alkaline metals in the glass.

Further tests of this nature should be conducted to determine more completely the conditions under which false particulate can occur and the amounts to be expected for industrial source categories. Such information would provide a data base for determining the advisability of excluding certain classes of filters for use in stack sampling. In addition, other glass components of the sampling system (probe liner, filter holder, and connectors), which

are usually borosilicate, should be similarly evaluated to determine if they contribute to false particulate formation.

CONCLUSIONS

Particulate collection filters were exposed to gas streams containing combinations of sulfur dioxide, sulfuric acid vapor, and water at temperatures well above the acid-water dewpoint to identify conditions leading to the collection of sulfate on the filters. The presence of such false particulate would result in an overestimate in mass for particulate stack sampling. From this work, the following conclusions are drawn:

- Streams containing SO_2 at concentrations of 500 ppm and 2000 ppm did not result in collected sulfate on either clean filters or on filters spiked with Mn^{+2}.

- Streams containing sulfuric acid vapor (with or without the coexistence of SO_2) resulted in the collection of varying amounts of sulfate depending upon the filter type.

- Evaluation of commercial filters commonly used for stack sampling showed that the susceptibility to sulfate collection as false particulate is directly related to the glass composition of the filter. Typical levels of sulfate collected by exposure to a gas stream at 200°C (2000 ppm SO_2, 10 ppm H_2SO_4, 10% moisture) are:

Sulfate (mg/m)	Grade	Commercial Filters
<1	Quartz	ADL/Balston Microquartz, Gelman Microquartz
	High titania	Reeve Angel 934AH
6-7	Medium titania	Gelman A
	High barium	Whatman GF/A
13-14	Borosilicate	Gelman AE, MSA 1106BH, Reeve Angel 900, Schleicher and Shuell 810

RECOMMENDATIONS

The magnitude of false particulate collected as sulfate by some commercial filters indicates the need for a better understanding of the mechanism for sulfate collection. Further study should be conducted to address the following kinds of questions.

- What is the range of conditions (gas temperature, sulfuric acid concentration, moisture content) for which sulfate will be collected as false particulate?
- Is there a threshold level, after which no further sulfate will be collected?
- Do other borosilicate glass components of a sampling train (probe liner, filter holder, connectors) similarly involve collection of sulfate as false particulate?
- Can the level of sulfate collected be altered by filter pretreatment? For example, a high temperature exposure of borosilicate glass filters to steam may remove the reactive components.
- How does the presence of other particulate influence sulfate collection?

Such further work is needed to provide a rational basis for deciding if certain classes of filters should be excluded for purposes of stack sampling.

ACKNOWLEDGMENTS

The authors acknowledge the help of Larry Damokosh and Dr. Judy Harris for carrying out the sulfate analyses. Appreciation is extended to Dr. Kenneth Knapp of the EPA for his suggestions and comments on experiment planning and review.

Particulate Sampling in Process Streams in the Presence of Sulfur Oxides

Kenneth M. Cushing
Southern Research Institute

ABSTRACT

Particulate sampling methods are performed on industrial process streams to determine total mass concentrations and particle size distributions. In some instances, the amount of sulfur collected may be of primary interest; however, sulfur oxide environments can also mask and interfere with the determination of total particulate concentrations and size distributions.

Most sampling techniques incorporate some type of filter material on which the particles are collected, either by filtration or impaction. Recent laboratory and field data concerning interference and weight gains by filter materials in sulfur oxide environments will be presented, including data showing a correlation between type of filter material, total filter weight gains, and the specific laboratory or field environment (concentration of sulfur oxides, temperature, etc.). A brief discussion will focus on a passivation technique for glass fiber filters.

Sampling of ultrafine particles is usually performed with some type of extraction-dilution system. It has been ob-

served that under certain combinations of SO_x concentration and dewpoint, fine sulfuric acid mists can be formed. Data related to this phenomenon will be reported.

INTRODUCTION

During the past six years Southern Research Institute personnel have performed many particle sizing research tests on control devices treating industrial process streams. In many cases these process streams have had high sulfur dioxide fractions, and this has led to difficulties in obtaining accurate and reliable data. In this paper two specific problems are addressed: SO_2 uptake by glass fiber filter media and SO_3/H_2SO_4 masking of ultrafine particle measurements.

SO_2 UPTAKE BY GLASS FIBER FILTER MEDIA

In order to determine the particle size distribution of material entering or exiting a control device, cascade impactors have been widely employed because of their simplicity of operation, size discrimination range (0.5-20 μm), and ability to operate in situ. In order to reduce particle bounce and reentrainment in cascade impactors, as well as to provide a lightweight media on which to collect milligram quantities of dust, glass fiber substrates are frequently used in most commercial devices. Unfortunately, these glass fiber substrates are susceptible to weight gains due to reaction of the sulfur dioxide with basic sites in the glass fibers.

Prior to Southern Research Institute's investigations into this problem, two previous experimental programs dealt with SO_2 uptake on glass fiber materials.

The work of Charles Gelman and J. C. Marshall (1) of the Gelman Instrument Company, makers of various filter media and equipment, indicates that SO_2 absorption is the cause of the anomalous mass gains. They acknowledge that a high pH glass fiber can absorb sulfur dioxide and thus cause erroneously high particulate weights.

According to Gelman and Marshall, the SO_2 reaction on glass fibers could cause "a 30% error in the measurement of total suspended particulate matter" in an urban atmosphere. It is possible that flue gases would give even higher errors, especially if the gases have a high moisture content, because the reactivity of SO_2 appears to increase at higher humidities.

Both quartz and glass fiber filter material was tested by Gelman. The quartz was found to be non-reactive with SO_2. The glass fiber materials, Gelman Type II and a newly developed SpectroGrade prepared with H_2SO_4, were low in SO_2 pickup; however, the SpectroGrade glass, prepared with HCl, picked up significant amounts of SO_2. (See Table 1.) Their explanation is that glass fibers prepared with H_2SO_4 reacted to form $CaSO_4$ which prevents further reaction with SO_2 to form sulfates. The test used for SO_2 reactivity was to expose the filters to a water saturated atmosphere of SO_2 for 20 hours. Mass change and initial pH of each filter were measured. Gelman does not elaborate on the meaning of "prepared with H_2SO_4."

Another type of SpectroGrade coated with an organic silicone resin showed low SO_2 pickup. This type of SpectroGrade with the silicone treatment is now a standard type supplied by Gelman. Use of the siliconized SpectroGrade at elevated temperatures, however, can result in the disappearance of the coating and SO_2 absorption by the filter medium since the filter is not prepared with H_2SO_4.

Table 1. Sulfur Dioxide Pickup
(After Gelman and Marshall) (1)
mg/Sheet - 20 Hour Exposure

	mg	Initial pH
SpectroGrade-HCl Siliconized	3	7.1
SpectroGrade HCl	17	9.4
SpectroGrade H_2SO_4	3	6.8
Type II Fiber H_2SO_4	3	6.8
Quartz	0	7.0
Quartz Alkali Strengthened	23 (est.)	9.5

Although the work by Gelman and Marshall showed quartz fiber media to be non-reactive with SO_2, the material has been found to be too fragile to be used successfully as an impactor substrate material.

Whereas the Gelman and Marshall program was aimed at reducing the interference to particulate mass gains by filter media, the work of Barton and McAdie (2) in 1970 was designed to make filter media acceptable for sulfuric acid aerosol collection. They cite a study by Lee and Wagman (3) in 1966 which reported that atmospheric sulfur dioxide could be oxidized catalytically on the glass surface and thus seriously interfere with the determination of actual H_2SO_4 aerosol levels. Barton and McAdie developed a technique to reduce these blank effects. The filter material was soaked for two or three days in a 20% solution of H_2SO_4 followed by a thorough washing in distilled water, 80% isopropanol, and acetone, respectively, in order to deactivate any surface contaminants which could be responsible for the apparent irreversible absorption of sulfuric acid by the glass fibers. These test results are shown in Table 2. Also reported in this table are the results of Scaringelli, Boone, and Jutze (4) who used an acetic acid wash. Their method allowed only a 50% recovery of H_2SO_4. It can be seen, however, that the method of Barton and McAdie allowed full recovery of the H_2SO_4 solution.

The purpose of the Southern Research screening tests sponsored by the EPA was to gain an understanding of the SO_2 induced mass changes that occur and to facilitate the selection of glass fiber filter materials suitable for use as impactor substrate media. A suitable

Table 2. Absorption of H_2SO_4 by Glass Fiber Filters (After Barton and McAdie) (2)

	H_2SO_4, μg per 10 ml, 80% isopropanol	
Filter Treatment	Added	Found
No filter	6.0	6.3 ± 0.4
H_2SO_4 treatment	6.0	7.0 ± 0.4
No filter	14.8	14.8 ± 0.3
HOAc treatment	14.8	7.2 ± 0.4
HOAc treatment with refluxing	14.8	3.0 ± 0.5
H_2SO_4 treatment	14.8	15.2 ± 0.3
No filter	18.0	17.9 ± 0.5
H_2SO_4 treatment	18.0	18.5 ± 0.5

substrate material would be one which has stable low mass characteristics and is mechanically strong to resist cutting, tearing, and loss of material. Since the mass changes are apparently a result of chemical reactions involving the production of sulfates, the laboratory work was principally concerned with exposure of the substrate materials to sulfuric acid and/or a wet SO_2 gas. The stability of mass changes over long time periods was investigated in order to evaluate the prospects for preconditioning techniques as a means for controlling mass changes. Two laboratory test methods were employed. One approach used a flow of saturated gaseous SO_2 through the filter material, and the second involved soaking the material in hot sulfuric acid solution.

In this laboratory study, glass fiber substrate materials were exposed to air, SO_2, and water vapor at an elevated temperature. Figure 1 shows a diagram of the conditioning apparatus. Dry air was preheated in the conditioning oven and then bubbled through a heated water container at 60°C (140°F). Next, SO_2 was introduced to the heated and humidified air stream. All lines carrying SO_2 laden air were then passed through a chamber containing the filter media being tested. The chamber was designed so that conditioning gases flowed through the filter stack being conditioned.

Both gravimetric and pH determinations were used to investigate the rate of SO_2 uptake by the sample material. The procedure used to determine the filter pH was a modification of Gelman's method for 8" x 10" filter sheets (1). Two 47 mm filters were used for each pH determination.

In one series of tests, four different kinds of glass fiber substrate materials were treated in the laboratory conditioning chamber on an hour-by-hour basis. After each hour of conditioning, the substrates were weighed, desiccated, reweighed, and the weights were recorded. It was found that desiccation resulted in no change in the weights, so this practice was discontinued. The four substrate materials tested were Reeve Angel 934AH, Gelman AE, Gelman SpectroGrade, and Whatman GF/A. All filters were 47 mm in diameter. Eight groups of twenty filters each were prepared and conditioned in the following order:

1. Reeve Angel 934AH
2. Gelman AE
3. Gelman SpectroGrade
4. Whatman GF/A
5. Reeve Angel 934AH
6. Gelman AE
7. Gelman SpectroGrade
8. Whatman GF/A

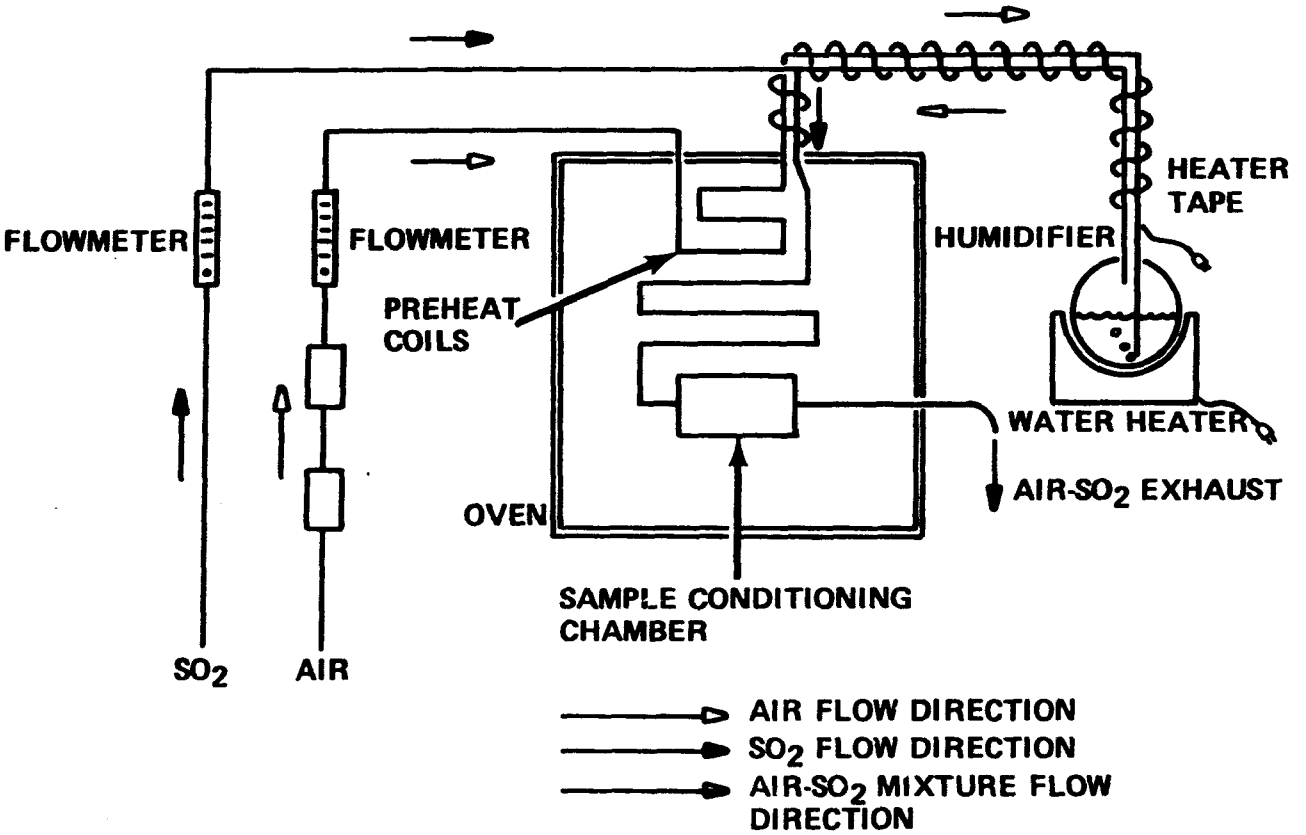

Figure 1. Diagram of experimental set-up for filter substrate conditioning experiment.

Gas flow was such that the Reeve Angel material was exposed first. Figure 2 shows the results for the first nine hours of conditioning. The conditioning temperature was 220°C (428°F). Water saturated air with 5% SO_2 was pumped through the chamber at a rate of 2.1 lpm. Note that after nine hours of conditioning the Reeve Angel material had not gained but lost weight. However, the weight loss was miniscule and probably due to handling. All others had gained significant amounts.

Sulfuric Acid Wash Treatment of Filter Media

Another approach to passivating impactor substrates was also investigated. Bundles of Reeve Angel 934AH and Gelman AE 47 mm filters were soaked in hot concentrated sulfuric acid-water (50/50) mixtures for 90 minutes. These filters were then washed in distilled water, washed again in ethanol (ETOH) or isopropanol (IPA), dried, baked, and desiccated. Upon conditioning for one hour under the conditions described above (220°C [438°F], air-water gas mixture with 5% SO_2), eighteen Gelman AE 47 mm filters gained 11.9 mg or 0.66 mg/filter. Twenty untreated Gelman AE 47 mm filters gained 67.7 mg or 3.39 mg/filter with the same conditioning. Therefore, the sulfuric acid-wash can make a difference when the filters are known to gain weight. The Reeve Angel material again showed no weight gains.

The hour-by-hour conditioning of the four different types of glass fiber filter substrate materials was continued, and mass gains were monitored for a total of 26 hours of conditioning. In addition, the sulfuric acid washed Gelman AE and Reeve Angel 934AH materials were laboratory conditioned on an hour-by-hour basis for a total of 18 hours. Figure 3 shows the mass gain per 47 mm filter versus laboratory conditioning time. Data for Gelman AE, AE acid washed, Gelman SpectroGrade, and Whatman GF/A are presented. Reeve Angel 934AH plain and acid washed filter materials were also conditioned, but since mass increase in this material was negligible, these data were not graphed. The Gelman AE acid washed material gained approximately one third as much mass as the plain Gelman AE. Figure 3 also shows that even after 26 hours of laboratory conditioning mass gains may be expected with further conditioning.

Gas analyses were conducted on the conditioning gas at the inlet to the conditioning chamber: SO_2 and SO_3 concentrations were measured at approximately 10,000 ppm, and 3 ppm to 5 ppm, respectively. Iron is a catalyst for the conversion of SO_2 to SO_3 at the conditioning temperature (220°C, 428°F). The conversion efficiency is small, less

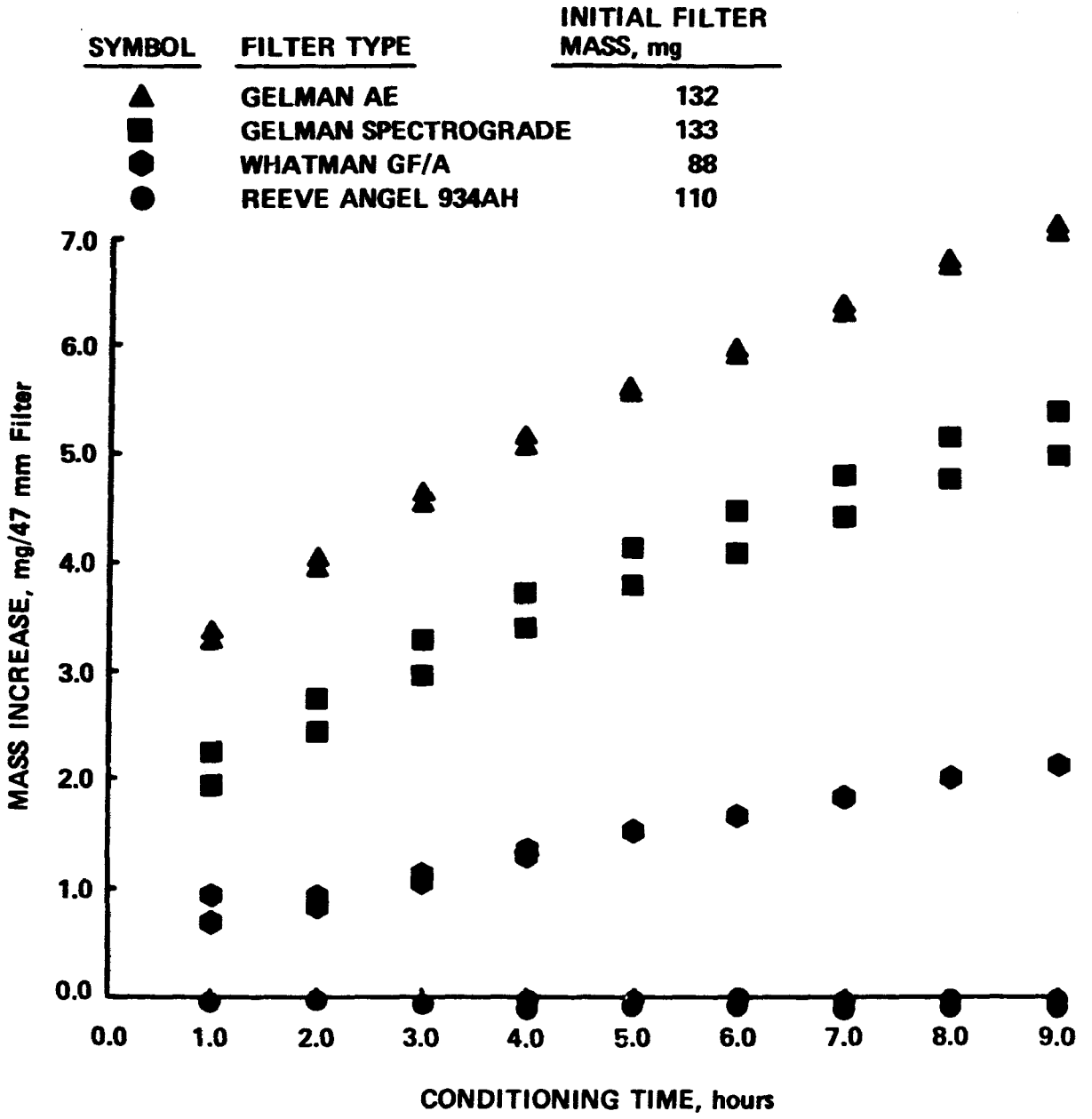

Figure 2. Mass gains of four types of glass fiber filter materials versus exposure time to a water-air-5% SO_2 gas mixture at 260°C (500°F).

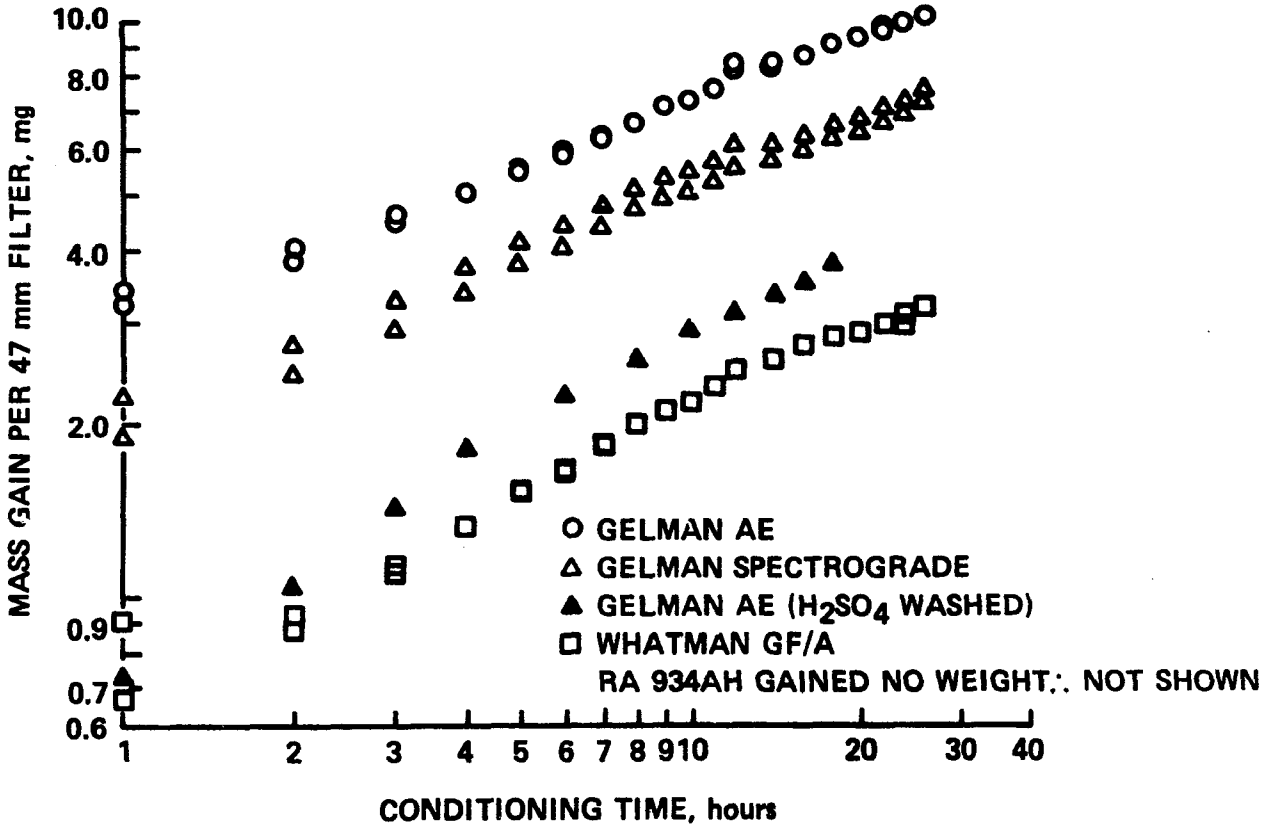

Figure 3. Mass increase per 47 mm filter as a function of laboratory conditioning time.

than 1% but still enough SO_3 is produced to be detected. Since all the SO_2 carrying lines and conditioning chamber are stainless steel, we should expect that the filters which have been SO_2 conditioned have also been exposed to SO_3.

Table 3 summarizes the end-point results presented in Figure 3. These data are presented in the order in which the 47 mm filters were conditioned in the stainless steel conditioning chamber (alundum filter holder). Results are presented on a mass gain per filter and percent mass gain basis.

In another series of tests, chemical analyses were made on the laboratory conditioned and unconditioned filters. Table 4 shows the barium, calcium, and soluble sulfate concentration in two types of glass fiber filter material conditioned at Southern Research: Reeve Angel 934AH and Gelman AE. These 47 mm filters were analyzed when received, after being baked-out and desiccated, and after being conditioned. The Reeve Angel material shows large amounts of calcium and miniscule amounts of barium and soluble sulfates, even after 12 hours of conditioning. The Gelman AE materials show large amounts of calcium as well, but after conditioning there is a great gain in soluble sulfates. This is reflected in the mass gains for this material. Each 47 mm filter gained on an average 2.93 mg. The initial pH of the Gelman AE material after baking was 9.8. With two hours of conditioning the pH dropped to 8.8. This is in contrast to the behavior of the Reeve Angel material. The pH of this substrate material stayed rather constant at about 5.9 to 6.7 before and after conditioning. Mass gains on conditioning for any length of time were very small.

These results indicate that a laboratory induced sulfate mass gain can be made to occur in glass fiber filter materials. Whether or not this mass gain or "conditioning" lasts is another question. To determine if the conditioning is a temporary effect, samples of these filters (16 to 20 filters per sample) were conditioned for 2 to 12 hours. Some were exposed to ambient air after conditioning, while others were desiccated.

Figures 4 and 5 show the results of these tests for the Reeve Angel 934AH material. Figure 4 shows the percent weight change versus days after conditioning for groups of filter conditioned for 2 hours and 12 hours. One group was exposed to ambient air after conditioning, and another group was desiccated after conditioning. In both cases minute mass gains were seen for 12 hour conditioning, and minute mass losses were seen for 2 hour conditioning. In either case there appears to be no reaction after conditioning resulting in an appreciable mass gain or loss. Figure 5 shows the pH of single filter samples measured after conditioning for 2 and 12 hours. As in

Table 3. Mass Gains of 47 mm Glass Fiber Filter Substrate Materials from Laboratory Conditioning

Material	Batch Number	Number of 47 mm Filters Conditioned	Conditioning Time (hours)	Mass Before Conditioning (grams)	Mass After Conditioning (grams)	Mass Gain per Filter (mg)	Percent Mass Gain
Reeve Angel 934AH	3307	20	26	2.1888	2.1881	-0.04	-0.03
Gelman AE	8204	20	26	2.6644	2.8735	10.46	7.84
Gelman SpectroGrade	8192-20232	20	26	2.6717	2.8160	7.22	5.40
Whatman GF/A	3563	20	26	1.7695	1.8349	3.27	3.70
Reeve Angel 934AH	3307	20	26	2.2149	2.2166	0.09	0.08
Gelman AE	8204	20	26	2.6266	2.8375	10.55	8.03
Gelman SpectroGrade	8192-20232	20	26	2.6522	2.8051	7.65	5.77
Whatman GF/A	3563	20	26	1.7361	1.8272	4.56	3.64
Reeve Angel 934AH (Acid Washed)	4292	20	18	2.0968	2.0975	0.04	0.03
Gelman AE (Acid Washed)	8206	20	18	2.6939	2.7699	3.80	2.82

Table 4. Barium, Calcium, and Soluble Sulfate Content in Two Glass Fiber Substrate Materials

	Reeve Angel 934AH Substrate Material					
	Barium		Calcium		Soluble Sulfate	
	Ba^{++} Mass (μg)	%BaO	Ca^{++} Mass (μg)	%CaO	SO_4^{-} Mass (μg)	$\%SO_4$
Original	63	0.06	14202	17.9	3.5	0.003
After Bakeout	54	0.05	14055	17.8	3.5	0.003
After Conditioning (2 Hours)	135	0.13	14531	18.2	4.5	0.004
After Conditioning (12 Hours)	<10	<0.01	13820	17.6	92	0.08

	Gelman AE Substrate Material					
	Barium		Calcium		Soluble Sulfate	
	Ba^{++} Mass (μg)	%BaO	Ca^{++} Mass (μg)	%CaO	SO_4^{-} Mass (μg)	$\%SO_4$
Original	<10	<0.01	6094	6.5	<10	<0.01
After Bakeout	<10	<0.01	5470	6.1	<10	<0.01
After Conditioning (2 Hours)	<10	<0.01	5758	5.9	3013	2.24

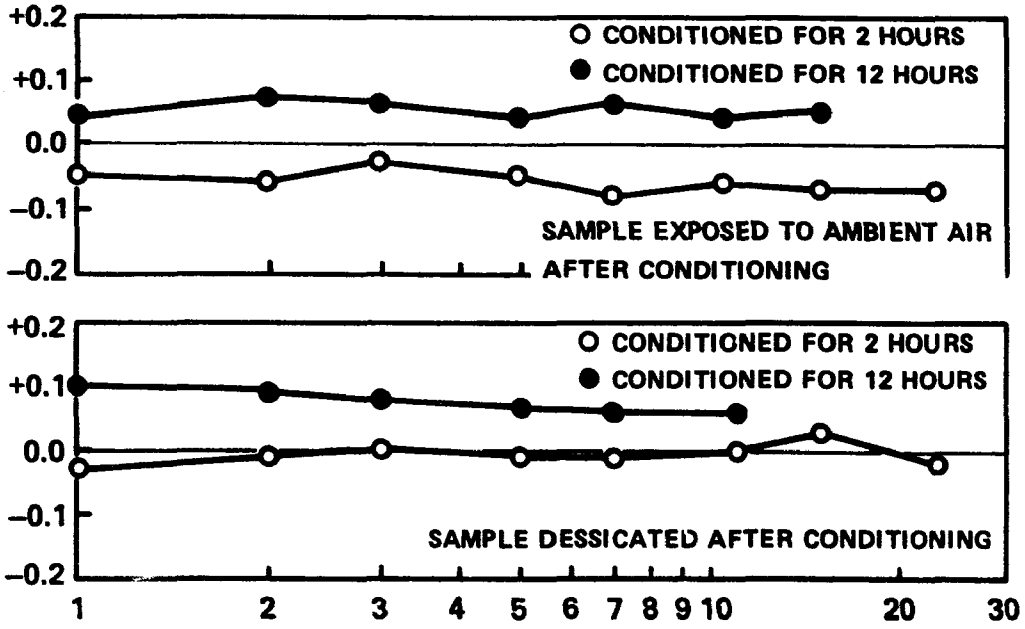

Figure 4. Percent weight change for Reeve Angel 934AH glass fiber filter substrate material as a function of time after conditioning.

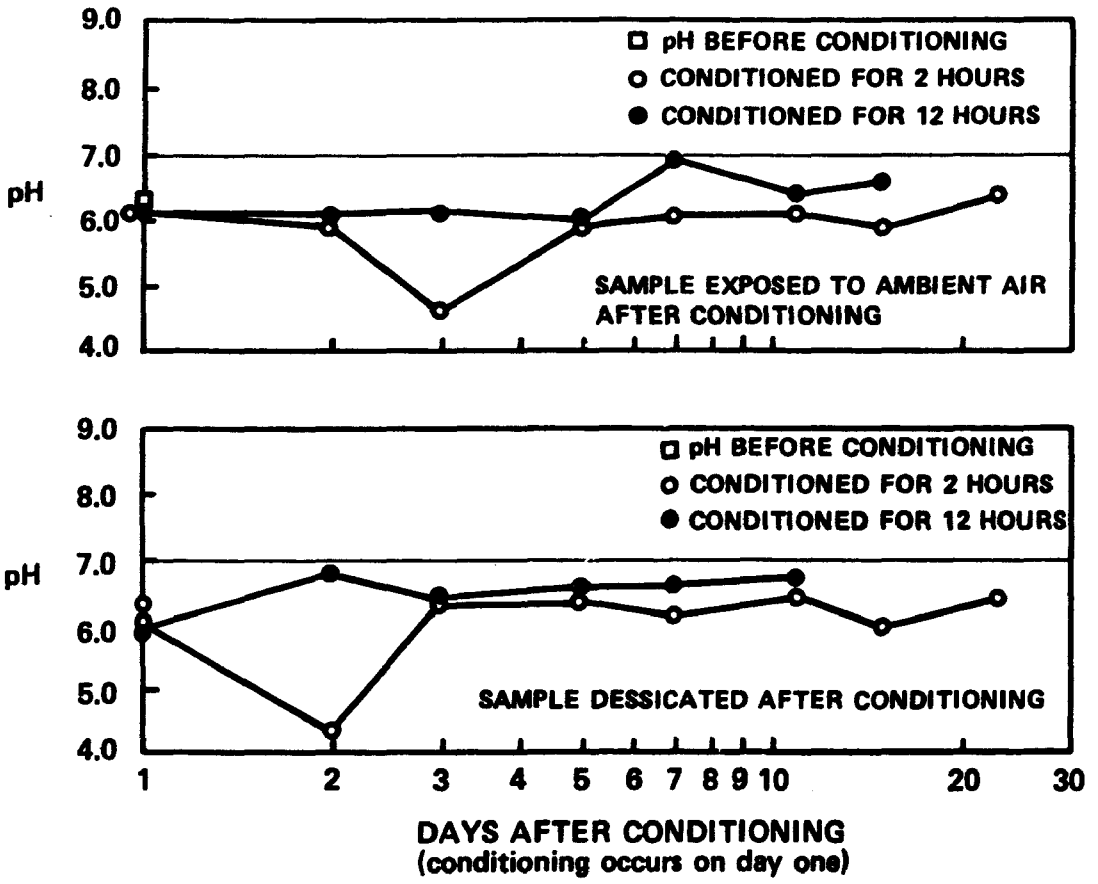

Figure 5. pH of Reeve Angel 934AH glass fiber filter substrate material as a function of time after conditioning.

Figure 4, one group was exposed to ambient laboratory conditions while another group was desiccated. This substrate material appears to have essentially no change of pH upon conditioning, and it is possible that since the material was only slightly acidic, changes in the pH of water used in the pH determination could have caused the changes shown in Figure 5. Whenever pH of a filter sample was measured, the pH of the water used was also measured. We believe this to be the case for the low pH recorded on day 2 of the desiccated sample and day 3 of the exposed sample. In this case the raw distilled water used in the pH determination had a measured pH of 4.32.

From these tests it would appear that, if pH is a good monitor, the conditioning has a lasting effect. Samples of this material, conditioned for 12 hours, which were stored under desiccation for as long as 77 days, show no mass change and small change in pH (6.10 before, 6.77 after).

A more detailed discussion of this work has been published in a report entitled "Inertial Cascade Impactor Substrate Media for Flue Gas Sampling" (5).

SO_3/H_2SO_4 MASKING OF ULTRAFINE PARTICLE MEASUREMENTS

Southern Research Institute has for the past several years been involved in determining particulate concentrations and size distributions for particles in the submicrometer size range. Much of this work has been directed toward characterizing the emissions from particular industrial sources and toward determining the efficiency at which industrial gas cleaning equipment removed particles in the 0.01 to 1 μm diameter size range.

Typical sample gas conditions are shown in Table 5. At any one source, the gas conditions may be any mixture within the ranges shown in the table, and, in fact, these may not represent the actual extremes. Because of the high particulate concentrations, both by mass and by number, the presence of large quantities of condensable vapors (i.e., water and H_2SO_4) and high concentrations of corrosive gases (H_2SO_4, SO_2 and others) extensive sample conditioning and dilution become mandatory. The required dilutions approach 5000:1 in some instances, and dilutions by factors of about 500:1 are quite commonly needed. In many instances these dilutions are set, not by requirements for diluting condensable vapors sufficiently to insure that sample gas stream to the instrumentation is not saturated, but by limiting factors in obtaining reliable data from

Table 5. Typical Flue Gas Sample Conditions

	Range	Typical Value
Temperature:	Ambient to 800°C	150°C
Absolute Pressure:	490 to 850 mm Hg	750 mm
Pressure Differential to Ambient:	± 75 mm Hg	-25 mm
Moisture (Vol. Percentage)	1 - 40%	10%
CO_2 (Vol. Percentage)	0 - 15%	12%
SO_2 (Vol. Percentage)	0 - 1.4%	0.2%
SO_3/H_2SO_4 (Vol. Percentage)	0 - 0.25%	0.0005%
Particulate Mass Concentrations	to 20 g/m^3	Inlets 5 g/m^3 Outlets 0.05 g/m^3
Concentration by Number of Particles Larger Than 0.01 μm	to 3 x 10^7/ml	2 x 10^7 inlet 2 x 10^5 outlet

the available detectors. Reliable concentration data for the purposes of diffusional analysis can be obtained only within the linear response concentration limits of the condensation nuclei counters used as detectors. These limits are 10^5 particles/ml for the instruments which we normally use (GE Laboratory Model CNC's and Environment One Model Rich 100 devices). In almost all the cases, dilutions by at least 100:1 have been necessary simply to reduce the concentrations to the linear range limits of the condensation nuclei counters.

On several field tests an interference phenomenon has been observed that appears to be an acid condensation fume. Figure 6 is a sample data set which illustrates this phenomenon. As the sample gas flowrate to the diluter was increased (thus reducing the dilution factor), the measured diluted concentrations increased linearly with the sample flowrate until a critical value was reached. At this point slight increases in sample flowrates led to very large nonlinear increases in apparent aerosol concentrations.

It would appear that when SO_3/H_2SO_4 (existing in the flue as a vapor) is cooled below a characteristic dewpoint, it condenses to form an acid fume and gives rise to the phenomenon shown in Figure 6. The condensation aerosol thus produced has a very small mean size because a diffusion battery having 50% penetration by 0.016 μm diameter particles will pass only a few percent of the condensation aerosol particles. The dewpoint is sensitive to the concentrations of both H_2O and SO_3. Thus, the condensation fume can be avoided by either using sufficiently high dilutions or by removing the SO_3/H_2SO_4 while in a gaseous state. (Once H_2SO_4 has condensed very high temperatures are required for re-evaporation.) Dilution is effective in avoiding the condensation fume. It is for this reason that the phenomenon is not normally encountered at inlet sampling ports to control devices where high dilutions are used. However, dilution alone may be inadequate because frequently the minimum dilution at which the onset of the condensation fume occurs can be so high that the diluted particle concentrations are below the minimum detection limits of the sizing instruments.

Gilmore Sem (6) has also reported experiencing this condensation fume when using an extraction dilution system similar to the one developed by Southern Research. His data are shown in Figure 7. These data were taken at the inlet to a baghouse on a western coal-fired utility boiler. The dilution factor of 21 used at the inlet was apparently not sufficient to prevent formation of these particles. Sem calculated that the undiluted number concentration, if they existed in the stack, would be 23 x 10^8 particles/cm^3. Coagula-

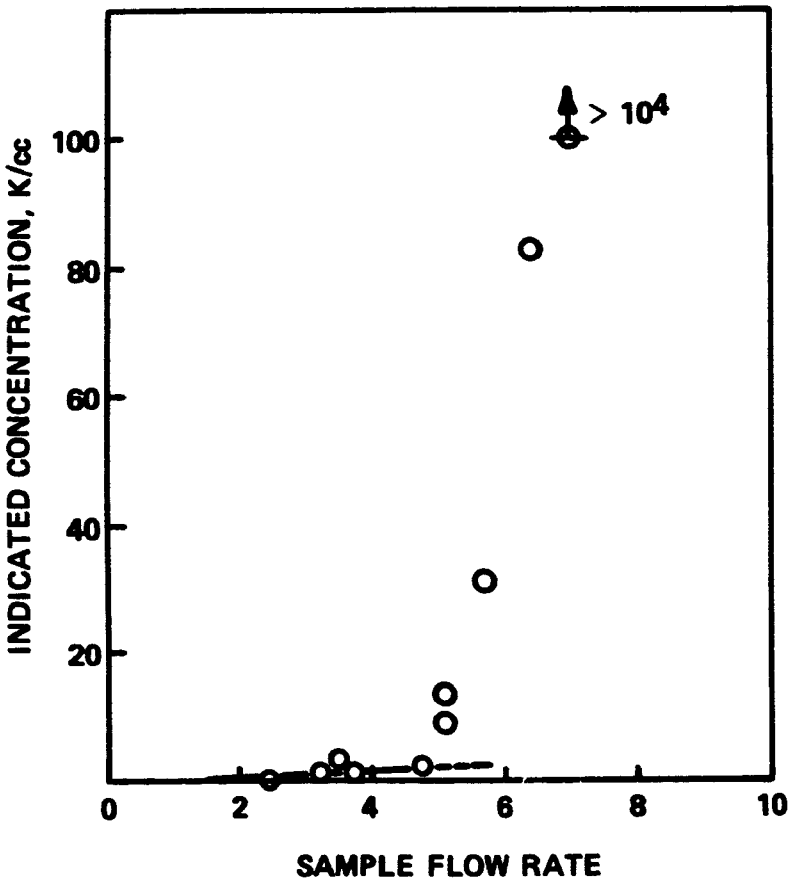

Figure 6. Behavior of diluted sample concentration at onset of sulfuric acid condensation.

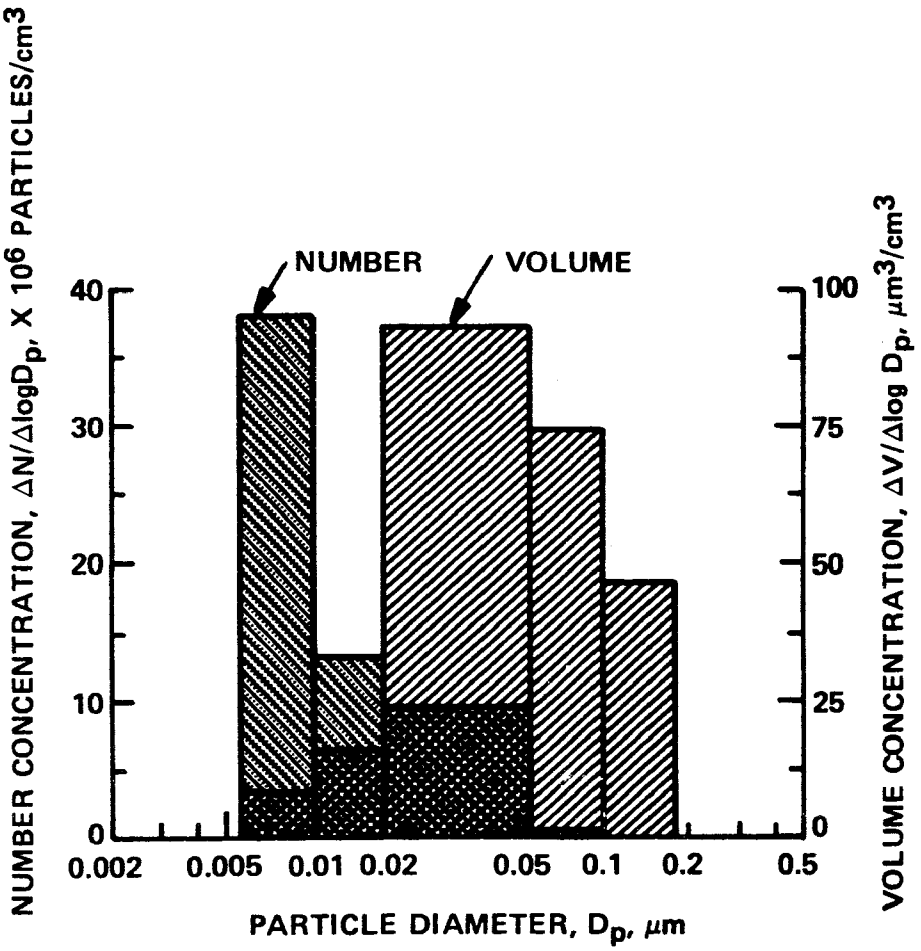

Figure 7. Typical size distribution at the inlet to the baghouse collector on a coal-fired steam boiler, measured and shown diluted 21x. The large number of very small particles may be formed by SO_x condensation in the diluter. After Sem (6).

tion rates at this concentration would be very rapid, causing such particles to grow in size by collision with others, resulting in a lower number concentration. Thus, it does not appear that these particles could have been older than several seconds, pointing to the sampling and conditioning system as the probable source.

To cope with this condensation problem, an oven containing SO_3 absorbers was incorporated into the Southern Research Sample Extraction and Dilution System shown in Figure 8. In this system a 0.5 ACFM sample flow is removed from the process exhaust stream and is pulled through a rigid probe, a flexible connector hose, and a cyclone into a "T" where the flow splits. The excess flow (needed to maintain a constant 0.5 ACFM flow through the cyclone) is dumped to ambient, and the desired sample flow (0.003 to 0.5 ACFM) goes into the diluter via a calibrated orifice and the SO_x absorber bank. The cyclone, orifice, and SO_x absorber bank are housed in a heated oven so that all components of the system, except the diluter, can be maintained at 400°F to prevent condensation. Pressure taps for the cyclone and the orifice allow continuous monitoring of the cyclone flowrate and the orifice flowrate by reading the pressure drop across the respective component. The oven was designed to house an adequate number of heated SO_x absorbers for reducing the vaporous SO_3/H_2SO_4 concentrations by diffusion to an absorber reagent. The number of absorbers required depends on the sample flowrate through the absorbers (residence time), the reagent used in the absorbers, and the initial levels of the SO_3 in the stack gas. Several reagents were considered (barium oxide, calcium oxide, PbO, granulated copper, calcium carbonate, silica gel, and activated charcoal), but only three were readily available in a granulated form: granulated copper, PbO, and activated charcoal. These three were used in a field test at a copper smelter operation where the SO_3 content of the stack gas ranged up to 0.25%. PbO and copper were found to be inadequate at this high SO_3 level even when six absorbers were used. Activated charcoal, however, was successful when six absorbers were used. In the configuration shown, activated charcoal allowed continuous running times of about six hours, although there were intermittent concentration increases which exceeded the removal capability of the absorbers and allowed a fume to form momentarily. Activated charcoal was, therefore, selected as the standard reagent. At many locations, SO_3 levels in the stack gas are so low that an acid fume is not encountered, and at others the concentrations can be adequately reduced by using only a few absorbers.

It should be noted that iron can act as a catalyst in the conversion of SO_2 to SO_3. For this reason, all parts of the SEDS which are made of stainless steel and come into direct contact with the

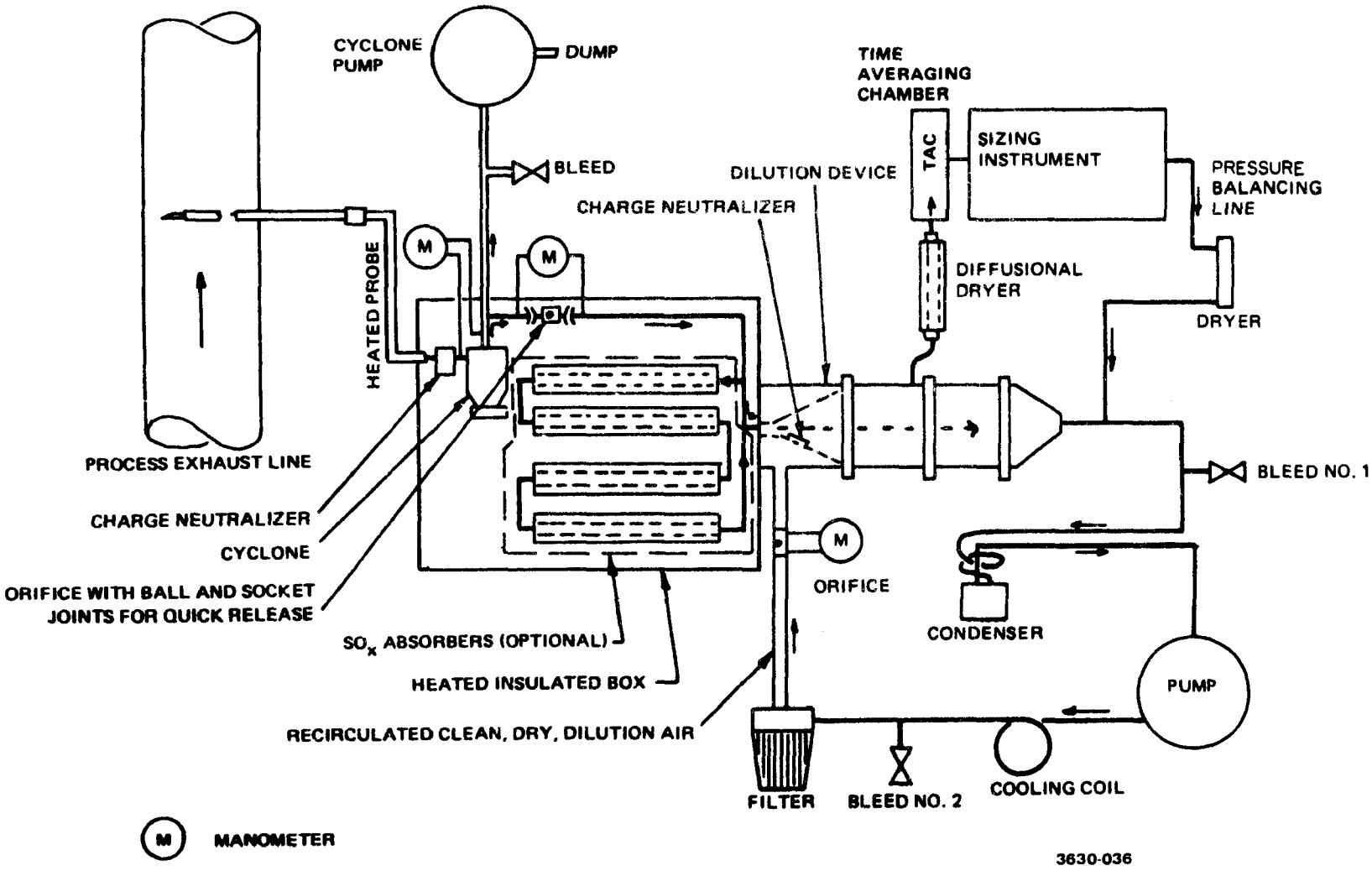

Figure 8. Sample extraction-dilution system (SEDS).

hot undiluted sample gas were passivated (removal of the iron from the exposed surfaces of the stainless steel) by immersion in hot nitric acid so as to avoid the generation of SO_3/H_2SO_4.

SUMMARY

Sampling for total mass particulate or particle number concentrations in gas streams containing sulfur oxide fractions can result in inaccurate data unless precautions are taken to passivate glass fiber media or properly condition the sample streams. Techniques have been mentioned by which glass fiber materials can be conditioned against the uptake of SO_2. SO_x absorbers are also useful for the removal of SO_3/H_2SO_4 prior to sample stream cooling and dilution in an ultrafine particle measuring apparatus.

REFERENCES

1. Gilman, C., and J. C. Marshall. High Purity Fibrous Air Sampling Media. American Industrial Hygiene Association Journal, 36(NA):512-517, 1975.

2. Barton, S. C., and H. G. McAdie. Preparation of Glass Fiber Filters for Sulfuric Acid Aerosol Collection. Environmental Science and Technology, 4(9):769-770, 1970.

3. Lee, R. E., and J. Wagman. A Sampling Anomaly in the Determination of Atmospheric Sulfate Concentration. American Industrial Hygiene Association Journal, 27(3):266-271, 1966.

4. Scaringelli, F. P., R. E. Boone, and G. A. Jutze. Journal of the Air Pollution Control Association, 16(6):310, 1966.

5. Felix, L. G., G. I. Clinard, G. E. Lacey, and J. D. McCain. Inertial Cascade Impactor Substrate Media for Flue Gas Sampling. EPA-600/7-77-060, U.S. Environmental Protection Agency, Research Triangle Park, North Carolina, 1977. 89 pp.

6. Sem, G. Submicron Particle Size Measurement of Stack Emissions Using the Electrical Mobility Technique. In: Proceedings of the Workshop on Sampling, Analysis, and Monitoring of Stack Emissions, Electric Power Research Institute Report SR-41, Palo Alto, California, April 1976.

Primary Aerosol Sulfur Size Distribution Measurements Using a Low Pressure Impactor

Richard C. Flagan
California Institute of Technology

ABSTRACT

The use of a reduced pressure cascade impactor to measure aerosol sulfur size distributions in flue gases from fossil fuel combustion will be examined. The impactor was developed to determine the contribution of sulfates to atmospheric submicron aerosols. A minimum cutoff diameter of 0.05 μm was achieved by operating four stages of the impactor well below atmospheric pressure. The small deposits on each impaction stage are ideal for sulfur analysis using a sensitive (1 ng sulfur detection limit) flash vaporization/flame photometric detection system. The impactor was designed and calibrated to size segregate particles smaller than about 8 μm diameter from a room temperature aerosol. Re-entrainment and bounce-off are small as long as the total loading on each stage is small and there are few particles larger than about 10 μm diameter.

Several changes in the operation of the reduced pressure are necessary if a hot gas stream containing high aerosol concentrations is sampled. Large particles should be removed upstream of the impactor. Dilution of the hot gases is necessary to provide reasonably long sample times before re-entrainment becomes a problem and to reduce the temperature without significantly altering the particle size. Redesign of the impactor for operation at elevated temperatures will be considered.

INTRODUCTION

For pollutant aerosols, the distribution of chemical species with respect to particle size is important in the evaluation of health effects and transport behavior. Cascade impactors commonly used for the size segregation of aerosols in chemical analysis can collect particles as small as 0.3 to 0.5 μm. Smaller particles which pass through the impactor are collected on the after-filter.

Recent studies of fine particles in the flue gases of coal-fired power plants have shown that large numbers of submicron particles are produced (1)(2). Moreover, the fine particles are found to be enriched with volatile species including a number of heavy metals and sulfur (3). In order to determine the importance of these emissions and to understand their formation, it will be necessary to determine their chemical composition. Fine ash and soot particles may be formed by homogeneous nucleation in the high temperature combustion zone. It has been suggested that 0.3%-3% of the ash in coal may be vaporized during pulverized coal combustion (4). This volatile ash may then condense and coagulate, forming a narrow size distribution at about 0.1 μm mean diameter according to recent calculation. Since this is near the minimum in the collection efficiency of most gas cleaning devices, much of that fine particulate matter will be emitted into the atmosphere. Disproportionate quantities of the heavy metals that are volatile at combustion temperatures may, thus, be emitted into the atmosphere.

Sulfate aerosols are also probably formed by condensation. Most of the sulfur in coal is oxidized to form SO_2, but only small amounts form SO_3 in the flame. Additional SO_3 may be formed by heterogeneous reactions on particles or heat transfer surfaces. Only at quite low temperatures will the SO_3 react with water or other species forming condensed phase sulfates or sulfites. Sulfate aerosol may be formed either upstream or downstream of the gas cleaning equipment, depending upon temperature, ash composition, and other possible variables. Thus, sulfate aerosols may not be removed by the gas cleaning equipment.

Sulfur represents an additional problem, since it may condense in sample lines even though it is a vapor in the flue gases. For this reason it is desirable to operate gas sampling and analysis equipment at flue gas temperatures. If this is not possible, dilution systems may be used, but very large dilution ratios will be required to prevent condensation (5).

Reduced pressure cascade impactors have been developed for the study of submicron particles in the atmosphere (6)(7). At low pressures the mean free path of the gas molecules is comparable to the diameter of the particles. The aerodynamic drag on the particles is reduced, making it possible to collect the fine particles by inertial impaction. Particles as small as 0.05 μm diameter have been collected with low pressure impactors.

Roberts and Friedlander (8) have developed a sensitive method for the analysis of aerosol sulfur. The aerosol is collected on small (0.1" x 0.8" x 0.001") stainless steel strips mounted on the collection surface of a single jet cascade impactor. The sulfur deposited on the strip is pyrolyzed by rapidly heating the strip to about 1200°C and the sulfur is then detected using a flame photometric detector. The detection limit of this method is about 2 ng sulfur. The total sulfur content is measured by this method, but the chemical species are not identified. Roberts' method for aerosol sulfur detection has been used with the low pressure cascade impactor to determine the sulfur size distribution in urban aerosols.

This combination should be useful for the measurement of sulfur in combustion generated aerosols. The low pressure impactor has been developed and calibrated for operation at ambient temperature and pressure. The present study examines the possibility of design modifications for elevated temperature operation.

INSTRUMENT DESCRIPTION

To make use of Roberts' technique, a low pressure impactor was developed with one circular jet per stage. The impactor has eight stages, and samples at a rate of one liter per minute. The aerodynamic cutoff diameters, corresponding to particles collected with an efficiency of 50%, are 0.05, 0.075, 0.11, 0.26, 0.50, 1.0, 2.0, and 4.0 μm. Particles larger than 0.5 μm are sampled at atmospheric pressure using the first four stages of the Battelle impactor (Delron #DC15, Powell, Ohio). Four additional stages, operating at pressure of 8-150 mm Hg, absolute size segregate the smaller particles. These pressures (Table 1) refer to the stagnation pressure below the jet. A critical orifice, 0.036 cm in diameter, separates the atmospheric and low pressure stages and determines the sample flow rate. The impactor is cylindrically shaped, with a diameter of 2.5", standing 18" high. For operation it requires a vacuum pump with a displacement of at least 100 Lpm. In this

lab, either the Leybold Hereas Trivac S4A or Sargent Welch 1403 was used.

Each stage of an impactor is characterized by its collection efficiency as a function of particle size. The diameter of a particle of unit density which is collected with a 50% efficiency is referred to as the aerodynamic cutoff diameter. In the design of the impactor, two things are considered: (1) the choice of jet diameters at the specified flow rate to obtain the desired cutoffs, and (2) impactor geometry and jet Reynolds number to minimize the cross sensitivity between stages.

Table 1. Low Pressure Impactor Design and Operational Parameters

Stage Number	D_j (cm)	P[a] (mm Hg)	V_j (m/sec)	Re_j	Cutoff (μm)
1	.249	744	3.5	560	4.0[b]
2	.140	743	11	990	2.0[b]
3	.099	740	22	1400	1.0[b]
4	.064	720	54	2170	0.50[b,c]
Orifice	.036	150	-	-	-
5	.110	140	93	1270	0.26[c]
6	.099	106	150	1430	0.11[c,d]
7	.099	50	300	1480	0.075[d]
8	.140	8	300	1050	0.05[d]

[a]1 atm = 745 mm Hg
[b]Calibration data from Delron Research Products (Powell, Ohio)
[c]This work
[d]Method of calibration described in Part II

For all stages, the jet to plate spacing is one half the jet diameter and the length of the jet throat is 6 mm.

For this impactor it was desired to build four low pressure stages to give approximately equal logarithmic intervals in the size range between 0.05 and 0.5 μm. To attain the reduced pressures, these four stages are preceded by a critical orifice which limits the flow rate to 1 Lpm; the orifice and these four stages follow the four atmospheric pressure stages of the Battelle impactor.

The jet diameters and operating pressures of the low pressure stages are chosen on the basis of the cutoff diameter calculated from the Stokes number, defined as

$$St = \frac{\rho_p d_p^2 V C}{18 D_j}$$

ρ_p = particle density
d_p = particle diameter
V = jet velocity
D_j = jet diameter
C = slip factor
μ = air viscosity

The collection efficiency of each impaction stage exhibits the same functional dependence on the Stokes number, provided the geometry and flow regime of the stages are similar. Of particular interest is the value of the Stokes number at a 50% collection efficiency, St_{50}. From this number the aerodynamic cutoff diameter is calculated for a specified jet diameter, pressure, and mass flow rate.

For the impactor, St_{50} for the atmospheric pressure stages is 0.09 $\pm$ 0.01, and this value was used to design the low pressure stages. Although the low pressure stages have geometry and jet Reynolds numbers similar to the atmospheric pressure stages, the Mach numbers are significantly higher, and this may change the value of St_{50}. Thus it is necessary to calibrate the low pressure stages.

Inspection of Eq. 1 shows that for a fixed mass flow rate, smaller particle cutoff diameters may be achieved by either decreasing the jet diameter or decreasing the pressure. The reduction in the drag on a particle at the lower pressure is reflected in the increased value of the slip factor, C, which is a function of the ratio of particle diameter to the mean free path of the air molecules. The multijet low pressure impactors of McFarland et al. (9) and Buchholz (10) achieve successively smaller size cuts

by decreasing the jet diameters while maintaining a constant pressure. All of the low pressure stages of the McFarland impactor operate at 24.3 mm Hg, and those of the Buchholz impactor operate in the range of 32-39 mm Hg. By contrast, for this impactor the low pressure stages operate at pressures from 8 to 140 mm Hg. Here the successively smaller size cuts are achieved not by decreasing the jet diameter but by decreasing the pressure. This variation in the operating pressure of each stage arises from the compressibility of the flow at the higher jet velocities used here.

The particles are classifed according to their aerodynamic drag at this reduced pressure. The aerodynamic diameter of the particle is

$$d_a = \sqrt{\frac{\rho_p}{\rho_o} \frac{C_s}{C_a}}\, d_s \qquad [2]$$

where d_s is the Stokes diameter and C_s and C_a are the slip corrections to the Stokes drag for particles of diameter d_s and d_a, respectively. The slip correction is given by

$$C = 1 + \frac{2\lambda}{d_p} [1.257 + 0.04 \exp(-.55 d_p/\lambda)]$$

where λ is the mean free path. For particles much larger than the mean free path, $C = 1$ and $d_a = \sqrt{\rho}\, d_s$. In the free molecular limit, $d_a = \rho\, d_s$.

Stages 4, 5, and 6 were calibrated using monodisperse polystyrene latex spheres (Dow Chemical) (6). A ThermoSystems, Inc., Model 3071 Electrostatic Classifier was used to produce a near monodisperse aerosol of sodium fluorescein (uranine) for calibration of stages 4, 5, 6, 7, and 8 (7). The collection efficiency curves from these studies are shown in Figure 1. Stages 4, 5, and 6 have relatively sharp efficiency curves. Some particles much smaller than the cutoff diameter, d_{50}, are collected on the eighth impactor stage.

The combination of the impactor stages and the after-filter collected 97%-100% of all the particles in the size range 0.057 to 0.39 μm (7). The collection efficiency for smaller particles was lower, 82% and 75% for 0.034 μm and 0.0078 μm particles, respectively. Diffusional losses are expected to become significant

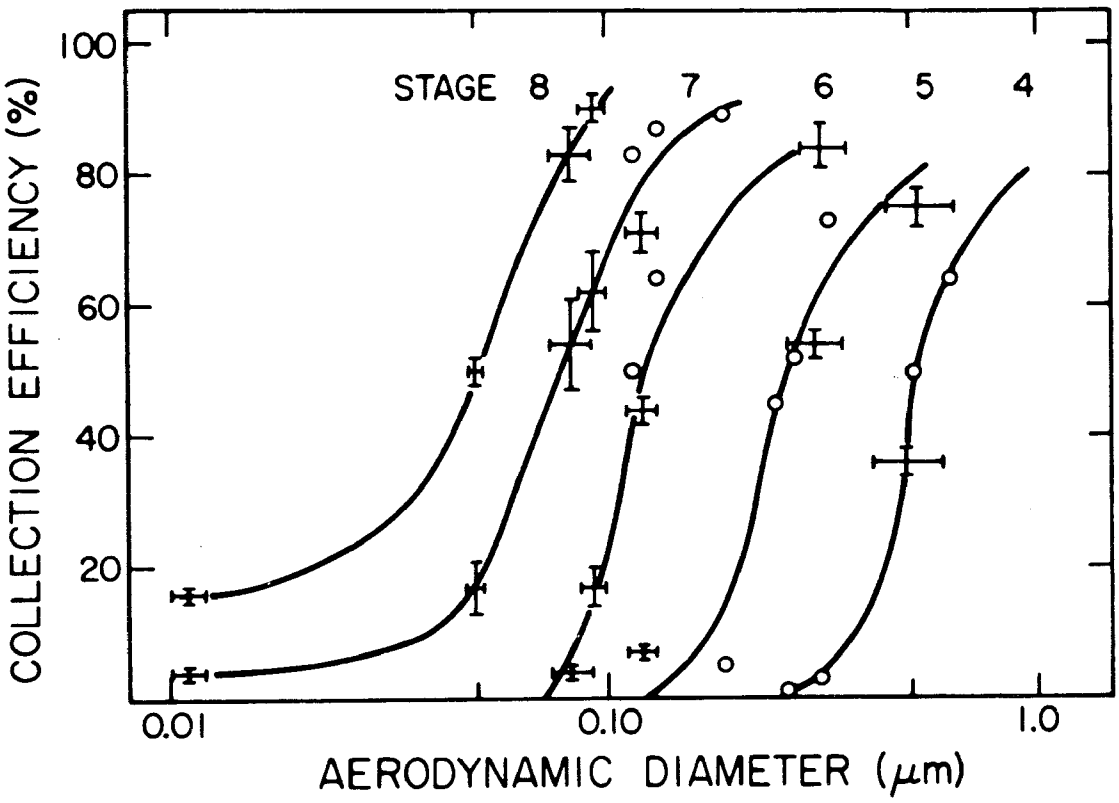

Figure 1. Low pressure impactor calibrations at ambient pressure and temperature (7).

for small particles in the low pressure stages of the impactor. The calculated wall losses in the free molecular regime are 7% for the 0.034 μm particles and 35% for the 0.0078 μm particles. Most of these losses occur between the eighth stage and the after-filter.

Particle rebound was not found to be a serious problem when coated impaction surfaces are used. The large particles which would rebound from the lower stages are collected with high efficiency on the upper stages. The problem could be more severe when the gas stream contains substantial quantities of particles much larger than the cutoff diameter of the first impactor stage. When a pulverized coal aerosol was sampled, 10 to 50 μm particles were observed on the seventh and eighth stages. It may be necessary to remove large particles from the sample upstream of the impactor in order to prevent the lower stages from being contaminated.

IMPACTOR PERFORMANCE PREDICTIONS

A stage of the low pressure impactor is sketched in Figure 2. The pressure, temperature, and velocity at point 2 determine the cutoff diameter of the stage. These conditions determined by the mass flow rate, the stagnation pressure and temperature, P_1° and T_1°, and the jet diameters d_j. The flow from 1 to 2 can be treated as a nozzle flow using the Bernoulli equation for compressible flow

$$\frac{1}{2}(V_2^2 - V_1^2) = \frac{\gamma}{\gamma - 1}\left[\frac{P_1}{\rho_1} - \frac{P_2}{\rho_2}\right] \qquad [3]$$

The density at 2 can be related to the velocity by continuing, i.e.,

$$\rho_2 = 4\dot{m}/(V_2 \pi d_j^2) \qquad [4]$$

The pressure ratio for a non-ideal nozzle is Crocco (11)

$$\frac{P_2}{P_1} = \left(1 - \frac{W^2}{\eta}\right)^{\frac{\gamma}{\gamma - 1}} \qquad [5]$$

where the reduced velocity is defined as

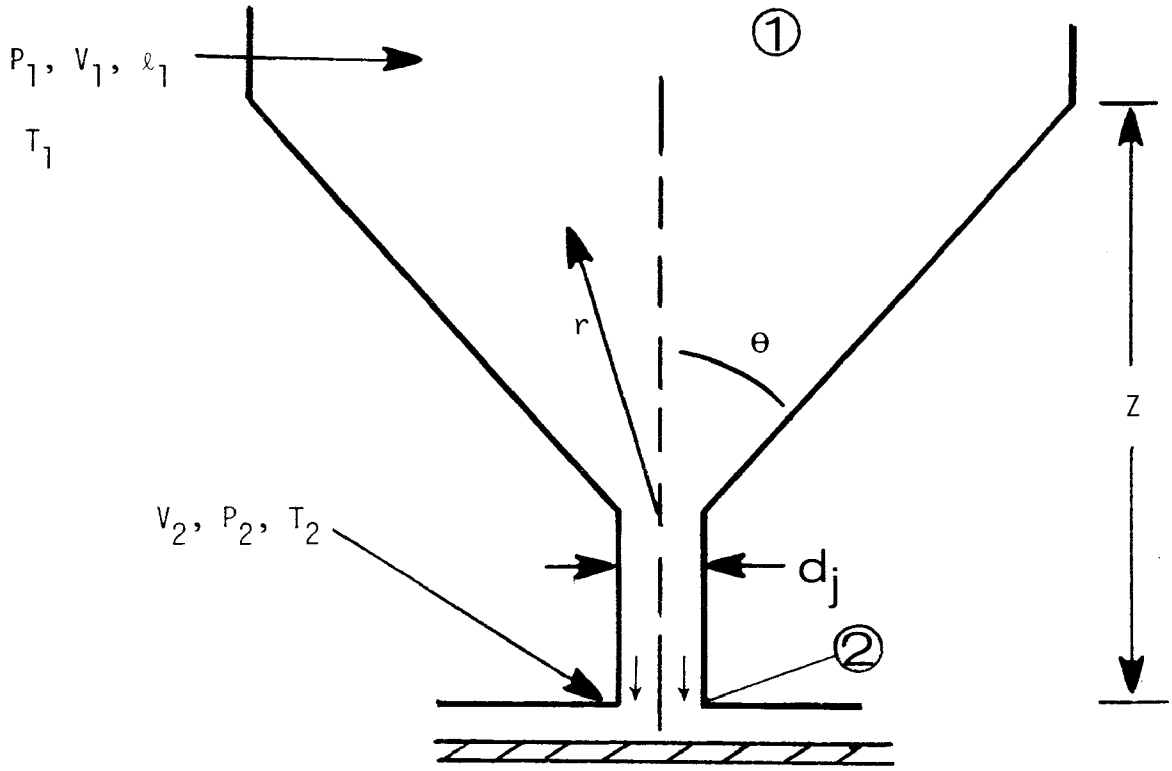

Figure 2. Impactor geometry.

$$W \equiv V_2/(2c_pT_1^\circ)^{1/2} \qquad [6]$$

and η is the nozzle efficiency. Combining Equations 3-6, we find

$$\frac{1}{2} V_2^{\,2} = \frac{\gamma}{\gamma-1} \frac{P_1}{1} \left[1 - \frac{\rho_1 V_2 \pi d_j^{\,2}}{4\,\dot{m}} \left(1 - \frac{\gamma-1}{\gamma} \frac{V_2^{\,2}}{2RT_1\eta} \right)^{\frac{\gamma}{\gamma-1}} \right] \qquad [7]$$

Equation 7 can be solved numerically to determine V_2. P_2 is then evaluated using Eq. 5. The temperature is calculated using Eq. 4 and the equation of state for an ideal gas.

The converging flow of a conical nozzle results in an efficiency of

$$\eta_c = (1 + \cos\theta)^2/4 \qquad [8]$$

Where θ is the half-angle of the converging section (11). The 45° half-angle of the Battelle impactor gives $\eta_c = 0.72$. The actual efficiency is lower. Impactor stage pressure drops comparable to those observed for the subsonic stages, stages 1-6, are predicted for a nozzle efficiency of $\eta = 0.5$, see Table 2.

The calculated cutoff diameters are also compared with the calibration data of Hering et al. (6)(7) in Table 2. The predictions are very close to the observed values, even though the Mach numbers of the jets are as high as 0.5 on stage 6. The flow through stages 7 and 8 is choked. Calculated cutoff diameters for the sonic stages do not agree with the measured values. Calibration provides the only reliable means of determining the cutoff diameters of these stages at the present time.

Several factors will alter impactor performance at elevated temperatures. The mass flow rate in the impactor, which is controlled by choked flow through the critical orifice, varies inversely with the square root of the stagnation temperature. The viscosity increases with increasing temperature, as does the mean free path. Thus, particle drag will increase in the con-

tinuum regime and decrease in the free molecular regime when the gas temperature is increased.

The predicted cutoff diameters of Hering's impactor operated at elevated temperatures are summarized in Table 3. Stages 1 and 2 are expected to collect larger particles as the temperature is increased. The performance of stage 3 (1 μm) is not expected to change significantly. The cutoff diameters for stages 4-6 should decrease at higher temperatures.

Table 2. Comparison of Impactor Calibration with Predicted Performance

Stage	D_j (cm)	P (mm Hg)	P_{calc}	V (cm/s)	d_{50} (μm)	d_{calc}
1	.249	744	745	344	4.0	4.4
2	.140	743	744	1090	2.0	1.8
3	.099	740	740	2190	1.0	1.0
4	.064	720	715	5400	.50	.49
Orifice	.036	150	-	_	-	-
5	.110	140	134	6620	.26	.23
6	.099	106	100	15600	.11	.11
7	.099	50	-	-	.075	-
8	.140	8	-	-	.05	-

T° = 295K
P° = 745 mm Hg

Table 3. Predicted Impactor Performance in Elevated Temperature Operation

Stage	D_j (cm)	T=295K d_{50} (μm)	T=400K d_{50}	T=600K d_{50}
1	.249	4.4	4.6	4.8
2	.14	1.8	1.9	2.1
3	.099	1.0	1.1	1.0
4	.064	.40	.48	.44
Orifice	.046			
5	.110	.23	.18	.13
6	.099	.11	.079	.053
7	.099	.075*	-	-
8	.140	.05*	-	-

*Measured by Hering et al. (7)

In summary, it should be possible to use the low pressure impactor for in situ size segregation of the submicron particles. The temperature will, however, affect the flow rate and cutoff diameters. It will certainly be necessary to recalibrate the instrument for elevated temperature operation. Finally, the impactor calibration data of Hering et al. (7) show that particles much larger than d_{50} are likely to bounce off the impactor stage. In order to prevent contamination of the smaller particle size fractions, it probably will be necessary to remove large particles from the sample upstream of the impactor inlet.

REFERENCES

1. McCain, J. D., J. P. Gooch, and W. B. Smith. J. Air Pollut. Contr. Assoc., 25:117, 1975.

2. Flagan, R. C., and S. K. Friedlander. Particle Formation in Pulverized Coal Combustion. In: Recent Developments in Aerosol Science, Shaw, D., ed. (in press).

3. Davison, R. L., D. F. S. Natusch, and J. R. Wallace. Environ. Sci. Techn. 8:1107, 1974.

4. Ulrich, G. D., J. W. Riehl, B. R. French, and R. Desrosiers. Mechanism of Submicron Fly-Ash Formation in a Cyclone, Coal-Fired Boiler. ASME International Symposium on Corrosion and Deposits, Henniker, New Hampshire, 1977.

5. Dolan, D. F., D. B. Kittelson, and K. T. Whitby. ASME Paper No. 75-WA/APC-5, 1975.

6. Hering, S. V., R. C. Flagan, and S. K. Friedlander. Design and Evaluation of a New Low Pressure Impactor, I, 1978.

7. Hering, S. V., S. K. Friedlander, J. J. Collins, and L. W. Richards. Design and Evaluation of a New Low Pressure Impactor, II, 1978.

8. Roberts, P. T., and S. K. Friedlander. Atmos. Environ. 10:403, 1976.

9. McFarland, A. R., H. S. Nye, and C. H. Erickson. EPA Report No. EPA-650/2-74-014, 1973.

10. Buchholz, H. Staub Reinholt der huf (English Translation) 30:15, 1970.

11. Crocco, L. Fundamentals of Gas Dynamics. H. W. Emmons, ed. Princeton University Press, 1958.

Use of a High-Flow Stack Sampler for Determination of Particulate Sulfate Emissions

A. Jack O'Neal, Jr.
Harold Cowherd
Long Island Lighting Company

ABSTRACT

The Long Island Lighting Company developed a high-flow stack gas sampler suitable for use by power station technicians. It allows for the collection of large quantities of particulate material (300 mg-500 mg) for physical and chemical analysis in 10-15 minutes of sampling time. The device is particularly well suited for evaluating the relative effects of changes in furnace conditions, and it also appears to have acceptable accuracy on an absolute basis. Sulfate concentrations are determined from the filter extract gravimetrically by barium precipitation.

The sampler was qualified by evaluating both the filter characteristics (standard high-volume ambient sampler filters can be used) and non-isokinetic sampling. Even though large gas flows at high SO_2 concentrations (~1500 ppm) are passed through the filter, artifact sulfate formation appears to be minimal. Filter retention was evaluated by analyzing the content of a liquid impinger that received a portion of the gas stream on the downstream side of the filter.

Primary sulfate emissions were evaluated for both high (2.8%) and low (0.3%) sulfur residual oil-fired boilers, and were found to be about 0.5% of the total sulfur emissions. This figure compares well with Brookhaven National Laboratory data obtained under similar conditions, but using the controlled condensation method.

242

INTRODUCTION

Conventional stack gas sampling, at best, is tedious, expensive, and time-consuming and was initially designed to examine efficiencies of dust collectors. Today, one needs to know not only dust collector efficiency but also the very nature of combustion products which escape collection and become stack emissions.

Over the past 15 years a growing body of evidence tells us that the nature of combustion products is largely dominated by conditions of the fire, some 4-6 seconds before sampling at stack entry. Believing this, LILCO decided to find the cause-effect relationships between furnace conditions and the nature of stack gases. However, the use of conventional equipment would virtually prohibit such a study unless one had unlimited time, money, and manpower, so it was necessary to design a stack gas sampler which would meet the following criteria:

1. A large enough mass (300-600 mg) of particulates must be collected to allow thorough and accurate physical and chemical analyses;

2. Five to fifteen minutes of actual sampling should produce 300-600 mg of material;

3. Results should be quite reproducible;

4. It should be a one-man operation; and

5. The sampling procedure should be easily learned by the average technician.

SAMPLING EQUIPMENT

Figure 1 presents a schematic of the prototype high-flow stack gas sampler that was designed and fabricated to conform to the constraints of this project. The unit was constructed essentially of 2" and 3" 316 stainless steel schedule 5 pipe, except for the filter holder which was constructed of two modified Hi-Vol stainless steel diffuser sections and was designed to accept the standard 8 x 10" Hi-Vol glass fiber filter. A 38" long and a 100" long sampler probe were designed for use with the instrument. Both probes were of 2" nominal diameter. The probe assembly was designed to pass through a 4" schedule 40 gas duct sample port.

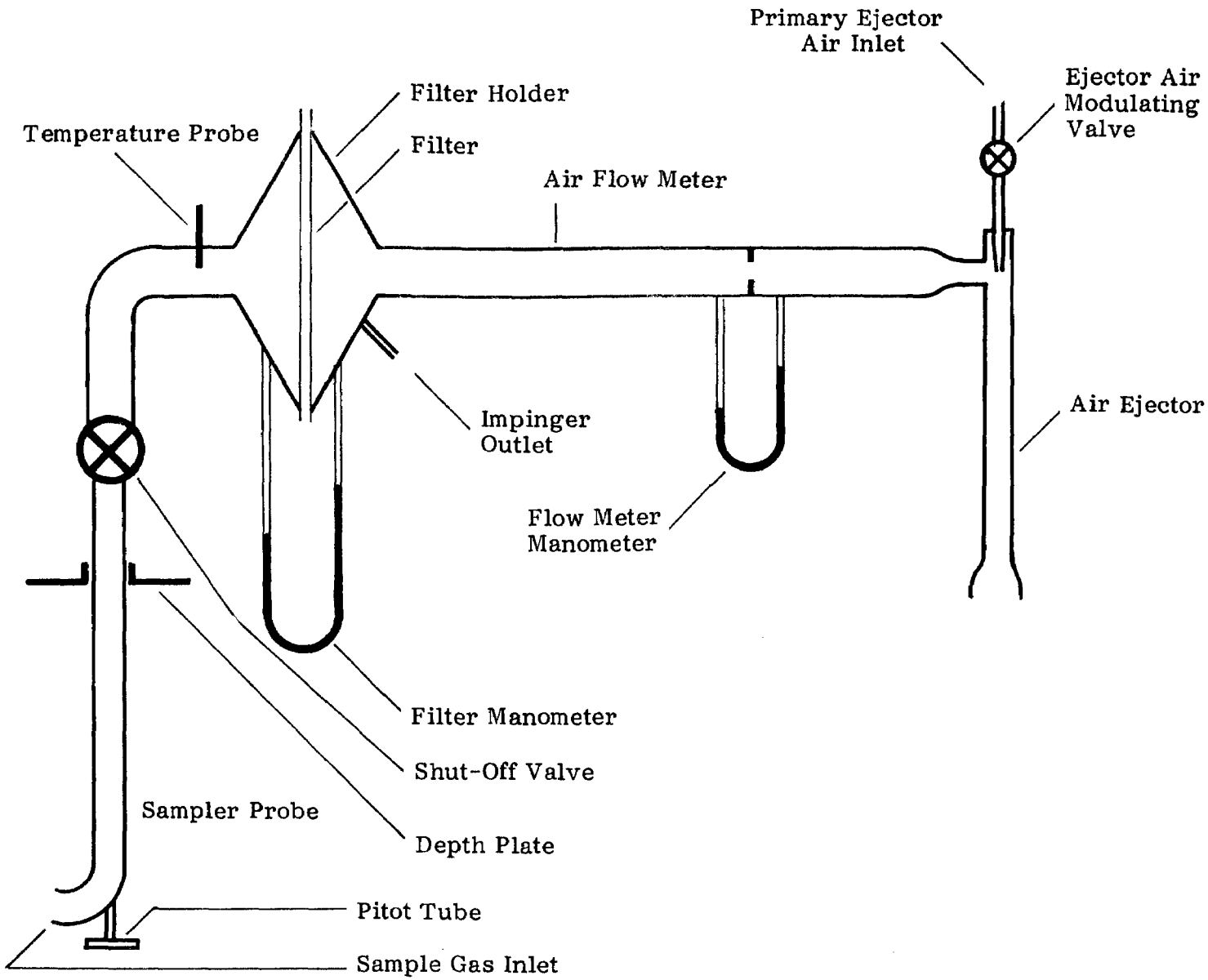

Figure 1. Schematic: Hi-flo stack gas sampler.

In operation, the sample probe was inserted into the gas stream through the gas duct sample port. The depth of insertion was controlled by setting the adjustable depth plate. After opening the shut-off valve, the sample gas was induced to flow into the sample probe, through the shut-off valve, across the particulate filter, and through the measuring orifice plate, by the pressure drop potential created by the compressed air operated ejector. The pressure drop across the particulate filter, the orifice plate, and the gas duct was measured by manometers and the temperature of the gas in the duct and the sample gas entering the filter was measured using standard thermocouples. A pitot tube was mounted at the bottom of the sample probe and was used to measure gas duct velocity head and to determine when the probe inlet was facing directly into the gas stream.

Interchangeable air flow meter orifice plates of 1.00, 1.25 and 1.50" diameter and ejector primary air nozzles of .25, .375 and .50" diameter were fabricated to provide flexibility to the design.

CALIBRATION

The airflow meter was flow calibrated for all three orifice plates while installed in the sampler in the normal operating configuration. The exit of the sampler ejector was connected to the inlet of a Rootsmaster, Model ALP 125 gas meter calibrator. Gas sampler orifice plate pressure drops were recorded for values of calibrator volume flow rate. After the calibration of the assembly was completed, the air flow meter section was removed from the assembly, and its exit was connected to the calibrator. This configuration was calibrated using the 1.25" orifice plate only. Except for the very lowest air flow, the calibration results were identical to those previously obtained for this orifice plate.

PRELIMINARY RESULTS

Preliminary testing of the prototype gas sampler (under various furnace conditions) has been completed. The tests have established the following:

1. The concept of high volume flow sampling is a feasible concept.

2. The repeatability of sample collection is well within the acceptability range. Standard deviation for multiple samples is equal to 10% of actual values.

3. A sample of sufficient amount can be collected within less than fifteen minutes, depending upon unit loading and fuel sulfur content.

4. Isokinetic sampling is not as critical, at least for this instrument, as was initially thought. (See Figure 2.)

5. The filters maintian their integrity after exposure to the 300°F stack gas and can be used for further analysis after weighing to determine the collected sample weight.

6. Filter retention can be examined by pulling filtered gas through a glass orifice immersed in a column of demineralized water. (See schematic in Figure 1 for sample source, marked Impinger Outlet.) The water was analyzed for flue gas particulate constituents, and only barely discernible traces were found. Thus, we believe the glass fiber filter pad has excellent retention with a labeled porosity of 0.3 microns.

During preliminary testing, condensation of the stack gas in the sampler did not appear; however, it did appear during later stack sampling when experimental incineration of boiler cleaning solvent was being conducted. Condensation appeared in both the sample collection section and the pitot tube section of the probe. This problem is common with stack gas sampling equipment; however, for this instrument, it is not as prevalent in the summer as in the other seasons. We are in the process of devising a means of alleviating this problem at the present time.

SOME RESULTS OF ACTUAL TESTING

Data have been obtained on two LILCO units to date, both oil-fired, the same design, and the same size at 185 MW, normal load. Barrett No. 2 burned a 0.3% sulfur oil containing about 0.01% to 0.02% ash; magnesium oxide additive is fed equal to oil ash on a pound-per-pound basis. Thus, each 341 lb. barrel of oil contained about 0.07 lbs. of oil ash plus 0.07 lbs. of MgO. The furnace normally operates between 0.8% and 1.1% excess oxygen at 185 MW. There is an operating cyclone ash collector where all collections

TEST DATE: 8/31/76

LOCATION: GLENWOOD POWER STATION, UNIT 50
SOUTH AIR HEATER EXIT DUCT (GAS SIDE)

UNIT POWER OUTPUT: 46.5 MW

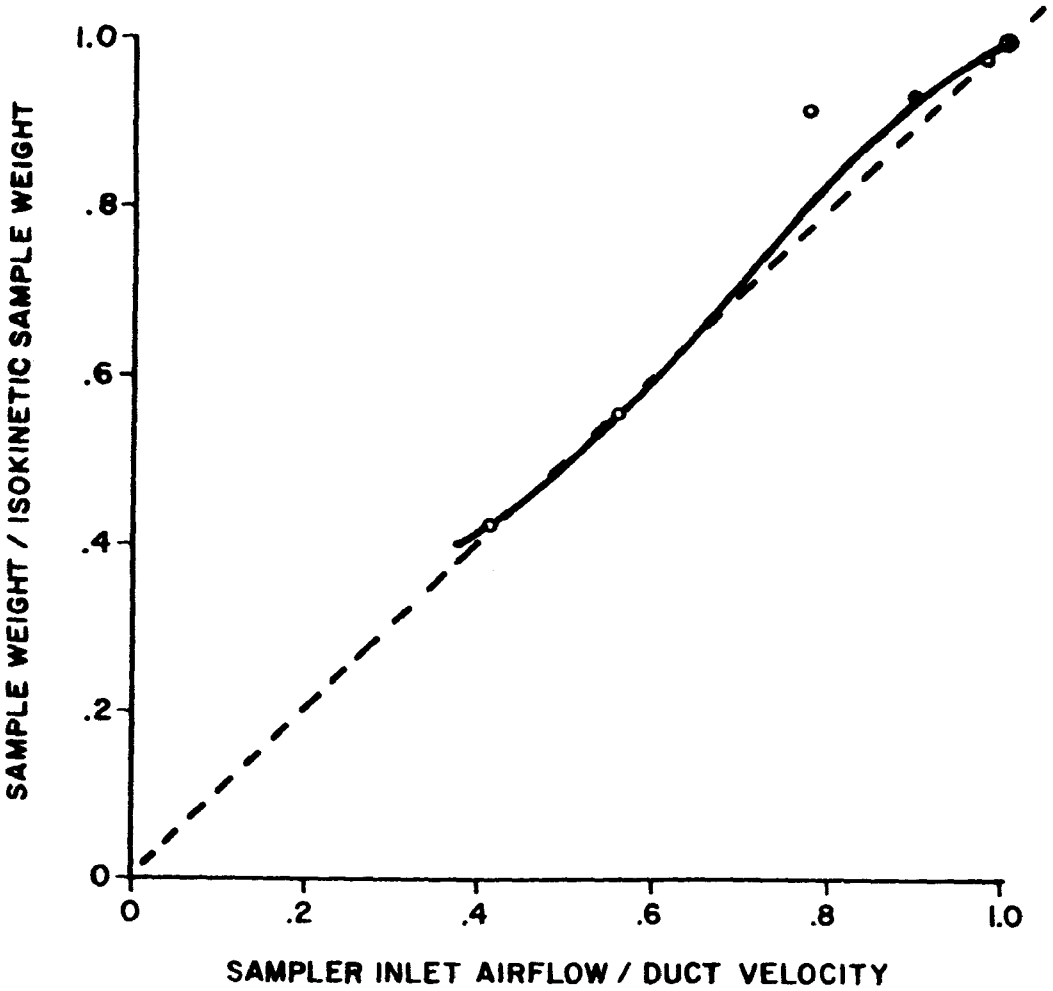

Figure 2. Hi-flo stack gas sampler effect of non-isokinetic sampling.

are re-injected back into the furnace. Table 1 shows the data from four tests on October 23 and four tests on October 24, 1976.

There was a time lapse between the Barrett tests and the ones on Port Jefferson No. 4 unit in August through November of 1977. The instrument was used in that interim to justify incineration of boiler organic cleaning solvents as an environmentally acceptable disposal technique (1).

Between August 18 and November 15, 1977, 36 tests were performed on Port Jefferson No. 4 unit. Some were performed when the boiler was clean, others when it was dirty; some tests utilized steady-state furnace conditions, others when furnace conditions were being altered. Teflon-backed filters and glass fiber filters were compared. During all tests the oil was essentially constant in quality with sulfur averaging 2.34%, vanadium pentoxide 0.055%, and ash (including MgO additive) 0.14%, by weight of the oil.

The sample site was at the outlet of the west induced draft fan where duct velocity ranged between 19 and 41 m/sec, depending on MW output and furnace conditions. The ratio of probe velocity/duct velocity ranged widely, but most tests were performed between 0.7 and 1.1. The sample site was downstream of an always-operating electrostatic precipitator which had a calculated collection efficiency between 58% and 71%, depending on gas velocities and dust burden in the ESP inlet gases. All ESP collections were re-injected back into the radiant furnace, but not continuously. Some gas samples were taken during re-injection, but most were not.

Filters were tared quickly after 24 hours in a desiccated container. After sampling, the filters were treated exactly as in the pre-tare procedure, the increase in weight representing the particulates collected during sampling. A sizable area was cut from the filter, precisely measured in area, digested in mild HCl and filtered. The filtrate was made ammoniacal to precipitate the R_2O_3 group and filtered. The filtrate was adjusted to the M.O. endpoint, treated with bromine and boiled. Ten percent barium chloride was added dropwise to precipitate all sulfates as barium sulfate which was filtered, ignited, and weighed.

Some of the more significant observations were as follows:

1. At constant 185 MW load and constant excess furnace air, burner tilt depression from +15° to +5° caused a reduction of 10% in particulate emissions. The concentration declined from 53.03 to 47.87 mg/m^3, and the mass declined from 32.02 to 28.90 kg/hr.

Table 1. Total Suspended Particulates and Sulfates on 0.3% S Oil

Filter #	TSP mg	Total SO_4 mg	Sample Volume *m^3	TSP mg/m^3	SO_4 mg/m^3
468	521.3	161.2	22.55	23.11	7.15
469	392.0	117.7	15.99	24.52	7.36
471	567.5	163.4	32.32	24.34	7.01
472	575.1	175.1	28.62	20.09	6.12
				Average	6.91
473	811.6	190.2	21.62	37.54	8.80
474	769.6	190.9	22.21	34.65	8.60
475	645.5	164.4	22.58	28.59	7.28
476	732.7	185.2	18.64	39.31	9.94
				Average	8.66

*At 20°C and 76.0 cm Hg

2. One of the causes of high particulate emissions was a rapid increase in MW load during testing.

3. Degree of boiler dirtiness seemed to have an important effect on both particulates and sulfates. See Figure 3 for the effect on concentration of these materials in mg/m^3. See Figure 4 for the effect on mass emitted per unit time in terms of kg/hr.

4. Approximately 12% of suspended solids were deposited in the probe before the filter with no apparent selectivity as to chemical components. After five consecutive samplings with a freshly-cleaned probe, the probe was washed and found to contain 12% of the mass accumulated on the five filter pads. The data in this paper have <u>not</u> been adjusted for this factor.

5. Approximately 145,000 kg of total ash input were needed to put the P.J. #4, 185 MW boiler into a dirty condition which would require washing.

6. Only about 0.1% of the input carbon showed in stack gases. Only 10% of input metals showed in stack gases (Table 2).

7. We can, therefore, make a general observation on total sulfate particulates. If we assume all the sulfur is converted completely to SO_4 (sulfate) in 2.4% sulfur oil, we find only about 0.3% of this in the stack gases. We find twice this, or 0.6% conversion on 0.3% sulfur oil, making the same assumption as on the 2.4% sulfur oil. See BNL data on LILCO units in these proceedings for agreement even though the methods are different.

8. So far, there is no significant difference in artifact sulfate between Teflon-backed and glass fiber filters. We will examine these materials further, but we prefer the glass fiber filter at the moment because of its low carbon content. The carbon content of particulates is important to LILCO, and the very high carbon blank in Teflon-backed filters tends to make our carbon findings suspect. GMW 810 Glass Fiber Filters, General Metal Works, Inc., Cleves, Ohio, is identification of the LILCO glass fiber filters. Pallflex, Model TX40HI-20 identifies the Teflon-backed filters used.

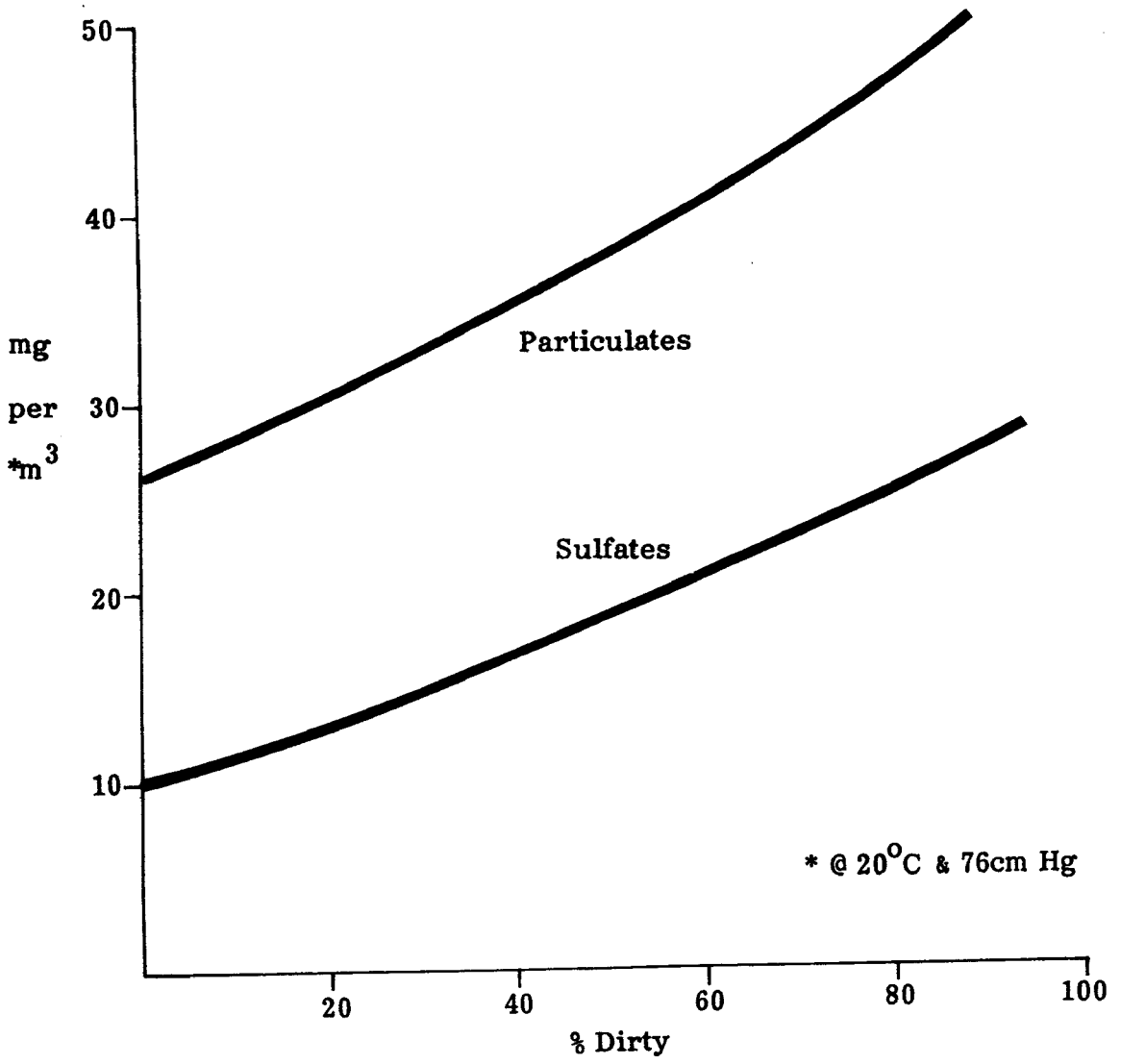

Figure 3. ESP outlet particulates vs. boiler dirtiness: mg/m @ 185 MW, #6 oil containing 2.4% S & 0.14% ash.

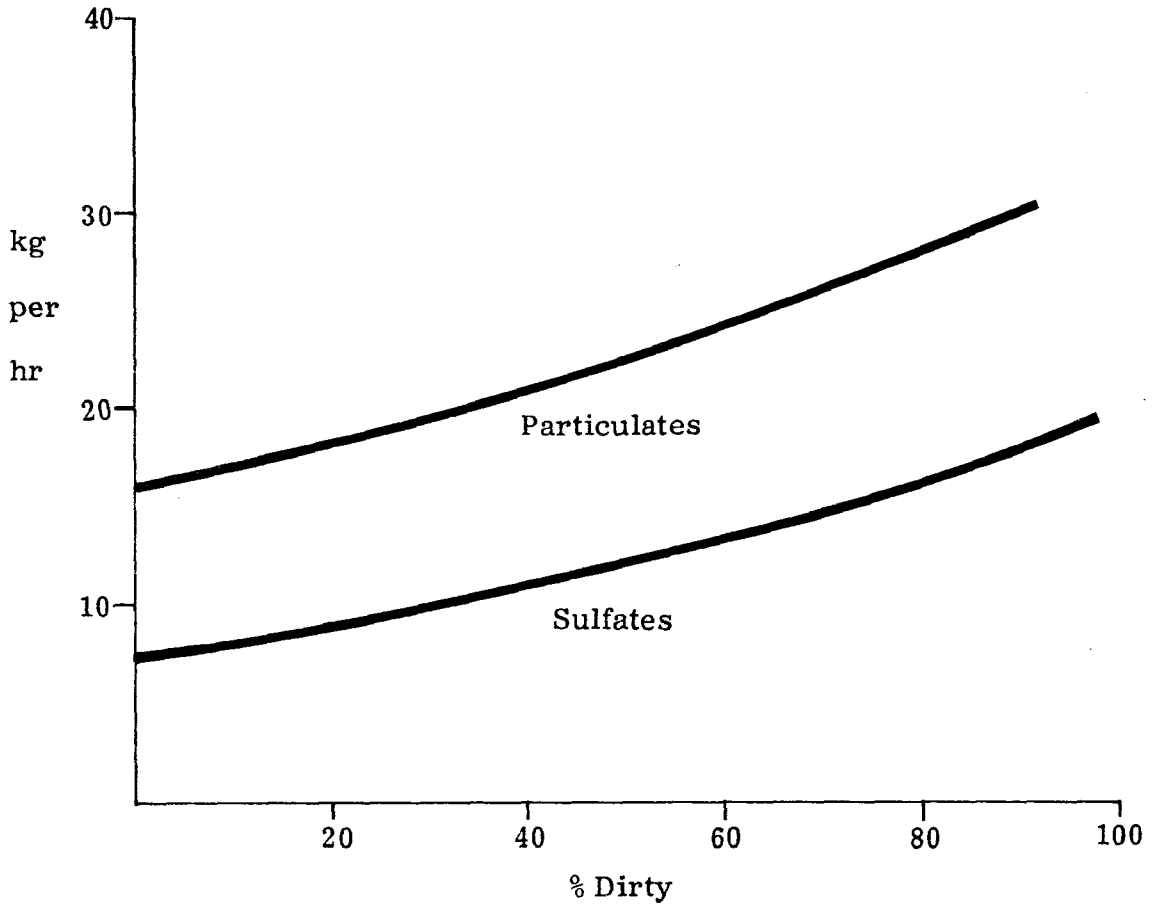

Figure 4. ESP outlet particulates vs. boiler dirtiness: kg/hr. @ 185 MW, #6 oil containing 2.4% S & 0.14% ash.

9. It appears there is less-than-linear reduction in sulfate particulate when fuel oil sulfur is reduced substantially, say from 2.4% to 0.3%. Table 3 shows the effect on two LILCO units of the same size, one on 2.4% sulfur and 0.14% ash, the other on 0.3% sulfur and 0.04% ash. High sulfur was burned at furnace excess O_2 of about 0.7%, low sulfur at about 1.0% excess O_2. The high sulfur unit had an ESP, the low sulfur unit a cyclone collector. Both units operated at 185 MW gross.

Table 2. Percentage of Input Metals Retained in System

F	74% to 97%
Cu	81% to 90%
Ni	89% to 93%
V	84% to 96%
Mg	98% to 99%
Na	77% to 94%

Table 3. Sulfate Emissions in mg/m^3

Boiler Conditions	2.4% S Oil	0.3% S Oil
Clean	10.0	-
50% dirty	18.0	7.8
100% dirty	28	-

REFERENCE

1. O'Neal, A. J., Jr., H. Cowherd, and D. J. Hassebroek. Experimental Incineration of Boiler Internal Cleaning Solvent at Long Island Lighting Company. Combustion, August 1977.

Inorganic Compound Identification by Fourier Transform Infrared Spectroscopy

Robert J. Jakobsen
R. M. Gendreau
William M. Henry
Battelle-Columbus Laboratories

Kenneth T. Knapp
U.S. Environmental Protection Agency

ABSTRACT

EPA-sponsored work at Battelle has led to a method which permits the identification of inorganic compounds, even in complex mixtures. Development of this needed capability has enabled us to identify specific sulfates and oxides in both coal and oil fly ash emission samples. This technique is based on both the sensitivity and the data handling capabilities of Fourier Transform infrared systems along with the proper preparation, handling, and conditioning of samplies and reference standards. The technique could aid in the development of compliance regulations by providing the ability to identify and measure specific compound emissions.

INTRODUCTION

Vast tonnages of particulates are emitted annually from sources using or processing fossil fuels. These fossil fuels are nearly totally inorganic species, and surprisingly little is known as to their specific chemical nature. Intelligent health effects testing and data interpretations depend on such knowledge, as do studies of control process effects. Past chemical analyses of fossil fuel emissions mainly have consisted of elemental determinations of metals and anions with some compound identification provided by use of the limited capabilities of x-ray diffraction.

While conventional dispersive infrared spectroscopy has been widely used for the identification of organic compounds, its use for inorganic identifications was mostly limited to the detection

of certain anions. This limited use was especially true for highly complex inorganic mixtures such as coal and oil fly ash emission samples. Infrared spectroscopy, as well as most analytical tools, was rarely used for inorganic compound speciation and never when the speciation involved different cations with the same anion (i.e., identification of individual compounds in a mix of inorganic sulfates).

However, the advent of commercial Fourier Transform infrared systems (FT-IR) provided analytical spectroscopy with both extra sensitivity and extra data-handling capabilities. We, therefore, began a program to investigate the use of FT-IR for inorganic compound identification. This paper reports the first results of this investigation which can be briefly summarized as follows:

(1) A method has been developed which permits the identification of inorganic compounds even in complex mixtures.

(2) Using this method, we have been able to identify specific sulfates in both coal and oil fly ash emission samples.

This technique is based on the use of FT-IR, the proper preparation and handling of both samples and reference standards, and the assistance of elemental chemical analyses.

An explanation of the differences between FT-IR and conventional dispersive infrared spectroscopy is not germane to the purposes of this paper. However, it is necessary to emphasize that the interferometer of the FT-IR systems provides great sensitivity, and the dedicated computers of FT-IR systems permit both storage of spectra and the capability to subtract spectra. Thus, as will be discussed later, reference standards can be prepared in a variety of ways, and the spectrum of each preparation can not only be run, but it can be stored for future uses (for comparison with sample spectra or in subtraction routines). Likewise, samples can be prepared in several ways with each sample spectrum being saved. Equally important to a storage capability is the capability to subtract spectra. Subtraction of spectra both enhances the ability to detect small differences and can be used to remove unwanted absorption bands. Such infrared absorption bands often mask bands of other components and, when removed, permit additional identifications.

Instrumental sensitivity is also important to inorganic compound speciation. This is especially true for opaque samples such as the coal fly ash emissions in which there are sizeable amounts of elemental carbon. In addition, sensitivity is also needed for the observation of small differences by subtraction of spectra.

REFERENCE STANDARDS AND SAMPLES

As stated previously, a most important aspect of our method development has been the preparation and/or handling of both samples and reference standards. Such reference standards are a necessary part of any method based on infrared identifications; because the spectra of the reference standards or known compounds are used to identify components of the sample either by direct comparison of spectra or through the subtraction routines. Thus it is important that the reference standards be in the same physical and chemical condition as the sample. Figure 1 demonstrates how easily a standard or sample can change and shows how difficult it can be to have both the standard and the sample in the same state or condition. This figure shows spectra of $MgSO_4 \cdot 7H_2O$ (run as KBr pellets) when the standard came from a freshly opened bottle (Figure 1A) and after the sample stood overnight in air (Figure 1B). The spectral differences probably reflect changes in hydration state, but they could also represent changes in crystalline structure. Of most importance, however, is the fact that these changes drastically alter the spectrum. If a sample containing $MgSO_4$ was in a condition such that it gave one of the spectra of Figure 1 and the reference standard gave the other spectrum, identification of $MgSO_4$ in the sample would be difficult, if not impossible. Thus, it is essential to have in storage or file spectra of reference standards in as many states or conditions as possible. The alternative to this is to find a way of preparing both standards and samples in a reproducible manner.

In order to evaluate whether such reproducibility could be achieved and what conditions would bring this about, we prepared a physical mixture of 13% $NiSO_4 \cdot 6H_2O$, 41% $MgSO_4 \cdot 7H_2O$, and 46% $VOSO_4$. Infrared spectra of each of these compounds are shown in Figure 2A, B, and C, respectively. These reference spectra were run early in the program and stored in the memory of the FT-IR system. Later when the physical mixture of these compounds was prepared, the reference spectra were recalled from memory, and the computer was used to generate a spectrum of the mixture. This computer-generated spectrum is shown in Figure 3C. The spectrum of the actual physical mixture can be seen in Figure 3B. A comparison of the spectra of Figures 3B and 3C shows that the computer-generated mixture spectrum and the spectrum of the actual physical mixture are similar but not identical. This again illustrates the difficulty in having even reference standards in the same or reproducible state. As it turned out, the compounds used to obtain the reference spectra for the computer-generated spectrum and the compounds used for the physical mixture came from different bottles or different manufacturers. Thus, even though

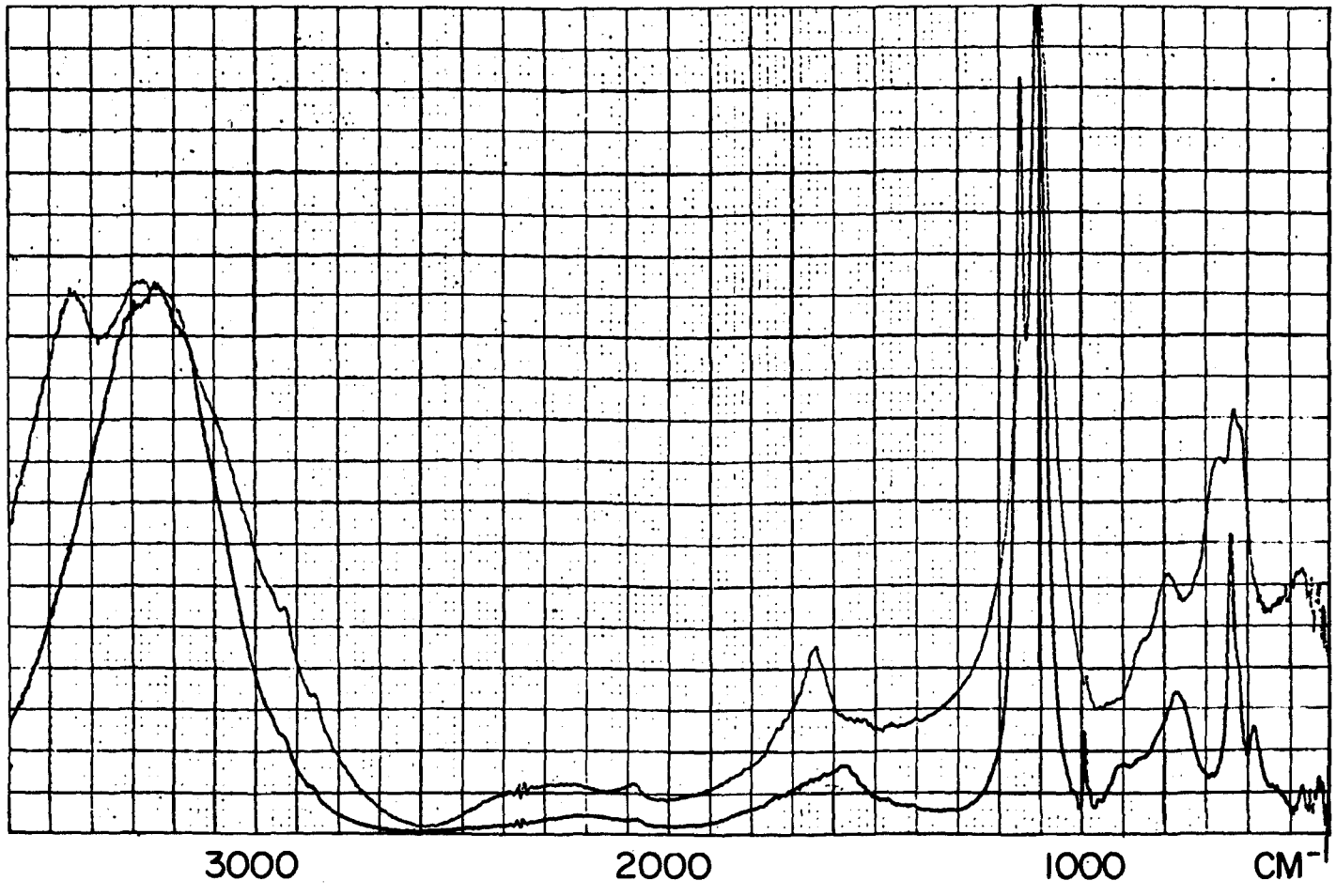

Figure 1. Infrared spectra of $NiSO_4 \cdot 6H_2O$ for freshly prepared sample and one day old sample.

Figure 2. Infrared spectra of (A) $NiSO_4 \cdot 6H_2O$; (B) $MgSO_4 \cdot 7H_2O$; (C) $VOSO_4$.

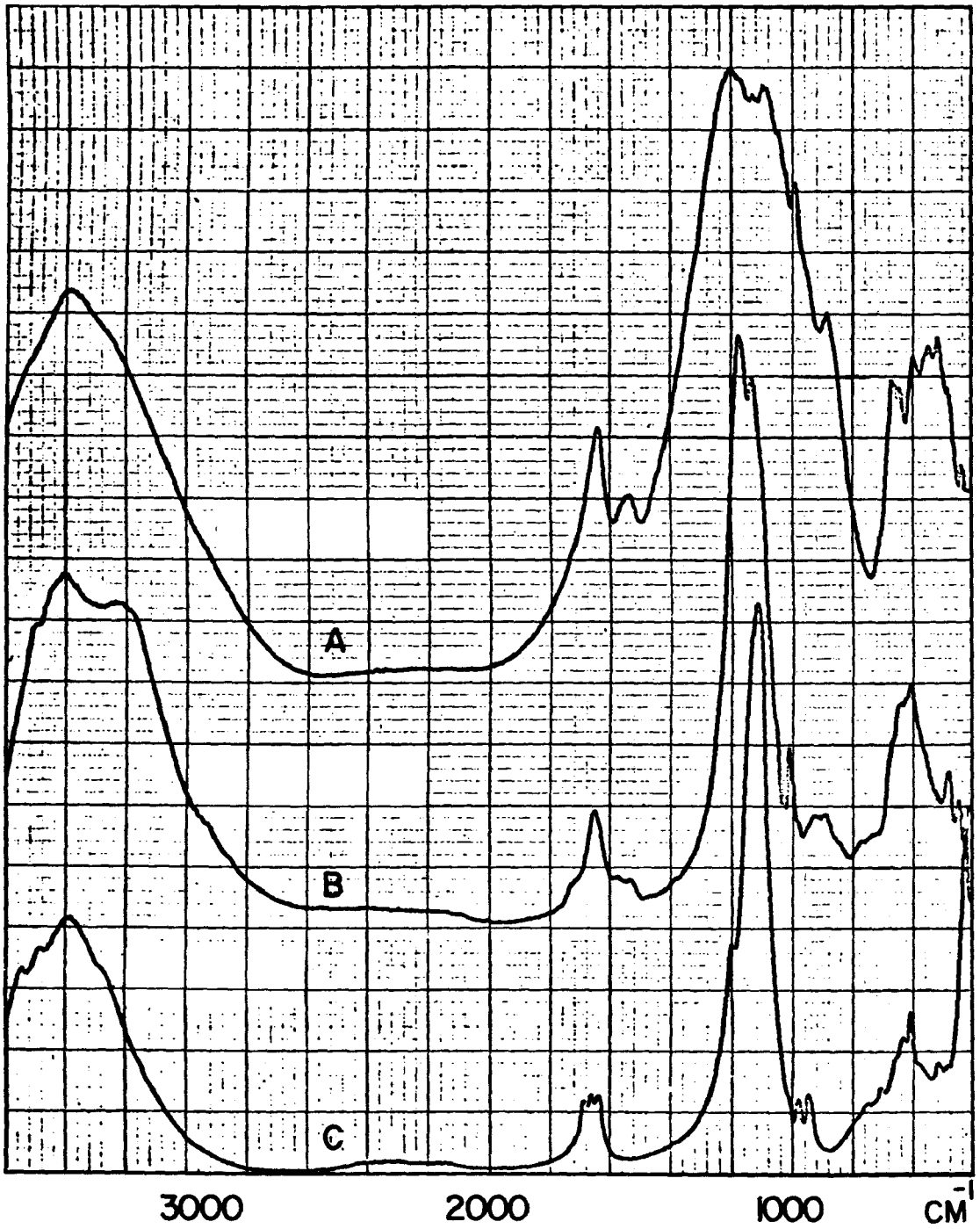

Figure 3. Infrared spectra of a mixture of $NiSO_4 \cdot 6H_2O$ (13%), $MgSO_4 \cdot 7H_2O$ (41%), and $VOSO_4$ (46%) (A) after dissolving H_2O and drying; (B) actual physical mixture; (C) computer generated spectrum of mixture (from components in Figure 2).

the spectra should have been identical, some of the sulfates were in different physical or hydration states. However, it should also be observed in Figures 3B and 3C that the computer can be used to determine if the reference standards are in the same physical state. This variation in physical state has been the main problem in past work attempting to use infrared spectroscopy for inorganic compound identification and the ability to detect such variations in the first step in successful inorganic speciation.

The physical mixture, described above, was dissolved in water, the water was evaporated, and the residue was dried. A spectrum of this dried residue is shown in Figure 3A. Note that there are significant changes in the spectrum of the physical mixture as a result of being dissolved in water (compare Figure 3A and 3B). Not only are there new infrared bands, but the strong S-O vibration (1050-1200 cm^{-1}) has broadened considerably. Thus, the physical state and the infrared spectra of inorganic compounds can be considerably altered as would be expected as a result of being dissolved in water. This is not always the case; we have found that some inorganic compounds remain unchanged after being dissolved in water. In either case it is important to know if being dissolved in water affects the compound for reasons to be described in subsequent discussion. Therefore, it is necessary to get spectra of the reference standards before and after being dissolved in water. The same is true for fly ash samples, but here we can use the computer to determine if dissolving in water has altered the physical or chemical state of the samples.

Figure 4 shows spectra of the same physical mixture after being dissolved in water and after baking in argon at various temperatures for eight hours. There are some minor differences in band intensity between the unbaked sample (Figure 3A) and the baked samples, but there are virtually no differences between the samples baked at 80°, 120°, and 350°C. The major spectral difference between the baked and unbaked samples appears to be a sharpening of the infrared bands in the baked samples.

Thus, we establish a procedure for handling samples as follows:

(1) Obtain infrared spectra of the fly ash samples before and after heating in argon at 350°C for eight hours.

(2) Do a water extraction of the sample, separate the water soluble and the water insolubles, and dry each fraction.

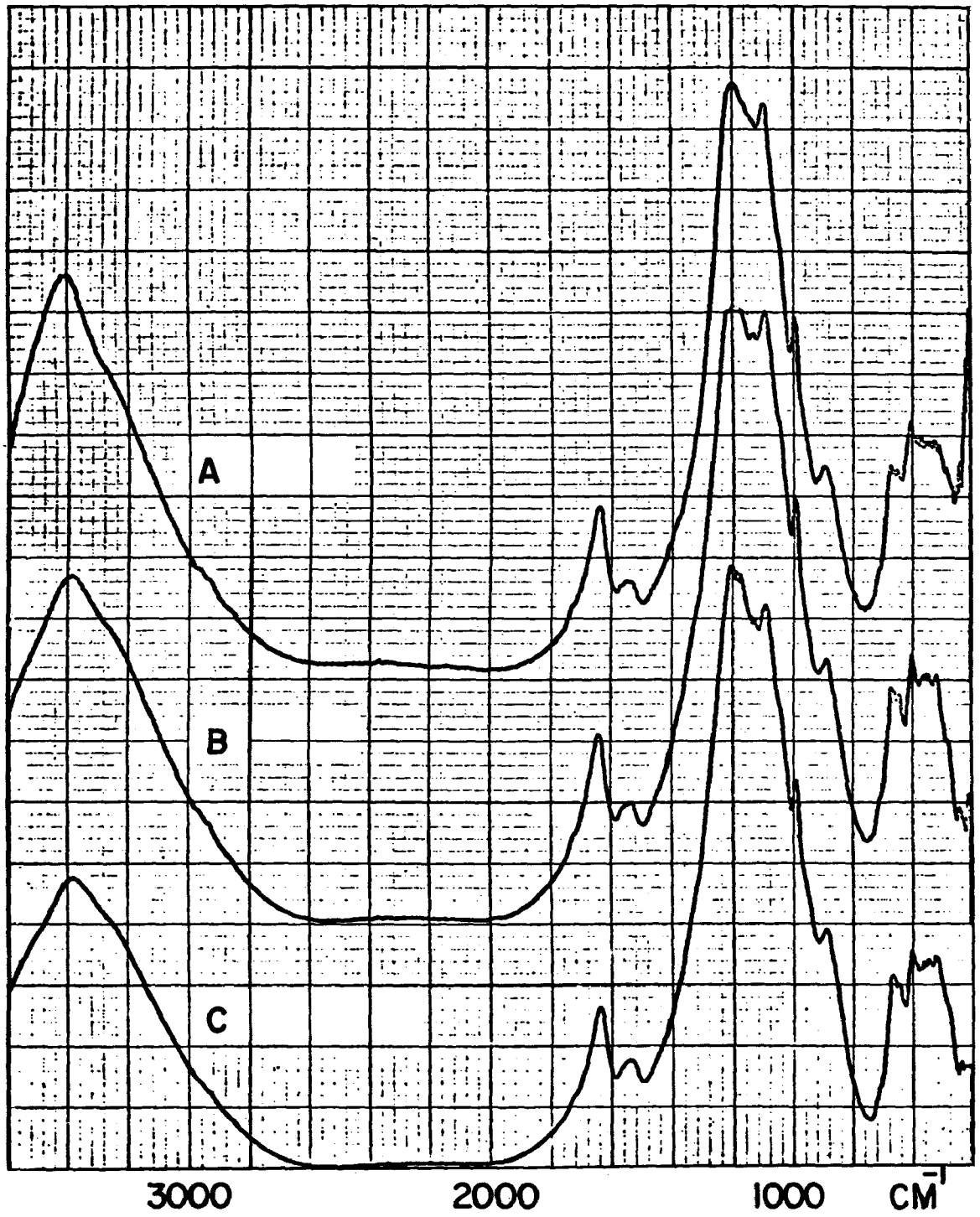

Figure 4. Infrared spectra of a mixture of $NiSO_4 \cdot 6H_2O$, $MgSO_4 \cdot 7H_2O$ and $VOSO_4$ after heating for 8 hours in argon at (A) 350°C; (B) 120°C; (C) 80°C.

(3) Obtain infrared spectra of the water solubles and the water insolubles before and after heating in argon at 350°C for eight hours.

Essentially the same procedure is followed for the reference standards, with the obvious exception that for a pure compound there is only a water soluble or water insoluble fraction. It is necessary to follow this procedure for the reference standards and permanently store the spectra of each reference standard under all the conditions of the procedure. However, we have not been able to save all these spectra due to the limited storage capacity of our current computer. This inability to save all the needed reference spectra has been the major limitation to our work to date, but this will be alleviated this summer when we acquire a new FT-IR system with unlimited storage capacity.

The above-listed procedure was selected for the samples because separating the water solubles (most sulfates) and the water insolubles (oxides and silicates) aids in the interpretation of the infrared spectra. This separation aids the spectral interpretation by removing interfering absorption bands. Each sample and each sample fraction are run both heated and unheated in order to follow changes due to the heating and because the heating (or baking) tends to put samples and reference standards in a reproducible physical or hydration state.

Some of these techniques are shown in Figures 5 and 6. These figures show spectra of a Picway coal fly ash and of the fractions obtained from our fractionation procedure. Figure 5 shows the fractions before heating or baking while Figure 6 shows the fractions after baking in argon at 350°C. Note that the spectrum (Figure 6C) of the water soluble baked fraction is considerably different from the other spectra in Figure 6. This brings up the question of whether dissolving the sample in water altered the physical state of the fraction. In Figure 7A, the spectrum of the water soluble fraction shown in Figure 6C is repeated, while Figure 7B shows the subtraction of the total sample (Figure 6A) and the water insoluble fraction (Figure 6B). This subtracted spectrum represents a computer-generated spectrum of the water soluble fraction. Comparison of Figures 7A and 7B show that they are virtually identical, establishing that the water soluble components were not altered by being dissolved in water. Thus, the computer can be used to determine when there are changes in the physical state of the samples due to the extraction procedures.

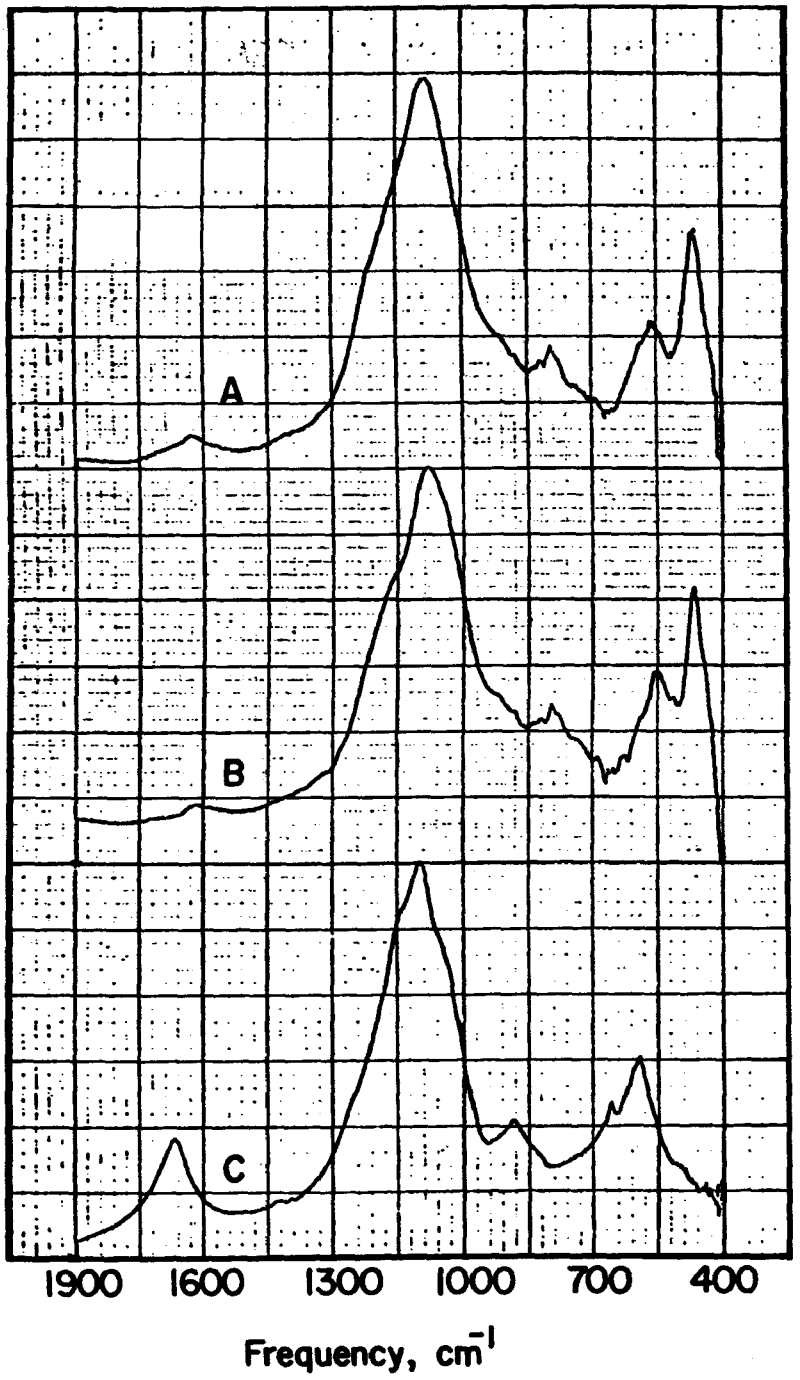

Figure 5. Infrared spectra of Picway coal fly ash (no heating) of (A) total sample; (B) water insoluble fraction; (C) water soluble fraction.

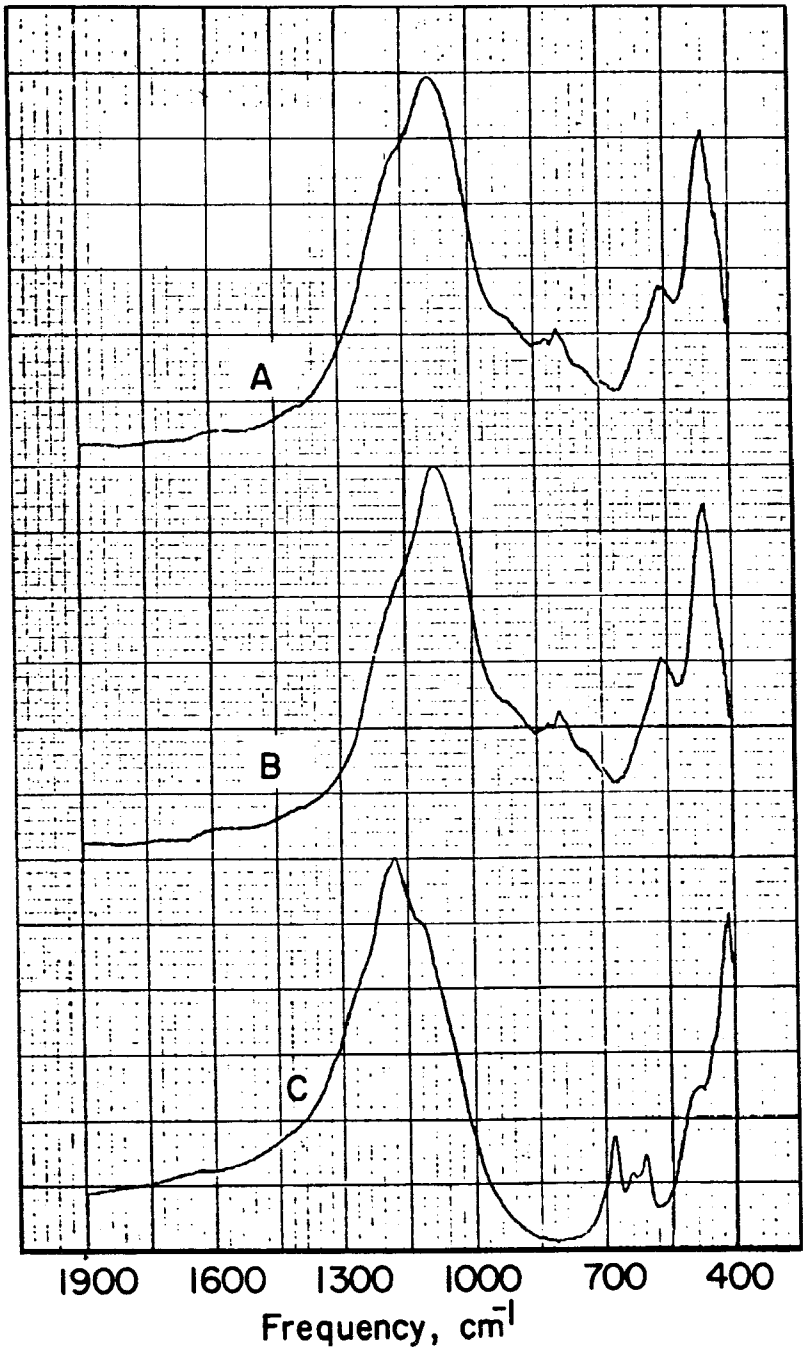

Figure 6. Infrared spectra of Picway coal fly ash (heated at 350°C for eight hours) of (A) total sample; (B) water insoluble fraction; (C) water soluble fraction.

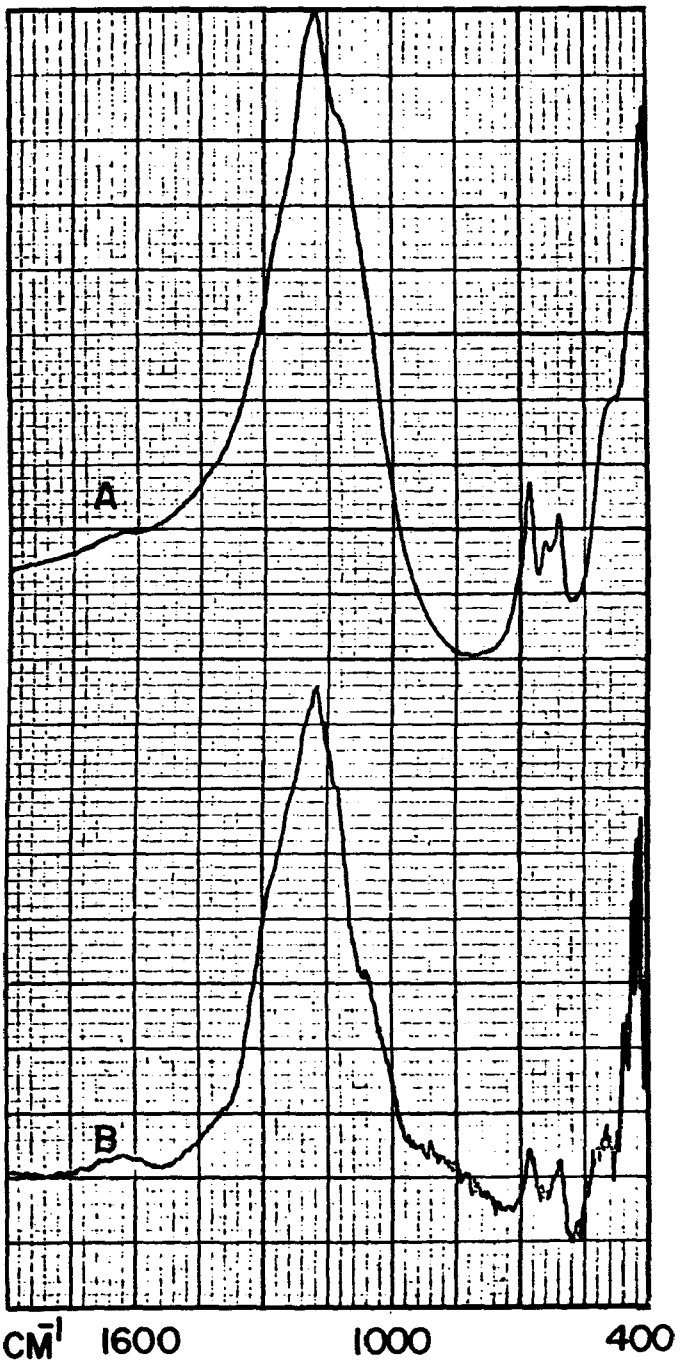

Figure 7. Infrared spectra of Picway coal fly ash (heated at 350°C for eight hours) of (A) water soluble fraction; (B) subtraction of total sample minus water insoluble fraction (i.e., computer generated spectrum of water soluble fraction).

OIL FLY ASH RESULTS

Using the fractionation procedure described above, six oil-fired fly ash samples were analyzed. The results of this analysis are shown in Table 1. As can be seen in Table 1, a large percentage of each oil fly ash is water soluble, and this fraction is mainly composed of sulfates. In Table 1, the percentage of water soluble components, the percentage of NH_4, and the percentage of the four most abundant elements are listed for each fly ash. The infrared results for each fly ash are also listed in Table 1 with the most abundant sulfate (based estimations from infrared band intensities) listed first, the second most abundant next, etc. It can be seen in Table 1 that this infrared method identified several sulfates in each fly ash, and these identifications were, in general, supported by the elemental analyses. Thus, FT-IR coupled with elemental analyses (especially to guide the initial subtractions) can identify individual sulfate compounds in a mixture of sulfates.

COAL FLY ASH RESULTS

The water soluble content of the coal fly ash samples is, in general, much lower than for the oil fly ash samples. Thus, while the water solubles are still important, the water insolubles assume a much greater importance than for the oil fly ash samples.

Figure 8 shows infrared spectra of the water soluble portion of Millcreek (Figure 8A) and Picway (Figure 8B) coal fly ashes. Note that the spectra are very similar and even though there are several informative infrared bands in the 600-700 cm^{-1} region, it is difficult to identify individual sulfates from such spectra. All that can be said is that there are large amounts of $CaSO_4$ and/or $Fe_2(SO_4)_3$ present. However, having the capability to subtract infrared spectra can be very useful, especially when the two spectra are very similar. Figure 9 shows the subtracted spectrum of the Millcreek and Picway fly ash samples (Figure 8B) and a scale expanded version of this subtraction (Figure 8A). The absorption band pointing downwards (1210 cm^{-1}) clearly indicates the presence of $Al_2(SO_4)_3$ in the Picway sample. Since the spectra (Figure 8) are so similar, $Al_2(SO_4)_3$ must also be present in the Millcreek sample, but there is more of it relative to the other sulfates in the Picway fly ash. Also the bands in the 600-700 cm^{-1} region indicate the presence of both $CaSO_4$ and $Fe_2(SO_4)_3$ and this indicates there is more of these components in the Millcreek sample than in the Picway sample since the bands in the 600-700 cm^{-1} region are pointing upwards. Thus, from the subtracted spectra, $Al_2(SO_4)_3$, $CaSO_4$, and $Fe_2(SO_4)_3$ can be identified in both

Table 1. Infrared Results for Oil Fly Ashes

Oil Fly Ash		% H_2O Sol.	% NH_4	% Indicated Elements			
#1	E[a]	58	0 NH_4	4.7Mg	3.9Na	1.0Ni	0.6Ca
	IR			$MgSO_4$	Na_2SO_4	--	$CaSO_4$
#2	E	23	0.1NH_4	2.2V	1.2Mg	0.6Ni	0.3Na
	IR			$VOSO_4$	$MgSO_4$	$NiSO_4$	--
#3	E	--	--	--	--	--	--
	IR			$VOSO_4$	Na_2SO_4	$CaSO_4$	--
#4	E	72	0.8	9.0V	5.0Mg	1.1Ni	0.5Na
	IR			VSO_4[b]	$MgSO_4$	$NiSO_4$	$VOSO_4$ Other[c]
#5	E	98	0.2	12.9V	2.7Mg	2.3Ni	2.0Na
	IR			$VOSO_4$	$MgSO_4$	$NiSO_4$	--
#6	E	83	7.3	2.4Mg	0.8V	0.4Fe	0.3Ni
	IR		NH_4HSO_4 $(NH_4)SO_4$	$MgSO_4$	--	--	$NiSO_4$ $CaSO_4$ $VOSO_4$

[a]E = Elemental Analysis
[b]VSO_4 is used to indicate a vanadium sulfate other than $VOSO_4$
[c]For fly ash #4, a 5th unidentified sulfate has been detected

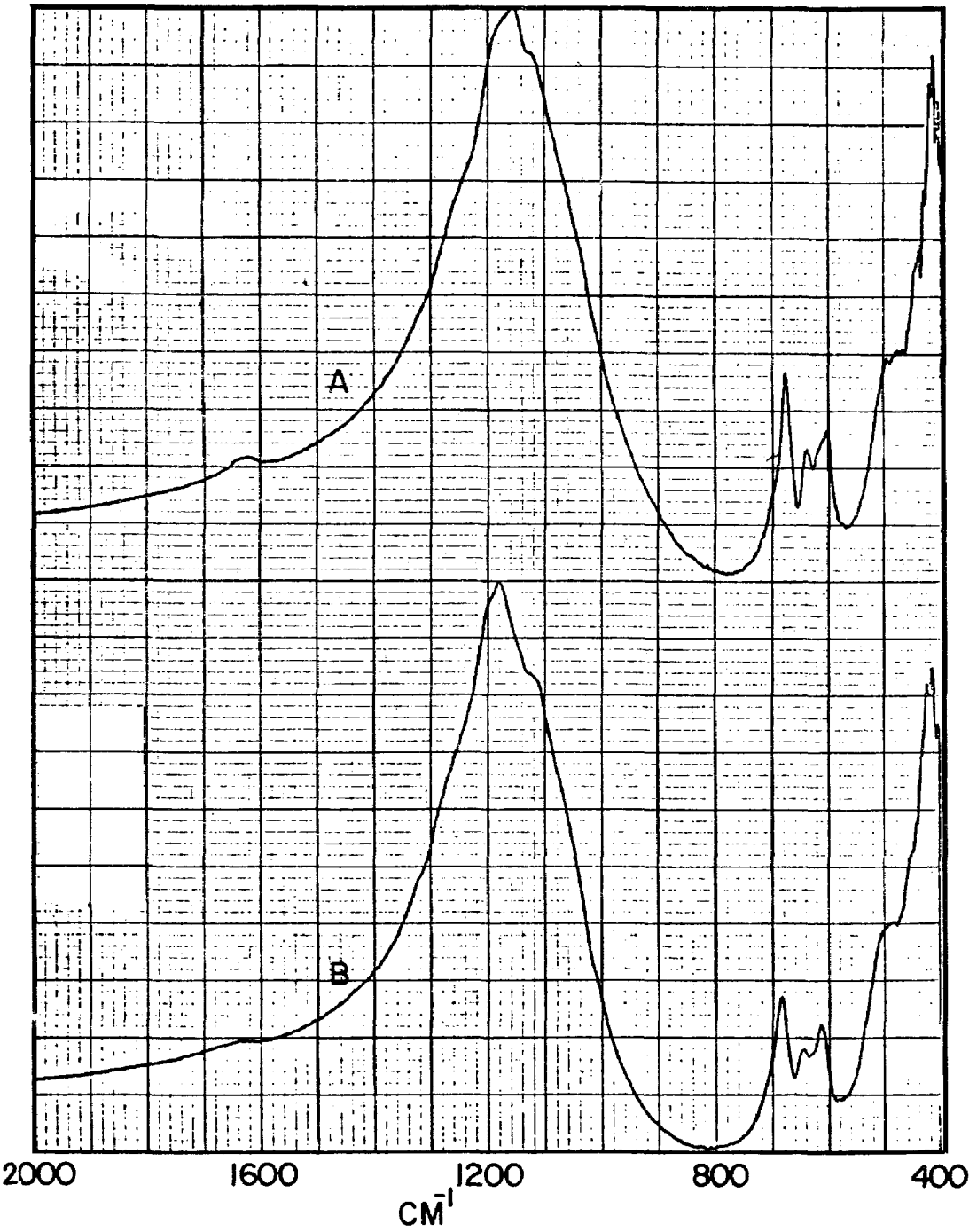

Figure 8. Infrared spectra of water soluble fraction of coal fly ashes of (A) Millcreek; (B) Picway.

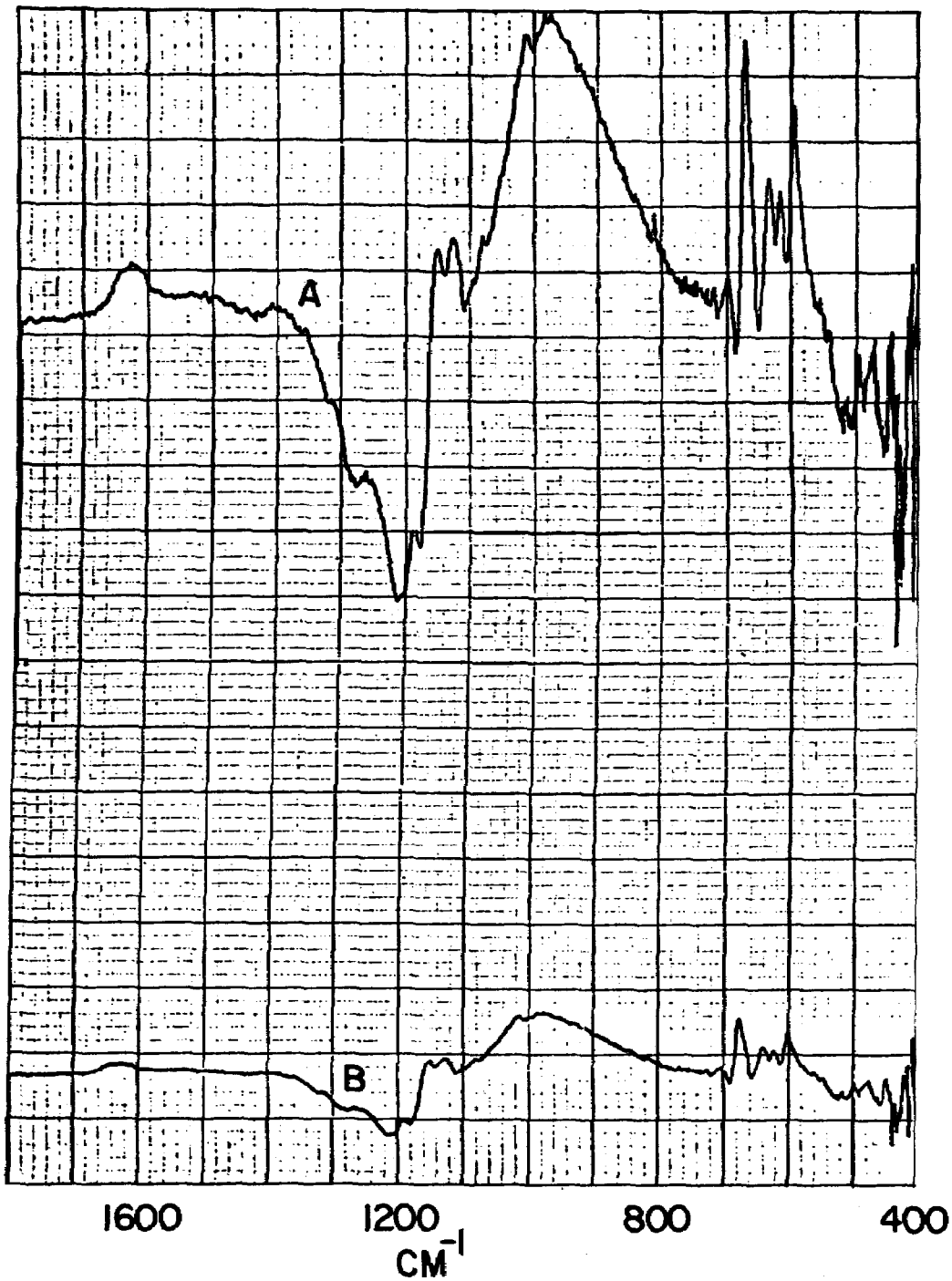

Figure 9. Subtracted infrared spectra (water soluble fractions of Millcreek minus Picway) with (A) scale expanded; (B) no scale expansion.

samples; the amount of $Al_2(SO_4)_3$ relative to the other sulfates is higher in the Picway sample; and the amount of $CaSO_4$ and $Fe_2(SO_4)_3$ is higher in the Millcreek sample. This is substantiated by the elemental analysis which is given in Table 2. Here it can be seen that even though the total quantity of soluble material is greater in the Millcreek sample, the total amount of possible $Al_2(SO_4)_3$ relative to the other possible sulfates is greater in the Picway fly ash.

Table 2. Elemental Analysis for Coal Fly Ash Samples

Coal Fly Ash	H_2O Sol.	Percent of Total		
			E	
Picway	14	0.6Al	0.6Fe	0.2Ca
Millcreek	35	1.9Fe	1.6Al	1.6Ca

The spectrum of the water insoluble fraction of the Picway coal fly ash is shown in Figure 6B and will not be repeated here. The spectrum of the Millcreek insoluble fraction is almost identical to the Picway fraction except that the Millcreek spectrum shows a greatly reduced 560 cm^{-1} (Fe_3O_4) infrared band. Thus, the spectra of the insoluble fractions show large amounts of SiO_2 and Fe_3O_4 with more Fe_3O_4 in the Picway sample. No Al_2O_3 was detected in either sample in spite of the fact that relatively large (about 10%) amounts of Al were found in each sample. This probably indicates that the SiO_2 component contains an aluminum iron silicate. We have not obtained as yet many reference spectra of silicates; thus such identifications are not possible at this time.

GLASS MELTS

The spectra of the water insoluble fractions of the coal fly ashes not only raise the questions of obtaining reference spectra for the identification of silicates but also raise the question of the amorphous (glass) versus crystalline content of these fractions. This can be especially critical in the area of inorganic compound identification because x-ray diffraction is dependent on crystallinity to be effective. Thus a technique for compound

identification in glassy samples is vitally needed. Our work in this area is just beginning, so only preliminary data are listed below.

Table 3. Composition of Glass Melts

Glass	%		
-----	Al_2O_3	Fe_2O_3	SiO_2
G-1	51	20	29
G-2	40	15	45

Two oxide samples, of the composition shown in Table 3, were prepared. For each sample, the oxides were mixed thoroughly, melted at high temperatures, quenched, and ground to less than 300 mesh. Infrared spectra of each sample were obtained both before and after melting. The spectra before melting are shown in Figure 10, while the spectra after melting are shown in Figure 11. The spectra of the two mixes before melting are quite similar (Figure 10) with the major difference being the increased band intensities at 790 and 1100 cm^{-1} in G-2. These bands are both due to SiO_2. A comparison of the height of the 790 cm^{-1} band (baseline corrected) indicates 50%-75% more SiO_2 in G-2 than in G-1. That this is true can be seen in Table 3 which gives the actual composition of the samples. A series of subtractions of G-2 minus G-1 were performed to determine which sample contained a higher Fe_2O_3 to Al_2O_3 ratio. Very little difference was observed in these subtractions which led to the conclusion that the ratio of Fe_2O_3 to Al_2O_3 was about equal in the two samples. Reference to Table 3 indicates that although the absolute amounts of Fe_2O_3 and Al_2O_3 vary between the two samples, the Fe_2O_3/Al_2O_3 ratio remains nearly constant.

Figure 11 shows the spectra of the two samples after melting. Note that these spectra are completely different from the corresponding unmelted spectra. This probably reflects the extreme treatment the samples received. NBS standards of SiO_2 which are either totally crystalline or totally amorphous do not show the drastic spectral changes seen between Figures 10 and 11. In spite of the major differences upon melting, we can detect (Figure 11) bands at 1110, 930, and 800 cm^{-1} in both melts. The 1110 cm^{-1} band is stronger in G-2 and a 560 cm^{-1} band appears in G-1. The

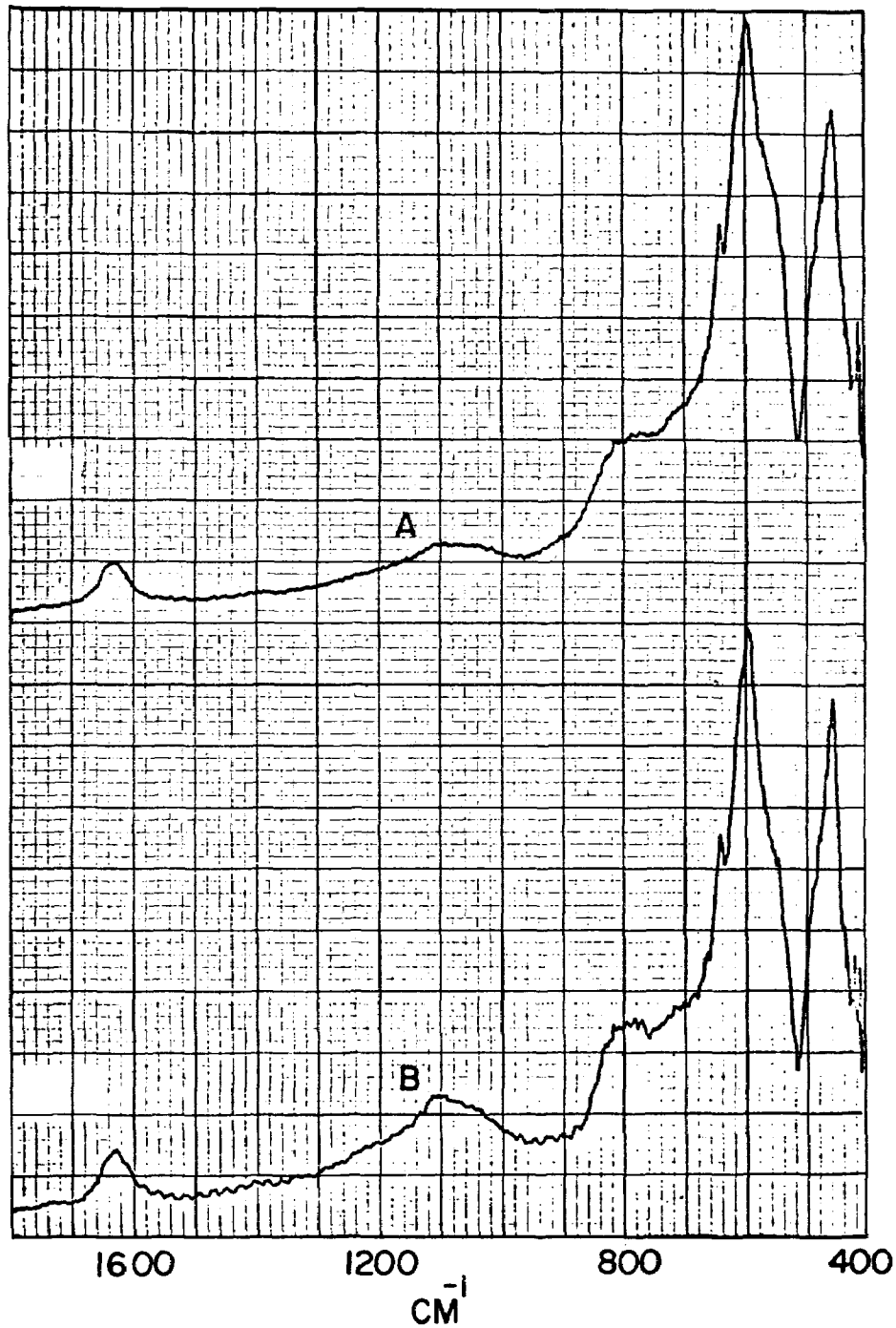

Figure 10. Infrared spectra of synthetic oxide mixtures before melting for (A) G-1; (B) G-2.

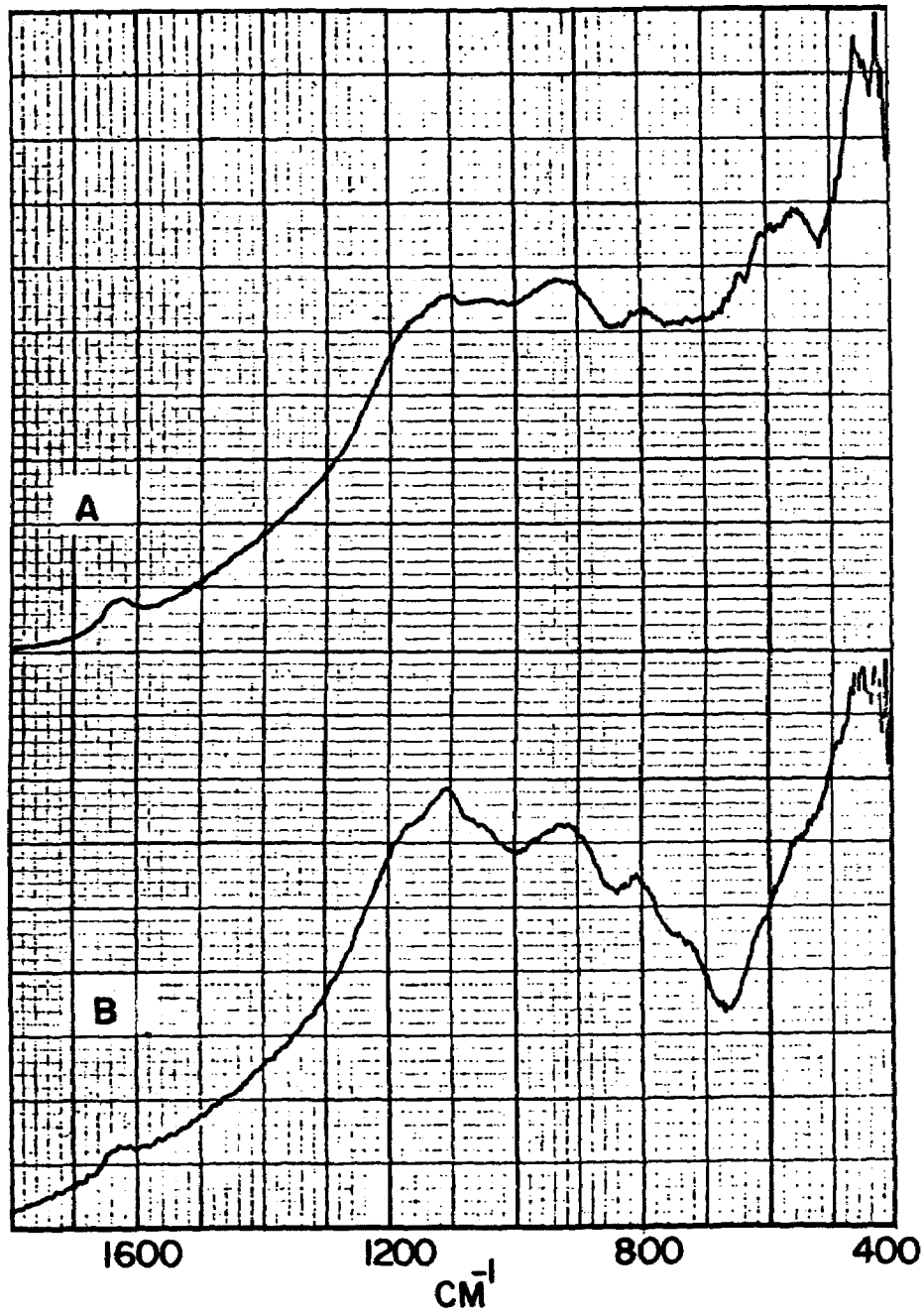

Figure 11. Infrared spectra of synthetic oxide mixture after melting for (A) G-1; (B) G-2.

1110 cm^{-1} band reflects the Si-O content of the samples and shows that G-2 has more SiO_2 than G-1 (also note SiO_2 content in Table 3). The 560 cm^{-1} likely means that we have more combined Fe_2O_3 and Al_2O_3 relative to SiO_2 in G-1 than in G-2. Thus, even though these samples were subjected to drastic conditions and the melt spectra are different from most glass spectra, information about the composition of the glass can still be obtained.

SUMMARY

The results obtained from the use of the methodology described in this paper demonstrate that FT-IR, when coupled with careful sample preparation and guided by the elemental analysis, can provide unique information on inorganic compound speciation. Preliminary information indicates that this information can be obtained on glassy as well as crystalline samples. Relative quantification of the compounds identified is already possible and being done, but absolute quantification will require getting accurate extinction coefficients for all the reference standards and for a variety of conditions. This is not possible at the present time because of lack of computer storage space for spectra.

Because of the lack of computer storage for both qualitative and quantitative work, we have not yet fully exploited the potential of this method for inorganic compound identifications. This is especially true for silicates and for mixed salts. Until we routinely begin to acquire far infrared (400-100 cm^{-1}) spectra, our capability to identify many oxides and to identify halogen salts is limited. In spite of these limitations the FT-IR technique has provided a unique method for inorganic speciation.

Report of the Working Group on Measurement of Particulate Sulfur Oxides Emissions

Richard C. Flagan, *Reporter*

The objective of this working group was to make recommendations for future research on sampling and analysis of primary sulfur oxide aerosols. Primary sulfur oxide aerosols are included in particulate matter present in the plume after initial dilution with ambient air but prior to any secondary reactions. This includes aerosols produced by condensation of sulfur trioxide or sulfuric acid vapor.

RECOMMENDATIONS

Research is needed to relate in-stack measurements of gases and aerosols to the total primary sulfur oxide aerosol which exists in the plume several stack diameters from the stack exit. The time scale for any primary aerosol formation upon initial dilution and cooling is short compared to the time required for any secondary oxidation of sulfur compounds (secondary aerosols).

Measurements need to be made to determine the contribution to particulate emissions resulting from transient phenomena including start-up, boiler deposit build-up, soot blowing, precipitator cleaning, shut-down, and malfunctions. Research needs to be done to determine the adequacy of and, possibly, the development of measurement methods for studying the transient aerosol emissions.

Research is needed to understand the physical and chemical transformations of particulate matter during and after sampling the flue gas. This would include studies of sample aging. Input from the analyst is essential to the understanding of the significance of any transformations.

Detailed studies of the sulfur aerosol speciation are necessary for an understanding of the effects of primary sulfur oxide aerosols.

Guidelines need to be developed for the consistent presentation of aerosol data.

1. It should be recognized that "total" aerosol samples usually exclude very large particles. The particle size dependent collection characteristics of the sampling system should be determined and reported.

2. Where particle size is determined, the definition of particle size must be clearly stated.

3. Particle size distribution data should not be normalized as percent versus size because of the inherent bias introduced by the sampling system collection characteristics. Data presentation such as $\Delta M/\Delta \log d_p$ versus $\log d_p$ should be employed.

Appendix

PARTICIPANTS AND OBSERVERS

Jeffrey W. Adams
Arthur D. Little, Inc.
Acorn Park
Cambridge, Massachusetts 02140
617/864-5770 x.3036

Aubrey P. Altshuller
Director
Environmental Sciences
Research Laboratory
Environmental Protection Agency
Environmental Research Center
MD/59
Research Triangle Park
North Carolina 27711
919/541-2191

John Bachmann
Environmental Protection Agency
Environmental Research Center
MD/12
Research Triangle Park
North Carolina 27711
919/541-5231

Elizabeth M. Bailey
Division of Environmental
Planning
Tennessee Valley Authority
Muscle Shoals, Alabama 35660
205/383-4631 x.2788

Roy L. Bennett
Research Chemist
Environmental Sciences
Research Laboratory
Environmental Protection Agency
Environmental Research Center
MD/46
Research Triangle Park
North Carolina 27711
919/541-3173

Richard K. Chang
Department of Engineering and
Applied Science
Yale University
New Haven, Connecticut 06520
203/432-4470

James L. Cheney
Environmental Protection Agency
Environmental Research Center
MD/46
Research Triangle Park
North Carolina 27711
919/541-3172

Harold Cowherd
Environmental Engineering
Long Island Lighting Company
175 East Old Country Road
Hicksville, New York 11801
516/733-4700

Kenneth M. Cushing
Research Physicist
Southern Research Institute
2000 Ninth Avenue South
Birmingham, Alabama 35205
205/323-6592

Daryl DeAngelis
Research Engineer
Monsanto Research Corporation
1515 Nicholas Road
Dayton, Ohio 45407
513/268-3411

Russell N Dietz
Chemical Engineer
Brookhaven National Laboratory
Building 426
Upton, New York 11973
516/345-3059

James Dorsey
Industrial Environmental
Research Laboratory
Environmental Protection Agency
Environmental Research Center
MD/62
Research Triangle Park
North Carolina 27711
919/541-2557

Brian Doyle
Principal Engineer
KVB, Inc.
246 North Central Avenue
Hartsdale, New York 10530
914/949-6200

Edgar S. Etz
Research Chemist
Center for Analytical Chemistry
National Bureau of Standards
Chemistry Building
Room A-121
Washington, D.C. 20234
301/921-2862

Richard C. Flagan
California Institute of
Technology
MS 138-78
Pasadena, California 91125
213/795-6811 x.1383

William M. Henry
Projects Manager
Battelle-Columbus Laboratories
505 King Avenue
Columbus, Ohio 43201
614/424-5210

James B. Homolya
Environmental Protection Agency
Environmental Research Center
MD/46
Research Triangle Park
North Carolina 27711
919/541-3085

James E. Howes, Jr.
Senior Researcher
Battelle-Columbus Laboratories
505 King Avenue
Columbus, Ohio 43201
614/424-5269

Skillman C. Hunter
KVB, Inc.
17332 Irvine Boulevard
Tustin, California 92680
714/832-9020

Peter Jackson
Central Electric Generating
Board
Marchwood Engineering
Laboratories
Marchwood Southampton
England SO44ZB

Ashok K. Jain
Research Engineer
NCASI
Box 14483
Gainesville, Florida 32604
904/377-4708

Robert J. Jakobsen
Battelle-Columbus Laboratories
505 King Avenue
Columbus, Ohio 43201
614/424-5617

Kenneth T. Knapp
Chief, Particulate Emissions
Research Section
Environmental Sciences
Research Laboratory
Environmental Protection Agency
Environmental Research Center
MD/46
Research Triangle Park
North Carolina 27711
919/541-3085

Arthur Levy
Manager
Combustion Systems Technology
Battelle-Columbus Laboratories
505 King Avenue
Columbus, Ohio 43201
614/424-4827

Dale Lundgren
Environmental Engineering
Sciences
University of Florida
Gainesville, Florida 32611
904/392-0846

Ray F. Maddalone
Section Head
TRW Defense and Space
Systems Group
One Space Park 01/2020
Redondo Beach, California 90278
213/535-1458

Richard E. Marland
Office of the Assistant
Administrator for Research
and Development
Environmental Protection Agency
RD 672
401 M Street, S.W.
Washington, D.C. 20460
202/755-2532

William R. McCurley
Research Engineer
Monsanto Research Corporation
1515 Nicholas Road
Dayton, Ohio 45418
513/268-3411

John Nader
Chief
Stationary Source Emissions
Research Branch
Environmental Protection Agency
Environmental Research Center
MD/46
Research Triangle Park
North Carolina 27711
919/541-3085

David F. S. Natusch
Professor
Department of Chemistry
Colorado State University
Fort Collins, Colorado 80523
303/491-5391

A. Jack O'Neal, Jr.
Chief Chemist
Electric Production Department
Long Island Lighting Company
P.O. Box 426
Glenwood Landing, New York 11547
516/671-6783

Richard Rhudy
Project Manager
Electric Power Research Institute
Box 10412
Palo Alto, California 94303
415/855-2421

Roosevelt Rollins
Environmental Protection Agency
Environmental Research Center
MD/46
Research Triangle Park
North Carolina 27711
919/541-3171

Arthur M. Squires
Department of Chemical
Engineering
Virginia Polytechnic Institute
Blacksburg, Virginia 24061
703/951-5972

Paul Urone
National Environmental
Investigation Center
Denver Federal Center
Building 53 - Box 25227
Denver, Colorado 80225
303/234-4661

Jack Wagman
Environmental Protection Agency
Environmental Research Center
MD/46
Research Triangle Park
North Carolina 27711
919/541-3009

Arthur S. Werner
Manager
Analytical Laboratory
GCA/Technology Division
Burlington Road
Bedford, Massachusetts 01730
617/275-9000

TECHNICAL REPORT DATA
(Please read Instructions on the reverse before completing)

1. REPORT NO. EPA-600/9-78-020a	2. RECIPIENT'S ACCESSION NO.
4. TITLE AND SUBTITLE WORKSHOP PROCEEDINGS ON PRIMARY SULFATE EMISSIONS FROM COMBUSTION SOURCES Volume 1. Measurement Technology	5. REPORT DATE August 1978
	6. PERFORMING ORGANIZATION CODE
7. AUTHOR(S)	8. PERFORMING ORGANIZATION REPORT NO.
9. PERFORMING ORGANIZATION NAME AND ADDRESS Kappa Systems, Inc. 1501 Wilson Boulevard Arlington, Virginia	10. PROGRAM ELEMENT NO. 1AD712 BC-52 (FY-78)
	11. CONTRACT/GRANT NO. 68-02-2435
12. SPONSORING AGENCY NAME AND ADDRESS Environmental Sciences Research Laboratory - RTP, NC Office of Research and Development U.S. Environmental Protection Agency Research Triangle Park, N.C. 27711	13. TYPE OF REPORT AND PERIOD COVERED Final
	14. SPONSORING AGENCY CODE EPA/600/09
15. SUPPLEMENTARY NOTES	

16. ABSTRACT

Technical papers on techniques for measuring primary sulfate emissions from combustion sources, presented at a workshop sponsored by the U.S. Environmental Protection Agency, are compiled in Volume 1 of a proceedings.

The objectives of the workshop were to review and discuss current measurement methods and problem areas for sulfur oxides emission with attention focused on sulfuric acid, sulfates, and sulfur-bearing particulate matter; to review and discuss emission data from various combustion sources operating under different conditions which include various pollutant controls, fuel composition, excess boiler oxygen, etc.; and to delineate and recommend areas in need of research and development effort.

Scientists were invited to present the result of their studies on primary sulfate emissions. The 3-day workshop devoted one day to measurement technology, a second to characterization, and a third to critical assessment of the presented papers and development of summary working group reports on each half-day session of the initial 2 days. Thirty-one papers were presented by 29 participants on measurements and characterization. Four working group reports were developed and summarized in the last day.

17. KEY WORDS AND DOCUMENT ANALYSIS

a. DESCRIPTORS	b. IDENTIFIERS/OPEN ENDED TERMS	c. COSATI Field/Group
* Air pollution		13B
* Sulfates		07B
* Emission		21B
* Combustion products		14B
* Measurement		
* Collecting Methods		

18. DISTRIBUTION STATEMENT RELEASE TO PUBLIC	19. SECURITY CLASS (This Report) UNCLASSIFIED	21. NO. OF PAGES 289
	20. SECURITY CLASS (This page) UNCLASSIFIED	22. PRICE

EPA Form 2220-1 (Rev. 4-77) PREVIOUS EDITION IS OBSOLETE